Complexity

Tales of Two Societies: On the Complexity of the Coevolution between the Physical Space and the Cyber Space

Lead Guest Editor: Shu-Heng Chen
Guest Editors: Simone Alfarano and Dehua Shen

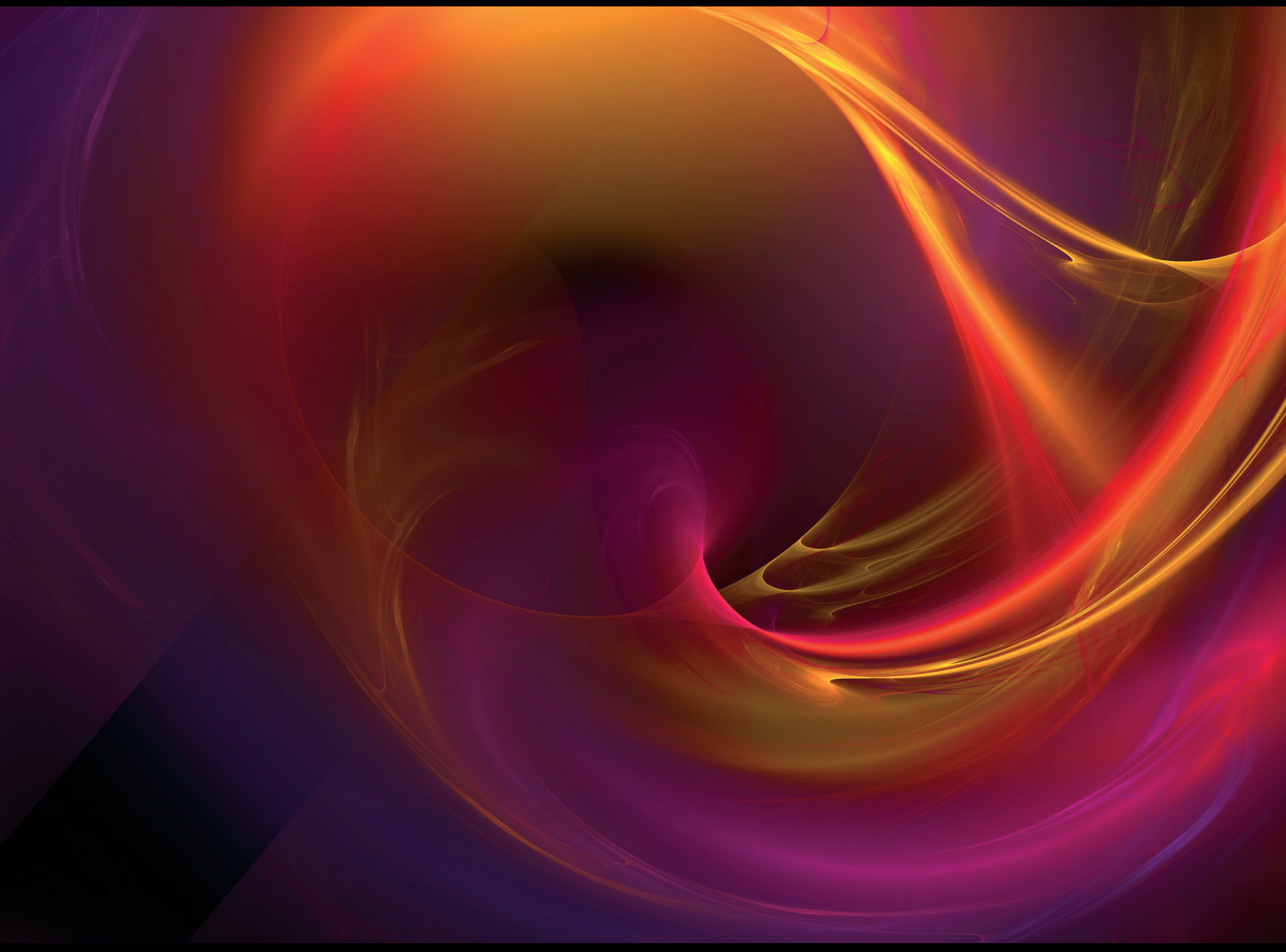

Tales of Two Societies: On the Complexity of the Coevolution between the Physical Space and the Cyber Space

Complexity

Tales of Two Societies: On the Complexity of the Coevolution between the Physical Space and the Cyber Space

Lead Guest Editor: Shu-Heng Chen
Guest Editors: Simone Alfarano and Dehua Shen

Contents

Institutional Investor Information Sharing, Stock Market Extreme Risk, and Financial Systemic Risk
Xiao-Li Gong and Zhi-Qiang Du
Research Article (10 pages), Article ID 5745916, Volume 2020 (2020)

Complexity to Forecast Flood: Problem Definition and Spatiotemporal Attention LSTM Solution
Yirui Wu, Yukai Ding, Yuelong Zhu, Jun Feng, and Sifeng Wang
Research Article (13 pages), Article ID 7670382, Volume 2020 (2020)

Dynamic Cross-Correlations between Participants' Attentions to P2P Lending and Offline Loan in the Private Lending Market
Yingxiu Zhao, Wei Zhang, and Xiangyu Kong
Research Article (8 pages), Article ID 1635793, Volume 2019 (2019)

Hindawi
Complexity
Volume 2021, Article ID 4703820, 13 pages
https://doi.org/10.1155/2021/4703820

Research Article

Defining Heritage Science: A Consilience Pathway to Treasuring the Complexity of Inheritable Human Experiences through Historical Method, AI, and ML

Andrea Nanetti

Nanyang Technological University, Singapore

Correspondence should be addressed to Andrea Nanetti; nanetti.andrea@gmail.com

Received 29 July 2020; Revised 4 September 2020; Accepted 12 November 2020; Published 15 February 2021

Academic Editor: Shu-Heng Chen

Societies have always used their heritage to remain resilient and to express their cultural identities. Today, all the still-available experiences accrued by human societies over time and across space are, in principle, essential in coping with the twenty-first century grand challenges of humanity (refer to the 17 UN Sustainable Development Goals). Artificial intelligence and machine learning algorithms can assist the next generation of historians, heritage stakeholders, and decision-makers in (1) decoding unstructured knowledge and wisdom embedded in selected cultural artefacts and social rituals, (2) encoding data in machine-readable systems, (3) aggregating information according to the user's needs in real time, and (4) simulating the consequences of either erasing, neglecting, putting in latency, or preserving and sharing specific human experiences. What our global society needs is a multilingual and transcultural approach to decode-encode the treasure of human experience and transmit it to the next generation of world citizens. This approach can be the pathway to work on a new science of heritage, its ethics, and empathy.

1. Introduction

Since 1834, when Michael Faraday first talked about "heritage science" in his Royal Institution Christmas Lecture, this science of heritage has evolved from a disciplinary field focused on conservation sciences to its more recent opening as a domain to a broader range of research disciplines able to reflect better the breadth and depth required by our complex societies in dealing with its heritage (i.e., what may and should be sustainably inherited). The *Singapore Heritage Science Conference* series (2014–2016 (see Figure 1)) and the three-day event, *Dancing over Ideas of Research* (2018), provided a discussion forum on the role of heritage science in today's society (refer to [2, 3]). These two conferences confirmed that the multidisciplinary domain of heritage science focuses on recording, accessing, interpreting, conserving, and managing cultural heritage seen as the treasure of human experiences.

Today, heritage science considers the knowledge and values acquired in all relevant disciplines, from arts and humanities (e.g., philosophy, ethics, art and art history, economics, sociology, and anthropology) to fundamental sciences (e.g., chemistry, physics, mathematics, and biology), as well as to computer science, engineering, communication, and media studies. In particular, the 2nd Singapore Heritage Science Conference, "Heritage and the Creative Industries," held on 15-16 January 2015, wrestled with the tensions between age-old practices and our modern digital lifestyles. New media and non-conventional communications have risen as a challenge, creating new possibilities for cultural expressions and the advancement of learning. However, during the conference, there was a sense that we might be losing our humanity as lives become more and more digital, and the criteria of digital-data preservation are left to the neoliberal rules of the free market. In hearing experts—like Harold Thwaites in his keynote address—talk about past experiences and draw from them creative inspirations for the future, one could realise that human qualities like ethics, empathy, identity, and spirituality are bonding resources that serve to bind people together. In short, to be human is to

Figure 1: This rendering—realized in 2014 by Muhammad Mustajab Bin Mohamad, Higher Executive Officer (Publicity, outreach & Alumni Relations) at the Nanyang Technological University School of Art, Design and Media—presents the 1st Singapore Heritage Science Conference concept as conceived by the conference chairs, Dr Andrea Nanetti and Dr Siew Ann Cheong. It shows an adult hand passing the world (identified as a complex mechanism with ASEAN at the centre) to a younger one. It is a good icon to summarise an approach to art, culture, and heritage in an AI perspective, where machine-generated algorithms may enhance the human transmission of data, information, knowledge, wisdom, and their relationships. This work was licensed under a Creative Commons Attribution-NonCommercial 4.0 International License (CC BY-NC 4.0) by Nanyang Technological University Singapore in 2014. For the Singapore Heritage Science Conference series (2014-2016, refer to www.paralimes.org for programmes, abstracts, and recordings of the presentations of the four conferences: 1st (January 2014) Heritage as a Complex System; 2nd (Jan. 2015) Heritage and the Creative Industries; Special edition (Nov. 2015) Exploring Maritime Heritage Dynamics; 3rd (Jan. 2016) The Treasure of Human Experiences. "Heritage poses the challenge of innovation in a new way: how does the new integrate with the old?" This was the key question raised by Helga Nowotny (founding member and former president of the European Research Council) in her keynote address at the 1st Singapore Heritage Science Conference on Heritage science as a complex system: The embarrassment of complexity: A phase of transition? The conference was organized and chaired by Andrea Nanetti and Siew Ann Cheong at Nanyang Technological University Singapore for the Complexity Program and the School of Art, Design and Media (6-7 January 2014, Figure 1). This event pioneered a new science of heritage as a state-of-the-art multidisciplinary domain able to investigate and discover integrated action plans and solutions in response to, and in anticipation of, the challenges arising from cultural heritage issues in society. Heritage is closely linked to the history and identity of communities. The complete video record of the conference is available from: http://www.paralimes.ntu.edu.sg/Pages/Home.aspx. The intellectual discussions facilitated by the Complexity Programme under the vibrant direction of Jan Vasbinder at Nanyang Technological University (NTU) Singapore between 2013 and 2018 have been extremely relevant in nurturing the idea of this new science of heritage and making the acquaintance with many renowned scholars from all-over the world, with whom I have discussed this idea and shared research projects.

be connected to other humans, to our environments, and, for some, to a cosmic significance. The conference presentations have been fully video recorded and are digitally available from http://www.paralimes.ntu.edu.sg/NewsnEvents/HeritageandtheCreativeIndustry/Pages/Video%20Gallery.aspx.

This essay aims to discuss the shifting of the multidisciplinary domain of heritage science into an interdisciplinary algorithmic perspective, viz., able to take full advantage of computational tools and possibly avoid the biases of blind faith in technology and progress. Such a new science of heritage must sit on the shoulders of the giants in different research fields to overcome the dichotomy between the humanities and the sciences [4–8]. This process aims to lead to the interdisciplinary formalisation and integration of multidisciplinary bookish scholarship and practical experience of heritage (i.e., the inheritability of artefacts, oral traditions, scientific knowledge, social rituals, and other cultural practices that embody human experiences of the world and the human condition itself).

This new science of heritage should also find ways to raise awareness of the importance of immunisation against blind faith in technology and progress. Odysseas Elyt is epitomised this critical challenge in 1974: "I apologize for the easy symbolism, but the truth of our age 'amounts' to just this: an incredible technical progress strives to cure the ills caused to man by an incredible technical progress" (refer to [9]:35-36). Poets and essayists explored the human condition (including emotion, aspiration, conflict, and mortality) in search for this "vaccine" in relation to ways of living together without violence, for the salvation of humankind and possibly generate a new form of being. The inevitable "souffrance" of the living beings described in Giacomo Leopardi's garden—which with Emanuele Severino we can epitomise as "The game of mankind's destiny" in apparent anticipation of Nietzsche's thought—asks us if humans can withstand the immensity without losing themselves in its vertigo. In 1819, the 21-year-old Leopardi had already taken up the thought of Blaise Pascal (1623–1662): "The eternal silence of these infinite spaces frightens me" [10]. The context of this quotation from Pascal is the following: *205. When I consider the short duration of my life, swallowed up in the eternity before and after, the little space which I fill and even can see, engulfed in the infinite immensity of spaces of which I am ignorant and which know me not, I am frightened and am astonished at being here rather than there; for there is no reason why here rather than there, why now rather than then. Who has put me here? By whose order and direction have this place and time been allotted to me?* Memoria hospitis unius diei praetereuntis *[Bible,* Sapientia/*Book of Wisdom, 5:15 "the remembrance of a guest of one day that passeth by" (transl. Douay-Rheims)]. 206. The eternal silence of these infinite spaces frightens me. 207. How many kingdoms know us not! 208. Why is my knowledge limited? Why my stature? Why my life to one hundred years rather than to a thousand? What reason has nature had for giving me such, and for choosing this number rather than another in the infinity of those from which there is no more reason to choose one than another, trying nothing else?*. Leopardi reworked Pascal's thoughts in his famous lyric *L'Infinito*: "Così tra questa/immensità s'annega il pensier mio: /e il naufragar m'è dolce in questo mare" (so my mind sinks in this immensity: /and

	Physics (only what can be measured belongs to physics)	History (evidence witnessed via personal observation or experience > knowledge acquired by investigation)
Space	Geometry	Geography
Time	Chronometry	Chronology
Memory	The part of a computer in which data or program instructions can be stored for retrieval (discard?)	The faculty by which the mind stores and remembers information (memory > selection > eschatology)

	History/humanities	Physics/computing
Data	Things known or assumed as facts, making the basis of reasoning (Philosophy).	The quantities, characters, or symbols, on which opearations are performed by a computer.
Information	Facts provided or learned about something or someone.	Data as processed, stored, or transmitted by a computer.
Facts	(i) A piece of information used as evidence or as part of a report or news article. (ii) The truth about events as opposed to interpretation (Law). (iii) The available body of facts or information indicating whether a belief or proposition is true or valid. (iv) Information given personally, drawn from a document, or in the form of material objects, tending or used to establish facts in a legal investigation or admissible as tesimony in court.	Synonymous with information.
Evidence	(i) The available body of facts or information indicating whether a belief or proposition is true or valid. (ii) Information given personally, drawn from a document, or in the form of material objects, tending or used to establish facts in a legal investgation or admissible as testimony in court (lab).	Collection of data demonstrating the reproducibility (consistency) of an information/fact.
Event	A thing that happens, especially one of importance.	A single occurrence of a process (physics).

Figure 2: The first table (space, time, and memory) is published here for the first time. For the second table (History/Humanities and Physics/Computing), refer to [12]; Table 18.1. In the same paper, Figure 18.1 on page 338 shows the stages a discipline must progress through to become computational: data collection, data management, data visualisation, and model and simulation.

foundering is sweet in such a sea) (see Leopardi, *Canti*: 106-107, where the translator titles incorrectly this idyll *Infinity* (which in Italian would have been *Infinità*) instead of *The infinite*. The poem was first published in [11]:903). We need a metamorphosis, a gesture of civilisation, which—as the poet Giuseppe Ungaretti said to Pier Paolo Pasolini in an interview in 1965—"is an act of human bullying against nature." As the journalist, Jonah Lehrer, explains in *How we decide* (2009), "rational we are not born, we become. That is, we are born Dionysiac, but to excel we also need to become Apollonian."

The vision rendered here is that neglecting heritage, the treasure of human experience, would leave humanity impoverished and less prepared for the uncertainties and increasing complexities of living together on planet Earth. Human societies have always used their heritage, viz., the inheritable treasure of human experiences (i.e., knowledge and values) accumulated across space and over time, to remain resilient, express cultural identities in their national narratives, and imagine desirable futures by integrating the new with the old (refer to [13]). Nowadays, it seems that the rapid development of society is endangering this spontaneous process of adaptation to change (refer to [14]). Given the increasing pace of technological innovation, many traditional modes of knowledge and value transmission have become obsolete or are at the risk of vanishing. Societies might lose their usual means before they could master new methods to keep their so-far treasured human experiences available in the present and for the future. This loss of cultural heritage would, thus, compromise societal resilience and adaptability to change at a time when they are needed more than ever. To deal with this challenge, public and private synergies in higher education and science and research (humanities complemented by other natural science disciplines) could and should play a major role in providing the vision to prototype, and engineer solutions, with

imagination (i.e., the faculty of conceiving new ideas and seeing external entities not present to the senses), empathy (i.e., a strong feeling of relationships with others), and curiosity (i.e., a strong desire to know and acquire knowledge by study, experience, or being taught).

Information-communication technology (ICT) has truly opened a new frontier for the advancement of data sharing, and we can agree with Sandra Rendgen that "professional data and information management will be a central cultural tool in the decades to come (refer to [15]:9)." However, ICT alone is not able to support substantial advancement of learning because the exponentially growing volume of digital data is a solution and a problem at the same time. Technology indeed allows us to access more and more information faster and faster from almost everywhere. However, current ICT is unable to retain, structure, and process the amount of digital data produced by society. Moreover, unstructured data per se are of little or negligible value. To become an asset, data need to be filtered, organised, and be machine-readable. This data processing requires considerable natural and human resources that our society may be unable or unwilling to allocate. Thus, due to the risk that many traditional modes of knowledge and value transmission might become obsolete or are at the risk of vanishing soon, our society needs to take the responsibility of deciding the selection criteria of what human knowledge and values to preserve and keep available for the next generation in a digital form.

In nature, genes have their physiological criteria to preserve or discard the information. Heredity—viz., the passing on of physical or mental characteristics genetically from one generation to another to ensure the existence of intelligent life itself—obeys to the laws of function and convenience in relation to the environment in which life spreads and evolves. Human genes are the naturally curated repository of all the experience accumulated by humanity on planet Earth. Human societies added cultural criteria as a complementary trove of valuable knowledge. Cultural heritage—viz., the experiences accrued by human societies that are transmitted by artificial (i.e., human-made) means such as orality, artefacts, and rituals—needs to be curated by humans. As mentioned above, traditional selection criteria are put at risk by today's rapid development of society, globalisation, and digital revolutions. Our society is, thus, urged to decide what to store and what to discard in the digital trove of the human experiences.

There is a cogent need of taking over the responsibility of discussing the best desirable principles for this new digital trove because society needs to reinforce, with more human selection criteria, the algorithms that are already dealing with the selection of valuable data. Today, these algorithms are increasingly written by machines and work mainly on pattern recognition to collect data that are considered worthy of being stored because of free-market rules. In the elaboration of the selection criteria for heritage science, it is essential to add ethics to pattern recognition if we want to avoid the risk of relying only on the authority of the free market whilst deciding on the usefulness of the treasure of human experiences (see the report *AI and the Ethical Conundrum. How organizations can build ethically robust AI system and gain trust* published by the Capgemini Research Institute in September 2020, which demonstrated that one-third of the leaders in charge of AI systems are not competent in understanding the potential biases of their own products. URL: https://www.capgemini.com/wp-content/uploads/2020/09/AI-and-the-Ethical-Conundrum-Infographic.pdf). In consideration of the fact that we can only assume what the next generation will need or appreciate in the future, transcultural and intergenerational empathy becomes an essential human value along with the functional and necessary preservation of the environmental characteristics compatible with human life on Earth. For the recent debate on "transculturalism" (an early twentieth-century cultural approach), refer to [16]. For the debate on the intergenerational discussion (in Lacan's psychoanalitic perspective), refer to [17]. For the environmental issues, refer to [18].

These motivations and considerations led the author of this paper to the establishment of the LIBER (Laboratory of Interdisciplinary Bookish and Experiential Research) under the aegis of Michelangelo Pistoletto's *Third Paradise* at the NTUS School of Art, Design and Media, in January 2019. In Latin, *liber* means both "book" and "free." *Liber*/book epitomises the treasure of human experiences as approached by the multidisciplinary domain of heritage science. *Liber*/free, as Maestro Pistoletto would say, epitomises the freedom to be responsible and uses all the arts and sciences to reconcile humanity with nature. The Nobel Laureate in Literature Odysseas Elyt is deeply felt this need of reconciliation for the sake of both humanity and individuals: "the lack of harmony between nature and man has led to the lack of harmony between soul and body . . . Since life cannot go back, it is men who have to go forward to try to catch it at least by the tail" (refer to [9]:33-34) the English translation is by Andrea Nanetti)." As Helga Nowotny discussed with Maestro Michelangelo Pistoletto and Nobel Laureate in Chemistry Ben Feringa at Nanyang Technological University Singapore on 22 January 2019 (Figure 3), our path forward may both be a Fourth Industrial Revolution along with increased inequality and poverty, driven by power and profit; or it may be a Third Paradise, which marks "the passage to a new level of planetary civilisation, essential to ensure the survival of the human race (refer to http://terzoparadiso.org/en/what-is accessed on 20 July 2020)," promoting or affording a balanced connection between humanity and nature [19].

The rationale of LIBER is that all the still-available experiences shared by human societies over time and across space are, in principle, essential in coping with the twenty-first century grand challenges of humanity [20]. We can agree with the philosopher and poet Giacomo Leopardi (1798–1837) that there is stagnation if society is incapable of redesigning its heritage for the future. Leopardi expresses a deep aversion to the present when it loses its connections with the past. He was indeed horrified by the present when it

is stripped of its connections with the past (refer to [21]). The vision is that, with a clearer understanding of where we came from, we can better understand who we are, where we are now, and what we want to become [22]. Today, heritage science can step up a new gear and provide a crucial contribution to implement this plan and empower human imagination and wisdom. This new heritage science should decode the knowledge and values that humanity embedded in tangible and intangible heritage, encode them in a digital knowledge aggregator (i.e., "knowledge engineering tool that allows its user to assemble information of different kinds from different sources, guided by what the user *wants to do* with the synthesized whole"), (refer to [23]:159) and make relevant information available to decision-making (where, when, and how it is needed), algorithmically (i.e., using computational procedures).

2. Discussing Old and New Human Ambitions

The starting point must be the human condition, which is the most vital and burning issue of all time [24]. In terms of algorithmic thinking, a preliminary ethic consideration needs to be highlighted before starting the computational engine and let AI affirm an automatic form of conduct through ML: humankind, humanity, societies, institutions, and the individual human beings that live in each present may have conflicting expectations and different motivations. Humankind identifies a living species that benefits from the privileges of Darwinian evolution. Humanity, viz., human beings collectively, embraces notions and conceptions not only related to humankind but also to the totality and each of the individual human beings living on Earth in the present. Modernity, with Johann Wolfgang Goethe, believed that exchanging information was an attribute of nature, whereas retaining given information belonged to human culture [25]. Today, this statement must be rephrased because we know that nature retains information in inheritable genes, whereas the human cultural endeavour is the use of information to imagine, design, and implement desired and shared futures wisely. In this social enterprise, research-intensive universities—where the research interests of faculty are shared with students—see an increasingly growing demand for internationalisation and interdisciplinarity (refer to [26]:55-57, and [27]). The vision is that internationalisation and interdisciplinarity processes can increase their sustainability and resilience with the inclusion of transculturalism, local knowledge, and heritage (refer to [22]:88).

At the foundation of this vision stays the fact that individual human beings are all different. As they look different outside, they are different inside. Their minds and consciousnesses show a great deal of variety. There is no normality. Heritage makes no exception. It is valued by each society differently. Unity can only be reached as an agreement to pursue shared projects for the future. Heritage science is all about the future. In this sense, the Renaissance concept of *virtus* (virtue, in Latin) is still applicable today to frame the discussion on a new science of heritage and empower the design of the future that we dream and desire as both a democratic society and individuals. The Italian Renaissance word *virtude* not only identifies a physical and mental value like the ancient Roman *virtus* but always implies the ability to determine the future, the ability to foresee problems, and to reorganise the present accordingly (refer to [28]:191). In this specific perspective, Niccolò Machiavelli's *Discorsi sopra la prima deca di Tito Livio* ("Discourses on Livy," ca 1517)—with the thought turned above all to young people and to those of the generations to come—addresses the fact that humans are unable to understand the history, and this is "the cause of the pettiness of modern times compared to the ancients (refer to [29]:182-183)." Today, machines are trained to take advantage of history, and they do it as they are instructed. But, how to decide what to teach to machines?

Individuals, institutions, and societies can agree on common goals that they want to achieve for the good of everybody (refer to [30]). For this huge but inevitable task, humans have developed education and laws to mitigate the exploitation of humans perpetrated by humans against other humans. They have the legacy of Mahatma Gandhi to use peaceful means, not violence, to bring about political or social change (refer to [31]:135-161). Therefore, with reference to the principles of right and wrong behaviour, scholars in research institutions and professionals in the industry are morally responsible for what they teach algorithms to do. In academia and the market, Research Integrity and Responsible Conduct policies (environment, experience, and ethos) are still unequal to the task of addressing questions such as "who decides what to teach to algorithms," "how the teaching process is performed" and "how the learning experience is monitored."

This algorithmic processes also need to take into consideration another basic distinction in order to be effective in the domain of heritage science. Knowledge and values perform differently in terms of how they passed on from one generation to the next. Epistemology—the theory of knowledge, especially regarding its methods, validity, and scope, and the distinction between justified belief and opinion—teaches us that data, information, knowledge, and, possibly, wisdom grow with humanity (refer to [23]: 163-164). They can be accumulated, put in latency, and transmitted from one generation to another both naturally, via genes, following the rules of evolution, and artificially through artefacts, education, and experience (refer to [32]). Still, values change across space and over time according to both axiology (i.e., the study of the nature of value and valuation and of the kinds of things that are of aesthetic, epistemic, moral, religious, and sentimental value) and economics (i.e., the appreciation and evaluation of what is worth to be produced, consumed, transferred, and considered wealth). For axiology, refer to [33]. For economics, refer to [34]. Thus, values need to be constantly shared (i.e., possessed in common with others) and continuously confirmed to operate cultural selections in the treasure of human experiences and design the future that we, individual humans and societies, dream and desire.

In practice, we can embrace Umberto Eco's concept of *Maximal Encyclopedia*, as expressed in the conclusions of his essay *From the Tree to the Labyrinth*. On the one hand, "if

cultures survive, one reason is that they have succeeded in reducing the weight of their encyclopaedic baggage by placing so many notions in abeyance, thus guaranteeing their members a sort of vaccination against the Vertigo of the Labyrinth." On the other hand, it "is not the fact that cultures *pare down* their encyclopaedias (which is, in any case, a physiological phenomenon), but rather that what has been placed in abeyance can always be recovered. For this reason, the regulatory idea of a *Maximal Encyclopaedia* is a powerful aid to the *Advancement of Learning*—and having to confront ever and anon the Vertigo of the Labyrinth is often the price we must pay for calling into question the laziest of our ontologies." This *Maximal Encyclopaedia* is the "truly virtual encyclopaedia" to which every encyclopaedia refers "through a series of cross-references." It is "the sum total of everything that was ever said, or at least of everything that could, in theory, be discovered, to the extent to which it has been expressed through a series of materially identifiable interpretants . . . a sort of World Wide Web far richer than the one to which we have access through the Internet (refer to [35]: quotations at pp. 93, 94, 88, and 94 respectively)." Eco's book was originally published as [36]. For a previous version of the same text, see also [37], Ch. 2 ("Dictionary vs. Encyclopedia"):46-86.

In 2016, after what Shawn Graham, Ian Milligan, and Scott Weingart called the "Digital Humanities Moment (refer to [38]: 37-72)," when historians started delving into data management and experimenting with various software to shed new light on their data sets, these authors seemed to find it more challenging to move forward to take full advantage of the fact that computation itself is *morphing*, as William Brian Arthur would say (refer to [39]:150-151). Indeed, machine learning algorithms, one of the computation's key technologies, underwent a radical change and has now opened new horizons to the automation and speed of pattern recognition as outlined by Pedro Domingos (Figure 4) (see [40]:1-22, Ch. 1. The Machine Learning Revolution). Graham et al. recognised this change as an opportunity for the third wave of computational history because entry barriers to powerful computing and big data have never been lower for historians [38].

As Carpo would say, "the first digital turn changed the way of making history, the second is changing the way of thinking [41]." This second change can initiate an interdisciplinary field of algorithmic research in which, as an example, Natural Language Processing (NLP) and Historical Methods are able to shift from mere automatic pattern recognition to the (semi)automatic mapping of meaningful information (i.e., associate semi-structured or unstructured elements of the historical domain with one or more elements of a second set of different entities of the same general type). According to Erik Cambria and Bebo White, to do so, NLP needs to evolve from its current "Syntactics Curve" (i.e., a stage that provides a "Bag-of-Words") to a new "Pragmatics Curve" (providing a "Bag-of-Narratives"), through an intermediate "Semantics Curve" ("Bag-of-Concepts") (refer to [42]:51, Figure 1); here,; Figure 3. This is the proposed pathway to steer a new consilient science capable of propelling a more mature field of both NLP and Digital Humanities into a new Science of Heritage via Computational History [12, 43] (in this field, a newopen-access publication by Andrea Nanetti on *History and Computers* is forthcoming).

In 2015, Domingos stated that "The engine that turns data into knowledge is no longer a black box: you know how the magic happens and what it can and cannot do [40]: 291." In this ambition, technology has both opportunities and limits. In 2009, William Brian Arthur published the results of his research on *The Nature of Technology* with the clear statement that "more than anything else technology creates our world. It creates our wealth, our economy, our very way of being." However, we still not have a clear understanding of how innovation works. There is no theory of change, and the established hegemony of a technoscientific culture is becoming a significant source of social uncertainty and instability that the human sciences need to address (refer to [44]:38-39). Technology does not work alone. Race, religion, and language are more and more sources of uncertainty. Often, India, China, and Africa are playing critical roles in the global arena. From the perspective of Kuhn's *Structure of Scientific Revolutions* [45], the global technoscientific civilisation is the newest paradigm shift. In an interview, held on the occasion of the International Congress, "At the dawn of eternity. The first 60 years of The original structure" (Brescia, 2-3 March 2018), the philosopher Emanuele Severino talked about what he defined as "the philosophical subsoil of our time" and its three great inhabitants: Friedrich Nietzsche, Giacomo Leopardi, and Giovanni Gentile (refer to http://www.raicultura.it).

In 1999, in the *Italian Alphabet*'s episode titled, "In search of poetry," Giuseppe Bertolucci stated that "poetry is . . . trying, in that, being able to overcome this state of horrible mechanization to restart (humanity) towards the spontaneity and authenticity of the human person." For Severino, "it will no longer be the capital that uses technology, it will no longer be democracy or Islam or Christianity or nationalisms or states to use the technology, but it will be the technology that uses them." In terms of the amelioration of the human condition, technology does not offer certainty for a better life. However, it appeals to individuals based on promises of a longer and healthier life, a more sustainable economy, a more stable society, a more available education, and so on. Technology asks for the faith that all of this will happen at some point in the future. Academic disciplines, such as the History of Science and Technology (HST) and Science Technology and Society (STS), are studying these topics as crucial factors for a sustainable future [46]. In this pathway, the need for a new science of heritage to treasure human experience becomes more apparent.

The human being can be at the centre of this pathway, a way of achieving what the Greek/Roman stoic concept had defined as *φιλαντρωπία*/humanitas (refer to [47]:173, and [48]:429-430) and can be translated in today's international English as "empathy." This concept is epitomised by Publius Terentius Afer as *Homo sum, humani nihil a me alienum puto/I am human, I consider nothing human to be alien to me* in his comedy *Heautontimorumenos* based on Menander's *Ἑαυτὸν τιμωρούμενος* (*The Self-Tormentor* refer to Publii Terentii Afri [ca 190-185-159 BCE], *Heautontimorumenos*, Act I, Scene 1, Line 25/77) and by Marcus Tullius Cicero's *studia humanitatis ac litterarum* in his oration in defence of

Figure 3: Michelangelo Pistoletto's Third Paradise. Art installation. Nanyang Technological University Singapore, School of Art, Design and Media. The plant used in the installation, *Alternanthera sessilis*' "Red," is not present in nature but grows only in greenhouses. We are the ones who keep this "artifice" alive, which is a way to experience the beauty of being free to choose the ethics of responsibility and commitment in life. This image was licensed under a Creative Commons Attribution-NonCommercial 4.0 International License (CC BY-NC 4.0) by Nanyang Technological University Singapore and Fondazione Pistoletto in 2019 [1].

the poet Archia (*Etenim omnes artes, quae ad humanitatem pertinent, habent quoddam commune vinclum et quasi cognatione quadam inter se continentur/In truth, all the arts which concern the civilising and humanising of men [better read: all the sciences which relate to the human nature and condition], have some link which binds them together, and are, as it were, connected by some relationship to one another*) (see Marci Tullii Ciceronis [106-43 BCE], *Pro Archia peoeta*, translated from Latin to English by C. D. Yonge, London: Henry G. Bohn, 1856; in particular, and the quotes, 2 and II.3, respectively).

In the diverse philosophical and political identities of the Renaissance cultural movement known as Humanism, the treaties on pedagogy have been often seen as the common ground for the education of the ideal member of civil society. This literary subgenre was introduced by Pier Paolo Vergerio's seminal work, *De ingenuis moribus et liberalibus studiis* ("on the Manners of a Gentleman and Liberal Studies") (see [49]). In [49], which was completed in Padua in 1402-1403 and soon followed by other humanists, the *studia humanitatis* or *studia humaniora* (the study of the *humanae litterae*, human studies, or the studies befitting a human being) ([50]:185), who is referring to [51]:365, were meant neither to train people for professional development nor to initiate youth to the contemplative life. Rather, the reading and discussion of human endeavours in grammar, rhetoric, poetry, history, and moral philosophy "aimed to shape the soul, to form the moral and aesthetic sense, to create citizens ready for the *vita activa* [active life] (see [52]:427);" "in the attempt to educate both princes and private citizens to serve the needs of the state. . . a preparation for a life of virtue (see [50]: 28)."

The values of this *paideia*/*παιδεία* (education) were of the essence in the culture of Renaissance. In English, see [53, 54]). However, in these two books, it is difficult to see any consistent advancement of learning when compared to [55], who provided a still-unrivalled contribution to the appreciation of the fundamental reasons of radical human renewal that ensured the successful spread of humanistic culture in Europe (see [56]:482–490). In particular, we can refer to the three qualities of *utilitas*/usefulness, namely, *honor*/honour (i.e., the quality of doing what is morally right), *decus*/distinction (i.e., the quality of being excellent), and *commodum*/convenience (i.e., the quality of being suitable to serve the needs of the society), as they were elaborated by both the Church and the humanistic culture of the time (refer to [57–59]). Today, in the aftermath of the WASP-Gentlemen's evident inadequacy to overcome its intrinsic nature, *φιλαντρωπία*/humanitas/empathy seems to be the key to understand the other and can serve contemporary globalised youth to connect as human beings beyond race, religion, and culture.

In Europe, an example of this philosophical and practical understanding of empathy, as *social catena* (human chain), the ultimate human quality and hope, can be found in Giacomo Leopardi's poem, *Broom* (*La Ginestra*, v. 149) composed at Villa Ferrighi (Torre del Greco) in 1836 (see [60]:286-309). The poem was first published by A. Ranieri (refer to [61]:119-127). This thought results from a vast philosophical erudition that ranges between eras and disciplines through ancient and modern languages, encompassing the heritage that was available in Europe at his time. After taking stock of what science had discovered on the materialist structure of reality, he asserted the groundlessness of human values and the total indifference of nature towards the destiny of mankind. Leopardi indeed anticipated Nietzsche in overturning the religious and humanistic values of the Christian order of the world and setting the human condition in a new framework (refer to [21]).

Franz Kafka, in a letter to Oskar Pollak dated 9 November 1903, expressed similar hopes and needs when he

wrote: "... Verlassen sind wir doch wie verirrte Kinder im Walde. Wenn Du vor mir stehst und mich ansiehst, was weißt Du von den Schmerzen, die in mir sind und was weiß ich von den Deinen. Und wenn ich mich vor Dir niederwerfen würde und weinen und erzählen, was wüßtest Du von mir mehr als von der Hölle, wenn Dir jemand erzählt, sie ist heiß und fürchterlich. Schon darum sollten wir Menschen vor einander so ehrfürchtig, so nachdenklich, so liebend stehen wie vor dem Eingang zur Hölle (we are abandoned like lost children in the forest. When you stand in front of me and look at me, what do you know about the pains that are in me and what do I know about yours. And if I prostrate myself in front of you and cry and tell you, what would you know more about me than about hell, if someone told you that it was hot and terrible. For that reason alone, we humans should stand before one another so reverently, so thoughtfully, as lovingly as in front of the entrance to hell) (see [62])."

Within this cultural context, heritage science can have the vision to the following:

(1) Develop transcultural advancement of understanding the human condition with a "glocal" approach (i.e., for global futures with local heritage). The neologism glocal was apparently coined by Manfred Lange who, in his work for the May 1990 Global Change Exhibition, sought to capture the complex interplay between the local, the regional, and the world-wide" as reported in [63]: 80.

(2) Nurture global citizenship as κοσμοπ ολιτεία/cosmopolitanism—according to Diogenes Läertius' [180-240 CE] *Vitae Philosophorum* (Βίοι καὶ γνῶμαι τῶν ἐν φιλοσοφίᾳ εὐδοκιμησάντων/Lives and Opinions of Eminent Philosophers), when the pre-Socratic philosopher Diogenes of Sinope (or Diogenes the Cynic [circa 412-323 BCE]) was asked where he came from, "he answered: 'I am a citizen of the cosmos' [κοσμοπολίτης/kosmopolitês (cosmopolite or cosmopolitan)]" (VI, 63). This can be done in the real world, which is *l'aiuola che ci fa tanto feroci* (Dante Alighieri, *Paradiso*, XXII, 151: *The little threshing-floor which makes us so fierce*) [64], with the ethics of "freedom as a generator of responsibility" (refer to [65]: 64-73). For the evolution of the relationship between freedom and responsibility from World War II to today, see [25].

(3) Eventually, educate the next generation of human scientists and decision-makers who are called upon to take up the grand challenges of humanity in the 21st century [66], for life on planet Earth, and for what may lie beyond [67]. See, among others, the 17 Sustainable Development Goals that the United Nations are targeting to be achieved by 2030 (https://www.un.org/sustainabledevelopment/sustainable-development-goals), the BBC list published by Bryan Lufkin on http://www.bbc.com/future/story/20170331-50-grand-challenges-for-the-21st-century (accessed on 13 February 2021).

In nurturing this vision for a new science of heritage, the inspiration comes from *Ars Generalis Ultima* (The Ultimate General Art), aka *Ars Magna* (The Great Art), by Ramon Llull (1232–1316), who introduced the encyclopaedic ideal, the use of mathematics, and visual mnemotechnics to pioneer what is now called the theory of computation (refer to [68]). A powerful thinking tool can be found in the Seven Circumstances ("Who, What, Where, When, Why, How, and By What Means") used by Aristotle to examine human actions (refer to Aristotle, *Nicomachean Ethics*, 1111a3-8), more recently propagated by Rudyard Kipling (surprisingly without "by what means" and as such used in the curricula of the US schools of journalism). This method was also applied by Giambattista Vico, who, at the dawn of Enlightenment, in his *magnum opus*, the *Scienza Nuova* (1725, New Science [69]), argued that a new grammar was needed to select and define the essential components (facts) and to validate these facts based on evidence by answering the questions "Who," "What," "Where," and "When." With this grammar, scholars can "come to terms" to structure a new language. Afterwards, logic can be applied to process data. Facts can be better understood and related to each other after removing contradictions, that is, after answering the question, "Why" (e.g., in a cause-and-effect relationship). To complete this "trivium metaphor," (McLuhan's *Global Village* can be seen as an epigone of this tradition; refer to [70]) the rhetoric to be put in place to produce wisdom needs to answer the questions, "How" and "By What Means," based on evidence (i.e., taking into consideration only facts validated in the grammar with a full demonstration of "Who," "What," "Where," and "When"). Furthermore, this trivium teaches us that working on relationships without having verified its agents is like putting logic before grammar. It can easily result in conclusions without foundations. Sometimes, this procedure is used to intentionally manipulate facts and produce misinformation.

3. Exploring a New Methodology for a New Science of Heritage

After having discussed why, what, who, where, when, and how, let us discuss the systematic means, the methods that can be used by this new science of heritage. To feed AI and machine learning in facilitating human thinking and finding solutions to complex problems, Andrea Nanetti, at the LIBER Lab, in the NTU School of Art, Design and Media, proposes to students and faculty a tetrahedron of research methodologies (artistic, design, and academic) grounded in art, culture, and heritage (see Figure 5). Here, this openness to multidisciplinary approaches to knowledge is seen as a first step, not only towards the implementation of holistic methodologies in general but also for designing and writing algorithms that can be interdisciplinary (i.e., the synthesis of two or more disciplines, establishing a new level of discourse and integration of knowledge). According to Julie Thompson Klein, interdisciplinary initiatives are characterised by the form or structure they take (e.g., team work), their motivation (e.g., to serve societal needs), how the disciplines interrelate (e.g., physics can be taught in the service of history), or by their integration level (e.g., from cross-reference to oneness).

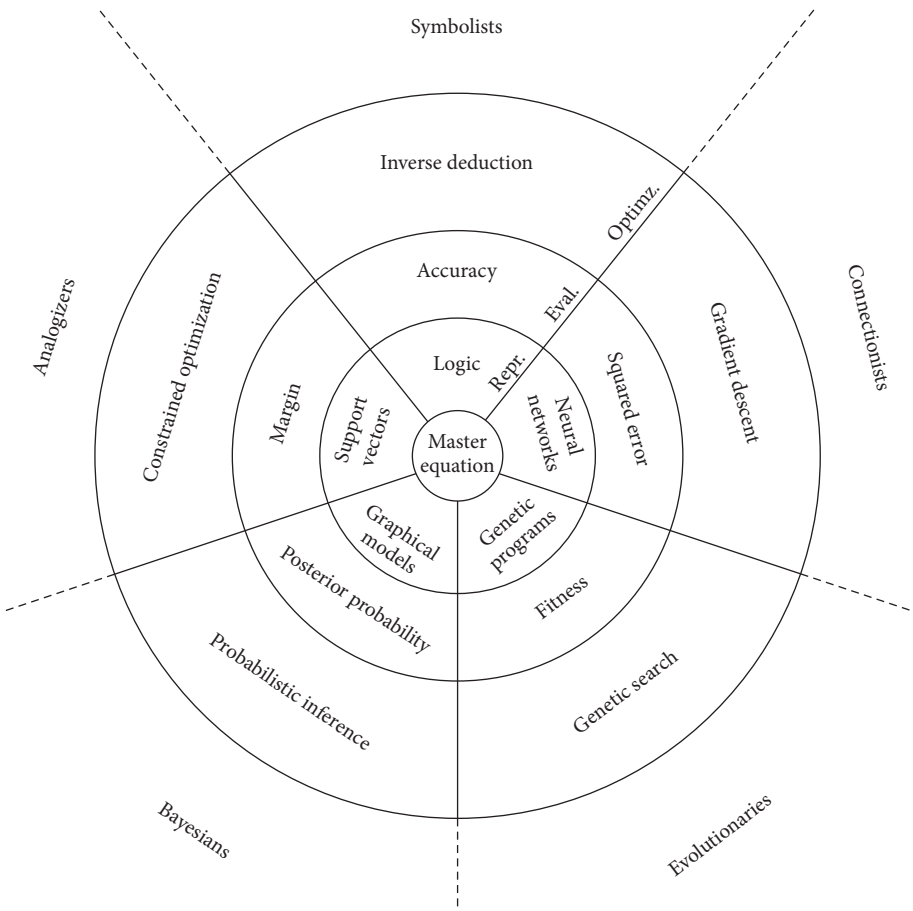

Figure 4: Pedro Domingos' diagram (p. 240) of the "five tribes of machine learning and their master algorithms: symbolists and inverse deduction; connectionists and backpropagation; evolutionaries (read evolutionists) and genetic algorithms; Bayesians and probabilistic inference; and analogizers (read analogists) and support vector machines" (p. 291).

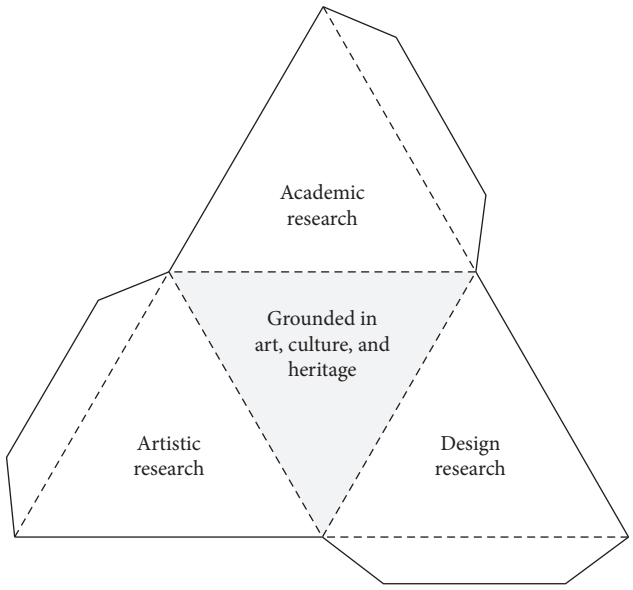

Figure 5: Cut-and-tape tetrahedron of research approaches (artistic, design, and academic) grounded in art, culture, and heritage to raise questions and prescribe transdisciplinary solutions to complex problems. This work was licensed under a Creative Commons Attribution-NonCommercial 4.0 International License (CC BY-NC 4.0) by Andrea Nanetti in 2017.

Hannah Arendt (1906-1975), portrait (1941) by photographer Fred Stein. Digital Image from WorldHistoria.

Power: the capacity or ability to direct or influence the behaviour of others or the course of events

Violence: the unlawful exercise of physical force or intimidation by the exhibition of such force

Strength: the influence or power possessed by a person, organization, or country

© Oxford Dictionary of English

Figure 6: "Hannah Arendt is preeminently the theorist of beginnings. All her books are the tales of the unexpected . . ., and reflections on the human capacity to start something new pervade her thinking. . . Often the way she sheds light into neglected corners of experience is by making new distinctions, many of them threefold as if conventional dichotomies were too constricting for her intellectual imagination. *The Human Condition* [first edition 1958] is crammed with distinctions: between labor, work, and action; between power, violence, and strength; between the Earth and the world" (see [24]).

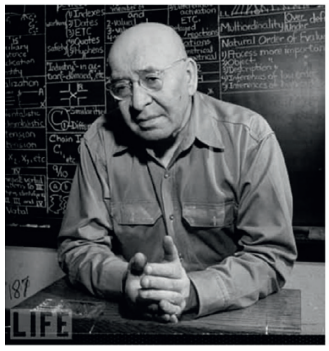

Alfred Habdank Skarbek Korzybski (1879-1950), independent scholar, in ca. 1949. Photographic portrait by unknown. © Life Magazine. Image from: http://i.kinja-img.com/gawker-media/image/upload/bvgbeuraxhursmmvmnsj.jpg

Rejection of the principle of identity and the recognition of so-called "multiordinal terms." The principle of identity is structurally impossible, and orientation based on it is "delusional" and "cannot lead to adjustment and sanity." "The mechanism of identification" should be "eliminated by special training" which is "therapeutic in effect." The author proposes a simple structural diagram, "structural differential," with which "the general verbal rejection of 'identity' is translated into ordering, which becomes a visual, kinesthetic, neuro–psychological method to train in non-identity or discrimination, and so to eliminate the always dangerous identifications, which play such an important part in all maladjustments."

Refer to https://psycnet.apa.org/record/1934-01910-000

Figure 7: Visual, kinaesthetic, neuropsychological method. Introduced by Alfred Korzybski to train in nonidentity. In his book entitled "Science and sanity. An Introduction to Non-Aristotelian Systems and General Semantics" [71], Korzybski states and demonstrates that Aristotelian systems are inadequate to face the challenges of our society. Socrates (469-399 BCE), his student Plato (427-347 BCE), and Plato's student Aristotle (384-322 BCE) formulated the complete system of knowledge and education of their time, which was perpetrated until today. Aristotle "aimed to formulate a general method for "all" scientific work." He was so comprehensive that, so far, it has been changed only field by field. Korzybski uses the history of mathematics to highlight how non-Aristotelian methods were needed and developed for the advancement of learning in this specific field (Introduction to the second edition, 1941, pp. xlix-l). However, "no methodological general theory based on the new developments of life and science had been formulated until general semantics and a general, extensional, teachable, and communicable, non-Aristotelian system was produced. The main difficulties ahead are neurosemantic and neurolinguistic because for more than 2,000 years, our nervous systems have been canalized in the inadequate, Aristotelian orientations, which are reflected even in the structure of the language we habitually us" (ibidem, pp. xlix-l).

This contrasts with multidisciplinary, which is a process for providing a juxtaposition of disciplines that is additive, not integrative. Transdisciplinary approaches provide holistic schemes that subordinate disciplines, looking at the dynamics of whole systems, such as structuralism or Marxism. Cross-disciplinary methods refer to examples from one discipline that can be used in others. For these distinctions, refer to [26]: 55. The rationale is that different academic disciplines have different assumptions and understandings of the same things, and all these different approaches need to be taught to machines in the perspective of a new science of heritage. As an example, we can highlight the ways of recording space-time in physics and history or the different understanding of words, such as data, information, facts, evidence, event, in history, and computing (Figure 2).

The proposal is to support the axiomatic formalisation of heritage as a new science able to build semantic taxonomies and train ML algorithms through the application of four key methods: (1) the triplets (threefold distinctions) applied by Hannah Arendt to start thinking about the human condition (Figure 6); (2) the visual, kinaesthetic, neuropsychological method introduced by Alfred Korzybski to train in nonidentity (Figure 7); (3) the D.A.N.C.I.N.G. method (Definition, Assumption, Notion, Conception, Interpretation, Narrative, Gamut) to understand complex words (Figure 8); and, last but not least,

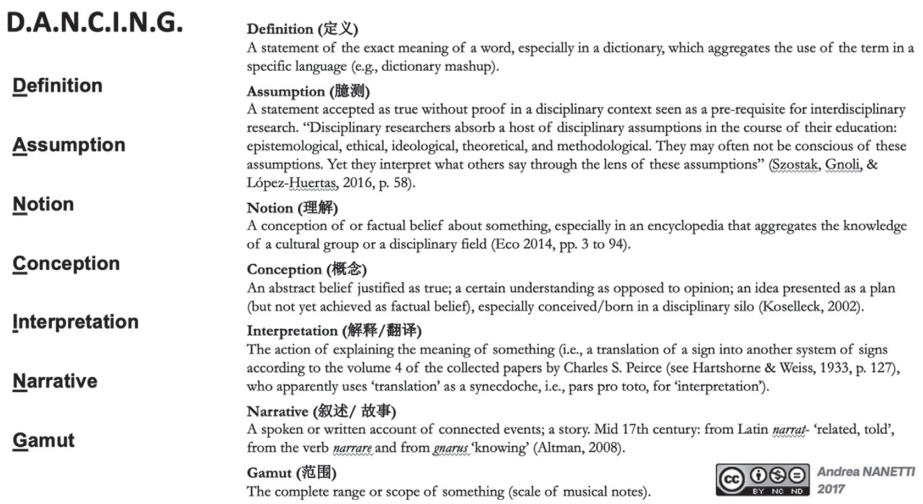

Figure 8: The D.A.N.C.I.N.G. method is a systematic procedure for the understanding of words that connote the complexity of human things, human nature, and the human condition (e.g., beauty, knowledge, science, art, technology, truth, justice, and love). The dancing method was created by Andrea Nanetti for the digital advancement of learning in 2017. Since then, this method has been successfully introduced by Nanetti in research and teaching at Nanyang Technological University, Singapore, and in master classes and keynotes, internationally, to provide a quick and robust multidisciplinary understanding of complex words whilst starting a new enquiry or simply addressing a topic to an audience. This method has been proved to be handy to guide humans and can be transferred to algorithms in the accomplishment of the whole gamut of different ways of seeing fundamental words. The Dancing Method was licensed under a Creative Commons Attribution-NonCommercial 4.0 International License (CC BY-NC 4.0) by Andrea Nanetti in 2017 [72–74].

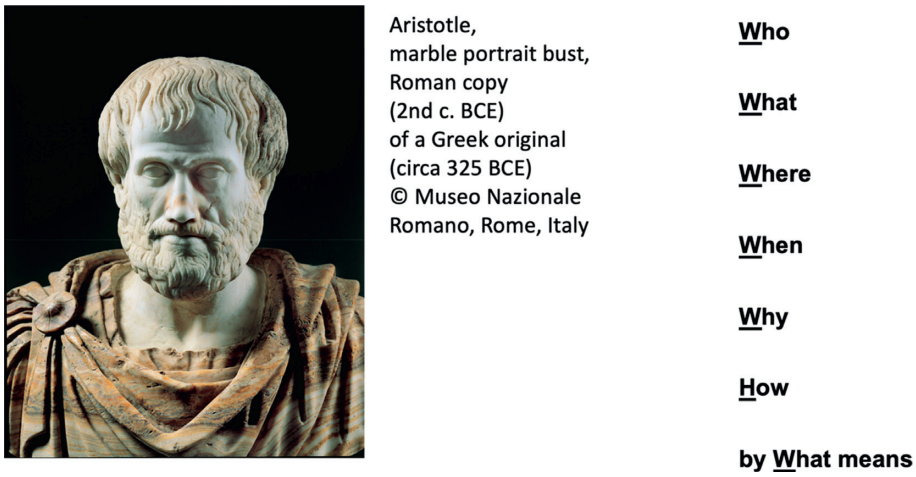

Figure 9: The seven circumstances are relevant to examine human actions. The earliest evidence of the use of this ur-method is in Aristotle, Nicomachean Ethics, 1111a, 3–8.

(4) the seven circumstances used by Aristotle to examine human actions (who, what, where, when, by what means, why, and how) (Figure 9).

4. Conclusions

In conclusion, the mission for heritage science should be to answer the question: what kind of heritage should our society take care of and by what means can it be safeguarded and transmitted? In addition, how could we leverage the increasing prevalence of technological developments to highlight and explain cultural and societal changes and illustrate potential future scenarios and *visionaries*, transmitting accumulated knowledge and discussing values (i.e., what is important in life) that we want to share? These are the key questions that need to be answered. The foundation of a new formal science of heritage needs the consolidation of a grammar that can be used worldwide and understood in different cultural contexts. This science could then showcase success stories, where cultural heritage has been convincingly employed to revitalise a community beset by natural or man-made disasters. It could also teach society to learn from stories of its failures, where communities endowed with rich cultural heritage should have been capable of coping with crises but made a series of poor decisions that lead to significant loses in their identities, cohesiveness, and heritage (Figure 1).

Data Availability

The data used to support the finding of the study are included within the article.

Conflicts of Interest

The author declares that there are no conflicts of interest.

Acknowledgments

This article, which is both a position and a review paper, has been written in the campus of Nanyang Technological University, Singapore, during the COVID-19 circuit-breaker, after office hours, in 2020. The thoughts and ideas presented in this work were defined and discussed earlier: firstly, with several colleagues, on different occasions, during the Forum "Next Generation, Please!" organised in the framework of the UNESCO Creative Cities Network by *Cittadellarte-Fondazione Pistoletto* (Italy, Biella, 23 May 2019); secondly, when I was a visiting Scholar at *Università di Venezia Ca' Foscari* (from 15 June to 15 August 2019); and, thirdly, on the occasion of a lecture on *Big Data and the Advancement of Learning. For a Sustainable and Open Knowledge Society*, which I gave for Department of Network and Data Science and Provost's Office at Central European University on 5 March 2020, which was my last overseas travel before the confining to my dwelling because of the spread of COVID-19. To all these institutions and their people goes my deepest gratitude for their generosity and the spirit of academic freedom that ultimately inspired this work.

References

[1] M. Pistoletto, "The third paradise," 2020, http://terzoparadiso.org/en/what-is.

[2] G. Bast, ""DANCING over ideas of research": Eine zukunftsorientierte kooperation mit Singapur im kunst- und bildungsbereich," in *Austria Kultur International Jahrbuch der Österreichischen Auslandskultur*, pp. 65–67, Bundesministerium für Europa, Integration und Äußeres – Sektion für Kulturelle Auslandsbeziehungen, Vienna, Austria, 2018.

[3] R. Comunian, A. Rickmers, and A. Nanetti, "The creative economy is dead—long live creative-social economies," *Social Enterprise Journal*, vol. 16, 2020.

[4] C. P. Snow, *The Two Cultures and the Scientific Revolution: The Rede Lecture 1959*, Cambridge University Press, Cambridge, UK, 1962.

[5] E. O. Wilson, *Sociobiology: The New Synthesis—25th Anniversary*, Harvard College, Cambridge, MA, USA, 2000.

[6] E. O. Wilson, *Biological Diversity: The Oldest Human Heritage*, University of the State of New York, State Education Dept., New York State Museum, Albany, NY, USA, 1999.

[7] E. O. Wilson, *Consilience the Unity of Knowledge*, Westminster: Knopf Doubleday Publishing Group, 1st edition, 2014.

[8] E. G. Slingerland and M. Collard, *Creating Consilience: Integrating the Sciences and the Humanities*, Oxford University Press, Oxford, UK, 2012.

[9] O. Elytis (Offering) My Cards To Sight [*Ανοιχτά χαρτιά (συλλογή κειμένων)*], Athens: Asterias Editions, 1973..

[10] B. Pascal, *Les Pensées*, E. P. Dutton & Co., Inc., New York, NY, USA, 1958, https://ebooks.adelaide.edu.au/p/pascal/blaise/p27pe/complete.html, 2nd edition.

[11] G. Leopardi, "L'infinito," *Il Nuovo Ricoglitore*, Ossia Inc., Bellevue, WA, USA, 1825.

[12] A. Nanetti and S. A. Cheong, "Computational history: from big data to big simulations," in *Big Data in Computational Social Science and Humanities*, S.-H. Chen, Ed., pp. 337–363, Springer International Publishing AG, Cham, Switzerland, 2018.

[13] B. Kahane, "La dimension identitaire de l'information à l'ère des algorithmes et de l'intelligence artificielle," in *La Transmission en Question(s)*, pp. 633–656, Éditions in PRESS, Paris, France, 2020.

[14] T. Moreau, "Héritage, transfert, mémoire. Ce qui se reçoit, s'élabore, se transmet—avec qui?" in *La Transmission en Question(s)*, pp. 361–370, Éditions in Press, Paris, France, 2020.

[15] S. Rendgen and J. Wiedemann, *Information Graphics*, Tashen, Cologne, Germany, 2013.

[16] M. Herren, M. Rüesch, and C. Sibille, *Transcultural History: Theories, Methods, Sources*, Springer-Verlag, Berlin, Germany, 2012.

[17] M. Recalcati, *Il Complesso di Telemaco. Genitori e Figli dopo il Tramonto del Padre*, Feltrinelli Editore, Milano, Italy, 2013.

[18] https://www.unenvironment.org United Nations Environment Programme.

[19] A. Nanetti, *The Third Paradise at NTU Singapore in Michelangelo Pistoletto, Between Obverse and Reverse, [Catalogue of the Exhibition, Partners and Mucciaccia, Singapore, 19 Jan–27 July 2019]*, Carlo Cambi Editore, pp. 70–74, Rome, Italy, 2019.

[20] A. Nanetti, "Expanding the thinkable future beyond inherited pasts and visible presents," in *Proceedings of the 2019 Gingko Meeting*, Vienna, Austria, 2019.

[21] R. P. Harrison, "La magia di leopardi," 2014, https://www.451online.it/la-magia-di-leopardi/.

[22] A. Nanetti and A. Simpson, "Sharing our heritage to shape our future. How effective are multi-user sharing platforms in supporting collaborative visioning for the future, and why is heritage centre-stage?" in *Proceedings of the 5th International Conference on Social Media Technologies, Communication, and Informatics*, pp. 82–90, Wilmington, DE: IARIA XPS Press, Barcelona, Spain, November 2015.

[23] N. Andrea, A. Cattaneo, S. Ann Cheong, and C.-Y. Lin, "Maps as knowledge aggregators : from renaissance Italy Fra Mauro to web search engines," *The Cartographic Journal*, pp. 159–167, 2015.

[24] H. Arendt, *The Human Condition*, The University of Chicago Press, Chicago, IL, USA, 2nd edition, 1958.

[25] A. Gailus, "Forms of life: nature, culture, and art in Goethe's Wilhelm Meister's apprenticeship," *The Germanic Review: Literature, Culture, Theory*, vol. 87, no. 2, pp. 138–174, 2012.

[26] J. T. Klein, *Interdisciplinarity: History, Theory and Practice*, Wayne State University Press, Detroit, MI, USA, 1990.

[27] Deborah DeZure, What is Interdisciplinary Learning? on http://departments.knox.edu/facdev/archives/POD_packets/Packet1/Interdisciplinary%20Teach%23EC3.htm, 2020.

[28] N. Gardini, *Rinascere. Storie e Maestri di un'Idea Italiana*, Garzanti, Milano, Italy, 2019.

[29] M. Viroli, *Il Sorriso di Niccolò. Storia di Machiavelli*, Editori Laterza, Bari, Italy, 1998.

[30] M. Ignatieff, *The Ordinary Virtues: Moral Order in a Divided World*, Harvard University Press, Cambridge, MA, USA, 2017.
[31] G. Pontara, *L'Antibarbarie. La Concezione Etico-Politica di Gandhi e il XXI Secolo*, Edizioni Gruppo Abele, Torino, Italy, 2nd edition, 2019.
[32] S. Sim and B. Seet, Eds., *The Chronicles of Evolution*, Wildtype Books, Singapore, 2018.
[33] S. L. Hart, "Axiology—theory of values," *Philosophy and Phenomenological Research*, vol. 32, no. 1, pp. 29–41, 1971.
[34] J. Reardon, M. A. C. Madi, and M. Scott Cato, "Economic value," in *Introducing a New Economics: Pluralist, Sustainable and Progressive*, pp. 153–166, Pluto Press, London, UK, 2018.
[35] U. Eco, *From the Tree to the Labyrinth. Historical Studies on the Sign and Interpretation*, Harvard University Press, Cambridge, MA, USA, 2014.
[36] U. Eco, *Dall'Albero al Labirinto. Studi Storici sul Segno e l'Interpretazione*, Bompiani, Milano, Italy, 2007.
[37] U. Eco, *Semiotics and the Philosophy of Language*, Indiana University Press, Bloomimgton, IN, USA, 1983.
[38] S. Graham, I. Milligan, and W. Scott, Eds., *The Historian's Macroscope*, Imperial College Press, London, UK, 2016.
[39] W. B. Arthur, *The Nature of Technology. What it is and How it Evolves*, Free Press, New York, NY, USA, 2009.
[40] P. Domingos, *The Master Algorithm: How the Quest for the Ultimate Learning Machine Will Remake Our World*, Basic Books, New York, NY, USA, 2015.
[41] M. Carpo, *The Second Digital Turn: Design beyond Intelligence*, MIT Press, Cambridge, MA, USA, 2017.
[42] E. Cambria and B. White, "Jumping NLP curves: a review of natural language processing research," *IEEE Computational Intelligence Magazine*, vol. 9, no. 2, pp. 48–57, 2014.
[43] A. Nanetti, "Overcoming linguistic obstacles and cultural barriers in the transcultural (re)-reading of primary sources and secondary literature for afro-Eurasian pre-modern history (1205–1533)," in *Order/Disorder in Asia: Historical Perspectives*, R. Mukherjee, Ed., The Asiatic Society, Kolkata, India, 2021.
[44] L. Tomasin, *L'Impronta Digitale. Cultura Umanistica e Tecnologia*, Carocci Editore, Rome, Italy, 2017.
[45] T. S. Kuhn, *The Structure of Scientific Revolutions*, University of Chicago Press, Chicago, IL, USA, 4th edition, 2012.
[46] W. E. Bijker, T. P. Hughes, T. J. Pinch, and D. G. Douglas, *The Social Construction of Technological Systems: New Directions in the Sociology and History of Technology*, MIT Press, Cambridge, MA, USA, 2012.
[47] C. Higgins, "Humanism, cosmopolitanism, and the ethics of translation," *Educational Theory*, vol. 64, no. 5, pp. 429–437, 2014.
[48] J. E. G. Zetzel, "Cicero and the scipionic circle," *Harvard Studies in Classical Philology*, vol. 76, pp. 173–179, 1972.
[49] D. Robey, "Humanism and education in the early quattrocento: the de ingenuis moribus of P. P. Vergerio [1370–1444]," *Bibliothèque d'Humanisme et Renaissance*, vol. 42, pp. 27–58, 1980.
[50] B. G. Kohl, "The changing concept of the studia humanitatis in the early renaissance," *Renaissance Studies*, vol. 6, no. 2, pp. 185–209, 1992.
[51] P. O. Kristeller, "Humanism and scholasticism in the Italian renaissance," *Byzantion*, vol. 17, pp. 346–374, 1944.
[52] S. Ferente, "La civiltà dei maestri," in *Atlante Della Letteratura Italiana*, vol. 1, pp. 427–432, Einaudi, Torino, Italy, 2010.
[53] R. Black, *Humanism and Education in Medieval and Renaissance Italy. Tradition and Innovation in Latin Schools from the Twelfth to the Fifteenth Century*, Cambridge University Press, Cambridge, UK, 2001.
[54] P. F. Grendler, *Schooling in Renaissance Italy: Literacy and Learning, 1300–1600*, The Johns Hopkins University Press, Baltimore, MD, USA, 1989.
[55] E. Garin, *Il Pensiero Pedagogico dell'Umanesimo*, Coedizioni Giuntine Sansoni, Florence, Italy, 1958.
[56] S. Zanardi, "La pedagogia dell'Umanesimo nell'interpretazione di Eugenio Garin," in *Dimensioni dell'Educare e il Gusto della Scoperta nella Ricerca. Studi in Memoria di Duilio Gasparini*, pp. 482–490, Armando Editore, Rome, Italy, 2011.
[57] C. Frova, "Processi formativi istituzionalizzati nelle società comunali e signorili italiane: una politica scolastica?" in *Culture et Idéologie dans la Génèse de l'État Moderne*, pp. 117–131, École Française de Rome, Rome, Italy, 1985.
[58] S. Marcucci, *La Scuola tra XIII e XV Secolo. Figure Esemplari di Maestri*, Istituti Editoriali e Poligrafici Internazionali, Pisa, Italy, 2002.
[59] P. Rosso, "La scuola nelle corti tardomedievali dell'Italia nord-occidentale: circolazione di maestri e di modelli," *Mélanges de l'École Française de Rome—Moyen Âge*, vol. 127, 2015.
[60] G. Leopardi, *Canti, Poems Bilingual Edition Translated and Annotated by Jonathan Galassi*, Farrar, Straus, and Giroux, New York, NY, USA, 2010.
[61] A. Ranieri, Ed., *Opere di Giacomo Leopardi*, Felice Le Monnier, Florence, Italy, 1845.
[62] F. Kafka, *Briefe 1902–1924*, S. Fischer, Frankfurt, Germany, 1958.
[63] J. Schnapp, "Animating the archive," in *Animated Archive*, pp. 72–80, Electa, Milano, Italy, 2013.
[64] The English translation is by Courtney Langdon, Cambridge: Harvard University Press, 1921.
[65] M. Pistoletto, *The Third Paradise*, Marsilio Editori, Venice, Italy, 2010.
[66] J. W. Vasbinder, B. Gulyás, and J. Y. H. Sim, *Grand Challenges for Science in the 21st Century*, World Scientific, Singapore, 2018.
[67] C. J. Preston, "The synthetic age," *Outstanding Evolution, Resurrecting Species, and Reengineering Our World*, The MIT Press, Cambridge, MA, USA, 2018.
[68] A. Bonner, *The Art and Logic of Ramon Llull. A User's Guide*, Brill Academic Publishers, Leiden, Netherlands, 2008.
[69] L. Pompa, *[Giambattista Vico] the First New Science*, Cambridge University Press, Cambridge, UK, 2002.
[70] M. McLuhan, *The Gutenberg Galaxy: The Making of Typographic Man*, Routledge and Kegan Paul, London, UK, 1962.
[71] A. Korzybski, *Science and Sanity. An Introduction to Non-Aristotelian Systems and General Semantics*, International Non-Aristotelian Library Pub. Co., New York, NY, USA, 5th edition, 1994.
[72] R. Altman, *A Theory of Narrative*, Columbia University Press, New York, NY, USA, 2008.
[73] C. Hartshorne and P. Weiss, Eds., *The Collected Papers of Charles Sanders Peirce*, Harvard University Press, Vol. 4, Cambridge, MA, USA, 1933.
[74] R. Szostak, C. Gnoli, and M. López-Huertas, *Interdisciplinary Knowledge Organisation*, Springer, Berlin, Germany, 2016.

Hindawi
Complexity
Volume 2020, Article ID 8015979, 15 pages
https://doi.org/10.1155/2020/8015979

Research Article

Coordinating Manipulation in Real-time Interactive Mechanism of College Admission: Agent-Based Simulations

Lan Hou,[1] Tao Jia,[1] Xiangbing Wang,[2] and Tongkui Yu[1]

[1]*College of Computer and Information Science, Southwest University, Beibei, Chongqing 400715, China*
[2]*School of Economics and Management, Guizhou University of Engineering Science, Bijie, Guizhou 551700, China*

Correspondence should be addressed to Tongkui Yu; ytkui@swu.edu.cn

Received 28 March 2020; Revised 5 September 2020; Accepted 19 September 2020; Published 6 October 2020

Academic Editor: Dehua Shen

The matching in college admission is a typical example of applying algorithms in cyberspace to improve the efficiency of the corresponding process in physical space. This paper studies the real-time interactive mechanism (RIM) recently adopted in Inner Mongolia of China, where students can immediately observe the provisional admission results for their applications and are allowed to modify the application before the deadline. Since the universities accept the applications according to the ranking of the scores, RIM is believed to make the competition more transparent. However, students may coordinate to manipulate this mechanism. A high-score student can perform a last-minute change on the university applied, opening a slot for a student with a much lower score. With agent-based simulations, we find that a large portion of students will choose to perform coordinating manipulation, which erodes the welfare and fairness of society. To cope with this issue, we investigate the Multistage RIM (MS-RIM), where students with different ranges of scores are given different deadlines for application modification. We find that the multistage policy reduces the chance of manipulation. However, the incentive to conduct manipulation is increased by a higher success rate of manipulation. Hence, the overall social welfare and fairness are further diminished under MS-RIM with a small number of stages, but are improved if the stage number is large.

1. Introduction

With the development of information and communication technology, the college admission process in the physical space has been transferred to the online information system. Many algorithms, such as deferred acceptance mechanism [1, 2], parallel choice mechanism [3, 4], and real-time interactive mechanism [3, 5], have been designed to reengineer the information process efficiently. The results from the cyberspace are then used to improve the welfare and fairness in the college-student matching of the real world [3–6].

The *sequential choice mechanism* (SCM) has been used in college admission of China for decades [7]. In this mechanism, each student submits a shortlist of preferred universities. A university will admit students who have listed it as the first choice in the first place. If the university has available quotas after the first round of admission, it will then consider applicants who list it as their second choice and so on. This mechanism is similar to the immediate acceptance mechanism, or Boston mechanism [8, 9]. In an age of underdeveloped communication technology, this algorithm was widely used due to its simplicity. However, the sequential mechanism has severe limitations: it is not strategy-proof [2, 8] and vulnerable to manipulation [10, 11]. Students need to choose their first choice carefully. Because once a student is rejected by her first-choice university, she will likely be rejected by her second-choice, as the quota of the university may have already been used up. Therefore, students with more information could choose candidate universities more wisely than others. Empirical evidence also shows that a large portion of high-score students failed to be admitted to any colleges only due to inappropriate choices [7].

To fix this problem, *a parallel choice mechanism* (PCM) has been gradually adopted by most provinces in China since 2008. In this mechanism, students can select several

"parallel" universities within each choice band. The automated admission information system processes the applications of students from the highest score to the lowest score. Hence, a student will be admitted into the first university in his list which has an unfilled quota. Under this mechanism, all the choices of a high-score student will be considered "parallelly" before moving on to the next student, which greatly increases the chance to be admitted. Empirical evidence also shows that the implementation of the parallel choice algorithm greatly alleviates the problem of students with high test scores not being admitted to any college [4]. Experimental evidence shows that the performance of the parallel choice mechanism is better than the immediate acceptance mechanism [12]. The parallel choice mechanism resembles the deferred acceptance mechanism [2], which is first proposed by Gale and Shapley [1] and widely adopted in two-sided matching [13, 14]. Deferred acceptance mechanism is proved to have some nice properties such as strategy-proof, stability, and elimination of justified envy [2, 13, 14]. The deferred acceptance mechanism asks the students to submit a full preference list of all the colleges. However, in common practice, students are only allowed to submit a list containing a limited number (e.g., 6 in the parallel choice mechanism in some provinces of China) of colleges. Imposing a constrain on the length of the preference lists compels students to adopt a strategic behavior when choosing which ordered list to submit [15] and hinders stable matching [16]. Experimental evidence shows that the students' incentives are drastically affected and more individuals manipulate their preferences under the constrained choice [17]. Chen and Kesten evaluated the sequential, parallel, and deferred acceptance mechanisms by the laboratory experiments. They found that, while the performance of the parallel choice mechanism is better than that of the sequential mechanism, it is worse than that of the deferred acceptance mechanism [12]. It implies that the advantages of the deferred acceptance mechanism are not fully exploited under the parallel choice mechanism due to the limited preference lists.

Inner Mongolia has adopted a novel mechanism called the *real-time interactive mechanism* (RIM) since 2008, which is expected to alleviate the problem caused by the limited length of the preference list in the parallel choice mechanism. In RIM, students can observe the tentative admission results online and modify their choices at any time before the deadline. This mechanism is similar to the iterative deferred acceptance mechanism [18], which is expected to improve both fairness and social welfare in that it is under perfect information [5]. There is experimental evidence showing that a higher proportion of stable outcomes and truth-telling rates are reached under the iterative deferred acceptance mechanism than the standard deferred acceptance mechanism [19, 20].

However, one type of manipulation is possible in the real-time interactive mechanism by the coordination of a high-score student and a low-score student [18]. Because students can modify their applications at any time before the deadline, the high-score student can "hold" a seat in a university and "release" it at the last minute so that the low-score student can take it. The utility of the low-score student is improved because she is admitted by a better university. The high-score student will also be admitted by her truly preferred university due to her score advantages. Hence, their total utility is improved (we assume that the coordinating students have other channels to transfer their utilities in real life and both of them only care about their average utility in our model). However, such coordinating manipulation may erode social welfare and fairness due to distorted outcomes. In practice, the issue of "seat-holding" manipulation has become critical. The authority is aware of it and claims that this behavior will be monitored and prohibited in the new college admission system 2020 [21].

By the approach of agent-based simulations [22, 23], we first study the rationale of the coordinating manipulation under the real-time dynamic mechanism and the impact of coordinating manipulation on social welfare and fairness. We then investigate whether the multistage policy of RIM can alleviate the coordinating manipulation problem. To identify the number of students who would like to take the coordinating manipulation, we use the value at the steady state where both manipulation and nonmanipulation students have no incentive to switch their strategies. We find that a considerable portion of students will take the coordinating manipulation, and both the welfare and fairness of the society are lower than the situation when there is no manipulation. Furthermore, we propose a variant of RIM with multiple stages (MS-RIM), where students with different scores have different deadlines to submit their applications, with higher score students earlier and lower score students later. Simulations show that the multistage policy has complex effects on matching results of RIM. The strategy can reduce the chance of coordinating because of the different deadlines to submit applications. However, it amplifies the students' incentive to conduct coordinating manipulation due to the scarcity of manipulation opportunity and consequent higher reward. Moreover, it helps to avoid the congestion that all manipulation students transfer their seats almost simultaneously and increases the success rate of the manipulation. The combination of the three effects indicates that when the number of stages is small, social welfare and fairness are diminished by the increased successful manipulations. Only when the number of stages is sufficiently large, the successful manipulation number decreases and the social welfare and fairness are improved.

The organization of this paper is as follows. Section 2 describes the background of this experiment. Section 3 introduces the agent-based model of the real-time dynamic mechanism of college admission. Section 4 presents and discusses the results and then comes to conclusions in Section 5.

2. Background

2.1. Real-Time Interactive Mechanism. The real-time interactive mechanism was firstly trialed in the college application and admission process of Inner Mongolia for a portion of the students in 2006 and 2007. It was then applied to all students since 2008, with a few modifications and improvements in the following years.

Before the application and admission process, the universities submit their enrolment plans and are assigned some quotas, and the students take the college entrance examination and obtain their scores, which is the main criteria of the admission. The number of students with different scores is publicly available, as well as the universities' enrolment plans and their lowest scores of admitted students in the previous years. The students are advised to well recognize the rank of their score among all students and choose some preferred and probably achievable universities.

When the admission process starts, every student needs to log in to the online admission system and choose a university to apply. On receiving a student's new application, the computerized system will insert this student to the ranking list of all students that apply to the same university according to their scores in the descending order. A student can see her position on the list and roughly know if she will be admitted immediately after submitting the application. The cut-off score, the minimum score of those students within the enrolment quotas of a school, will be updated in real-time and made public regularly.

At any time before the system closes, the students can check if they could be admitted and decides whether to make a new application. Students can modify their choices as many times as possible before the deadline.

When the system is closed, the students whose score is ranked within the quota of their applied university will be officially admitted. Otherwise, they will be rejected by this university and cannot be admitted by other universities too.

The advantage of the real-time interactive mechanism is information transparency. A student can observe whether he could be admitted by the applied university immediately after the application submission, and this enables students to apply the universities both preferred and achievable, which is impossible under other mechanisms.

2.2. Coordinating Manipulation of High- and Low-Score Students. The real-time interactive mechanism is not perfect. One shortcoming of this mechanism is that it is vulnerable to a type of manipulation by the coordination of a student with a high exam score and another student with a low exam score.

At the beginning of the admission procedure, the high-score student does not apply to his favorite university, but applies to the university that the low-score student prefers. This means that the high-score student "holds a seat" from a university for the low-score student. In the last few minutes before the deadline, the high-score student can "release this seat" so that the low-score student can apply for this university before other students notice this vacancy. After releasing a seat, the high-score student immediately applies to his truly preferred university. As a result, the high-score student can be accepted because of the advantage of his score, and the low-score student can be admitted by a better university due to a successful manipulation.

Although a successful manipulation can benefit the two manipulation students, this may make unfairness to other students and welfare loss to society. If there were no manipulation, another student with a score between the high-score and low-score student can be admitted by the university that admits the low-score student. Moreover, the high-score manipulation student switches to a university at the last minute before the deadline, and this usually pushes another student out of the enrolment quota of the applied university without the chance to apply to other universities due to the limited time.

2.3. Multistage Real-Time Interactive Mechanism. Since 2008, the admission process is carried out by multiple stages, which we called the multistage real-time interactive mechanism (MS-RIM). Students with different scores are given different deadlines to submit their applications, and the deadline for students with higher scores is earlier than those with lower scores. For example, students whose scores range from 600 to 629 need to submit their applications before 4 pm, and students whose scores range from 570 to 599 submit their applications before 5 pm, and so forth.

This multistage policy is introduced to tackle the network congestion problem because many students modify their applications just before the deadline. Especially, when a high-score student switches to a university, some low-score students who are ranked lower near the cut-off score will be afraid of being refused by this university and switch to apply to other universities, and they will then push other students to switch universities too. The multistage policy provides students with different scores different deadlines, and this alleviates the number of switches and improves the problem of network congestion.

It is still unclear how the multistage policy influences coordinating manipulation. Because the deadline to submit applications varies for students with different scores, some of them will have no opportunity to conduct the coordinating manipulations. However, coordinating manipulations remains a big issue in practice despite the implementation of the multistage policy for many years.

We conduct simulations to confirm that, although the multistage policy can really reduce the occurrence of the coordinating manipulation, it increases the incentive of students to manipulate the mechanism.

3. Methods

We study the college application and admission process under real-time interactive mechanism by agent-based simulations, which provide an ideal tool to model complex adaptive systems by a bottom-up approach [22, 23]. By modeling the behaviors of the individual students, we can observe how the interactions self-interested individuals build up the macrolevel phenomena such as the welfare and fairness of the resultant matching. An agent-based simulation is also flexible to perform scenario analysis which is usually necessary for practical policy making. This approach has been adopted to study the college matching problem [24, 25].

The simulation model settings are initialized as follows:

(1) A set of students $N = \{1, 2, \ldots, n\}$ whose exam scores are randomly generated from the uniform distribution from *score_min* to *score_max*.

(2) A set of universities is denoted by $S = \{s_1, s_2, \ldots, s_m\}$.

(3) The enrolment quotas of the universities are denoted by $Q = \{q_1, q_2, \ldots, q_m\}$, which means that the number of students that university i will admit is q_i.

(4) The preferences of students over universities are denoted by $P = \{P_1, P_2, \ldots, P_n\}$, where P_i is a permutation of all universities, for example, P_i: s_1, s_2, s_3, ... , s_m, which means that, for student i, university s_1 is his first choice, university s_2 his second choice, university s_3 his third choice, and so forth. We assume there is a public ranking of universities, such as the Best Global Universities Ranking by U.S. News and World Report. The student preference P is randomly generated by disturbing the public ranking, which means that students may have different preferences over universities, but in general, top-ranked universities are preferred by more students than low-ranked ones.

(5) The preferences of universities over students are denoted by $R = \{R_1, R_2, \ldots, R_m\}$. In this model, all universities' preferences over the students are completely based on their scores.

(6) The minimum score difference between the two manipulation students is *score_diff*. Since the high-score student will hold a seat for the low-score student in the coordinating manipulation, only the score difference between them is larger than *score_diff*, and then they can take the manipulation strategy.

(7) The proportion of students who attempt to find partners to take coordinating manipulation is denoted by ρ, which is called the *manipulation-seeking ratio*. In the simulation, a proportion ρ of the students are randomly selected as *manipulation-seeking students*. Each manipulation-seeking student has one chance to find a partner. For a manipulation-seeking student who has no partner (student A, for example), he will ask another student (say student B) which is randomly chosen from all other students. If B is also a manipulation-seeking student and has no partner, and their score difference is larger than *score_diff*, they will become partners and are ready to conduct the coordinating manipulation, and student B will not search for other partners anymore; otherwise, student A cannot conduct manipulation although he is willing to do so. Those who find partners to conduct coordinating manipulation are called *manipulation students*.

(8) The number of rounds in one simulation is T. The simulation runs in discrete steps, and every student has one chance to update his application at each round.

(9) The round when the high-score manipulation students release the seat that they hold for the low-score manipulation students is $t_{seat\text{-}transfer}$. We simulate with different $t_{seat\text{-}transfer}$ and the students will adapt to choose the optimal $t^*_{seat\text{-}transfer}$ to maximize their utilities.

(10) To simulate the situation that some students may fail to submit their applications due to the operation failure (such as network congestion, slow system response, and operation error), each student has a probability λ_t that his submission is unsuccessful. The failure probability varies with the round number t, and the closer the round number is to the deadline, the larger λ_t will be.

The simulation procedure is described as follows. The admission process runs for T rounds. In each round, every student has one chance to submit his application. The order of students to submit applications is rearranged randomly for each round. Before submitting applications, every student can inquire the information about university's quotas and cut-off scores of universities. The nonmanipulation students will report their true preferences, that is, they will apply to their most preferred university among all feasible universities whose quota is not filled or the applicant's score is higher than the last one in the university's application list. For manipulation students, the high-score manipulation student will apply for the most preferred feasible university of low score, and the low-score manipulation student will apply according to his true preferences before the seat-transfer time $t_{seat\text{-}transfer}$. At round $t_{seat\text{-}transfer}$, the high-score student releases the seat of the university that the low-score student preferred and then applies for his truly preferred feasible school, and at the same time the low-score student applies for this "released seat" immediately. All the operations of the students are vulnerable to failure with probability λ_t. The ranking of students in the university's application list is updated in the descending order as soon as a new application is submitted. After all students have submitted their applications, each student can observe the temporary matching result and know if their ranking is within the quota of the universities. Then, a new round starts and all students can modify their applications in the new round.

The admission process ends after T rounds of simulation, and the students whose scores are within the quotas of the applied universities are officially admitted. Then, the utilities of students and universities can be calculated according to the admission results and their preferences.

A student's utility is determined by the position of the university that admitted him in his preference. For example, when there are m schools, the utility of a student is $m/m = 1$ if he is admitted by his first-choice university and is $(m-1)/m$ if admitted by the second-choice university and so forth, and if he is admitted by the last preferred university, his utility is $1/m$. Certainly, the utility of unmatched students is zero.

The utility of universities can be calculated in the same manner. When there are n students, a university's utility from admitting the student with the highest score is $n/n = 1$ and is $(n-1)/n$ from admitting the second-highest score student and so forth. Since each university may accept more

than one, the total utility of a university is the sum of the utilities from all admitted students. If a university failed to enrol enough students, the utility from the vacant seat is 0. Then, the utility of a university can be adjusted by dividing the total utility with its quota q.

The parameter settings of our simulations are $n = 450$, $m = 30$, $q = 15$, $score\_min = 550$, $score\_max = 700$, $score\_diff = 20$, ρ ranges from 0 to 1, $T = 100$, $t_{seat\text{-}transfer}$ ranges from 1 to T, and $\lambda_t = t/1000$, and $t = 1$ to 100. Although, we set the max round number of one simulation as 100, the system stabilizes at about the 35th round.

4. Results and Discussion

4.1. Coordinating Manipulations at Steady State. Although every student can choose to coordinate with other students to manipulate the mechanism, it does not imply that all of them are willing to do so. As rational agents, they will make their choices according to the expected utility from different strategies. If the expected utility from manipulation is larger than that from nonmanipulation, more students will choose manipulation, otherwise, more students will adapt to nonmanipulation. Then, a *steady state* where the manipulation students and nonmanipulation students obtain the same utilities characterized the outcome of the manipulation game. At the steady state, the percentage of the manipulation and nonmanipulation students will not change despite that the self-interested students are free to make their choices.

There are a proportion ρ of the students (about ρn) who are willing to find partners to conduct manipulation, and about $(1-\rho)n$ students truthfully submit their applications. Among manipulation-seeking students, some of them can successfully find their partners, while others cannot. This is simulated by randomly matching them in pairs, and if the difference between the score of two partners is larger than *score_diff*, they can really conduct the coordinating manipulation. So, only the students who are willing to conduct manipulation as well as have successfully found the partners are called *manipulation students*. The students who do not really conduct manipulation are called *nonmanipulation students*, including those who are willing to manipulate but fail to find the partners.

To find the steady state, we simulate with different ρ that ranges from 0 to 1 and calculate the average utility of the manipulation students and nonmanipulation students, respectively, under different values of ρ. Some typical results are shown in Figure 1.

Since high-score and low-score students coordinate, we assume they can transfer utilities to each other by other channels in real life, and hence they can be regarded as a coalition and both of them make their decision according to their average utilities, as indicated by the red lines marked with circles.

One decision that the manipulation students need to make is when the high-score students will transfer the seat to the low-score students. If the seat-transfer happens too late, they will take the risk of application failure at the last minute due to network congestion or other issues. If they transfer too early, the low-score students may be pushed out of the list of their preferred university by other students who apply to this school in the following rounds. Hence, they will choose the optimal round to release the seats. In the simulation, we try all seat-transfer time and calculate the corresponding average utilities of the manipulation students; then, the seat-transfer time that provides the largest utility of manipulation students will be their optimal choice, for example, the 1st round before deadline when $\rho = 0.01$ in Figure 1(a) and the 10th when $\rho = 0.1$ and 11th when $\rho = 0.3$ in Figure 1(b) and 1(c). In Figures 1(e) and 1(f), the utilities of manipulation students are always lower than nonmanipulation students whenever they release the seats, so they will not choose to coordinate. In particular, we find that the utility difference between manipulation students and nonmanipulation students stabilizes at about the 15th round, so all figures shown in this paper display the results from the last round to 15th round.

Another decision of the students, on a higher level, is whether to conduct coordinating manipulation. This actually depends on how many students are doing so. When there are few students who attempt to coordinate, such as $\rho = 0.01$, 0.1, and 0.3 in Figures 1(a)–1(c), the utility of the manipulation students (at the optimal seat-transfer time) will be larger than that of nonmanipulation students; this is because the information provided in the tentative admission result is mostly real, and there are few switches of applied university of manipulation students before the deadline. Hence, the nonmanipulation students may learn to adopt the manipulation strategy for higher utility and the portion of the manipulation-seeking students (ρ) will increase.

However, if there are too many manipulation-seeking students, such as $\rho = 0.7$ and 0.9 in Figures 1(e) and 1(f), the utility of nonmanipulation students is slightly larger than manipulation students; this is because the information of the tentative admission result is not reliable and there are too many application switches before deadline. Hence, some manipulation students will choose not to take manipulation strategy even though they have the chance to do so, and the portion of manipulation-seeking students (ρ) will decrease.

As a result, the system will stabilize at a *steady state* where the utility of manipulation students is equal to that of the nonmanipulation students, at $\rho = 0.5$ in Figure 1(d), and no manipulation students want to switch to nonmanipulation students and vice versa. Figure 2 provides the relationship between manipulation-seeking ratio (ρ) and the utilities of different students with more values of ρ, and we can see the steady state at $\rho^* = 0.5$, with the utility of manipulation students larger than that of nonmanipulation students when $\rho < \rho^*$ and smaller when $\rho > \rho^*$. Therefore, the consequence of the students' rational choices is that about half of the students will try to find partners to conduct coordinating manipulation. Here comes Result 1.

Result 1. A considerable portion of students will conduct the coordinating manipulation under the real-time interactive mechanism.

Next, we will investigate how the manipulation impacts the social welfare and fairness of the matching by real-time

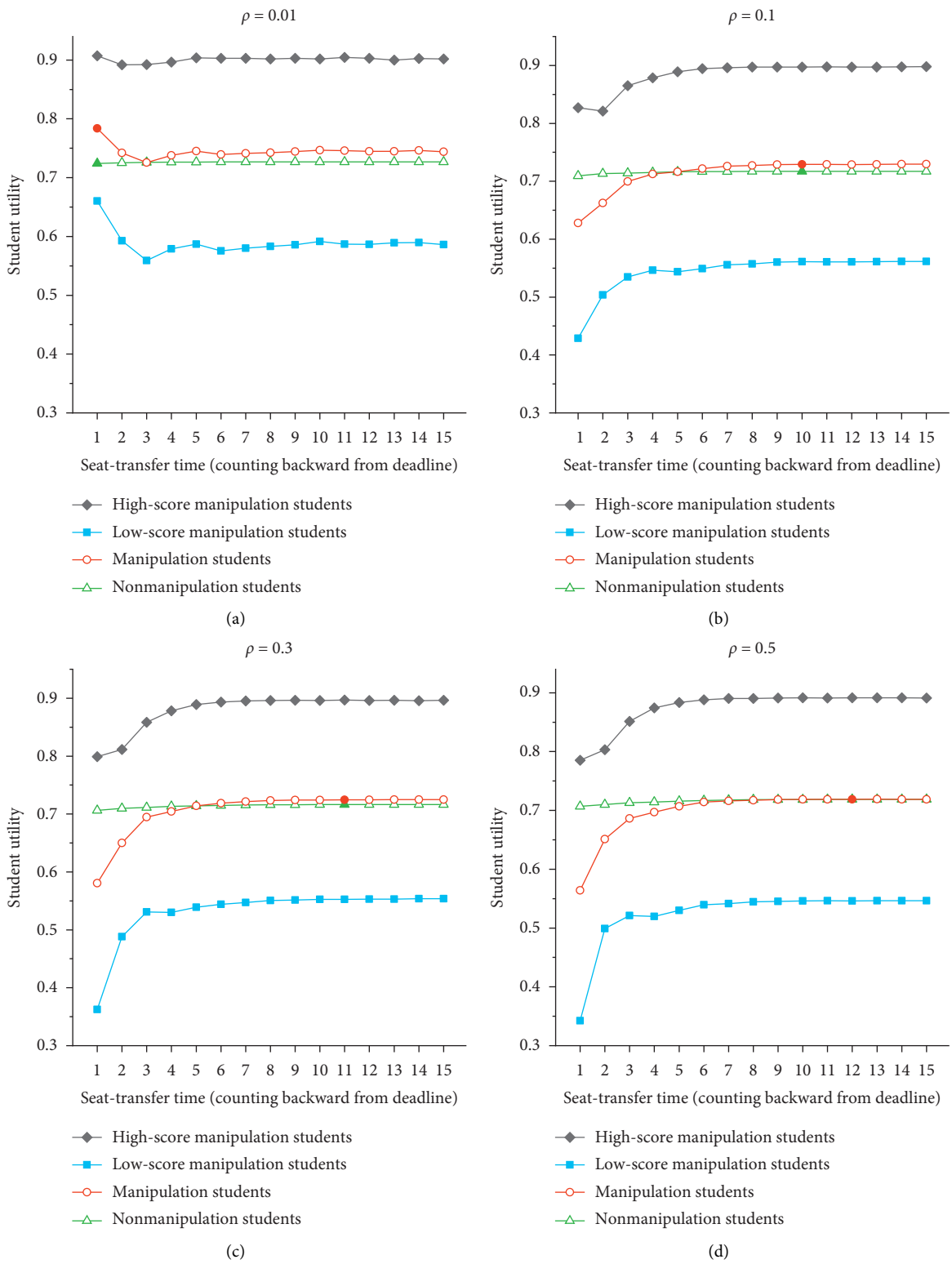

Figure 1: Continued.

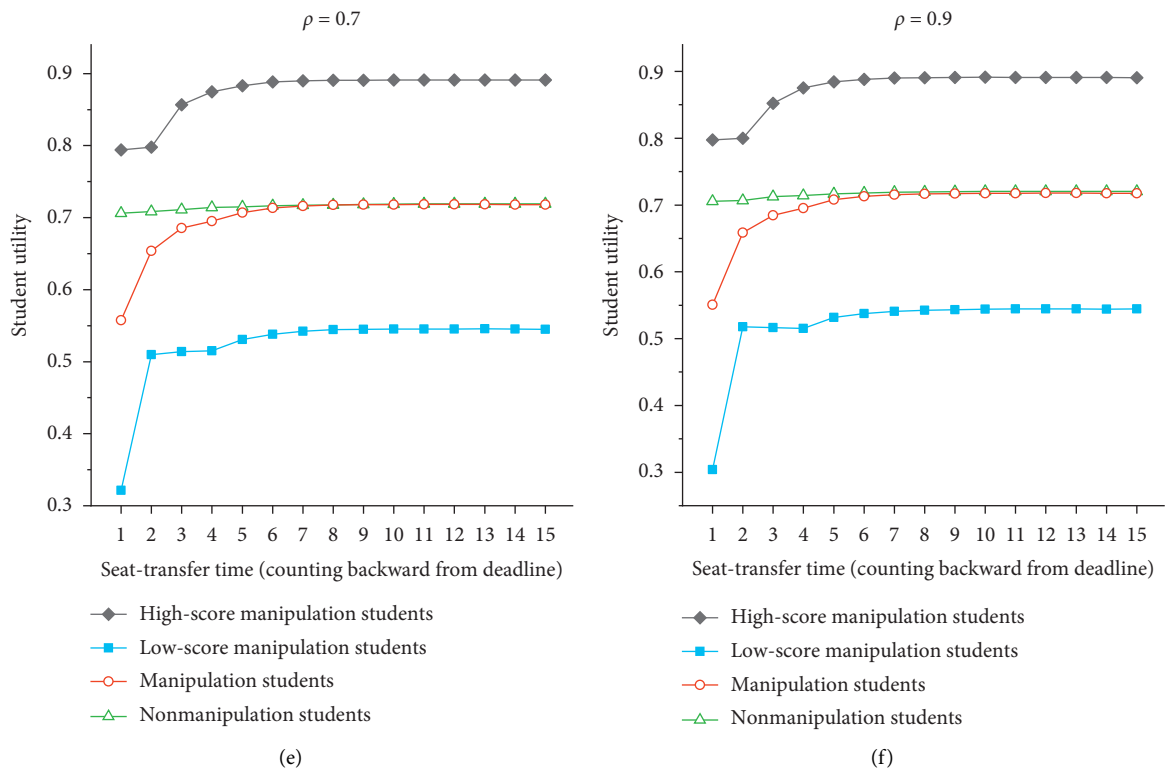

Figure 1: Utilities of manipulation and nonmanipulation students under different manipulation-seeking student ratio ρ. The x-axis represents the time when the high-score manipulation student transfers the seat to the low-score manipulation student, and it is the round number counted backward from the deadline. The y-axis represents the average utilities of students. The black line marked with diamonds is the average utility of the high-score manipulation students, the blue line marked with squares is for low-score manipulation students, the red line with circles is the average utility of all the manipulation students (both high- and low-score manipulation students), and the green line with triangle is for nonmanipulation students. The solid marks represent the optimal transfer time $t^*_{seat\text{-}transfer}$ of manipulation students. For each parameter setting, we run the simulation for 100 times and calculate the average utilities.

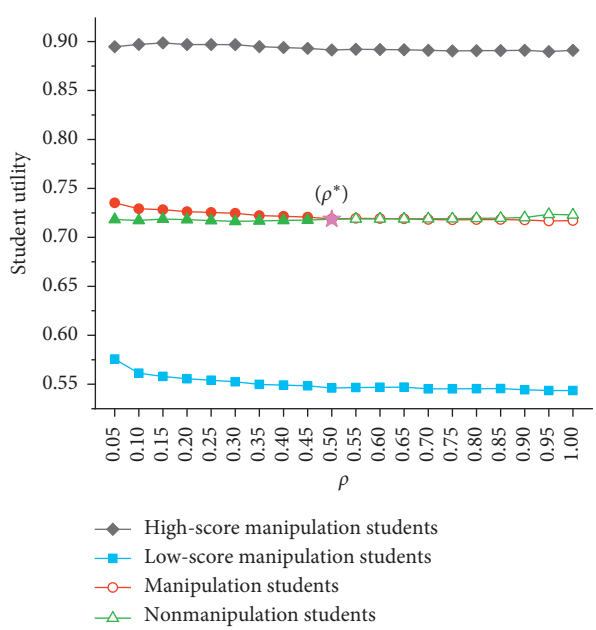

Figure 2: Relationship of manipulation-seeking ratio (ρ) and the utilities of different students. The utilities of students are calculated with the optimal seat-transfer time of manipulation students. The steady state (ρ^*) is marked with pentagram.

interactive mechanism. Social welfare is measured by the utility per capita for all students and all universities. We calculate the average utility of all students and that of all universities for $\rho = 0$ (no manipulation) and $\rho = 0.5$ (the steady state with manipulation). We can see that the average utility of all students from 0.7199 (no manipulation) to 0.7187 (steady state with manipulation), as shown in Figure 3(a). To investigate how the manipulation and nonmanipulation students with different scores are affected by the coordinating manipulation, we calculate the average utility of the top-ranked (with scores higher than the mean score of all students) and low-ranked (with scores lower than the mean score) manipulation and nonmanipulation students, as shown in Figures 3(b) and 3(c). The average utility of both the top- and low-ranked nonmanipulation students becomes smaller. The reason that the utility of top-ranked nonmanipulation students becomes worse off is that the high-score manipulation students will resubmit their applications after releasing the seat for the low-score manipulation student, and they will push some of the high-score nonmanipulation students out of the admission list of the applied university, then cause them to have no time to resubmit applications. For low-ranked nonmanipulation students, in addition to the above reason, it is also because some of the seats are held by the manipulation students and

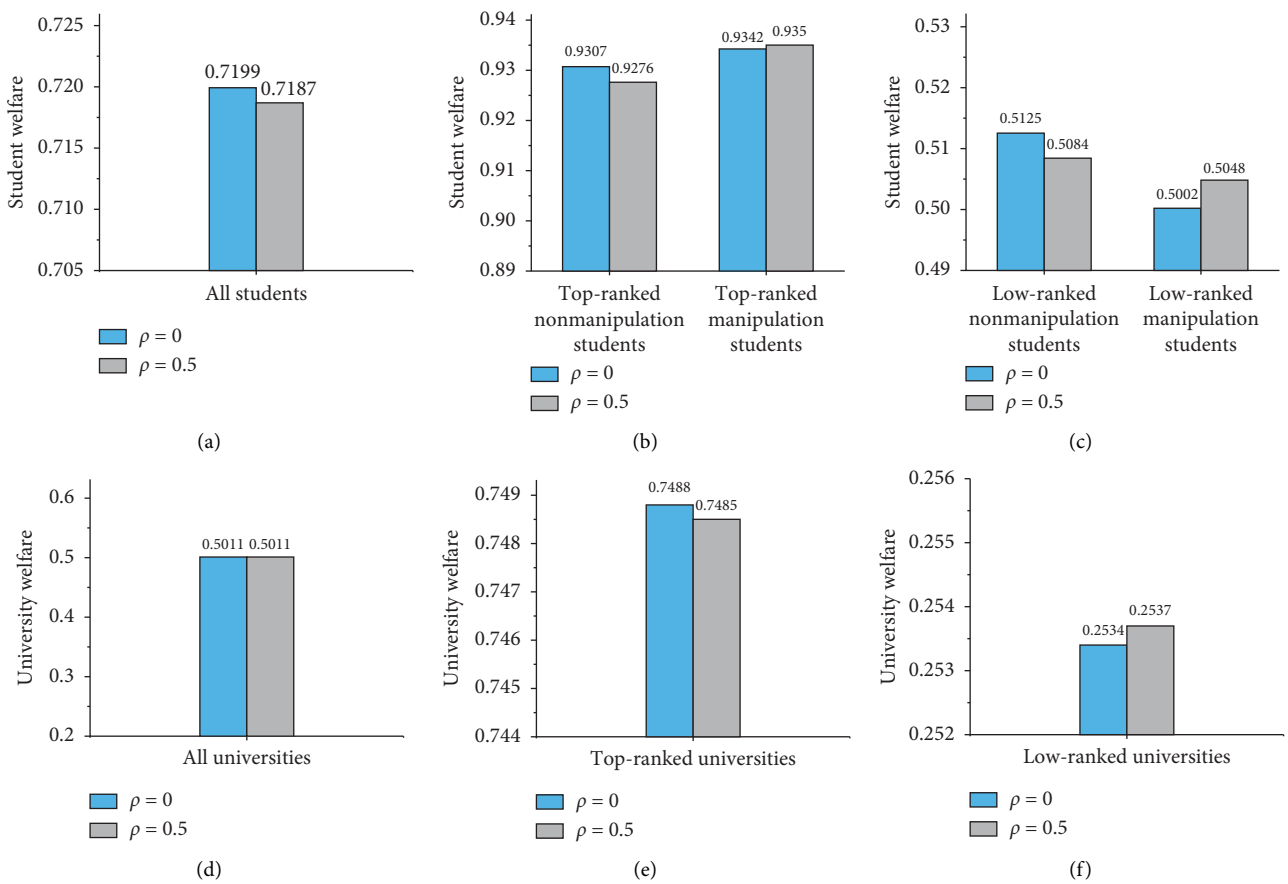

Figure 3: Student welfare and university welfare under the state with no manipulation ($\rho = 0$) and under the steady state with manipulation ($\rho = 0.5$). The top-ranked and low-ranked students are those whose scores are ranging from 625 to 700 and 500 to 624. The top-ranked and low-ranked universities are No. 1–15 and No. 16–30 universities in the public ranking, respectively.

the cut-off score of the university is raised, so they can only choose their less preferred universities.

The average utility of all universities for $\rho = 0$ (no manipulation) is the same as that for $\rho = 0.5$ (the steady state with manipulation), as shown in Figure 3(d). This is because all universities have the same preferences over students (all prefer students with a higher score), and the total utility of all schools does not change under any college-student matching as long as the quotas of all universities are fulfilled. However, the utility distribution among the universities is different, with the utility of the top-ranked universities (No. 1–15 in the public ranking) damaged while that of the lower-ranked universities (No. 16–30) improved, as indicated in Figures 3(e) and 3(f). This is because the low-score manipulation students can be admitted by better ranked universities through successful coordinating manipulation, which causes the top-ranked universities to accept low-score students and their utilities are damaged. On the contrary, there must be increases in utilities of low-ranked universities.

The fairness of a college-student matching is measured as follows. For each student, he can observe the cut-off scores (the minimum score of all admitted students) of all universities that he preferred but do not admit him, and if his score is larger than any one of the cut-off scores, he will feel unfair; otherwise, he will feel fair. Hence, the *fairness index* is defined as the proportion of students who feel fair among all students. Figure 4 compares the fairness of the situations with and without manipulations. When there is no manipulation, the property of no justified envy of deferred acceptance mechanism assures that there is no unfairness [2], which is consistent with the simulation results that the fairness index equals 1. However, at the steady state with manipulation, the fairness index declines to 0.9456, which implies that about 5% of students feel unfair. Hence, we have Result 2 as follows.

Result 2. The social welfare and fairness of the matching are both damaged under real-time interactive mechanism due to the manipulation behaviors.

4.2. Manipulation under MS-RIM. In this section, we investigate the manipulation behavior under the multistage RIM. The admission procedure runs for K stages, and each stage runs for T rounds. After the end of stage 1, the students with scores ranging from $score\_min + (score\_max\text{-}score\_min)\ (K-1)/K$ to $score\_max$ cannot submit their applications anymore. Similarly, students with scores ranging from $score\_min + (score\_max\text{-}score\_min)\ (K-2)/K$ to

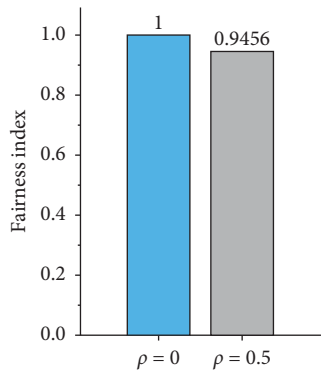

Figure 4: Fairness index under the state with no manipulation ($\rho = 0$) and the steady state with manipulation ($\rho = 0.5$).

score_min + (*score_max-score_min*) $(K-1)/K$ cannot submit their applications any more after the end of stage 2 and so on. The admission system closes after the last stage.

For each stage of an MS-RIM, we need to find the steady state (ρ^*) where the proportion of manipulation-seeking students does not change. Similar to the previous section, we simulate with different values of ρ ranging from 0 to 1 and choose the one that provides the same utility for both the manipulation and nonmanipulation students. Given the value of ρ, the utilities of students also depend on the seat-transfer time ($t_{seat\text{-}transfer}$) of manipulation students, that is, when the high-score students transfer seats to low-score students. As rational individuals, they will choose the optimal time that provides the maximum utility. Hence, for a given value of ρ, we simulate all seat-transfer time and choose the one that provides the highest utility for manipulation students, as indicated by the solid marks. We calculate the steady state stage by stage, and the manipulation-seeking ratio at the steady state may vary across stages.

For two-stage RIM, we firstly consider the decision of students in the 1st stage, whose scores are between 625 and 700. When few students attempt to coordinate ($\rho = 0.1$), the utility of the manipulation students (at the optimal seat-transfer time) will be larger than that of nonmanipulation students, as illustrated in Figure 5(a). It is expected that more students will adopt this strategy. When all students are willing to find partners to conduct coordinating manipulation ($\rho = 1$), the utility of manipulation students is still larger than nonmanipulation students, as in Figure 5(b). This implies that the steady state is $\rho^* = 1$ and all students are willing to conduct the coordinating manipulation eventually as the consequence of the rational choice of students. Given that the students in the first stage behave as the steady state indicates ($\rho^* = 1$ in this simulation), the steady state for the second stage (with students' scores from 550–624) can be obtained similarly by simulating with different values of ρ. And it is found that the steady state is also $\rho^* = 1$ because the utility of manipulation students is always larger than that of the nonmanipulation students for all ρ values, as illustrated by Figures 5(c) and 5(d).

For three-stage RIM, by the same method, we find that the steady state is $\rho^* = 1$ for all stages, implying that all students are willing to conduct coordinating manipulation due to the higher utility than nonmanipulation, as illustrated by the typical results in Figure 6. Two new observations should be noticed. The first is that the utility difference between the manipulation and nonmanipulation students at a steady state is larger in late stages than in the early stages. Certainly, the larger is the difference, the stronger incentive to conduct manipulation that the students will have, that is, the incentive to conduct manipulation is larger in the late stage than in the early stage. The second observation is that the optimal seat-transfer time ($t^*_{seat\text{-}transfer}$), when the high-score manipulation student releases the seat for the low-score student, in the 3rd stage of three-stage RIM is the last round before the deadline, that is, compared with manipulation in the early stage, the manipulation students in late stages transfer their seats at the time closer to the deadline. This is because the low-score manipulation students in this stage have the least scores (550–580), and they can only be accepted by the lower-ranked universities even if there was no manipulation. This implies that their "opportunity cost" is low, and they would like to take the risk to improve their utilities by transferring the seat at the last round.

To investigate the observations discussed above and how the multistage policy affects matching results of RIM, we also simulate the four-stage, five-stage, and six-stage RIM, and all the results are summarized in Table 1 (other parameters are the same as above).

Simulation results averaged for 100 runs. The ratio of students who are willing to conduct coordinating manipulation at the steady state is ρ^*; $t^*_{seat\text{-}transfer}$ is the optimal time for the manipulation students to transfer the seat from the high-score student to the low-score student; utility difference is the average utility of the manipulation students minus the average utility of the nonmanipulation students; the manipulation number is the number of students that find partners to conduct manipulation (that is, the scores' difference of the two paired student is larger than the critical value *score_diff*); the successful manipulation number is the number of manipulation students who successfully transfer the seat from the high-score student to the low-score students and do not need to be pushed out by other students in the following rounds; student (university) welfare is the average utility of all students (universities); the fairness index is the ratio of students who do not feel unfair.

The steady states are $\rho^* = 1$ for each stage of all versions of RIM except the one-stage version (the third column of Table 1). This means that all of the students are trying to find partners to conduct coordinating manipulation and the utility from the manipulation is always larger than nonmanipulation under MS-RIM. Hence, we have the following result.

Result 3. Students have a stronger incentive to conduct coordinating manipulation under MS-RIM than one-stage RIM.

The explanation for the result is that the benefit of the manipulation is smaller when there are more students to conduct coordinating manipulation. This is because the information on the tentative admission result is not reliable when most students report false preferences. Meanwhile, the

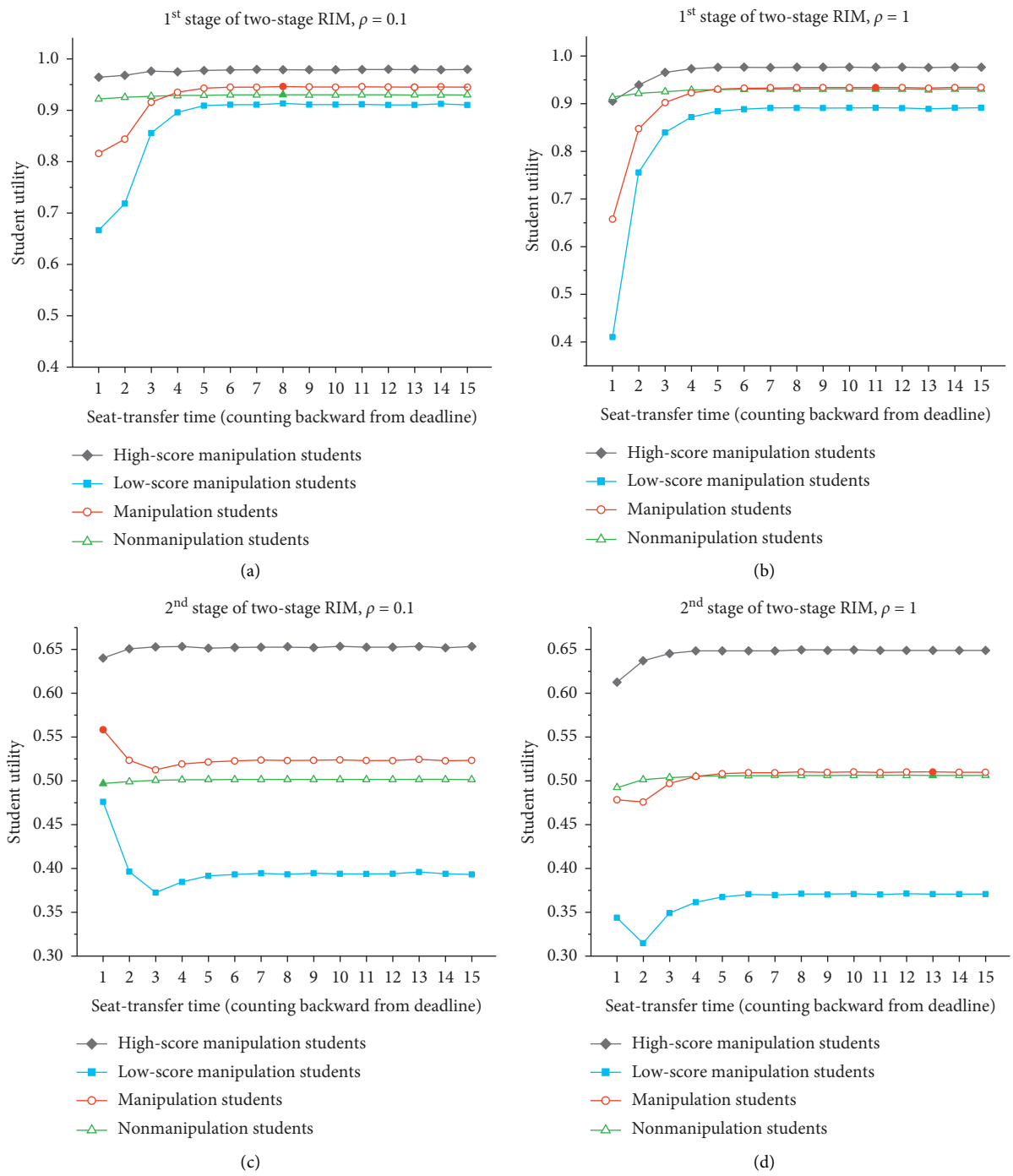

Figure 5: Utilities of manipulation and nonmanipulation students under different manipulation-seeking ratios ρ under two-stage of RIM. The utility of manipulation students is always larger than that of nonmanipulation students for different values; hence, the steady state is that all students are willing to conduct coordinating manipulation.

seat-transferring of the coordinating students may affect each other, for example, when a high-score student releases the seat for his partner and chooses his preferred university, another student who just applied this university may be pushed out of the admission list and he will immediately resubmit a new university then continuously pushing the other one out of the admission list, that is, there are too many application switches before the deadline. Under the multistage policy, students in different stages cannot coordinate; hence, the number of the students who can conduct coordinating manipulation becomes smaller, and the scarcity of the manipulation makes it more beneficial and therefore, the students are more willing to take this behavior.

We can also see that the utility difference between manipulation and nonmanipulation students is generally larger for late stages than early stages in a certain version of

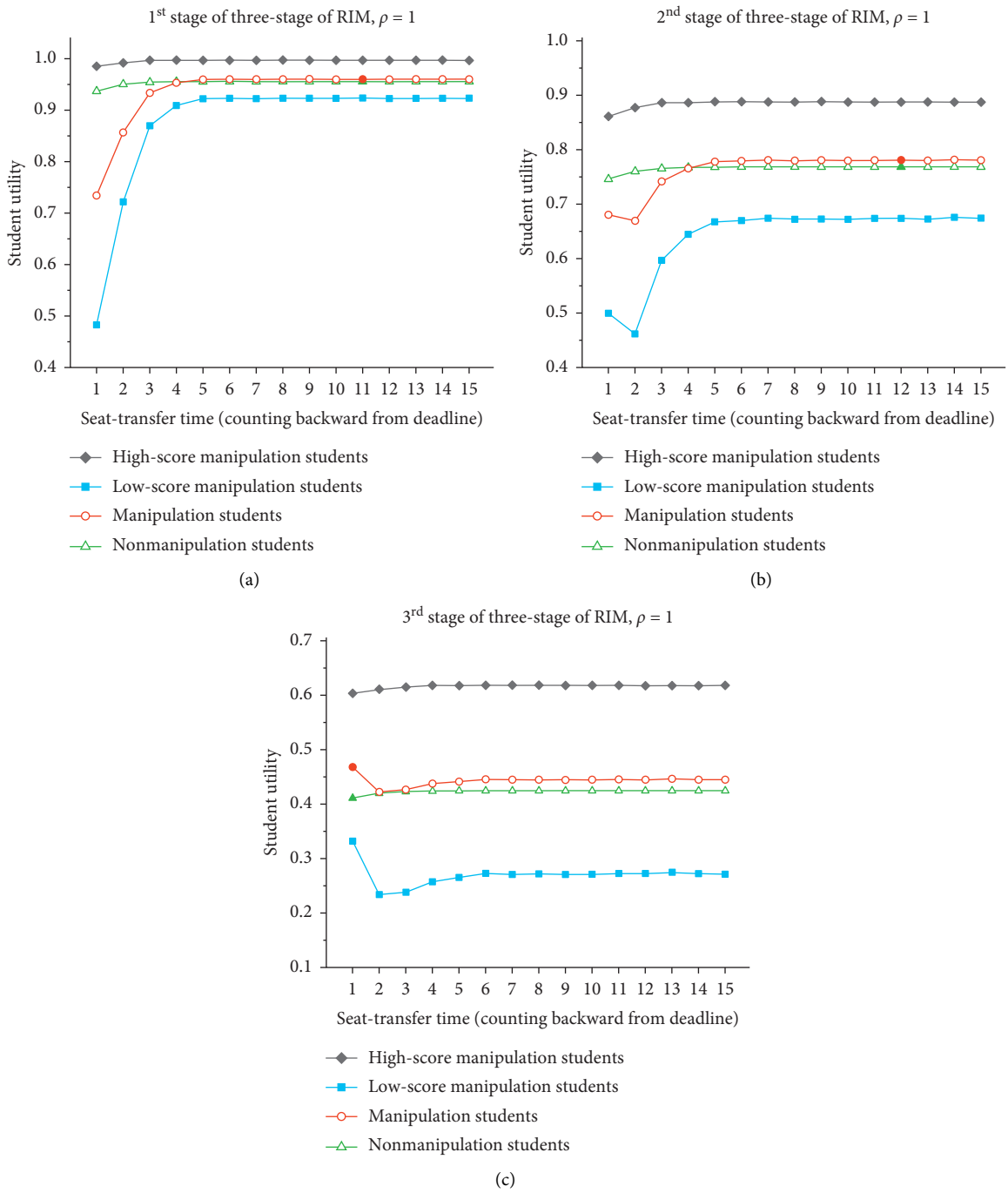

Figure 6: The utilities of manipulation students and nonmanipulation students when the manipulation students transfer the seat at different stages.

MS-RIM. Take four-stage RIM, for instance, the utility differences are 0.0007, 0.0018, 0.0154, and 0.0887 for the 1st, 2nd, 3rd, and 4th stage. The reasons for this result are two-fold. First, when the students conduct coordinating manipulation at any stage, they have the probability that the application for new universities will be unsuccessful due to the network congestion or operation failure. Since the students in the early stages have higher scores, they can usually be admitted by good universities due to their score advantages and then obtain high utilities, that is, the extra utility from successful manipulation over nonmanipulation is roughly the same for all stages, but the utility loss from unsuccessful manipulation in the early stage is larger than that in the late stage, which makes the expected utility gain from manipulation (both successful and unsuccessful) over nonmanipulation is smaller than that in the late stage. Second, the manipulation students in the late stages usually transfer the seat in the rounds closer to the deadline of the submission, that is, the optimal seat-transfer time ($t^*_{seat\text{-}transfer}$) becomes smaller in late stages, as shown in the fourth

Table 1: Simulation results of different versions of RIM.

Version of RIM	Stage number	ρ^*	$t^*_{seat\text{-}transfer}$	Utility difference	Manipulation number	Successful manipulation number (rate)	Student welfare	University welfare	Fairness index
One-stage RIM	Stage 1	0.5	12	0	170.1	15.94 (0.09)	0.7187	0.5011	0.9458
Two-stage RIM	Stage 1	1	13	0.0031	53.22	14.83 (0.28)	0.7184	0.5011	0.9282
	Stage 2	1	11	0.0037	54.62	11.18 (0.20)			
Three-stage RIM	Stage 1	1	11	0.0047	17.12	4.31 (0.25)	0.7157	0.4988	0.793
	Stage 2	1	12	0.0125	17.40	2.76 (0.19)			
	Stage 3	1	1	0.0564	17.28	9.27 (0.54)			
Four-stage RIM	Stage 1	1	12	0.0007	6.48	2.61 (0.40)	0.7178	0.5004	0.8743
	Stage 2	1	12	0.0018	5.77	4.46 (0.77)			
	Stage 3	1	10	0.0154	6.40	5.58 (0.87)			
	Stage 4	1	1	0.0887	6.08	3.40 (0.56)			
Five-stage RIM	Stage 1	1	12	0.0001	1.82	1.23 (0.68)	0.7196	0.5009	0.9507
	Stage 2	1	11	0.0083	2.10	1.99 (0.95)			
	Stage 3	1	6	0.0327	1.94	0.62 (0.32)			
	Stage 4	1	7	0.0560	2.12	1.95 (0.92)			
	Stage 5	1	1	0.0904	2.18	1.59 (0.73)			
Six-stage RIM	Stage 1	1	3	0.0017	0.52	0.47 (0.90)	0.7198	0.5010	0.9841
	Stage 2	1	4	0.0192	0.44	0.25 (0.57)			
	Stage 3	1	5	0.0338	0.68	0.50 (0.74)			
	Stage 4	1	4	0.0344	0.58	0.44 (0.76)			
	Stage 5	1	1	0.0376	0.52	0.47 (0.90)			
	Stage 6	1	1	0.0542	0.58	0.37 (0.64)			

column of Table 1. For example, the manipulation students in the fourth stage of the four-stage RIM transfer their seats in the last round before the deadline, i.e., $t^*_{seat\text{-}transfer} = 1$. The choice of the optimal transfer time is a trade-off between the probability of operation failure and the probability of being pushed out by other students. If the manipulation students transfer their seat early, the operation failure probability will be smaller because they have more rounds to resubmit their applications, while the probability of being pushed out is larger because more students can notice and apply for the university that the low-score manipulation students applied and push the low-score manipulation students out. The consequence of operation failure is that the students obtain no utility at all, even the normal utility if they did not conduct manipulation. The consequence of being crowded out is that they cannot obtain the extra utility that the manipulation behavior provides. In the late stage, the students have low scores and their utility is usually small if they do not conduct coordinating manipulation; hence, their utility loss when being crowded out is relatively small. Therefore, they will transfer their seats in the round closer to the deadline to decrease the probability of being crowded out to enjoy the extra utility from manipulation. And this result can be summarized as follows.

Result 4. Under a certain version of MS-RIM, the students have a stronger manipulation incentive in late stages than early stages; the manipulation students in late stages transfer their seats at the time closer to the deadline.

In summary, the multistage policy has complex effects on matching results of RIM. The direct effect is that it can reduce the opportunity for the students to coordinate, for example, in the two-stage RIM a student with a score 700 in the first stage cannot hold a seat for the student with a score 550 in the second stage because their deadlines to submit applications are different. This is called the *manipulation opportunity reduction effect* of the multistage policy. The multistage policy has an indirect effect that more students are willing to conduct coordinating manipulation, and the reason is that the utility from manipulation becomes higher when there are fewer students who can conduct manipulation, which lures more student to adopt the coordinating manipulation, for example, from $\rho^* = 0.5$, in one-stage RIM to $\rho^* = 1$ in all other versions of RIM. We call this effect the *manipulation incentive amplification effect* of the multistage policy. Combining these two effects, there are fewer and fewer students who will conduct coordinating manipulation as the stage numbers increases, as shown in the sixth column of Table 1 and illustrated in Figure 7(a). Furthermore, the multistage policy has another indirect effect, named *manipulation success-rate improvement effect*. In the one-stage RIM, all manipulation students transfer the seat from the high-score students to low-score students before the deadline and many manipulation students may be pushed out of the admission list of the applied university by other students and fail in the manipulation. However, under RIM with multistage, the number of manipulation students who simultaneously transfer their seats is smaller because of the different deadlines, and there are few switches of the applied university of manipulation students before the deadline, the probability of being pushed out will be smaller, so the success rate of manipulation becomes higher, as shown in the seventh column of Table 1 and illustrated in Figure 7(a). Therefore, the successful manipulation number (the number

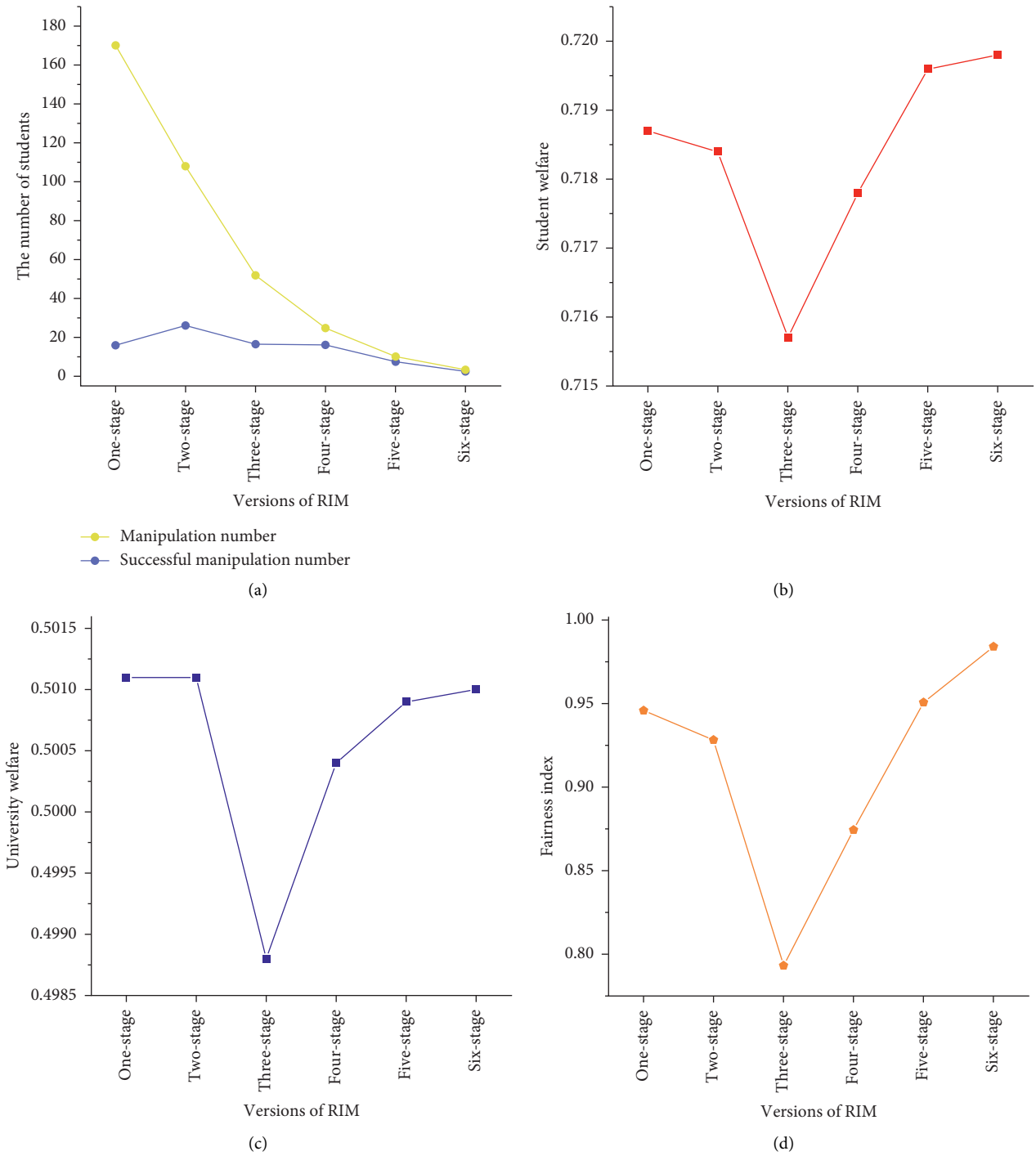

Figure 7: Simulation results under different versions of RIM.

of the students who conduct coordinating manipulation and successfully apply to the intended universities with no operation failure or being pushed out by other students) in two-stage, three-stage, and four-stage RIM are larger than one-stage RIM because the manipulation incentive amplification effect and manipulation success-rate improvement effect dominate the manipulation opportunity reduction effect when the stage number is small; the successful manipulation number drops down in five-stage and six-stage RIM because the manipulation opportunity reduction effect dominates.

The student welfare (the average utility of all students) decreases slightly under two-stage RIM than one-stage RIM, drops dramatically under three-stage RIM, recovers under four-stage RIM to about the level of one-stage RIM, and keeps increasing under five- and six-stage RIM, as shown in the eighth column of Table 1 and illustrated in Figure 7(b). This pattern is mainly determined by the number of

successful manipulations under different versions of RIM, and the larger is the successful manipulation number, the smaller is the student welfare. The sudden decrease under three-stage RIM is also on account of the optimal seat-transfer time in the third stage is the last round before the deadline, many students (both manipulation and non-manipulation students) are pushed out of admission lists and are not matched to any university and obtain zero utility.

The university welfare changes in the similar pattern of the student welfare as the state number of MS-RIM varies, as shown in the ninth column of Table 1 and illustrated in Figure 7(c). Because all universities have the identical preference to students according to their scores, the average university utility does not change no matter how the students and universities are matched as long as the quotas of all universities are fulfilled, and hence the university welfare is the same for one-stage and two-stage RIM because manipulation students transfer their seats very early and almost no student is pushed out at the last minute before the deadline under these two mechanisms. Under the three-stage RIM, however, all manipulation students in the third stage transfer their seats in the last round before the deadline, and many students are pushed out of admission lists of their applied universities and have no chance to resubmit their applications; hence, some universities cannot fulfill their enrolment quota and then obtain smaller utilities. The university welfare reduction under the four-, five-, and six-stage RIM is also due to the unfulfilled quota of universities, but the welfare reduction becomes smaller as the stage number increases thanks to the decline of the successful manipulation number.

The fairness index changes in a similar pattern, as shown in the ninth column of Table 1 and illustrated in Figure 7(d). More students feel unfair under the two-, three-, and four-stage RIM than under one-stage RIM, and fewer students are feeling unfair under five- and six-stage RIM. It can be expected that if there are enough many stages in an MS-RIM, the maximal score difference of the students in one stage will be smaller than the critical value for coordinating manipulation (*score_diff*) and there will be no coordinating manipulation anymore, and the social welfare and fairness reaches the maximum (equal to the value of the state with no manipulation ($\rho = 0$) in Figure 3). The results of the manipulation number, social welfare, and fairness are summarized as follows.

Result 5. Under MS-RIM with a small stage number, more students successfully conduct coordinating manipulation than one-stage RIM, and the social welfare and fairness are diminished; under MS-RIM with a large stage number, there are fewer successful manipulation students than one-stage RIM, and the social welfare and fairness are improved.

5. Conclusions

Matching plays an important role in several processes in our social system, such as dating, marriage, hiring, recommending, and more [26–30]. Here, we investigate another instance of matching: the college application and admission. The development of information and communication technology makes it possible for the college admission process to be automated online. The innovation of the matching algorithms in cyberspace can dramatically improve the efficiency of the corresponding process in physical space.

This paper studies the manipulation behaviors in the real-time interactive mechanism (RIM) recently adopted in Inner Mongolia of China and several other places globally. This mechanism has many advantages, such as transparency and real-time feedback. However, it is vulnerable to manipulation by the coordination of students. A high-score student can perform a last-minute switch on the university applied, opening a slot for a student with a much lower score. And this erodes the social welfare and fairness of the admission system.

Using the approach of agent-based modeling, we study the manipulation behavior in the real-time interactive mechanism. It is found that the benefit from manipulation is positive when there are few manipulation students but negative when manipulation occurs too frequently. Hence, a stable state where manipulation and nonmanipulation students have equal utility characterizes the outcome of the students' strategic choices. Simulations show that a large portion of students will choose to perform manipulation at the steady state and social welfare and fairness are damaged.

To cope with this issue, we investigate the multistage RIM (MS-RIM), where students with different ranges of scores are given different deadlines for application modification. By intensive simulations, we identify three effects of the multistage policy. It can reduce the chance of students to coordinate due to the different deadlines to submit applications. Nevertheless, it amplifies the students' incentive to conduct coordinating manipulation due to the scarcity of manipulation opportunity and consequent higher reward. Moreover, it helps to avoid the congestion that all manipulation students transfer their seats almost simultaneously and increases the success rate of the manipulation.

Due to the combined effects of multistage policy, more students conduct coordinating manipulation successfully under MS-RIM with a small number of stages, and the social welfare and fairness are diminished; while under MS-RIM with a larger number of stages, the successful manipulation number decreases and the social welfare and fairness are improved. However, a large number of stages imply that the mechanism needs to be executed for a very long time that may bring inconvenience. As an implication, some other policies are needed to really combat the coordinating manipulation in the real-time interactive mechanism, such as limiting the times that a student can resubmit his application unless he is pushed out of the admission list of the applied university.

Data Availability

The data used to support the findings of the study are available from the corresponding author upon request.

Conflicts of Interest

The authors declare that there are no conflicts of interest regarding the publication of this paper.

Acknowledgments

This work was supported partly by the National Natural Science Foundation of China (71201129 and 71561007), Fundamental Research Funds for the Central Universities (XDJK2016B008), Joint Fund Project in Science and Technology Department of Guizhou Province [Qian Ke He LH Zi [2017] 7001], and major projects of Natural Science Innovation Corps in Education Department of Guizhou Province [Qian Jiao He KY Zi [2017] 051].

References

[1] D. Gale and L. S. Shapley, "College admissions and the stability of marriage," *The American Mathematical Monthly*, vol. 69, no. 1, pp. 9–15, 1962.

[2] A. Abdulkadiroglu and T. Sonmez, "School choice: a mechanism design approach," *American Economic Review*, vol. 93, no. 3, pp. 729–747, 2003.

[3] Y. Chen and O. Kesten, "Chinese college admissions and school choice reforms: a theoretical analysis," *Journal of Political Economy*, vol. 125, no. 1, pp. 99–139, 2017.

[4] M. Zhu, "College admissions in China: a mechanism design perspective," *China Economic Review*, vol. 30, pp. 618–631, 2014.

[5] F. Li, "Economic thinking of the college admissions in China: comparison of the immediate acceptance mechanism, parallel mechanism and real-time dynamic mechanism," *Educational Research at Tsinghua University*, no. 5, pp. 48–55, 2011.

[6] P. A. Pathak, "The mechanism design approach to student assignment," *Annual Review of Economics*, vol. 3, no. 1, pp. 513–536, 2011.

[7] H. F. Nie, "A game-theoretical analysis of China's college admission mechanism," *China Economic Quarterly*, vol. 6, no. 3, pp. 899–916, 2007, in Chinese.

[8] A. Abdulkadiroglu, P. A. Pathak, A. E. Roth, and T. Sonmez, "The Boston public school match," *American Economic Review*, vol. 95, no. 2, pp. 368–371, 2005.

[9] H. Ergin and T. Sonmez, "Games of school choice under the Boston mechanism," *Journal of Public Economics*, vol. 90, no. 1-2, pp. 215–237, 2006.

[10] P. A. Pathak and T. Sonmez, "School admissions reform in chicago and england: comparing mechanisms by their vulnerability to manipulation," *American Economic Review*, vol. 103, no. 1, pp. 80–106, 2011.

[11] P. A. Pathak and T. Sönmez, "Leveling the playing field: sincere and sophisticated players in the Boston mechanism," *American Economic Review*, vol. 98, no. 4, pp. 1636–1652, 2008.

[12] Y. Chen and O. Kesten, "Chinese college admissions and school choice reforms: an experimental study," *Games and Economic Behavior*, vol. 115, pp. 83–100, 2019.

[13] G. Y. Shi, Y. X. Kong, B. L. Chen, G. H. Yuan, and R. J. Wu, "Instability in stable marriage problem: matching unequally numbered men and women," *Complexity*, vol. 2018, Article ID 7409397, 2018.

[14] Y. X. Kong, G. H. Yuan, L. Zhou, R. J. Wu, and G. Y. Shi, "Competition may increase social utility in bipartite matching problem," *Complexity*, vol. 2018, Article ID 4092056, 2018.

[15] G. Haeringer and F. Klijn, "Constrained school choice," *Journal of Economic Theory*, vol. 144, no. 5, pp. 1921–1947, 2009.

[16] R. M. Antonio, "Implementation of stable solutions in a restricted matching market," *Review of Economic Design*, vol. 3, no. 2, pp. 137–147, 1998.

[17] C. Calsamiglia, G. Haeringer, and F. Klijn, "Constrained school choice: an experimental study," *American Economic Review*, vol. 100, no. 4, pp. 1860–1874, 2010.

[18] I. Bo and R. Hakimov, *The Iterative Deferred Acceptance Mechanism*, SSRN, Rochester, NY, USA, 2018.

[19] I. Bo and R. Hakimov, "Iterative versus standard deferred acceptance: experimental evidence," *The Economic Journal*, vol. 130, no. 626, pp. 356–392, 2020.

[20] F. Klijn, J. Pais, and M. Vorsatz, "Static versus dynamic deferred acceptance in school choice: theory and experiment," *Games and Economic Behavior*, vol. 113, pp. 147–163, 2019.

[21] Inner Mongolia Admissions and Exam Infor-Net. Notice on the 2020 Inner Mongolia Gaokao College Application Submission. https://www.nm.zsks.cn/ptgxzs/ggl/202007/t20200720_40198.html.

[22] J. M. Epstein, "Agent-based computational models and generative social science," *Complexity*, vol. 4, no. 5, pp. 41–60, 1999.

[23] S. H. Chen, *Agent-Based Computational Economics: How the Idea Originated and where It is Going*, Routledge, New York, NY, USA, 2017.

[24] S.-H. Chen, C. H. Wang, and W. Chen, "Matching impacts of school admission mechanisms: an agent-based approach," *Eastern Economic Journal*, vol. 43, no. 2, pp. 217–241, 2017.

[25] C. H. Wang, B.-T. Chie, and S.-H. Chen, "Transitional student admission mechanism from tracking to mixing: an agent-based policy analysis," *Evolutionary and Institutional Economics Review*, vol. 14, no. 1, pp. 253–293, 2017.

[26] E. E. Bruch and M. E. J. Newman, "Aspirational pursuit of mates in online dating markets," *Science Advances*, vol. 4, no. 8, 2018.

[27] Y. Xie, S. Cheng, and X. Zhou, "Assortative mating without assortative preference," *Proceedings of the National Academy of Sciences*, vol. 112, no. 19, pp. 5974–5978, 2015.

[28] T. Jia, R. F. Spivey, B. Szymanski, and G. Korniss, "An analysis of the matching hypothesis in networks," *PLoS One*, vol. 10, no. 6, 2015.

[29] P. Haller and D. F. Heuermann, "Job search and hiring in local labor markets: spillovers in regional matching functions," *Regional Science and Urban Economics*, vol. 60, pp. 125–138, 2016.

[30] L. Lü, C. H. Yeung, Y.-C. Zhang, Z.-K. Zhang, and T. Zhou, "Recommender systems," *Physics Reports*, vol. 519, no. 1, pp. 1–49, 2012.

Hindawi
Complexity
Volume 2020, Article ID 5642730, 12 pages
https://doi.org/10.1155/2020/5642730

Research Article

Associated Credit Risk Contagion with Incubatory Period: A Network-Based Perspective

Kai Xu,[1] **Jianming Mo**,[2] **Qian Qian**,[3] **Fengying Zhang**,[4] **Xiaofeng Xie**,[5] **and Zongfang Zhou**[6]

[1]*Business School, Chengdu University, No. 2025, Chengluo Avenue, Longquanyi District, Chengdu 610106, China*
[2]*Chinese Finance Research Institute, Southwestern University of Finance and Economics, No. 55, Guanghua Village Road, Wenjiang District, Chengdu 610074, China*
[3]*School of Business, Sichuan Normal University, No. 5, Jinan Road, Jinjiang District, Chengdu 610101, China*
[4]*West China School of Nursing, Sichuan University, No. 37, Guoxuexiang, Wuhou District, Chengdu 610041, China*
[5]*West China School of Nursing/West China Hospital, Sichuan University, No. 37, Guoxuexiang, Wuhou District, Chengdu 610041, China*
[6]*School of Management and Economics, University of Electronic Science and Technology of China, No. 2006, Xiyuan Avenue, High-Tech District, Chengdu 611731, China*

Correspondence should be addressed to Kai Xu; xukai@cdu.edu.cn

Received 9 January 2020; Revised 20 June 2020; Accepted 17 July 2020; Published 17 August 2020

Academic Editor: Dehua Shen

Associated credit risk is a kind of credit risk among the associated credit entities formed by credit-related entities. Focusing on this hot topic of associated credit risk and the relevant contagion and considering the latent entities and their incubatory period, this paper builds an infectious dynamic model to describe the associated credit risk contagion of associated credit entities based on the mean-field theory of complex networks. Firstly, this paper analyzes the stable state of the associated credit risk contagion in the associated entity network, considering the latent entities and their incubatory period. Secondly, from the perspective of complex network and considering the incubatory period, a SHIS model is built to reveal how the incubatory period influences associated credit risk contagion. Finally, the sensitivity of some parameters is analyzed in the Barabási–Albert (BA) scale-free network. The results show the following: (i) the contagion threshold of associated credit risk is related to the incubatory period of latent entities, the recovery rate and infectivity of infected entities, and the newborn rate of credit entities; (ii) the infectious rate of infected entities, the mortality rate of credit entities, and the important factors stated in (i) are all significantly correlated with the density of infected entities.

1. Introduction

At present, the concept of credit risk has not formed a unified definition [1]. The conventional view is that credit risk refers to the risk that the counterparty or borrower is unable or unwilling to perform the contract; that is, the possibility that the default caused by the debtor's failure to repay the debts in the contract on time will bring losses to the creditors [1]. Nowadays, the world economic development has entered a new stage, and the credit relationship among enterprises, banks, insurance companies, and other credit entities is becoming increasingly closer and more extensive, thus forming associated credit entities. If the default of some credit entities increases the defaults or the default probability of the other credit entities that are associated with them, this credit risk is then called the associated credit risk among the associated credit entities [2]. It can be seen that the associated credit risk is a special kind of credit risk.

The U.S. subprime mortgage crisis spread rapidly to many countries around the world and eventually led to the bankruptcy or reorganization of several well-known investment banks, commercial banks, and insurance companies, resulting in turmoil in the entire financial market in 2008. The phenomenon appears that some subprime

borrowers have failed to repay their loans on time in the early spring of 2006, and this subprime mortgage crisis swept through major financial markets in the world, such as the United States and the European Union in August 2007. So the incubatory period of associated credit risk is noticeable. Affected by above subprime crisis, Greece's sovereign credit was downgraded, causing the European debt crisis to erupt and spread rapidly throughout the euro area at the end of 2009. It lasts for a long time from subprime crisis to European debt crisis, and these two big finance crises both cause significant fluctuations and losses of the global economy, which are both called systemic risk according to the literature [3]. The core of systemic risk concern is contagious [4]. Credit risk is a kind of nonsystemic risk, the core of credit risk concern is the credit entities' default, and the credit risk is also contagious [4]. If an entity does not pay enough attention to the incubatory period of associated credit risk and do not guard against credit risk in the incubatory period, it is likely that systemic financial risk will be caused by credit risk contagion, and just like above subprime crisis and European debt crisis mentioned, the regional economy and even the global economy will be severely damaged. Therefore, when identifying the associated credit risk and exploring the evolutionary law of associated credit risk contagion, the incubatory period of the associated entity should be considered.

For the evolutionary mechanism of the associated credit risk contagion, the above studies may be more reasonable if considering the latent entities and incubatory period. In fact, in the early stage of the contagion and evolution of associated credit risk, some credit entities have high credit levels including strong operational capability, highly profitable and liquidity, and reasonable governance structures. These credit entities have a specific resistance to the associated credit risk, which may have been infected, but the symptoms of the credit risk have not been shown, or they are unwilling to disclose or even intentionally hide their own credit risk for themselves. This period of hiding credit risk is called the incubatory period. However, with the increase in the ability of the associated credit risk to infect the associated entities and the change in the internal and external environment of the credit entities, the risk incubatory period of the latent entities may come to an end, and they may become infected entities with high credit risk. After effective control and management, such as rescue or immunization, the infected entities decrease their own credit risk, which may become susceptible entities again. Credit risk evolves in the associated entity network.

To summarize, in this paper, based on the classical SIS epidemiological model, a SHIS derived model is constructed to study associated credit risk contagion in an associated entity network to reveal the influence of incubatory period and relevant parameters on credit risk contagion. The highlights of this paper are to make use of the SHIS infectious dynamics model and introduce latent entities and the incubatory period to characterize the evolutionary contagion mechanism of associated credit risk in the associated entity network.

The remainder of this paper is organized as follows: Section 2 is an analysis of epidemiological model applied to associated credit risk contagion; Section 3 is a literature overview; Section 4 is a description of the basic epidemiological model; Section 5 includes assumptions, derived epidemiological model construction, and theoretical analysis; and Section 6 presents our simulation analysis of the derived epidemiological model. By using simulation software, we analyze the influence of different factors on associated credit risk contagion, including incubatory period. Section 7 is the conclusion of this paper and the prospects for future work.

2. Feasibility Analysis of Epidemiological Model Applied to Associated Credit Risk Contagion

May et al. find that financial risk contagion is similar to the epidemic spread, so the epidemiological model is used to describe the contagion of financial risk [5]. Luo et al. and Xu et al. also pointed out that risk contagion in the guarantee network is similar to the virus spread and briefly described similarity characteristic between them [6, 7]. Based on the previous research results, combined with the infectious evolution characteristics of the associated credit risk, we find that the infectious evolution of the associated credit risk in the associated entity network has many similarities with the spreading of the epidemic virus in the social network. For example, there is being infectious source, infectivity, immunity, and reversibility of circulation.

The evolution process of epidemic virus is similar to that of associated credit risk, which shows two kinds of characteristics: one is the similarity of infectious structure, and the other is the similarity of infectious mode. The infectious structure includes diffusion channels and infection targets, and the infectious mode includes infectious radiation and infectious process. The details are listed as follows.

The infectious structure is similar. The epidemic virus spreads in the social group network composed of individuals, the spreading channel is the path of the social group network which is the mutual relationship between individuals, and the spreading goal of the epidemic virus is the individual node of the social group network. However, the contagion of associated credit risk is spreading in the associated entity network, the spreading channel is the direct or indirect relationship between the associated entities, and the spreading goal of the associated credit risk is the node of associated entity network. Furthermore, due to the difference in individual autoimmunity in the social group network, the ability of resisting virus invasion is different. However, due to the difference in governance level (including operation, financing, profitability, and solvency) of associated entities in the associated entity network, the ability of resisting associated credit risk is also different. Therefore, in terms of infection structure, associated credit risk and epidemic virus are similar.

The infectious mode is similar. The spread of epidemic virus in the social group network takes the shape of radiation, while the associated entities with credit risk have radiation negative effects on other associated entities in the associated entity network. In addition, the virus generally

spreads through contacts in the contagion process of epidemic, while in the contagion process of associated credit risk, a node entity with credit risk is also preferred to have negative effects on the associated entity that has direct relationship with the infected node entity. Therefore, in terms of infectious mode, associated credit risk and epidemic virus are similar.

3. Literature Overview

This paper is closely related to three strands of the existing literature. First, our paper is linked to work on financial network and contagion. Second, our analysis is closely related to work on epidemiological model and credit risk contagion. The third strand of relevant literature investigates the associated credit risk contagion and relevant delayed effects.

First, this paper is linked to existing work on financial network and contagion. Elliott et al. studied the financial contagions and cascades of failures affected by integration and diversification in a network of financial interdependencies [8]. Based on susceptible-infected-recovered (SIR) model, Fisher established the financial network contagion model and found that shocks in this financial market exhibit complex evolutionary dynamics that either tend to increasingly fragile states or the elimination of a high number of competitors, detrimental to a more decentralized market order [9]. Unlike Fisher, Eboli represented a financial system as a flow network and model the process of direct balance-sheet contagion as a flow of losses crossing such a network and focused most of the analysis on the effects that the connectivity and centralization of a financial network have on its exposure to default contagion and then found that both the complete and the star networks show a robust yet fragile response to shocks [10]. Gencay et al. discussed that network uncertainty gives rise to an endogenous core-periphery structure which is optimal in mitigating financial contagion yet concentrates systemic risk at the core of big banks [11]. Dastkhan and Gharneh introduced a simulation model to analyze the contagion in financial markets based on the cross shareholding network of firms and the probability and the extent of contagion [12]. Bucci et al. developed an epidemiological approach to analyze the mutual influence between financial contagion and economic activity and showed that financial contagion in some specific regions may propagate quickly also in regions far away from those in which the contagion initially occurs, highlighting the role of regional policy coordination to avoid interregional contagion [13]. Hu and Li put epidemiological model into scale-free financial network and discuss the influence of infection rate on financial risk contagion [14].

In order to prevent financial and economic crisis, Dastkhan applied the forward-looking conditional value at risk (COVaR) as a market-based systemic risk measure to analyze the systemic risk in an emerging market and predict financial crisis [15]. However, Sarlin evaluated the performance of biologically inspired early warning systems for systemic financial crises based on a logit model, a standard back-propagation neural network, and a neurogenetic model [16]. Giudici et al. applied correlation network models that tap into the multivariate network structure, as a viable means to assess common exposures and complement direct linkages, and found that common exposures indeed are channels of contagion and should be accounted for when measuring systemic risk [17]. Apergis et al. found contagion occurred during the recent global financial crisis across European and US financial markets through the channels of higher order moments [18].

Second, this paper is closely related to work on epidemiological model and credit risk contagion. Chakrabarty and Zhang examined the negative consequences of the contagion effect using variables, such as the number of transactions, the size of transactions, and the volume of transactions [19]. Jorion et al. found that affiliated transactions lead to credit risk contagion among enterprises, and counterparty default is the potential cause of credit risk contagion [20]. Through numerical simulation, the contagion mechanism caused by the business relationships among enterprises in bank loan portfolios was studied [21]. Based on the epidemiological model, a network model is built with consideration of investor behavior and information disclosure strategy, and the mechanism of counterparty credit risk contagion is analyzed [22]. A counterparty credit risk contagion network evolution model SIRS is developed to study counterparty credit risk contagion in the CRT market and its influencing factors [23]. Chen et al. studied the causes, mechanisms, and control strategies of credit risk contagion among CDS counterparties and found that information asymmetry and innovation diffusion could cause credit risk contagion among CDS counterparties [24]. Later, Chen et al. introduced an evolving network model of credit risk contagion in the credit risk transfer (CRT) market and described the influence and active mechanism of the spillover effects of infected investors, behaviors of investors and regulators, emotional disturbance of investors, market noise, and CRT network structure on credit risk contagion [25]. However, Li et al. studied the credit risk with an affiliated guarantee relationship and found that the contagion intensity of credit risk was positively correlated with the proportion of equity [26]. Yang and Hu studied the risk contagion model of China's interbank market, characterized the interbank network structure by using a core-edge network, and found that the ability of Chinese banks to withstand risks has improved in recent years [27]. Wu et al. found that changes in bank credit ratings can cause risk contagion within the bank network that is composed of interbank lending relationships [28]. Based on the SIR model, Wang et al. built a network model with the consideration of investor behavior and information disclosure strategy and analyzed the mechanism of counterparty credit risk contagion [29]. Jiang et al. proposed two credit risk contagion models separately considering asymmetric information association and sentiment contagion and further analyzed the influence of network structure, information association, individual risk attitude, financial market supervision intensity, and individual risk resisting ability on individual risk contagion [23, 30]. It can be seen that the above-mentioned counterparty risk, correlation,

information asymmetry, authenticity, sentiment, and network structure trigger the credit risk contagion. Besides, Giusy et al. investigated the relationship between exposure to climate change and firm credit risk and indicated that the exposure to climate risks affects the creditworthiness of loans and bonds issued by corporates [31].

A lot of literature has emerged on sovereign credit default contagion. De Bruyckere et al. investigated contagion between bank and sovereign default risk in Europe over the period 2007–2012, and empirical certified that three contagion channels are at work: a guarantee channel, an asset holdings channel, and a collateral channel [32]. Breckenfelder and Schwaab studied spillovers from bank to sovereign risk in the euro area and surprisingly found that bank risk in stressed countries was not absorbed by their sovereigns but spilled over to nonstressed euro area sovereigns [33]. Greenwoodnimmo et al. developed an empirical network model to study credit risk spillovers among a group of eighteen sovereigns and their financial sectors from 2006 to 2015 [34]. Srivastava et al. applied an error correction model to document strong evidence of Granger causality in mean from the S&P option market to the sovereign CDS market in 98% of the 56 sovereigns [35]. Bostanci and Yilmaz studied the network structure of the volatility of the sovereign credit default swaps spreads and found that both trade and capital flows are important determinants of pairwise connectedness across countries [36].

Finally, this work is closely related to literature on associated credit risk contagion and relevant delay effect. Xu et al. combined an epidemic model and complex network theory and explored the impacts of risk information and individual responses on associated credit risk [37]. Based on the improved epidemiological model, Qian et al. studied the stable state characteristics of the associated credit risk contagion in immunization scenarios [38]. Based on the theory of infectious diseases, Li et al. established a stochastic dynamic model of credit risk contagion in enterprise groups and analyzed the stable condition of the model and the arrival time of default peaks [39]. Qian et al. constructed a dual-layer network and found that entrepreneurs' spreading willingness and the authenticity of information will affect the associated credit risk contagion [40]. The above literature research lays the theoretical foundation for this paper to use an epidemiological model and complex network theory to study the associated credit risk contagion.

About the delayed effects in complex networks, many studies related to viruses or infectious diseases are often presented. These literatures consider delay or incubatory period and study the propagation dynamics properties of virus including threshold, global stability, and immune strategy [41–45], which inspires us to study the credit risk contagion with incubatory period. Viviana and Lucia proposed a particular time-delay susceptible-infected-recovered model to investigate and describe the credit risk contagion in the market and studied the steady states according to different values of time delay and different bank support policies [46]. Li et al. studied the delayed effect of the contagion of associated credit risk in scale-free and small-world networks and further explored the impact of immune failure and immune invalidity on the contagion of the associated credit risk under incomplete immunization [2, 47, 48]. Based on above literatures, we consider the incubation period to study the associated credit risk contagion in the associated entity network.

4. Basic Epidemiological Model

Many social, biological, and communication systems can be properly described by complex networks whose nodes represent individuals or organizations and links mimic the interactions among them [49, 50]. The following main approaches were borrowed from biological epidemiology. The standard model used in the study of computer virus infections is the susceptible-infected-susceptible (SIS) epidemiological model [51]. In this SIS model, each node of the network represents an individual and each link is a connection along which the infection can spread, and individuals exist only two discrete states: "healthy" or "infected." At each time step, each susceptible (healthy) node is infected at rate ν if it is connected to one or more infected nodes. Infected nodes are cured and become again susceptible at rate δ, defining an effective spreading rate $\lambda = \nu/\delta$. Without loss of generality, we can set $\delta = 1$. This SIS model does not take into account immunization, and individuals run stochastically through the cycle susceptible $\longrightarrow$ infected $\longrightarrow$ susceptible. Thus, based on the SIS epidemiological model and literature [51], the dynamical mean field equation (1) is established as

$$\begin{cases} \dfrac{dS_k(t)}{dt} = I_k(t) - \lambda k\left[1 - I_k(t)\right]\Theta\left(I_k(t)\right), \\ \dfrac{dI_k(t)}{dt} = -I_k(t) + \lambda k\left[1 - I_k(t)\right]\Theta\left(I_k(t)\right), \end{cases} \tag{1}$$

where density $I_k(t)$ of infected nodes with given connectivity k, i.e., the probability that a node with k links, is infected [51]. The first formula of equation (1) considers infected nodes becoming healthy with probability $\delta = 1$. The second formula of equation (1) represents the density of newly generated infected nodes that is to the infection rate λ and the probability that a node with k links is healthy $[1 - I_k(t)]$ and obtains the infection via a connected node [38]. $\Theta(I_k(t))$ with any given link points to an infected node, which can be written as

$$\Theta\left(I_k(t)\right) = \frac{1}{\langle k\rangle}\sum_k kP\langle k\rangle I_k(t). \tag{2}$$

Through solving equations (1) and (2) in the stationary state $[dI_k(t)/dt = 0]$, the below self-consistency (3) is obtained [38] as

$$\Theta\left(I_k(t)\right) = \frac{1}{\langle k\rangle}\sum_k kP\langle k\rangle \frac{\lambda k\Theta\left(I_k(t)\right)}{1 + \lambda k\Theta\left(I_k(t)\right)}, \tag{3}$$

where $\Theta(I_k(t))$ is a function of λ. The self-consistency equation (3) allows the condition $\lambda\langle k^2\rangle/\langle k\rangle \geq 1$ only if

$\Theta(I_k(t)) \neq 0$ and $I_k(t) \neq 0$, so the epidemic threshold is defined as

$$\lambda_c = \frac{\langle k \rangle}{\langle k^2 \rangle}, \tag{4}$$

where $\langle k^2 \rangle$ is the second moment of degree distribution. If λ is above the threshold, i.e.,$\lambda \geq \lambda_c$, the infection spreads and becomes possible. Otherwise, $\lambda \leq \lambda_c$, and the infection dies out exponentially [51].

5. Derived Epidemiological Model

5.1. Assumptions. For the convenience of the research, this paper proposes the following assumptions based on the characteristics of the contagion evolution of associated credit risk.

Assumption 1: In the network composed of N associated entities, the associated entities exist only in three discrete states, "susceptible," "latent," or "infected," which are divided into three categories: susceptible entities, latent entities, and infected entities.

(1) Susceptible entity S: in the associated entity network, the susceptible entity refers to the entity with a lower credit risk that is vulnerable to be infected by the high credit risk entity associated with it, thus increasing the possibility of becoming a high credit risk entity. This kind of credit entity's own credit risk is at a low level, but it is easy to be infected by the high credit risk entity, and it is easier to be infected by the high credit risk entity closely related to it. For example, those enterprises and financial institutions with excessive financial leverage, high asset-liability ratio, and temporary shortage of cash flow are vulnerable to be infected by the credit risk because their ability to resist credit risk is weakened. There are a large number of them in the network of associated entities. Once infected, some susceptible entities need self-protection and operation and are unwilling to disclose or even intentionally hide their real credit risk. This period of hiding their own real credit risk is called incubatory period. These susceptible entities in incubatory period are transformed into latent entities.

(2) Latent entity H: in the associated entity network, the latent entity refers to the entity which has been infectious, and its credit risk is at a little high level but cannot infect other associated entities. That is, this kind of credit entity cannot enlarge the credit risk of other credit entities through the relationship between them. For example, those enterprises and financial institutions with profit margin remained at a high level, high accounts receivable, and high debt ratio, which have weak linkages with other susceptible entities. Under the influence of own internal factors and external macroenvironment, after some time τ ($\tau \geq 0$, incubatory period), such entities with high credit risk are transformed into infected entities.

(3) Infected entity I: in the associated entity network, the infected entity refers to the entity which has been infectious, and its credit risk is at an extremely high level and can infect the associated entities. That is, this kind of credit entity can magnify the credit risk of other credit entities through the relationship between them. The change in the proportion in the network indicates the contagion effect of associated credit risk. For example, those enterprises and financial institutions have suffered from severe operational problems such as long-term losses, insolvency, and serious shortage of cash flow.

Assumption 2: A susceptible entity can be changed into a latent entity at an invariant probability λ through the correlation with an infected entity. In this network, before a susceptible entity can be changed into an infected entity, it must undergo an incubatory period, and the latent entity can only be changed into an infected entity. Here, λ is the contagion probability ($0 < \lambda \leq 1$) of associated credit risk, which expresses the speed of contagion and diffusion of the associated credit risk in the network of associated entities. Infected entities are not immune and become susceptible entities after being cured or recovered. At this moment, if the susceptible entities contact an infected entity because of the relationship, they will be infected with a certain probability λ.

Assumption 3: An infected entity will be cured at a rate of δ and become susceptible entity, where δ is the recovery rate ($0 < \delta \leq 1$).

An associated entity network that is composed of associated entities is always dynamically changing. There are usually credit entities entering the network, and there will also be credit entities that naturally disappear or leave the network. In general, there is the following assumption.

Assumption 4. A credit entity that enters the network anew is called a newborn, and the new rate is M. Assume this newborn entity is susceptible. A credit entity that naturally disappears or withdraws from the network is dead, and the death rate is m. Suppose this dead entity is infected entity. The associated entity network is in the process of continuous development and expansion and so $0 < m \leq M < 1$.

5.2. Derived Model Construction. In a complex network of associated entities that is composed of N associated credit entities, the credit entities are nodes in the network, and the relationships among the nodes are the edges of the network. The degree k_i of node entity i is defined as the number of edges that are connected to the entity. The average of the degree k_i of all nodes in the network is called the network average, and it is denoted as $\langle k \rangle$. Denote $P(k_i)$ as the probability of randomly selecting a node i with degree k_i and so $\langle k \rangle = \sum_{i=1}^{n} k_i P(k_i)$. The densities of susceptible entities,

latent entities, and infected entities at time t and degree k are expressed as $S_k(t)$, $H_k(t)$, and $I_k(t)$, respectively, and here, the density is the proportion. Therefore,

$$S_k(t) + H_k(t) + I_k(t) = 1. \tag{5}$$

$P(t)$ denotes the probability that a credit entity is still in the incubatory state within period t after it enters the incubatory state (without considering death), and therefore, $\lim_{t\longrightarrow\infty} P(t) = 0$, $\lim_{t\longrightarrow 0} P(t) = 1$, and $\int_0^{\infty} P(v)dv$ is a finite positive number.

Considering the actual situation of enterprise type, nature, strength, and operation management, there are two typical situations. The first is that there are susceptible entities (S), latent entities (H), and infected entities (I) in the associated entity network. The second is that there are susceptible entities (S), latent entities (H), infected entities (I), and recovery entities (R) in the associated entity network. The first typical situation is studied in this paper, in which situation, S, H, and I are defined in Section 5.1.

It is assumed that there are only susceptible entities (S) in the associated entity network at the beginning. With the change in external objective macroenvironment and internal subjective factors, some susceptible entities with highly profitable and liquid and reasonable governance structures may be infected, but these credit entities have some specific resistance to the associated credit risk, and the symptoms of the credit risk have not been shown, which are called hidden entities (H). However, with the increase in infectious capacity of associated credit risk and the change in the internal and external environments of the credit entities, hidden entities may become infected entities (I). After effective control and management, such as rescue or immunization, the infected entities may get out of trouble and decrease their own credit risk, which may become susceptible entities (S) again. Credit risk evolves in the associated entity network. Therefore, the epidemiological model describing this kind of station is the susceptible $\longrightarrow$ incubatory $\longrightarrow$ infected $\longrightarrow$ susceptible (SHIS) model.

According to the above basic epidemiological model, hypothesis, and using dynamic mean-field theory, the first equation of the SHIS model can be described as

$$\frac{dS_k(t)}{dt} = M - \lambda k S_k(t)\Theta(t) - mS_k(t) + \delta I_k(t), \tag{6}$$

where M is described in Assumption 4, $\lambda k S_k(t)\Theta(t)$ denotes the decrease of susceptible entities due to infection, $mS_k(t)$ denotes the decrease of susceptible entities due to death, and $\delta I_k(t)$ denotes the increase of susceptible entities that come from infected entities due to treatment.

The second equation of SHIS model can be described as

$$H_k(t) = \int_0^t \lambda k S_k(\eta)\Theta(\eta)e^{-M(t-\eta)}P(t-\eta)d\eta, \tag{7}$$

where $H_k(t)$ denotes the number of susceptible entities entering into latent entities due to infection and e^{-zt} denotes the probability that a credit entity is still in the incubatory state within period t after it enters the incubatory state (without considering death). $\Theta(t)$ denotes that any given link points to an infected node at time t, and the degree-independent network is considered in this paper. Therefore, $\Theta(t)$ can be written as

$$\Theta(t) = \frac{1}{\langle k\rangle}\sum_{i=1}^{n}\varphi(i)P(i)I_i(t), \tag{8}$$

where $\varphi(k)$ is the infectivity function of the nodes with degree k.

Equation (7) is the Riemann–Stieltjes integral, and so

$$\frac{dH_k(t)}{dt} = \lambda k S_k(t)\Theta(t) + \int_0^t \lambda k S_k(\eta)\Theta(\eta)e^{-M(t-\eta)}M_t P(t-\eta)d\eta - MH_k(t). \tag{9}$$

The third equation (9) of SHIS model can be described as

$$\frac{dI_k(t)}{dt} = \int_0^t \lambda k S_k(\eta)\Theta(\eta)e^{-M(t-\eta)}M_t P(t-\eta)d\eta - (\delta + M)I_k(t). \tag{10}$$

Simplifying equation (10), we get

$$\frac{dI_k(t)}{dt} = \lambda k e^{-M\tau}S_k(t-\tau)\Theta(t-\tau) - (\delta + M)I_k(t), \tag{11}$$

where $\lambda k e^{-M\tau}S_k(t-\tau)\Theta(t-\tau)$ denotes the number of latent entities entering into infected entities due to infection, $\delta I_k(t)$ denotes the decrease of infected entities due to treatment, and $MI_k(t)$ denotes the decrease due to the newborn.

The SHIS model is complex and challenging to study. Therefore, only the probability function $P(t)$ is taken as the following state function:

$$P(t) = \begin{cases} 1, & t \in [0, \tau], \\ 0, & t > \tau, \end{cases} \tag{12}$$

where $t > \tau$, obtained from equation (9) as

$$\frac{dH_k(t)}{dt} = \lambda k S_k(t)\Theta(t) - \lambda k e^{-M\tau}S_k(t-\tau)\Theta(t-\tau) - MH_k(t), \tag{13}$$

where $0 \le t \le \tau$, obtained from equation (9) as

$$\frac{dH_k(t)}{dt} = \lambda k S_k(t)\Theta(t) - MH_k(t). \tag{14}$$

5.3. Theoretical Analysis. Equations (6), (7), and (10) depict the transformation relationship among the susceptible entities, latent entities, and infected entities. After a period of contagious evolution, if the contagion of the associated credit risk in the associated entity network is in a long-term disordered and uncertain state, the associated entity network is considered to be in an unstable state. Conversely, if the contagion of the associated credit risk tends to be stable, that is, the densities of the three types of entities in the associated entity network tend to be stable, the associated entity

network is considered to be in a stable state. This paper focuses on this stable state, that is, the stable risk state. Furthermore, in this stable risk state, the density of infectious agents in the associated entity network tends to be constant.

Therefore, in order to conduct the research conveniently, when $t > \tau$, this paper only discusses the following equation:

$$\frac{dI_k(t)}{dt} = \lambda k e^{-M\tau} S_k(t-\tau)\Theta(t-\tau) - (\delta + M) I_k(t). \quad (15)$$

The analytic solution of equation (15) is not easy to find, and the solution under a stable risk state is considered instead. The densities of the susceptible entities and infected entities with a degree k in the stable state are S_k^* and I_k^*, respectively; S^* and I^* are the densities of susceptible entities and infected entities in the whole associated entity network in stable state, respectively. The probability of a random edge being connected to an infected entity in a stable state is Θ^*.

Definition 1. When the contagion probability λ of the associated credit risk is less than a specific probability value λ_c, the associated credit risk is no longer contagious in the associated entity network, where λ_c is called the contagion threshold of the associated credit risk in the associated entity network.

Proposition 1. *The contagion threshold of the associated credit risk considering the incubatory period is $\lambda_c = (\delta + M)\langle k\rangle e^{M\tau}/\langle \varphi(k)\rangle$. When $\lambda < \lambda_c$, the associated credit risk is no longer contagious in the associated entity network, and equations (6), (7), and (10) converged to the equilibrium point $(M/m, 0)$; when $\lambda > \lambda_c$, equations (6), (7), and (10) converged to the equilibrium point (S^*, I^*).*

Proof. In the stable state, $dS_k(t)/dt = 0$ and $dI_k(t)/dt = 0$, and the solution of equations (6) and (11) in the stable state is obtained as

$$\begin{cases} S_k^* = \dfrac{M + \delta I_k^*}{\lambda k \Theta^* + m}, \\ I_k^* = \dfrac{\lambda k M \Theta^* e^{-M\tau}}{(\delta + M)(\lambda k \Theta^* + m) - \lambda k \delta e^{-M\tau}\Theta^*}, \end{cases} \quad (16)$$

where $\Theta^* = (1/\langle k\rangle)\sum_{i=1}^{n} \varphi(i) P(i) I_i^*$.

The following formula of equation (16) is put into equation (8), where Θ^* satisfies the self-consistency condition, obtained as

$$\Theta^* = \frac{1}{\langle k\rangle}\sum_{i=1}^{n} \varphi(i) P(i) \frac{\lambda i M \Theta^* e^{-M\tau}}{(\delta + M)(\lambda i \Theta^* + m) - \lambda i \delta e^{-M\tau}\Theta^*} = f(\Theta). \quad (17)$$

$\Theta^* = 0$ is a trivial solution of equation (11). Besides, $f(\Theta)$ is continuously differentiable, obtained as

$$f'(\Theta) = \sum_{i=1}^{n} \varphi(i) P(i) \frac{M^2 e^{M\tau}}{\langle k\rangle \lambda i (\delta + M)\delta^2 \Theta^2 (\lambda i \Theta + m)^2} > 0. \quad (18)$$

$f(\Theta)$ increases with Θ. When $f'(\Theta)|\Theta_{=0} > 1$, namely, $\lambda e^{-M\tau}\langle \varphi(k)\rangle/(\delta + M)\langle k\rangle > 1$, and there is a nontrivial solution to equation (17) within $0 < \Theta^* < 1$, and the contagion threshold is obtained as $\lambda_c = (\delta + M)\langle k\rangle e^{M\tau}/\langle \varphi(k)\rangle$. When this nontrivial solution Θ^* is put into (16), S_k^* and I_k^* are both obtained. Because $S^* = \sum_k P(k) S_k^*$ and $I^* = \sum_k P(k) I_k^*$, the equilibrium point (S^*, I^*) exists.

From the expression of λ_c, it is found that the contagion threshold of associated credit risk is not only related to the topological structure of the network but also related to the recovery rate of the infected entity, the newborn rate of the credit entity, the incubatory period of the latent entity, and the contagion ability function of the infected entity. As the recovery rate increases, the contagion threshold of the associated credit risk increases. As the freshness of the credit entity increases, the contagion threshold of the associated credit risk increases. As the incubatory period of the possible entity increases, the contagion threshold of associated credit risk increases. Finally, as the contagion ability of the infected entity increases, the contagion threshold of associated credit risk decreases. In next section, more detailed discussion will be studied by simulation analysis under some assumptions.

6. Simulation Analysis

In this section, the simulations are analyzed in BA scale-free network. The associated entity network is a complex system of multientities, multilinks, multitasks, self-organization, and self-learning. In recent years, with the evolution of the macroenvironment, such as market and microindividual factors, the associated entity network has presented complex network characteristics. In the associated entity network, there are a few entities that are connected with more related entities; there are also situations in which most entities are only connected with other minority entities, that is, preferential connectivity; and most of the real-world network scale is expanding, that is, growth. Therefore, the network presents scale-free characteristics. The existing literature shows that scale-free networks can accurately depict the characteristics of interbank overnight lending networks, intercountry banking networks, and different stock market networks [5–7] that can be used to study the contagious characteristics of associated credit risks [26, 27, 52]. In view of this, this paper chooses the BA scale-free network to analyze the contagious evolutionary law of the credit risk of associated entities. In the BA scale-free network, if k is continuous, the network's average degree is $\langle k\rangle = \int_w^{+\infty} kP(k)dk = 2w$, and the node degree distribution is $P(k) = 2w^2k^{-3}$, where w is the smallest degree of credit entity in the network.

Concerning the contagion ability function $\varphi(k)$, in order to get close to the real risk contagion network and better study the infectious characteristics of associated credit risk, the assumption of piecewise linear infectivity is adopted to describe $\varphi(k)$ in this paper [18], namely, $\varphi(k) = \min(\alpha k, A)$. When the degree k of an entity node is small, its contagion capacity is proportional to k, which is $\varphi(k) = \alpha k$. When k is overwhelmingly large and over one constant A/α, its

contagion capacity is A, namely, $\varphi(k) = A$. Here, $A > 0$ is a constant parameter where $0 < \alpha \leq 1$.

In BA scale-free networks, when $\varphi(k) = \alpha k$, the contagion threshold of associated credit risk is as

$$\lambda_c = \frac{(\delta + M)\langle k\rangle e^{M\tau}}{\langle \varphi(k)\rangle} = \frac{(\delta + M)e^{M\tau}}{\alpha}, \tag{19}$$

where $\varphi(k) = A$. The contagion threshold of associated credit risk is as

$$\lambda_c = \frac{(\delta + M)\langle k\rangle e^{M\tau}}{\langle \varphi(k)\rangle} = \frac{2(\delta + M)we^{M\tau}}{AP(A)}, \tag{20}$$

where $P(A) > 0$ is a constant and $AP(A) > 0$ is also a constant. To simplify the research, the network in the real world is limited, so $\varphi(k) = \alpha k$.

From the expression λ_c of equations (19) and (20), it is found that the contagion threshold of associated credit risk is related to contagion ability function, the recovery rate of the infected entity, the new rate, and the incubatory period of the latent entity.

The node distribution $P(k)$ and average degree $\langle k\rangle$ of the BA scale-free networks are both put into (17), and the following is obtained:

$$2w\left[(\delta + M)(\lambda i\Theta^* + m) - \lambda i\delta e^{-M\tau}\Theta^*\right] = \lambda iMe^{-M\tau}\int_1^n \frac{2\alpha w^2}{i^2}di. \tag{21}$$

Inserting equation (20) into equation (21), the analytical solution is obtained:

$$\Theta^* = \frac{\lambda\alpha Mwie^{-M\tau} - m(\delta + M)}{\lambda i(\delta + M - \delta e^{-M\tau})}. \tag{22}$$

Inserting equation (22) into equation (16), we can get

$$I_k^* = \frac{(\delta + M)\lambda m}{Mw\alpha(\delta + M - \delta e^{-M\tau})k} + \frac{M}{e^{M\tau}(\delta + M) - \delta}. \tag{23}$$

Therefore,

$$I^* = \sum_k P(k)I_k^* = \frac{2w(\delta + M)\lambda m}{3M\alpha(\delta + M - \delta e^{-M\tau})} + \frac{Mw^2}{e^{M\tau}(\delta + M) - \delta}. \tag{24}$$

Obviously, in BA scale-free networks, in addition to the network structure, the density of the infected entities in the whole network is also related to the new rate, mortality rate, incubatory period of the latent entities, recovery rate of the immune entities, infection rate, and infection coefficient of the infected entities. Moreover, when $\lambda < \lambda_c$, the associated credit risk is not contagious. When $\lambda > \lambda_c$, the associated credit risk is contagious. Therefore, the contagion effect of associated credit risk exists in associated entity networks.

6.1. Comparative Analysis without considering the Incubatory Period. Without considering the incubatory period, that is $\tau = 0$, the contagion threshold of associated credit risk is $\lambda_c^0 = (\delta + M)/\alpha$, and the overall density of infected entities in the stable state is $I^{*^0} = (2w(\delta + M)\lambda m/3M^2\alpha) + w^2$.

Considering the incubatory period, that is, $\tau > 0$, the contagion threshold of associated credit risk is $\lambda_c = (\delta + M)e^{M\tau}/\alpha$, and the overall density of infected entities in the stable state is $I^* = \sum P(k)I_k^* = (2w(\delta + M)\lambda m/3M\alpha(\delta + M - \delta e^{-M\tau})) + (Mw^{2k}/e^{M\tau}(\delta + M) - \delta)$.

Comparatively, $\lambda_c > \lambda_c^0$, which means that the contagion threshold of associated credit risk will be underestimated without considering the incubatory period, and $I^* < I^{*^0}$, which means that the density of infected entities in the stable state may be overestimated without considering the incubatory period. Refer to the parameters value of literature [37, 38, 40, 47, 52], parameter values are given in the below numerical simulation.

Figure 1 shows that the interaction of the infected entities density I^*, the incubatory period τ, and the infection probability λ in the stable state when $\alpha = 0.1$, $w = 2$, $M = 0.05$, $m = 0.01$, and $\delta = 0.5$. The density of infected entities without considering the incubatory period always outweighs the density of infected entities when considering the incubatory period, that is, $I^{*0} > I^*$.

6.2. Numerical Simulation and Analysis of the Density of Infected Entities. The interaction between the density of infected entities I, the incubatory period of latent entities τ, the infection probability λ, the infectivity coefficient α, the recovery rate of infected entities δ, the new rate of credit entities M, and the mortality rate of credit entities m in the BA scale-free network can be calculated.

It can be seen from Figure 2 that the changing relationship between the density of infected entities I and the incubatory period τ of latent entities considering different infection probabilities of infected entities $\lambda_1 = 0.1$, $\lambda_2 = 0.3$, and $\lambda_3 = 0.5$ when $\alpha = 0.1, w = 2, M = 0.05$, $m = 0.01$, and $\delta = 0.5$. As can be seen from Figure 2, (i) when the infection probability of infected entities remains unchanged, as the incubatory period of latent entities increases, the infectivity of the associated credit risk in the network decreases, and increasingly fewer associated entities are infected, which is consistent with the reality. (ii) When the incubatory period is unchanged, as the infection probability increases, the contagion effect of the associated credit risk in the network increases, and so the density of infected entities in the network will increase. That is, the number of infected entities in the network will increase as the contagion of the associated credit risk increases, which is consistent with reality. It can be seen that the incubatory period of latent entities and the infection probability of infected entities are important factors affecting the density of infected entities.

Figure 3 shows the changing relationship between the density of infected entities I and the incubatory period τ of latent entities considering different recovery rates of infected entities $\delta_1 = 0.4, \delta_2 = 0.6$, and $\delta_3 = 0.8$ when $\alpha = 0.1$, $w = 2$, $M = 0.05$, $m = 0.01$, and $\lambda = 0.1$. The following can be seen from Figure 3: (i) when the recovery rate of infected entities remains unchanged, as the incubatory period of latent entities increases, the infectivity of the associated credit risk in the network decreases, and increasingly fewer associated

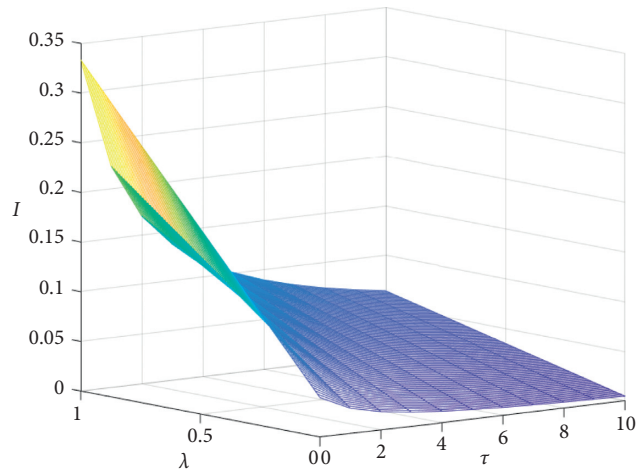

Figure 1: Interaction of the infected entities density I, incubatory period τ, and infection probability λ.

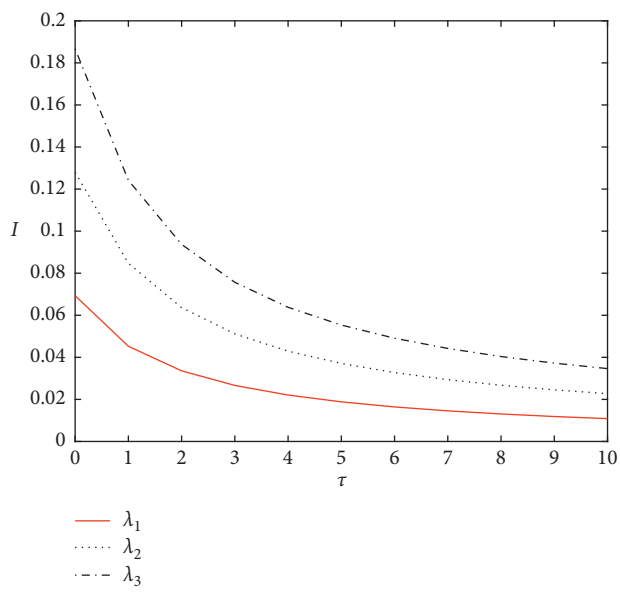

Figure 2: Interaction of the infected entities density I and incubatory period τ considering different infection probabilities λ.

entities are infected, which is consistent with reality. (ii) When the incubatory period is unchanged, before 1.5 units of time, as the recovery rate increases, the number of infected entities abnormally increases. This observation may be the reason why there is an increase in the number of infected entities who do not receive timely assistance and have weakened resistance, even though the recovery rate increases, which causes the overall density of infected entities to increase in a short time. When the incubatory period is unchanged, at 1.5 units of time, the change in the recovery rate will not affect the overall density of infected entities, and the density of infected entities is constant at this moment. When the incubatory period is unchanged, after 1.5 units of time, the density of infected entities decreases as the recovery rate increases. Therefore, when the incubatory period remains unchanged, the overall change in the density of

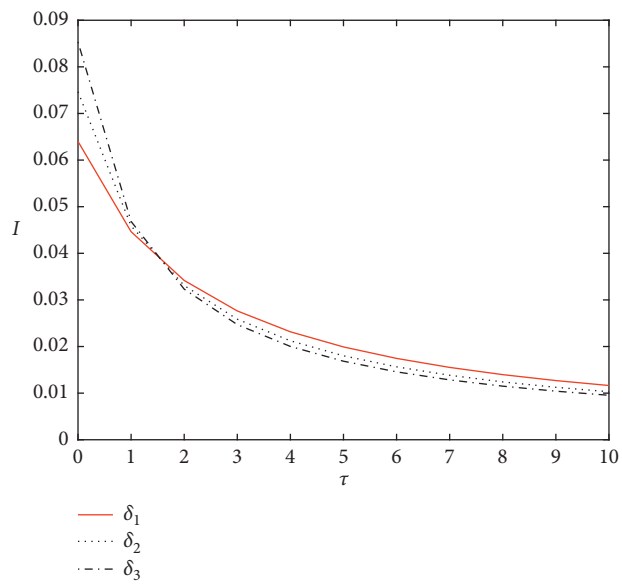

Figure 3: Interaction of the infected entities density I and incubatory period τ considering the different recovery rates δ.

infected entities is in line with the actual situation. It is concluded that the recovery rate of the infected entities and the incubatory period of the latent entities are important factors affecting the density of the infected entities.

Figure 4 shows that the relationship between the density of infected entities I and the incubatory period τ of latent entities considering different newborn rates of credit entities $M_1 = 0.01$, $M_2 = 0.05$, and $M_3 = 0.08$ when $\alpha = 0.1$, $\omega = 2$, $M = 0.05$, $m = 0.01$, and $\lambda = 0.1$. To more clearly explore the contagion of associated credit risk, the new rate here temporarily represents the initial value of the associated entities network, and so the change in the new rate represents the change in the initial value of the network. The following can be seen from Figure 4: (i) when the new rate remains unchanged, as the incubatory period of latent entities increases, the infectivity of the associated credit risk in the network decreases, and increasingly fewer associated entities are infected, which is consistent with reality. (ii) When the incubatory period remains unchanged, the marginal density of infected entities will increase as the new rate increases. That is, the higher the new rate is, the faster the density of infected entities will decrease. (iii) When the incubatory period remains unchanged, the higher the new rate is, the smaller the density of infected entities is. This observation may be due to the greater number of new entities, the increase in the network nodes, and the dilution of the density of infected entities. Therefore, the newborn rate of credit entities and the incubatory period of latent entities are important factors affecting the density of infected entities.

Figure 5 shows that the changing relationship between the density of infected entities I and the incubatory period τ of latent entities considering different mortality rates of credit entities $m_1 = 0.001$, $m_2 = 0.01$, and $m_3 = 0.1$ when $\alpha = 0.1$, $\omega = 2$, $\gamma = 0.5$, $M = 0.01$, and $\lambda = 0.1$. The following can be found: (i) with the increase in the incubatory period of latent entities, the infectivity of the associated credit risk

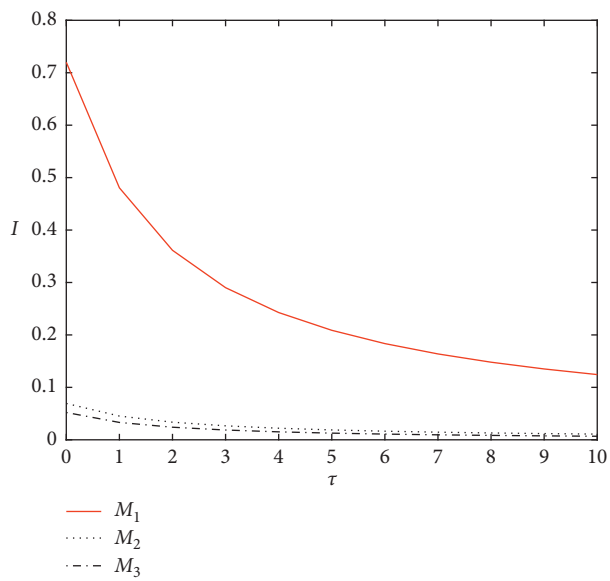

Figure 4: Interaction of the infected entities density I and incubatory period τ considering different newborn rates M.

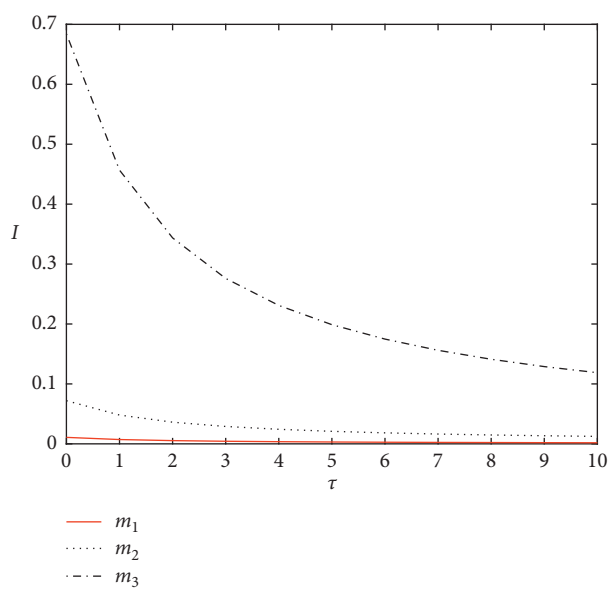

Figure 5: Interaction of the infected entities density I and incubatory period τ considering the mortality rate m.

in the network decreases, and increasingly, fewer associated entities are infected. That is, the density of infected entities tends to decrease, which is consistent with reality. (ii) When the incubatory period and other conditions remain unchanged, with the increase in the mortality rate, the density of infected entities will increase. That is, the density of infected entities will increase as the mortality rate increases. This observation may be because most of the dead entities are susceptible entities and new entities. Meanwhile, the infected entities have a lower mortality rate because of their enhanced resistance and self-healing consciousness, and so the density of infected entities will increase. Therefore, the mortality rate of credit entities and the incubatory period of latent entities are important factors affecting the density of infected entities.

7. Conclusions and Discussion

With economic globalization and the further development of market economies, the relationships among various credit entities, such as enterprises, banks, insurance companies, and guarantee companies, are becoming increasingly closer and more complex, and the credit transactions among various associated entities are increasingly frequent; therefore, the associated credit risks are widespread. The change in the associated credit risk not only has a chained effect but also has an incubatory period. Once the credit risk breaks out, it will quickly spread to other associated entities, thus harming the network of associated entities, even the financial system and the whole social economy, and even leading to the outbreak of systemic financial risk. Therefore, it is of great theoretical significance and practical value to explore the hidden contagious evolutionary mechanism of associated credit risk and to identify, prevent, and control associated credit risk. However, in practical economic development and business operations, the incubatory period of associated credit risk is not well understood, which leads to missed opportunities for risk control, credit crises, and even the outbreak of global financial crises. The main contribution of this paper is to use the SIS infectious dynamics model and introduce latent entities and the incubatory period to characterize the infectious evolutionary mechanism of associated credit risk in the network of associated entities. Furthermore, in the BA scale-free network, the numerical simulation analysis shows the following: (i) the contagion threshold of associated credit risk is related to the network structure, and it changes in the same direction as the incubatory period of latent entities, the recovery rate of infected entities, and the new rate of credit entities. Meanwhile, the contagion threshold changes in the opposite direction as the infective ability of infected entities. (ii) The longer the incubatory period of the latent entities is, the higher the recovery rate of infected entities is, the higher the mortality rate is, and the smaller the density of the infected entities is. (iii) The higher the probability of infected entities is, the greater the density of infected entities is, the higher the new rate of credit entities is, and the faster the density of infected entities will decrease. The above conclusions are consistent with the crisis phenomena in the real network of associated entities. Furthermore, this paper provides a new perspective for enterprises, banks, guarantee companies, and other credit entities to control associated credit risk. Our future research will apply the data of listed companies in Shanghai and Shenzhen stock exchanges of China to conduct an in-depth empirical study on the incubatory period and evolutionary mechanism of the associated credit risk contagion.

Data Availability

The simulation data used to support the findings of this study are available from the corresponding author (xukai@cdu.edu.cn) upon request.

Conflicts of Interest

The authors declare that there are no conflicts of interest.

Acknowledgments

This work was supported by the National Natural Science Foundation of China (nos. 71701166 and 71871147), Sichuan Social Science Planning Project (no. SC19B004), Soft Science Project of Chengdu Science and Technology Bureau (no. 2016-RK00-00010-ZF), a project supported by Sichuan Landscape and Recreation Research Center (no. JGYQ2018004), and Sichuan County Economic Development Research Center (no. xy2018016).

References

[1] Z. F. Zhou, *Associated Credit Risk and its Contagion Effect-Important Risk Sources in Modern Society, Economy and Market Environment*, Science Press, Beijing, China, 2018.

[2] Y. K. Li and Z. F. Zhou, "Contagion delayed effects of associated credit risk based on scale-free network," *Systems Engineering*, vol. 33, no. 8, pp. 74–79, 2015.

[3] O. De Bandt and P. Hartmann, *Systemic Risk: A Survey*, Social Science Electronic Publishing, Beijing, China, 2000.

[4] P. Smaga, *The Concept of Systemic Risk*, Systemic Risk Centre Special Paper, Beijing, China, 2014.

[5] R. M. May, S. A. Levin, and G. Sugihara, "Ecology for bankers," *Nature*, vol. 451, no. 7181, pp. 893-894, 2008.

[6] G. Luo, Y. W. Zhao, and Y. Wang, "Risk propagation patterns of guarantee network based on the theory of complex network," *Journal of University of Chinese Academy of Sciences*, vol. 32, no. 6, pp. 836–842, 2015.

[7] P. Xu and X. Yu, "Research on the application of risk contagion model of mutual guarantee financing for SMEs clusters," *Accounting Research*, vol. 2018, no. 1, pp. 82–88, 2018.

[8] M. Elliott, B. Golub, M. O. Jackson et al., "Financial networks and contagion," *American Economic Review*, vol. 104, no. 10, pp. 3115–3153, 2014.

[9] E. Fisher, "A biological approach for financial network contagion based on the Susceptible-Infected-Recovered(SIR) model," *Anã lisis Econã³mico*, vol. 21, no. 69, pp. 109–128, 2013.

[10] M. Eboli, "A flow network analysis of direct balance-sheet contagion in financial networks," *Journal of Economic Dynamics and Control*, vol. 2019, no. 103, pp. 205–233, 2019.

[11] R. Gencay, H. Pang, M. C. Tseng et al., "Contagion in a network of heterogeneous banks," *Journal of Banking and Finance*, vol. 2020, Article ID 105725, no. 111, p. 16, 2020.

[12] H. Dastkhan and N. S. Gharneh, "Simulation of contagion in the stock markets using cross-shareholding networks: a case from an emerging market," *Computational Economics*, vol. 53, no. 3, pp. 1071–1101, 2019.

[13] A. Bucci, D. La Torre, D. Liuzzi, and S. Marsiglio, "Financial contagion and economic development: an epidemiological approach," *Journal of Economic Behavior & Organization*, vol. 162, pp. 211–228, 2019.

[14] Z. H. Hu and X. H. Li, "Contagion and bailout strategy in complex financial network—SIRS model on the Chinese scale-free financial network," *Finance & Trade Economics*, vol. 2017, no. 4, pp. 101–114, 2017.

[15] H. Dastkhan, "Network-based early warning system to predict financial crisis," *International Journal of Finance & Economics*, vol. 2019, 2019.

[16] P. Sarlin, "On biologically inspired predictions of the global financial crisis," *Neural Computing and Applications*, vol. 24, no. 3-4, pp. 663–673, 2014.

[17] P. Giudici, P. Sarlin, and A. Spelta, "The interconnected nature of financial systems: direct and common exposures," *Journal of Banking & Finance*, vol. 2020, Artticle ID 105149, no. 112, p. 18, 2020.

[18] N. Apergis, C. Christou, I. Kynigakis et al., "Contagion across US and European financial markets: evidence from the CDS markets," *Journal of International Money and Finance*, vol. 96, no. 96, pp. 1–12, 2019.

[19] B. Chakrabarty and G. Zhang, "Credit contagion channels: market microstructure evidence from Lehman Brothers'bankruptcy," *Financial Management*, vol. 41, no. 2, pp. 2320–2343, 2012.

[20] P. Jorion and G. Zhang, "Credit contagion from counterparty risk," *The Journal of Finance*, vol. 64, no. 5, pp. 2053–2087, 2009.

[21] D. Barro and A. Basso, "Credit contagion in a network of firms with spatial interaction," *European Journal of Operational Research*, vol. 205, no. 2, pp. 459–468, 2010.

[22] S. Li and X. Sui, "Contagion risk in endogenous financial networks," *Chaos, Solitons & Fractals*, vol. 91, pp. 591–597, 2016.

[23] S. Jiang, H. Fan, and M. Xia, "Credit risk contagion based on asymmetric information association," *Complexity*, Article ID 2929157, vol. 2018, p. 11, 2018.

[24] T. Q. Chen, J. P. Wang, and J. N. Wang, "Research on credit risk contagion mechanism of counterparty based on CDS," *Financial Theory & Practice*, vol. 4, pp. 35–38, 2017.

[25] T. Q. Chen, B. Q. Xiao, and H. F. Liu, "Credit risk contagion in an evolving network model integrating spillover effects and behavioral interventions," *Complexity*, vol. 2018, Article ID 1843792,, p. 16, 2018.

[26] L. Li and Z. F. Zhou, "Credit contagion mechanism for interrelated guarantee," *Systems Engineering*, vol. 1, pp. 55–60, 2015.

[27] H. J. Yang and H. M. Hu, "Risk contagion of Chinese interbank markets based on core-periphery network," *Journal of Management Sciences in China*, vol. 20, no. 10, pp. 44–56, 2017.

[28] L. Wu, Y. M. Zhuang, and L. Zhang, "An analysis of credit risk diffusion in inter-bank market," *Journal of Southeast University(Philosophy and Social Science)*, vol. 19, no. 6, pp. 74–79, 2017.

[29] L. Wang, S. Li, T. Chen et al., "Investor behavior, information disclosure strategy and counterparty credit risk contagion," *Chaos, Solitons & Fractals*, vol. 119, pp. 37–49, 2019.

[30] S. Jiang and H. Fan, "Credit risk contagion coupling with sentiment contagion," *Physica A: Statistical Mechanics and Its Applications*, vol. 512, pp. 186–202, 2018.

[31] C. Giusy, G. Gianfranco, and S. Marco, "Climate change and credit risk," *Journal of Cleaner Production*, vol. 2020, Article ID 121634, no. 266, p. 18, 2020.

[32] V. De Bruyckere, M. Gerhardt, G. Schepens, and R. Vander Vennet, "Bank/sovereign risk spillovers in the European debt crisis," *Journal of Banking & Finance*, vol. 37, no. 12, pp. 4793–4809, 2013.

[33] J. Breckenfelder and B. Schwaab, "Bank to Sovereign risk spillovers across borders: evidence from the ECB's comprehensive assessment," *Journal of Empirical Finance*, vol. 49, pp. 247–262, 2018.

[34] M. Greenwood-Nimmo, J. Huang, V. H. Nguyen et al., "Financial sector bailouts, sovereign bailouts, and the transfer of credit risk," *Journal of Financial Markets*, vol. 42, pp. 121–142, 2019.

[35] S. Srivastava, H. Lin, I. M. Premachandra, and H. Roberts, "Global risk spillover and the predictability of sovereign CDS spread: international evidence," *International Review of Economics & Finance*, vol. 41, pp. 371–390, 2016.

[36] G. Bostanci and K. Yilmaz, "How connected is the global sovereign credit risk network," *Journal of Banking and Finance*, vol. 2020, no. 113, Article ID 105761, 2020.

[37] K. Xu, Z. F. Zhou, and Q. Qian, "The impact of risk information and behavioral response on associated credit risk contagion," *Technology Economics*, vol. 37, no. 8, pp. 116–122, 2018.

[38] Q. Qian and Z. F. Zhou, "Research on the associated credit risk within the immunization," *Operations Research and Management Science*, vol. 2018, no. 1, pp. 132–137, 2018.

[39] L. Li and Z. F. Zhou, "Dynamic infection mechanism research for credit risk within business group," *Management Review*, vol. 2015, no. 1, pp. 48–56, 2015.

[40] Q. Qian, Y. Yang, J. Gu, and H. R. Feng, "Information authenticity, spreading willingness and credit risk contagion–A dual-layer network perspective," *Physica A: Statistical Mechanics and Its Applications*, vol. 536, Article ID 22519, 2019.

[41] H. F. Zhang, J. Xie, H. Chen et al., "Impact of asymptomatic infection on coupled disease-behavior dynamics in complex networks," *EPL*, vol. 114, no. 3, p. 6, 2016.

[42] Q. Redouane and A. Hammoumi, "A stochastic delay model of HIV pathogenesis with reactivation of latent reservoirs," *Chaos Solitons & Fractals*, vol. 2020, no. 132, Article ID 109594, p. 11, 2020.

[43] T. Shi, T. Long, Y. Pan et al., "Effects of asymptomatic infection on the dynamical interplay between behavior and disease transmission in multiplex networks," *Physica A-Statistical Mechanics and Its Applications*, vol. 2019, Article ID 121030,, no. 536, p. 16, 2019.

[44] R. X. Zhang, Z. Jin, and S. P. Li, "Epidemic spreading with time delay on complex networks," *Acta Mathematicae Applicatae Sinica, English Series*, vol. 32, no. 2, pp. 319–326, 2016.

[45] C. Y. Xia, Z. Wang, J. Sanz, S. Meloni, and Y. Moreno, "Effects of delayed recovery and nonuniform transmission on the spreading of diseases in complex networks," *Physica A: Statistical Mechanics and Its Applications*, vol. 392, no. 7, pp. 1577–1585, 2013.

[46] F. Viviana and M. Lucia, "A nonlinear dynamic model for credit risk contagion," *Mathematics and Computers in Simulation*, vol. 174, no. 8, pp. 45–58, 2020.

[47] Y. K. Li and Z. F. Zhou, "Contagion delayed effects of associated credit risk based on scale-free network," *Journal of Systems Engineering*, vol. 30, no. 5, pp. 575–583, 2015.

[48] Y. K. Li and Z. F. Zhou, "Contagion and simulation of interfirm associated credit risk based on incomplete immunization," *Chinese Journal of Management Science*, vol. 25, no. 1, pp. 57–64, 2017.

[49] R. Pastor-Satorras and A. Vespignani, "Epidemic dynamics in finite size scale-free networks," *Physical Review E*, vol. 65, no. 3, Article ID 035108, 2002.

[50] R. Pastor-Satorras and A. Vespignani, "Epidemic spreading in scale-free networks," *Physical Review Letters*, vol. 86, no. 14, Article ID 3200, 2001.

[51] W. O. Kermack and A. G. Mckendrick, "Contributions to the mathematical theory of epidemics. II. the problem of endemicity," *Proceedings of The Royal Society A: Mathematical, Physical and Engineering Sciences*, vol. 138, no. 834, pp. 55–83, 1932.

[52] K. Xu, Z. F. Zhou, and Q. Qian, "Impact of information bidirectional dissemination and individual response on associated credit risk contagion," *Systems Engineering*, vol. 38, no. 2, pp. 11–19, 2020.

Hindawi
Complexity
Volume 2020, Article ID 8581793, 10 pages
https://doi.org/10.1155/2020/8581793

Research Article

Investor Sentiment in an Artificial Limit Order Market

Lijian Wei[1] and Lei Shi[2]

[1]*Sun Yat-sen Business School, Sun Yat-sen University, Guangzhou 510275, China*
[2]*Macquarie Business School, Department of Applied Finance, Macquarie University, Sydney, NSW 2109, Australia*

Correspondence should be addressed to Lei Shi; l.shi@mq.edu.au

Received 14 February 2020; Revised 19 April 2020; Accepted 28 April 2020; Published 30 June 2020

Academic Editor: Dehua Shen

This paper examines the under/overreaction effect driven by sentiment belief in an artificial limit order market when agents are risk averse and arrive in the market with different time horizons. We employ agent-based modeling to build up an artificial stock market with order book and model a type of sentiment belief display over/underreaction by following a Bayesian learning scheme with a Markov regime switching between conservative bias and representative bias. Simulations show that when compared with classic noise belief without learning, sentiment belief gives rise to short-term intraday return predictability. In particular, under/overreaction trading strategies are profitable under sentiment beliefs, but not under noise belief. Moreover, we find that sentiment belief leads to significantly lower volatility, lower bid-ask spread, and larger order book depth near the best quotes but lower trading volume when compared with noise belief.

1. Introduction

With FinTech, such as natural language processing, introduced into financial services, traders have increasingly used short-term intraday sentiment information derived from news wire articles. For example, "RavenPack" provides real-time structured sentiment data from social media that helps to decipher whether news or comments are good or bad for the listed company. If traders use these sentiment data to forecast the price, they may lead to underreaction or overreaction in short-term intraday data. In fact, empirical studies in both academic [1] and practice [2] find evidences of under/overreaction in intraday data.

Heston et al. [3] used five-minute frequency intraday data and found that the yield series had significant serial correlation. Furthermore, Gao [4] took US ETF funds and divide the trading day into 13 half-hour intervals. The return rate of the half hour after opening has a significant positive correlation with the return of the half hour before closing, and there is an intraday momentum effect. Komarov [5] uses half-hour intraday returns of the US stock markets and finds that morning earnings can predict the closing returns. Zhang et al. [6] use the Shanghai Composite Index and find that the returns in the first half hour and/or the penultimate half hour (the seventh half hour) can significantly predict the returns in and out of the sample in the last half hour. Jin et al. [7] conduct an investigation of intraday timeseries momentum across four Chinese commodity futures contracts, and their results indicate that the first half hour return positively predicts the last half hour return across all four futures.

In a seminal paper, Barberis et al. [8] (hereafter BSV98) propose a type of sentiment belief, which incorporates both conservative bias and representative bias, and show that the model is able to generate both under- and overreaction observed in monthly data. BSV98 employs a representative agent framework, without interactive trading among heterogeneous agents. As a result, the BSV model is not suitable for examining the impact of investor sentiment on market volatility, trading volume, and liquidity in financial markets, which predominantly are limit order markets with continuous double auction. Therefore, two important questions that remain are as follows: (1) can sentiment lead to under/overreaction in a limit order markets with intraday trading? (2) What is the impact of sentiment on market volatility and liquidity including the bid-ask spread, order book depth, and trading volume?

This paper aims to answer these two questions by analyzing an agent-based model with sentiment belief in an artificial limit order market. According to Paulinet al. [9], the agent-based modeling is a powerful tool for studying the complex financial systems, such as limit order markets, based on the big data and computing power. Paulin et al. [9] point out that the problem classic economic theories face is that "*even if the individual microbehaviors of system components are all perfectly understood, it remains extremely difficult to predict the overall macrobehaviors that the system might exhibit*." Agent-based modeling (ABM) overcomes this shortcoming by assuming "*agents are independent software entities that operate according to their own rules and objectives*." Especially in a limit order market, classic economic theory based on rational expectation would require each agent to *know* the optimal strategy of all other agents, i.e., their submission price and order quantity. However, this is an extremely complex problem to solve (even numerically) given its dimensionality. Therefore, ABM is the only feasible channel to study the emergent properties of market microstructure of financial assets from the microbehaviors of bounded rational and heterogeneous agents.

To setup a benchmark for comparison, we first consider noisy beliefs, as in De Long et al. [10], about the fundamental value which deviate randomly from rational expectations. We call the traders with noisy belief noise traders. Then, for our main simulation analysis, we model sentiment traders who follow a Bayesian learning scheme, similar to the one in BSV98; thus, sentiment traders are also called *BSV traders*. More specifically, BSV traders think that the expected log fundamental value follows a regime switching model with conservative bias and representative bias rather than a random walk. BSV traders believe that there is a continuation regime as well as a mean-reverting regime, and they use past trends to determine the likelihood of which regime they are currently in. Following Chiarella et al. [11], the order submission price and order size are determined by the forecasting price, the budget constraint, and the no-short-sell constraint via the constant absolute risk aversion (CARA) utility function. The order type (market or limit) is determined by the submission price and the bid and ask price; that is, if the submission price of buy (sell) order is no lower (higher) from the ask (bid) price, they will place market buy (sell) order; otherwise, they will submit limit buy (sell) order.

Our main finding is that BSV traders can have very a different impact on the limit order market compared to noise traders. First, BSV trading gives rise to profitable strategies that are based on under/overreaction, while noise trading does not. Second, we find that, under BSV trading, conditional on overreaction, trading volume, and volatility is significantly higher and order book depth significantly lower than the periods without overreaction. In contrast, there are no significant differences between overreaction and non-overreaction periods under noise trading. In general, BSV trading leads to significantly lower volatility, smaller bid-ask spread, larger order book depth near the best quotes, and lower trading volume compared to noise trading.

Our paper is contributed significantly to the literature. First, we extend Barberis et al. [8] to a limit order market and examine whether sentiment trading can lead to over/underreaction in short-term intraday data, which are consistent with the empirical findings in recent financial markets that introduce sentiment data via FinTech. While there are agent-based models which examine the BSV sentiment effect, such as Zhang et al. [12] and Zhang and Zhang [13], a market-maker trading mechanism is used rather than a limit order book and also their focus is on examining the long-run survival of irrational traders. Chen et al. [14] highlight that agent-based models need to employ the limit order book as a realistic trading mechanism to study richer market dynamics in intraday data. We extend Zhang and Zhang's [13] work in a realistic trading mechanism and study the impact of BSV-type sentiment on market volatility and liquidity, thus providing more useful implications to the regulators and investors.

Furthermore, in Chiarella et al. [15], based the simulated data with BSV-sentiment trading, it is found that the model reproduces a number of important stylized facts in limit order markets including fat tail and absence of autocorrelation in returns, volatility clustering, long memory in absolute returns, the bid-ask spread and the trading volume, the hump shape in the mean depth profile closer the best quotes of the order book, an increasing and nonlinear relationship between trade imbalance and midprice return, and also the diagonal effect (event clustering) in submitted order types. The focus of the current paper is on the under/overreaction effect and the impact of BSV sentiment on market volatility and liquidity.

2. The Artificial Limit Order Market

We consider a limit order market with traders, with different investment horizons, who arrive at the market randomly and submit orders to buy or sell shares of a risky security (e.g., stock). The fundamental value F_t of the risky asset follows a *geometric random walk*, i.e.,

$$\ln(F_{t+1}) = \ln(F_t) + \sigma\epsilon_{t+1}, \quad \epsilon_{t+1} \overset{\text{i.i.d}}{\sim} \mathcal{N}(0,1)), \tag{1}$$

where the volatility per period, σ, is constant and common knowledge among the traders. From (1), the log fundamental value is a martingale, i.e., $\mathbb{E}_t[\ln(F_{t+\tau})] = \ln(F_t)$ for $\tau \geq 1$.

Moreover, traders do not monitor the market continuously, trader i with an investment horizon, and τ^i enters the market following a Poisson process with a mean of $1/\tau^i$. Upon arrival, she knows the fundamental value of the current period F_t, together with its past values every τ^i period. Thus, trader i's information set is given by $I_t^i \equiv \{F_t, F_{t-\tau^i}, \cdots, F_{t-N^i\tau^i}\}$, where N^i measures the length of her observations. In addition to the risky stock, traders can also invest in a risk-free security with *zero* interest rate.

2.1. Traders' Beliefs

2.1.1. Noisy Beliefs. First, we consider the noisy beliefs, similar to De Long et al. [10], as a benchmark. We assume

traders' beliefs about the mean and variance of the log fundamental value deviate randomly from their values under rational expectations, i.e.,

$$\begin{aligned}\mathbb{E}_t^i[\ln(F_{t+\tau^i})] &= \ln(F_t) + \tilde{\theta}_t^i,\\ \mathbb{V}_t^i[\ln(F_{t+\tau^i})] &= \sigma^2\tau^i + (\theta^i)^2 - (\tilde{\theta}_t^i)^2,\end{aligned} \tag{2}$$

where $\tilde{\theta}_t^i \sim^{\text{i.i.d}} \text{Uniform}\,[-\theta^i, \theta^i]$. We refer to these traders *noise* traders. When $\theta^i = 0$, trader i has rational expectations; thus,

$$\begin{aligned}\mathbb{E}_t^i[\ln(F_{t+\tau^i})] &= \ln(F_t),\\ \mathbb{V}_t^i[\ln(F_{t+\tau^i})] &= \sigma^2\tau^i.\end{aligned} \tag{3}$$

2.1.2. Sentiment Beliefs. Next, for our main analysis, in the spirit of Barberis et al. [8] (hereafter BSV), we assume that traders' beliefs are driven by *behavioral sentiment*. More specifically, each trader believes that the log fundamental price $\ln(F_{t+\tau^i})$ follows:

$$\ln(F_{t+\tau^i}) = \ln(F_t) + \theta_{t+\tau^i} + \sigma\epsilon_{t+\tau^i}, \tag{4}$$

where $\epsilon_{t+\tau^i} \sim^{\text{i.i.d}} \mathcal{N}(0, \sqrt{\tau^i})$ and the mean growth rate $\theta_{t+\tau^i}$ follows a two-state Markov chain with transition matrix

	$\theta_{t+\tau^i} = \theta^i$	$\theta_{t+\tau^i} = -\theta^i$
$\theta_t = \theta^i$	$\pi_{t+\tau^i}$	$1 - \pi_{t+\tau^i}$
$\theta_t = -\theta^i$	$1 - \pi_{t+\tau^i}$	$\pi_{t+\tau^i}$.

(5)

Therefore, trader i believes that there is a good (bad) state in which the mean growth rate of the fundamental price is positive (negative). Given the current state, the probability of staying in the same state is given by $\pi_{t+\tau^i}$. When θ^i is different from zero, trader i's belief exhibits sentiment, believing in an underlying structure for the mean growth rate, which does not exist.

Furthermore, as in Barberis et al.'s study [8], trader i believes that the transition probability $\pi_{t+\tau^i}$ also follows a Markov chain with transition matrix:

	$\pi_{t+\tau^i} = \pi_L$	$\pi_{t+\tau^i} = \pi_H$
$\pi_t = \pi_L$	$1 - \lambda_1$	λ_1
$\pi_t = \pi_H$	λ_2	$1 - \lambda_2$.

(6)

Thus, traders believe there is one state $\pi_t = \pi_H$ in which the mean growth rate is more likely to remain the same as the last period and a state $\pi_t = \pi_L$ in which the mean growth rate is more likely to switch from one state to another, in which λ_1 and λ_2 measure the switching intensities. This Markov regime-switching model is motivated by two important psychological biases: *conservative bias* and *representative heuristic bias*. According to Barberis et al. [8], agents either react too little to cash-flow news (changes in the fundamental process) because they believe the mean fundamental growth rate is mean reverting, or they react too much to cash-flow news because they believe the mean fundamental growth rate is trending. The former is consistent with conservative bias and the fact that agents underweighs the information in individual cash-flow news, whereas the latter is consistent with representative bias since agents over-extrapolate the past trend and overweighs information contained in a series of positive/negative cash-flow news.

Traders do not observe the mean growth rate θ_t, and they update their probability beliefs about θ_t and π_t based on a Bayesian learning scheme (see the learning process in the Appendix). Given a sentiment trader's estimated probabilities $q_{\pi,t}^i$ and $q_{\theta,t}^i$, trader i makes a τ^i-period ahead forecast of the log fundamental price:

$$\mathbb{E}_t^i[\ln(F_{t+\tau^i})] = \ln(F_t) + \mathbb{E}_t^i[\theta_{t+\tau^i}]. \tag{7}$$

The details of the deviation of equation (7) are also documented in Appendix. The variance of log fundamental price perceived by sentiment trader i is given by

$$\mathbb{V}_t^i[\ln(F_{t+\tau^i})] = \sigma^2\tau^i + (\theta^i)^2 - (\mathbb{E}_t^i[\theta_{t+\tau^i}])^2. \tag{8}$$

We call these traders with behavioral sentiment BSV traders. Note that, without sentiment ($\theta^i = 0$), BSV traders' belief also becomes the one in equation (3). Therefore, sentiment is the key ingredient in generating heterogeneity in beliefs across BSV traders with different investment horizons (see the example in Appendix), and the key difference between noise traders and BSV traders is that BSV traders have a learning scheme under bias in belief while noise traders do not.

2.2. Traders' Optimal Demand and Order Submission. Following Chiarella et al. [11], we assume that traders maximize a CARA utility function by optimizing their demand in the risky stock, which is given by

$$z_t^{i*} = \frac{\mathbb{E}_t^i[\ln(p_{t+\tau^i})] - \ln(p_t^i)}{\alpha^i p_t^i \mathbb{V}_t^i[\ln(p_{t+\tau^i})]} - s_t^i, \tag{9}$$

where α^i is the absolute risk aversion coefficient, s_t^i is the number of shares of the risky asset held at time t, p_t^i is the order price, and z_t^i is the order size (quantity) submitted at time t (agent i maximizes a CARA utility function, i.e., $\max_{\pi_t} \mathbb{E}_t[-e^{-\alpha W_{t+\tau}}]$, and $W_{t+\tau} = W_t + \pi_t p_t \rho_{t+\tau}$ is assumed to be normally distributed, where p_t is the submission price, π_t is the quantity of risky asset held at time t, and $\rho_{t+\tau} = p_{t+\tau}/p_t - 1 \approx \ln(p_{t+\tau}/p_t)$ is the agent's expectation for future returns. Refer to Chiarella et al. [11] Appendix A for detailed derivations).

Next, trader i uses her belief about the fundamental value to estimate the mean and variance of the future market price:

$$\begin{aligned}\mathbb{E}_t^i[\ln(p_{t+\tau^i})] &= \mathbb{E}_t^i[\ln(F_{t+\tau^i})],\\ \mathbb{V}_t^i[\ln(p_{t+\tau^i})] &= \mathbb{V}_t^i[\ln(F_{t+\tau^i})].\end{aligned} \tag{10}$$

Now to determine the submission price p_t^i for trader i, we assume trader can neither short-sell nor borrow at the risk-free rate, which implies that

$$\begin{aligned}z_t^{i*} &\geq -s_t^i,\\ z_t^{i*} p_t^i &\leq c_t^i,\end{aligned} \tag{11}$$

where c_t^i is the amount of cash trader i holds at time t. The no-shorting and no-borrowing constraints are necessary to

derive the bounds $p_t^{i,m}$ and $p_t^{i,M}$ for the submission price. Without such constraints, agents may place large orders to buy or to sell far away from the best bid/ask, which is unrealistic. Alternatively, one could assume that each agent has the ability to borrow a certain amount $\tilde{c}^i$ and to take a short position $\tilde{s}^i$ and then the price bounds are determined such that $z_t^{i*} \geq -(s_t^i + \tilde{s}^i)$ and $z_t^{i*} p_t^i \leq (c_t^i + \tilde{c}^i)$ and $\tilde{s}^i$ and $\tilde{c}^i$ can also depend on market conditions.

From (11), we obtain the following bounds for the submission price p_t^i for trader i:

$$p_t^{i,m} \leq p_t^i \leq p_t^{i,M}, \tag{12}$$

where $p_t^{i,M} = \exp\{\mathbb{E}_t^i[\ln(p_{t+\tau^i})]\}$ and $p_t^{i,m}$ is determined implicitly by

$$\frac{\mathbb{E}_t^i[\ln(p_{t+\tau^i})] - \ln(p_t^{i,m})}{\alpha^i \mathbb{V}_t^i[\ln(p_{t+\tau^i})]} = c_t^i + s_t^i p_t^{i,m}. \tag{13}$$

Furthermore, we define p_t^{i*} as the *no trade price* for trader i, which solves

$$\frac{\mathbb{E}_t^i[\ln(p_{t+\tau^i})] - \ln(p_t^{i*})}{\alpha^i p_t^{i*} \mathbb{V}_t^i[\ln(p_{t+\tau^i})]} = s_t^i. \tag{14}$$

We assume trader i trades in the following way. She either tries to sell s_t^i shares of the risky asset at the maximum price of $p_t^{i,M}$ or buy $c_t^i/p_t^{i,m}$ shares at the minimum price of $p_t^{i,m}$ (this may seem rather extreme, however, assuming the order will be executed, buying at $p_t^{i,m}$ or selling at $p_t^{i,M}$ maximizes trader i's expected utility). If the best ask $a_t^1 < p_t^{i,m}$ or the best bid $b_t^1 > p_t^{i,M}$, then agent i submits a market buy or a market sell order; otherwise, she submits a limit buy or limit sell order. Note that this way of determining the submission price is different from Chiarella et al. [11], where agents randomly pick a price $p_t^i \in [p_t^{i,m}, p_t^{i,M}]$.

Furthermore, we assume the probability of submitting a buy or sell order is given by

$$\begin{aligned} P_{\text{buy}} &\equiv \mathbb{P}\left(z_t^{i*} = \frac{c_t^i}{p_t^{i,m}}\right) = \frac{p_t^{i*} - p_t^{i,m}}{p_t^{i,M} - p_t^{i,m}}, \\ P_{\text{sell}} &\equiv \mathbb{P}\left(z_t^{i*} = -s_t^i\right) = \frac{p_t^{i,M} - p_t^{i*}}{p_t^{i,M} - p_t^{i,m}}. \end{aligned} \tag{15}$$

Intuitively, the further the no-trading price is away from the minimum price, the higher the probability to buy; the further the no-trading price is away from the maximum price, the higher the probability to sell.

Lastly, we assume trader i's expected return and variance or return over her investment horizon are based on the expected value and variance of the log fundamental price and the submitted price, that is,

$$\begin{aligned} \mathbb{E}_t^i[r_{t+\tau^i}] &= \mathbb{E}_t^i[\ln(F_{t+\tau^i})] - \ln(p_t^i), \\ \mathbb{V}_t^i[r_{t+\tau^i}] &= \mathbb{V}_t^i[\ln(F_{t+\tau^i})]. \end{aligned} \tag{16}$$

Upon entering the market, trader i either places a market order or a limit order which will be stored in the limit order book. A transaction occurs when a market order hits a quote on the opposite side of the order book. Limit orders are executed using both price and time priorities. At time t, trader i submits a buy or sell order with price level p_t^i and order size z_t^i (z_t^i is the optimal order size based on p_t^i). The order leads to a trade when she submits a buy order and $p_t^i \geq a_t^1$ or when she submits a sell order and $p_t^i \leq b_t^1$, where b_t^1 and a_t^1 are the best bid and ask price, respectively. If there is enough depth at the best bid or best ask, then the entire order trader i submits is executed at a_t^1 or b_t^1; otherwise, part of the order may be executed at prices further away from the best bid or ask or it may become a limit order with price p_t^i as the new best bid or ask price. Furthermore, there can be multiple agents who arrive at the market at the same time, in which case we assume those agents trade in a randomized order.

Table 1 summarizes the order submission rules of trader i in which X is drawn from a uniform distribution on $[0, 1]$. Note that trader i's submission price is either $p_t^{i,m}$ (for buy orders) or $p_t^{i,M}$ (for sell orders). If the depth at the best bid (ask) is not enough to fully satisfy the order size, the remaining volume of the order is executed against limit orders in the book. The trader thus takes the next best buy (sell) order and repeats this operation as many times as necessary until the order is fully executed. This mechanism applies under the condition that quotes of these orders are above (below) price $p_t^{i,M}$ ($p_t^{i,m}$). If the limit order is still unmatched by the time $t + \tau^i$ it is removed from the book.

The artificial limit order market with continuous double auction is redeveloped from "FinancialMarketModel" (CSS 739 Class Project Team, Simulating Financial Markets using MASON Framework, Center for Social Complexity, George Mason University, USA, 2008) based on MASON platform simulation framework (Sean Luke, Claudio CioRevilla, Liviu Panait, Keith Sullivan, and Gabriel Balan; MASON: A Multiagent Simulation Environment. Simulation, 81: 517–525, 2005). The architecture of the artificial limit order market is outlined in Figure 1.

2.3. Simulation Design and Setting. Our analysis of the model is based on computer simulations. We assume traders' investment horizons τ^i follow a uniform distribution between $\tau(1-\Delta)$ and $\tau(1+\Delta)$ where the reference investment horizon $\tau = 60$ (approximate one hour) and the range is specified by $\Delta = 0.5$. Furthermore, we restrict the investment horizons to be integers.

Traders are initially given $s_0^i = 10$ shares of the risky asset and $c_0^i = s_0^i F_0$ amount of cash, where the initial fundamental price $F_0 = \$50$. At the beginning of each period t, each trader i has a probability $1/\tau^i$ of entering the market. Agents observe the fundamental value F_t after they enter the market before submitting an order. Upon entering the market, trader i cancels any unmatched limit order and submits a new order according to the order submission rules in Table 1.

The volatility of the log fundamental price per period is set to $\sigma = 4$ basis points (bp) (if each trading period is treated as one minute, then the annualized volatility is approximately 10% p.a.), and risk aversion is set to $\alpha^i = 0.1$ for all traders following Chiarella et al. [11]. For the BSV traders with behavioral sentiment, we assume $\pi_L = (1/3)$, $\pi_H = (3/4)$, $\lambda_1 = 0.1$, and $\lambda_2 = 0.3$ following BSV98 and

Table 1: Summary of submission rules of agent i, $0 \le X \le 1$, is drawn from a uniform distribution.

	Buy/sell		Limit/market	Volume
$X \le P_{\text{buy}}$	Buy	$a_t^1 \le p_t^{i,m}$	Market order	$\le c_t^i / p_t^{i,m}$
$X \le P_{\text{buy}}$	Buy	$a_t^1 > p_t^{i,m}$	Limit order	$c_t^i / p_t^{i,m}$
$X > P_{\text{buy}}$	Sell	$b_t^1 \ge p_t^{i,M}$	Market order	$\le s_t^i$
$X > P_{\text{buy}}$	Sell	$b_t^1 < p_t^{i,M}$	Limit order	s_t^i

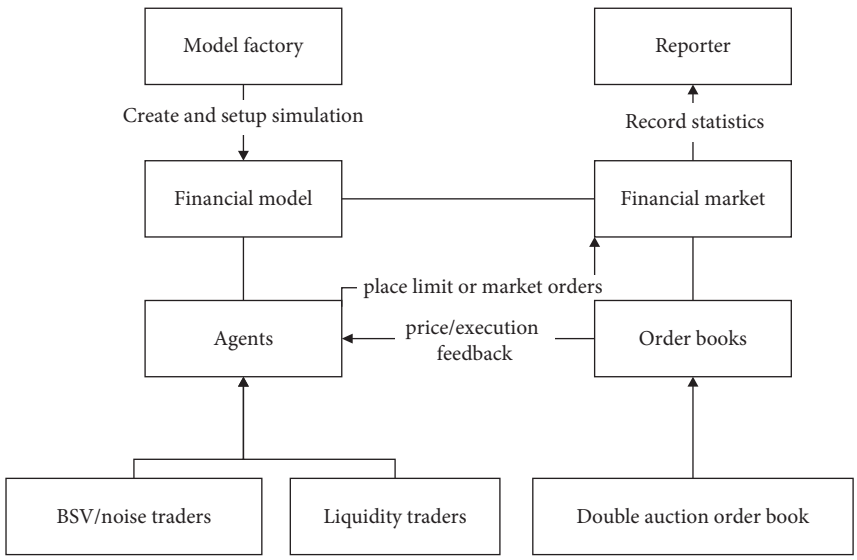

Figure 1: The architecture of artificial limit order market.

$\theta^i = \sigma\sqrt{\tau^i}$. Upon entering the market, trader i estimates the probabilities $q^i_{\pi,t}$ and $q^i_{\theta,t}$ based on her information $I^i_t = \{F_t, F_{t-\tau^i}, \cdots, F_{t-N^i\tau^i}\}$ with initial priors $q^i_{\pi,t-N^i\tau^i} = q^i_{\theta,t-N^i\tau^i} = 0.5$. We set $N^i = 60$ for every agent and the number of the agents to 1000 (we did some robustness tests with changing N^i to 90 or 30 and the total number of agents to 2000 or 500, and the results do not change significantly). The minimum tick size by which prices can differ is given by \$0.01. We assume that the *true* fundamental price process is a geometric random walk (the particular set of parameter values used in Section 2.3 has shown to reproduce many of the known stylized facts of financial markets including long memory in absolute returns, volumes and bid-ask spread, hump shape in mean depth profiles of order books, nonlinear relationship between order imbalance and midprice returns, and event clustering in order submission types, see Chiarella et al. [15]).

Apart from noise and BSV traders, we assume there are also liquidity traders. Liquidity traders' investment horizons and arrival rates follow the same uniform distribution as noise/BSV traders. They choose randomly between buy and sell orders with equal probability, after which they also choose randomly between market and limit orders with equal probability. The order size is randomly distributed between 1 and 10. Moreover, their limit orders are always at the best bid or ask price. Therefore, the liquidity traders do not set prices on the order book. They either provide or demand liquidity with equal probability. Given the total number of agents in the market, we assume 90% of them are noise/BSV traders and 10% of them are liquidity traders.

Intuitively, liquidity traders trade for exogenous reasons (e.g., unwind position to adhere to appropriate risk levels), and they may use market orders if they are impatient or limit orders at the best bid/ask if they have time to wait for more favourable prices. However, liquidity traders are not likely to place orders that are far away from the best bid/ask. Moreover, we assume they choose randomly between market and limit orders with equal probability because we think it is reasonable to assume that liquidity traders are equally likely to provide or consume liquidity to the market. Furthermore, order size is chosen randomly between 1 and 10 since traders are initially endowed with 10 shares of the risky asset, and the two choices need to be consistent to generate realistic results.

We design two simulation cases. The first one is the *noisy* case, which there are 900 noise traders and 100 liquidity traders, and we use this case as a benchmark. Then, we consider the other case, "BSV" case, in which there are 900 BSV traders and 100 liquidity traders.

The results reported are the outcome of 30 simulations of 72,000 periods with the first 60,000 steps used as a burn-in period (the results remain similar among different simulations).

3. Analysis of Simulation Results

In this section, we use the simulation results to examine under/overreaction effect and the impact of behavioral

sentiment on market volatility and liquidity. We first examine whether BSV sentiment can generate overreaction and underreaction in intraday data. Then, we examine the impact on intraday market volatility, liquidity including the bid-ask spread, the order book depth near the best quotes, and the trading volume.

3.1. Underreaction and Overreaction. According to BSV98, underreaction and overreaction are defined as

$$\mathbb{E}\left[r_{t+1} \mid z_t = G\right] > \mathbb{E}\left[r_{t+1} \mid z_t = B\right], \tag{17}$$

$$\begin{aligned}&\mathbb{E}\left[r_{t+1} \mid z_t = G, z_{t-1} = G, \cdots, z_{t-j} = G\right]\\ &\quad < \mathbb{E}\left[r_{t+1} \mid z_t = B, z_{t-1} = B, \cdots, z_{t-j} = B\right],\end{aligned} \tag{18}$$

respectively, i.e., returns tend to a higher following good news than following bad news; however, returns tend to lower following a series of good news than a series of bad news, which is in contrary to the *efficient market hypothesis* (EMH) that says any public information should be reflected by the equilibrium price such that no abnormal profit can be made. Therefore, under/overreaction serves as counterevidence against the EMH.

In the limit order market, we interpret an increase (decrease) in the midprice $\overline{p}_t = (1/2)(a_t^1 + b_t^1)$ as good (bad) news. Intuitively, an increase (decrease) in the midprice suggests that investors in the market are revising their expectation of the fundamental value of the risky asset upward (downward).

In order to test for underreaction specified in (17), we design the following *underreaction* (UR) trading strategy. Suppose the changes in the midprice, $\Delta\overline{p}_{t+1} = \overline{p}_{t+1} - \overline{p}_t$ act as trading signals, and the signal is positive when $\Delta\overline{p}_{t+1} > 0$ and negative when $\Delta\overline{p}_{t+1} < 0$ (in rational expectation equilibrium model, uninformed traders use the price as a public signal about future payoffs. For example, an increase in price signals to the uninformed traders that a positive private signal has been received by the informed traders. Therefore, we use price increase (decrease) as a buy (sell) signal for the under/overreaction trading strategies). Initially, if a trader observes a positive (negative) signal, she buys (short-sells) one share of the risky asset. Then, as soon as trading signal switches sign, she closes off the initial position. She repeats the strategy starting from the next period.

On the contrary, to exploit any overreaction present in the market, we construct the following trading strategy. An OR signal appears after 3 consecutive negative (positive) price changes; however, the strategy does not buy (sell) until an opposite signal appears. As a result, there are $j \geq 3$ consecutive price changes in the same sign before trade begins. For example, in Figure 2, there were 5 positive signals (exclude zero returns) before a negative return appeared, then strategy dictates to short-sell. Finally, the OR strategy waits the same number of periods before closing the position. Strategy repeats starting from the next period (we test $j \geq 1, 2, 3, \cdots, 9$; we find that when $j < 3$, the OR strategy is not profitable; and when $j \geq 3$, the OR strategy is profitable, but the opportunities of OR strategies decrease when j increases. Thus, we report the result of $j \geq 3$). Figure 2 provides graphic illustrations of the UR and OR trading strategies.

Table 2 reports the profitability of the UR and OR trading strategies; panel A assumes transactions occur at midprices, where panel B assumes that buy (sell) orders are executed at the best ask (bid). We have the following observations. First, both trading strategies deliver positive returns in a market populated by BSV and liquidity traders with the UR trading strategy being significantly more profitable than the OR strategy. In contrast, when the market is populated with noise and liquidity traders, the strategies deliver large negative returns. This confirms that the model generates realistic prices that are consistent with empirical evidence of under/overreaction. The UR strategy is much more profitable than the OR strategy since the UR strategy allows trading after every positive/negative signal, whereas the OR strategy activates only after a series of $j \geq 3$ consecutive signals of the same sign.

Second, after bid-ask spread is taken into account, the UR strategy remains profitable, whereas OR strategy has negative return in the market with BSV and liquidity traders. Intuitively, the OR strategy suffers from deterioration in market liquidity during the overreaction period; i.e., market depth reduces and spread widens after BSV traders trade overaggressively after observing a series of good/bad signals. We show evidence of this in Table 3.

3.2. Volatility, Spread, Volume, and Order Book Depth. We define following measures of market quality: *volatility* is the sample standard deviation of log-return of the midprice, that is, $\ln(\overline{p}_{t+1}) - \ln(\overline{p}_t)$ per trading period; the *bid-ask spread* is measured by the on average number of tick sizes between the best bid price and best ask price, that is, $a_t^1 - b_t^1$ per period; and *volume* is measured by the average number of shares being transacted per period. Moreover, we also compute the *average order book depth* near the best quotes. Average order book depth of the best 5 quotes on the ask (bid) side is denoted by *Da5* (*Db5*).

Results in Table 3 show that volatility, spread, and trading volume are all significantly smaller in a market populated by BSV traders than one populated by noise traders. The intuition is that, due to their Markov switching belief about the log-fundamental process, although BSV traders can underreact as well as overreact to news, they underreact more often. Investors are expected to underreact after every good or bad signal; however, they overreact only after they receive a series of positive or negative signals. Since the log fundamental process $\ln(F_t)$ is a random walk, the probability of observing a series of price increases or decreases is relatively small. Therefore, BSV traders submit less aggressive orders compared to noise traders given the same movement in the fundamental value. Results also show that order book depth is larger in a market populated by BSV traders than in market populated by noise traders. Intuitively, noise traders' expectations deviate randomly from the currently observed log-

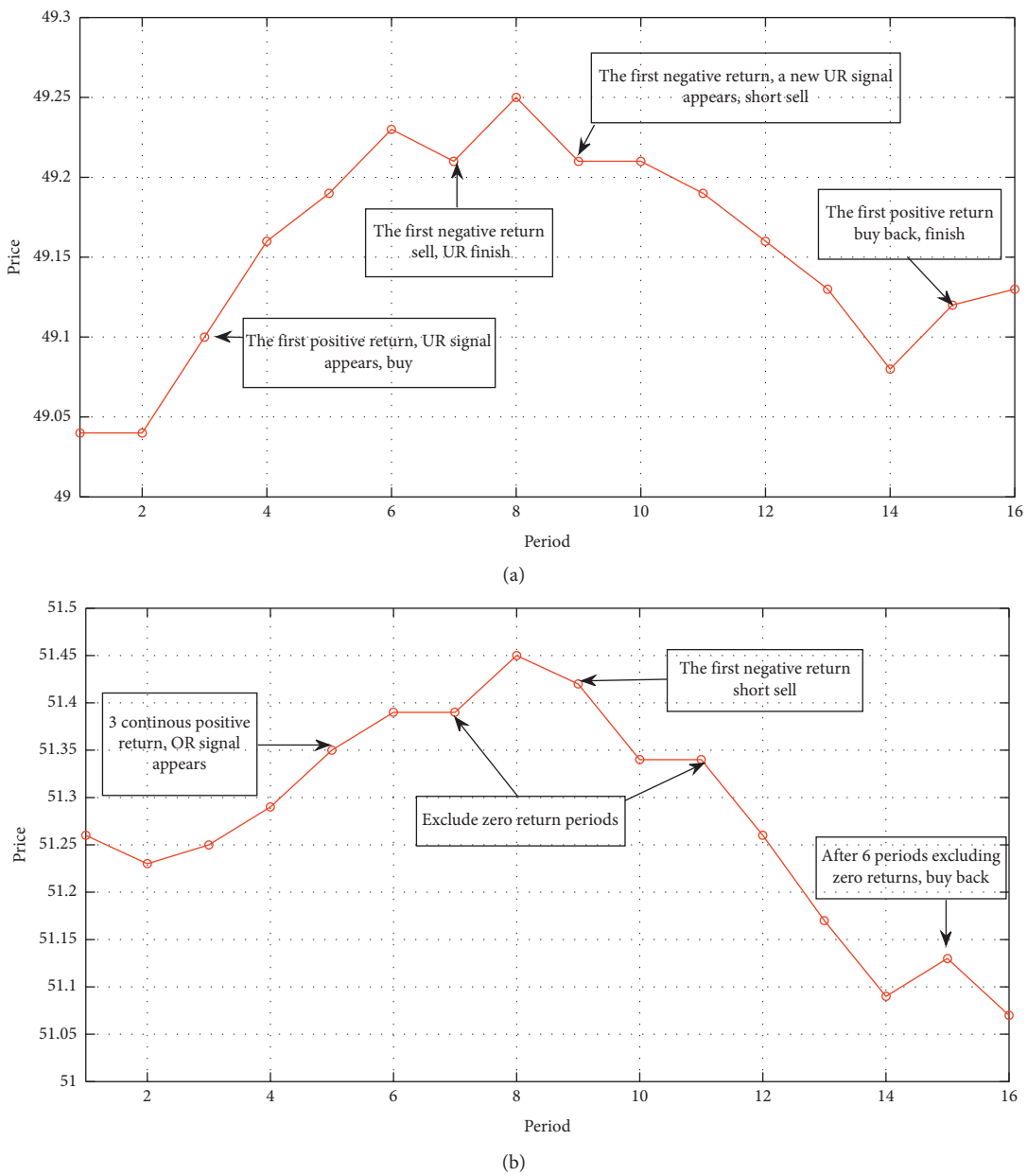

Figure 2: Graphic illustrations of the (a) underreaction (UR) and (b) overreaction (OR) trading strategies.

Table 2: Profitability of the *underreaction* (UR) and *overreaction* (OR) strategies.

Panel A	UR	OR
BSV	27.49	1.73
Noise	−53.34	−7.34
Panel B	UR	OR
BSV	13.20	−4.53
Noise	−266.45	−56.05

Panel A assumes that all transactions occur at the midprice, whereas panel B assumes that buy (sell) orders are executed at the best ask (bid).

fundamental value, $\ln F_t$, whereas BSV traders' expectations are closer to $\ln F_t$ since they follow the same learning scheme. Therefore, noise traders are more likely to place limit order further away from the best quotes.

In Table 3, we also compute the volatility, spread, volume, and order book depth conditioned on the occurrence of overreaction in the market. Overreaction is identified when there had been j ($j \geq 3$) consecutive increases (decreases) in the midprice $\overline{p}_t$, which provides j consecutive positive (negative) trading signals. Suppose the first of the j consecutive positive/negative trading signals was observed in the trading period $[t, t+1]$, then the overreaction period is given by $[t, t+2j+1]$ corresponding to the trading horizon of the overreaction trading strategy. Moreover, the overreaction (OR) period is not constant period, and it has been calculated by the OR trading strategy. For example, if there are 3 after 3 consecutive positive price changes, then it means that there is an OR period; when there is a negative price change, the OR period ends; for example, if the

Table 3: Market quality measures with BSV and noise trading.

	Volatility	Spread	Volume	Da5	Db5
BSV	1.84 [0.23]	2.11 [0.73]	34.38[10.21]	78.35[16.96]	122.36[43.31]
BSV-OR	3.01[0.55]*	2.24[0.64]	56.59[14.94]*	75.33[16.06]*	107.00[28.03]*
Noise	5.33[0.46]	4.19[0.25]	94.83[7.49]	72.00[9.00]	87.25[15.00]
Noise-OR	5.35[0.42]	4.13[0.24]	95.91[7.02]	72.72[8.43]	89.54[9.44]

Unconditional means are denoted by *BSV* and *noise*, respectively. Conditional means during overreaction periods is denoted by *BSV-OR* and *noise-OR*, respectively. *Conditional and unconditional means are significantly different at 1% level. The value in the square brackets is the variance of 30 simulations.

negative price change happens at the 5th period, the length of OR is 5–1 = 4; if it happens at the 9th period, the length of OR period is 9–1 = 8. In Table 3, BSV-OR (noise-OR) corresponds to the overreaction periods in a market populated by BSV (noise) traders.

Results indicate that, in a market populated by BSV traders, volatility, volume increase, and order book depth reduce significantly during the overreaction periods. In contrast, there are no significant differences in any of the observable quantities in a market populated by noise traders. The intuition is clear; only the BSV trader actually overreacts during the overreaction period, during which they trade more aggressively, leading to higher volatility and trading volume, also reduced order book depth. The noise traders, on the other hand, do not overreact; therefore, their trading behavior is not affected by the overreaction periods. Interestingly, the bid-ask spread does not show any significant increases in the overreaction period even in a market populated by BSV traders, which suggests that even when they overreact, BSV traders do not trade aggressively enough to widen the spread.

4. Conclusion

In this paper, we propose an agent-based model to examine the impact of behavioural sentiment on market volatility and liquidity in limit order markets. Compared to noise traders who do not engage in learning at all and their beliefs deviate randomly from fundamental price, sentiment traders with a Bayesian learning scheme may underreact or overreact to past changes in the fundamental price; thus, traders with different investment horizons may have different expectations about the future fundamental price. In an artificial limit order market, traders are allowed to submit market or limit orders, and submission price and order size are both determined by CARA utility maximization.

Simulation results show that sentiment and noise trading have very different impacts in a limit order market. Firstly, underreaction and overreaction trading strategies are only profitable in a market populated by sentiment traders. Moreover, conditional on overreaction (signal by consecutive positive/negative midprice returns), only sentiment trading leads to a significant increase in trading volume and volatility and reduction in order book depth. Overall, we find that sentiment trading leads to rich trading and price patterns, which resemble more of those in the real stock market.

For future avenues of research, it would be interesting to extend the model to include a chartist component in agent's beliefs and examine the joint impact of sentiment and return extrapolation on the price and liquidity dynamics. For instance, the complex interaction between sentiment and extrapolation may provide an explanation for flash crash, sudden liquidity dry-ups, and commonality in the order flows.

Appendix

The Learning Process of BSV Traders

We assume that BSV traders do not observe the mean growth rate θ_t, so they update their probability beliefs about θ_t and π_t based on Bayesian learning process. Let $q^i_{\theta,t} \equiv \mathbb{P}(\theta_t = \theta^i \mid I^i_t)$ and $q^i_{\pi,t} \equiv \mathbb{P}(\pi_t = \pi_L \mid I^i_t)$, where $I^i_t \equiv \{F_t, F_{t-\tau^i}, \cdots, F_{t-N\tau^i}\}$. Define $R_{t+\tau^i} \equiv \ln(F_{t+\tau^i}/F_t)$, and trader i updates her probabilities after observing $R_{t+\tau^i}$ as follows:

$$\begin{aligned} q^i_{\theta,t+\tau^i} &= q^i_{\pi,t}\mathbb{P}\left(\theta_{t+\tau^i} = \theta^i \,\middle|\, \pi_t = \pi_L, R_{t+\tau^i}\right) + \left(1 - q^i_{\pi,t}\right)\mathbb{P}\left(\theta_{t+\tau^i} = \theta^i \,\middle|\, \pi_t = \pi_H, R_{t+\tau^i}\right), \\ q^i_{\pi,t+\tau^i} &= q^i_{\theta,t}\mathbb{P}\left(\pi_{t+\tau^i} = \pi_L \,\middle|\, \theta_t = \theta^i, R_{t+\tau^i}\right) + \left(1 - q^i_{\theta,t}\right)\mathbb{P}\left(\pi_{t+\tau^i} = \pi_L \,\middle|\, \theta_t = -\theta^i, R_{t+\tau^i}\right), \end{aligned} \tag{A.1}$$

where

$$\begin{aligned} \mathbb{P}\left(\theta_{t+\tau^i} = \theta^i \,\middle|\, \pi_t, R_{t+\tau^i}\right) &= \frac{\mathbb{P}\left(R_{t+\tau^i} \,\middle|\, \theta_{t+\tau^i} = \theta^i\right)\mathbb{P}\left(\theta_{t+\tau^i} = \theta^i \,\middle|\, \pi_t\right)}{\sum_{\theta_{t+\tau^i}\in\{\theta^i,-\theta^i\}}\mathbb{P}\left(R_{t+\tau^i} \,\middle|\, \theta_{t+\tau^i}\right)\mathbb{P}\left(\theta_{t+\tau^i} = \theta \,\middle|\, \pi_t\right)}, \\ \mathbb{P}\left(\pi_{t+\tau^i} = \pi_L \,\middle|\, \theta_t, R_{t+\tau^i}\right) &= \frac{\mathbb{P}\left(\pi_{t+\tau^i} = \pi_L\right)\mathbb{P}\left(R_{t+\tau^i} \,\middle|\, \theta_t, \pi_{t+\tau^i} = \pi_L\right)}{\sum_{\pi_{t+\tau^i}\in\{\pi_L,\pi_H\}}\mathbb{P}\left(\pi_{t+\tau^i}\right)\mathbb{P}\left(R_{t+\tau^i} \,\middle|\, \theta_t, \pi_{t+\tau^i}\right)}, \end{aligned} \tag{A.2}$$

for $\theta_{t+\tau^i} \in \left\{-\theta^i, \theta^i\right\}$ and $\pi_{t+\tau^i} \in \{\pi_L, \pi_H\}$ and

$$\begin{aligned}
\mathbb{P}\left(R_{t+\tau^i} \mid \theta_{t+\tau^i}\right) &\propto \exp\left(-\frac{\left(R_{t+\tau^i}-\theta_{t+\tau^i}\right)^2}{\sigma^2\tau^i}\right),\\
\mathbb{P}\left(\theta_{t+\tau^i}=\theta^i \mid \pi_t\right) &= q^i_{\theta,t}\pi_t+\left(1-q^i_{\theta,t}\right)\left(1-\pi_t\right),\\
\mathbb{P}\left(\theta_{t+\tau^i}=-\theta^i \mid \pi_t\right) &= q^i_{\theta,t}\left(1-\pi_t\right)+\left(1-q^i_{\theta,t}\right)\pi_t,\\
\mathbb{P}\left(\pi_{t+\tau^i}=\pi_L\right) &= q^i_{\pi,t}\left(1-\lambda_1\right)+\left(1-q^i_{\pi,t}\right)\lambda_2,\\
\mathbb{P}\left(\pi_{t+\tau^i}=\pi_H\right) &= q^i_{\pi,t}\lambda_1+\left(1-q^i_{\pi,t}\right)\left(1-\lambda_2\right),\\
\mathbb{P}\left(R_{t+\tau^i} \mid \theta_t,\pi_{t+\tau^i}\right) &\propto \pi_{t+\tau^i}\exp\left(-\frac{\left(R_{t+\tau^i}-\theta_t\right)^2}{\sigma^2\tau^i}\right)+\left(1-\pi_{t+\tau^i}\right)\exp\left(-\frac{\left(R_{t+\tau^i}+\theta_t\right)^2}{\sigma^2\tau^i}\right),
\end{aligned} \tag{A.3}$$

for $\theta_t \in \left\{-\theta^i, \theta^i\right\}$ and $\pi_t \in \{\pi_L, \pi_H\}$.

Given her estimated probabilities $q^i_{\pi,t}$ and $q^i_{\theta,t}$, trader i makes a τ^i-period ahead forecast of the log fundamental price as the one in equation (7):

$$\mathbb{E}^i_t\left[\ln\left(F_{t+\tau^i}\right)\right] = \ln\left(F_t\right)+\mathbb{E}^i_t\left[\theta_{t+\tau^i}\right], \tag{A.4}$$

where

$$\begin{aligned}
\mathbb{E}^i_t\left[\theta_{t+\tau^i}\right] &= \mathbb{P}\left(\pi_{t+\tau^i}=\pi_L \mid I^i_t\right)\begin{pmatrix} q^i_{\theta,t} & 1-q^i_{\theta,t}\end{pmatrix}\begin{pmatrix}\pi_L & 1-\pi_L\\ 1-\pi_L & \pi_L\end{pmatrix}\begin{pmatrix}\theta^i\\ -\theta^i\end{pmatrix}\\
&+\mathbb{P}\left(\pi_{t+\tau^i}=\pi_H \mid I^i_t\right)\begin{pmatrix} q^i_{\theta,t} & 1-q^i_{\theta,t}\end{pmatrix}\begin{pmatrix}\pi_H & 1-\pi_H\\ 1-\pi_H & \pi_H\end{pmatrix}\begin{pmatrix}\theta^i\\ -\theta^i\end{pmatrix}.
\end{aligned} \tag{A.5}$$

Data Availability

The data were obtained from the simulation. The coding of the simulation is available from the corresponding author upon request.

Conflicts of Interest

The authors declare that they have no conflicts of interest.

Acknowledgments

Financial support from the National Natural Science Foundation of China, under grant NSFC 71671191, U1811462, and 71721001, is gratefully acknowledged.

References

[1] S. Klößner, M. Becker, and R. Friedmann, "Modeling and measuring intraday overreaction of stock prices," *Journal of Banking & Finance*, vol. 36, no. 4, pp. 1152–1163, 2012.

[2] A. Chekhlov, "Over- and under-reaction in liquid markets," *The Hedge Fund Journal*, 2010.

[3] S. Heston, R. Korajczyk, and R. Sadka, "Intraday patterns in the crosssection of stock returns," *Journal of Finance*, vol. 65, no. 4, pp. 1369–1407, 2010.

[4] L. Gao, Y. Han, S. Li, and G. Zhou, "Market intraday momentum," *Journal of Financial Economics*, vol. 129, no. 2, pp. 394–414, 2018.

[5] O. Komarov, "Intraday momentum," *SSRN Working Paper*, 2017.

[6] Y. Zhang, F. Ma, and B. Zhu, "Intraday momentum and stock return predictability: evidence from China," *Economic Modelling*, vol. 76, pp. 319–329, 2019.

[7] M. Jin, F. Kearney, Y. Li, and Y. Yang, "Intraday time-series momentum: evidence from China," *Journal of Futures Markets*, vol. 40, no. 4, pp. 632–650, 2020.

[8] N. Barberis, A. Shleifer, and R. Vishny, "A model of investor sentiment," *Journal of Financial Economics*, vol. 49, pp. 307–343, 1998.

[9] J. Paulin, A. Calinescu, and M. Wooldridge, "Agent-based modeling for complex financial systems," *IEEE Intelligent Systems*, vol. 33, no. 2, pp. 74–82, 2018.

[10] J. B. De Long, A. Shleifer, L. H. Summers, and R. J. Waldmann, "Noise trader risk in financial markets," *Journal of Political Economy*, vol. 98, no. 4, pp. 703–738, 1990.

[11] C. Chiarella, G. Iori, and J. Perellò, "The impact of heterogeneous trading rules on the limit order book and order flows," *Journal of Economic Dynamics and Control*, vol. 33, no. 3, pp. 525–537, 2009.

[12] Y. Zhang, W. Zhang, X. Xiong, and X. Jin, "BSV investors versus rational investors: an agent-based computational finance model," *International Journal of Information Technology & Decision Making*, vol. 5, no. 3, pp. 455–466, 2006.

[13] Y. Zhang and W. Zhang, "Can irrational investors survive? a social-computing perspective," *IEEE Intelligent Systems*, vol. 22, no. 5, pp. 58–64, 2007.
[14] S.-H. Chen, C.-L. Chang, and Y.-R. Du, "Agent-based economic models and econometrics," *Knowledge Engineering Review*, vol. 27, no. 2, pp. 187–219, 2012.
[15] C. Chiarella, X. He, L. Shi, and L. Wei, "A behavioural model of investor sentiment in limit order markets," *Quantitative Finance*, vol. 17, no. 1, pp. 71–86, 2017.

Hindawi
Complexity
Volume 2020, Article ID 8921030, 20 pages
https://doi.org/10.1155/2020/8921030

Research Article

Quantifying the Cross-Correlations between Online Market Participation Willingness and Stock Market Dynamics

Gang Chu,[1] Xiao Li,[2] and Yongjie Zhang[1]

[1]*College of Management and Economics, Tianjin University, Tianjin 300072, China*
[2]*School of Finance, Nankai University, Tianjin 300350, China*

Correspondence should be addressed to Xiao Li; xiaoli@nankai.edu.cn

Received 5 December 2019; Revised 29 April 2020; Accepted 27 May 2020; Published 24 June 2020

Academic Editor: Marcio Eisencraft

The investors' market participation willingness plays a vital role in the decision-making process of asset allocation. With the newly emerged dataset of investors' market participation willingness, this paper provides the first evidence on the dynamic relationship between market participation willingness and the market dynamics in the Chinese stock market. We select four typical Chinese stock market indices, i.e., SSE50 Index, CSI300 Index, Small and Medium Enterprise Market Index, and Growth Enterprise Market Index, to represent different aspects of the Chinese stock market. Moreover, we use mutual information to measure the overall dependence between market participation willingness and stock market and employ the DCCA cross-correlation coefficient and MF-DCCA to investigate the cross-correlation between market participation willingness and market dynamics. We find that there exist overall dependence and power-law cross-correlation between market participation willingness and the Chinese stock market, and the cross-correlations are significantly multifractal.

1. Introduction

Stock market participation is always an important topic in behavioral finance. Investors' market participation willingness directly affects investment decisions on how to allocate their assets to the savings or stock market. High market participation willingness means that more investors participate in the stock market and more capital flows into the stock market. The limited stock market participation is one of the most important market frictions and can help us understand some financial puzzles or anomalies which cannot be explained by frictionless neoclassical models [1]. Existing literature on market participation is more concerned with the determinants of market participation, while little is known about the influence of it on the stock market.

Previous studies have been paying more attention to the determinants of market participation. Some basic determinants of stock market participation have been recognized. The stock market participation willingness is influenced by family wealth [2], investors' financial education [3], IQ [4], gender [5], financial literacy [6], and personality traits [7]. However, in conventional economics of ideal markets and rational decision making, underlying determinants are usually neglected. Liang and Guo [8] highlighted that social interaction plays a significant role in transmitting relevant information to potential investors and found the marginal effect of social interactions on stock market participation. Bonaparte and Kumar [9] found that political activism increases people's propensity to participate in the stock market because their information-gathering costs are lower. Rao et al. [10] focused on the relationship between investor happiness and stock market participation, either directly or indirectly through mutual funds, by using data from China household finance survey (CHFS) and found that happiness affects investors' decisions regarding buying stocks or mutual funds.

As for the influence of market participation. Basak and Cuoco [11] constructed an equilibrium model to study the characterization of equilibrium prices and optimal consumption and investment policies, respectively, and investigated the equilibrium implications of restricted market participation. Guo [12] presents a consumption-based

model to explain the equity premium puzzle and finds that limited market participation led to lower risk-free rate generating a substantial liquidity premium. Polkovnichenko [13] also studied the implications of limited stock market participation for the equity premium, but he found that limited stock market participation does not play a significant role in explaining the equity premium puzzle. These studies only provide some evidence about the influence of market participation with theoretical models and a serious lack of empirical analysis support. The main reason for this is that the lack of proper data identifying the market participation willingness. Zhang [14] used US country-level racial composition as a proxy for market participation and found that stocks headquartered in countries with a higher percentage of the local white population have more liquidity. However, he only highlighted the influence of local market participation on local stocks, and we do not think the percentage of the white population is an indirect and improper proxy for market participation willingness. It is essential to provide more empirical evidence to explain the influence of market participation on the stock market. In addition, existing studies about market participation all focus on the developed countries' equity market, and the Chinese stock market is neglected. The Chinese stock market is one of the most important parts of the global financial market. Moreover, the Chinese stock market is dominated by individual investors, and their market participation willingness will have a significant impact on market performance. Therefore, the relationship between market participation willingness and the Chinese stock market may be different from that in the developed stock market.

The objective of this paper is to investigate the complex relationship between investors' market participant willingness and the Chinese stock market. Chinese stock market is dominated by individual investors, whose market participation willingness is more likely to affect the stock market. Since the stock market is a far more complex system with fractality properties [15–17], traditional methodologies under the framework of efficiency market hypothesis may not fully explain the relationship between investors' market participation willingness and the stock market. Recently, various methodologies under the theoretical framework of the fractal market hypothesis are put forward to investigate the multifractal property, such as multifractal detrended fluctuation analysis (MF-DFA) [18], multifractal detrended cross-correlation analysis (MF-DCCA) [19–21], and others. In this paper, we employ Yu'e Bao Sentiment Index (YSI) as a proxy for investors' market participation willingness and use the mutual information to measure the overall dependence between the investors' market participation willingness and the stock market; we also employ the DCCA cross-correlation coefficient and MF-DCCA method to investigate the cross-correlation between investors' market participation willingness and the stock market. Ruan et al. [22] used Yu'e Bao Sentiment Index as proxy for individual investor sentiment and employed the MF-DCCA method to investigate the cross-correlation between investor sentiment and stock market returns. Our paper differs from Ruan et al. [22] in a few key ways. First, the focus of Ruan et al.'s paper [22] is the relationship between investor sentiment and stock returns of Chinese stock market, while we focus on the investors' market participation willingness. Yu'e Bao Sentiment Index has been created to describe changes in users' willingness to enter the market. This index is designed based on data about hundreds of millions of users and millions of transactions, and thus we believe that this index is more appropriate to represent the investors' market participation willingness, rather than investor sentiment. Second, we thoroughly investigate the cross-correlation between investors' market participation willingness and stock market returns, trading volume, and stock market volatility, not just on the stock market return. Third, our study accounts for all major stock indices, including SSE50 Index, CSI300 Index, GEM Index, and SME Index, in Chinese stock market and is therefore generalizable. The SSE50 Index and CSI300 Index represent the mature and large-capitalization listed firms, which is not easy to be affected by market participation willingness. However, the GEM Index and SME Index represent the growing and small-capitalization listed firms, which is easier to be affected by market participation willingness. Thus, the dynamic relationship can be different when considering different types of stocks.

Our paper contributes to a growing literature in the following aspects. First, we focus on the relationship between investors' market participation willingness and the stock market. Existing literature about behavioral finance mainly focused on investor happiness [23, 24], investor sentiment [25–27], investor attention [28–30], and geographical information [31, 32]. This paper is the first one to give empirical analysis on the nonlinear cross-correlation between investors' market participation willingness and Chinese stock market performance. Second, we employ YSI as the proxy for market participation willingness in Chinese stock market. YSI is the newly emerged dataset on investors' willingness to participate in the stock market, which directly describes the market participation willingness based on the daily transaction behavior and data of over 200 million Yu'e Bao users. Third, we combine mutual information analysis and MF-DCCA analysis to examine the nonlinear relationship between investors' market participation willingness and Chinese stock performance. This new empirical perspective expands the existing literature.

The rest of this paper is organized as follows. Section 2 describes the data and preliminary test statistics. Section 3 introduces the methodology of mutual information and MF-DCCA. Section 4 represents the empirical results, and Section 5 makes a conclusion.

2. Data and Descriptive Statistics

This paper mainly uses the daily Yu'e Bao Sentiment Index (YSI) as the proxy for market participation willingness, which is derived from the TianHong Fund official website (http://www.thfund.com.cn/yuebao/emotions). Yu'e Bao is China's first-ever Internet fund specially designed for Alipay. It amasses roughly RMB 1.13 trillion in assets and 588 million users under management to 2019, marking it the largest money market fund in China. The YSI is constructed

by TianHong Fund by mining the fund data of Yu'e Bao users. This index is based on 200 million users and 10 billion pieces of data of the transaction, using big data analysis models and cloud computing technology to reflect the changes in users' willingness to enter the stock market. There is no doubt that Yu'e Bao Sentiment Index is an objective and accurate proxy for portraying investor's participation willingness in China. Meanwhile, compared with other market participation proxies, YSI can provide daily data excluding the IPO (Initial Public Offering) data. The time span of this index is from April 1, 2014, to May 10, 2018. We calculate the daily abnormal investor sentiment index (Ab_YSI) as the daily raw YSI as provided by TianHong Fund minus the average raw YSI over the prior 30 trading days, scaled by the average raw YSI over the prior 30 trading days. The detailed definition is as follows:

$$\text{Ab\_YSI}_t = \frac{\text{YSI}_t}{(1/30)\sum_{k=1}^{30}\text{YSI}_{i-k}} - 1, \tag{1}$$

where YSI_t is the Yu'e Bao Sentiment Index in day t.

To study the relationship between market participation willingness and stock market, we choose four major stock market indices, including SSE50 Index, CIS300 Index, SSE SME Composite (SME), and Growth Enterprise Market (GEM) Index. SSE50 and CSI300 indices are composed of listed companies with large market value and high liquidity, SME Index is composed of small size companies, and GEM Index is composed of high risk and rapid growth companies. We get the stock market index data from CSMAR (CSMAR financial dataset, China Stock Market Accounting Research financial dataset) financial database in the same sample period from April 1, 2014, to May 10, 2018. Formally, we estimate daily market returns and abnormal trading volume. We calculate daily abnormal volume as daily trading volume minus the average trading volume for a 30-trading-day period, divided by the average trading volume for a 30-trading-day period. The detailed definitions are as follows:

$$\text{Return}_t = \log\left(\frac{P_t}{P_{t-1}}\right), \tag{2}$$

where P_t is the stock market index return in day t.

$$\text{Ab\_Volume}_t = \frac{\text{Volume}_t}{(1/30)\sum_{k=1}^{30}\text{Volume}_{i-k}} - 1, \tag{3}$$

where Volume_t is the stock market trading volume in day t.

The variance of returns can be predicted using particular time series models, and the Generalized Autoregressive Conditional Heteroscedasticity (GARCH) seems to be the most successful [33, 34]. We use GARCH (1,1) to calculate the daily stock market returns volatility. The GARCH (1,1) model is as follows:

$$\begin{aligned} \varepsilon_t &= \sqrt{h_t}\nu_t, \\ h_t &= \alpha_0 + \beta_1 h_{t-1} + \alpha_1 \varepsilon_{t-1}^2, \end{aligned} \tag{4}$$

where h_t is the conditional variance.

Figure 1 illustrates the daily time series YSI, SSE50 Index, CSI300 Index, SME Index, and GEM Index. As shown in Figure 1, the trend of YSI is similar to Chinese stock market indices.

Table 1 reports the descriptive statistics for YSI, daily stock market returns, abnormal trading volume, and returns volatility, including the mean, standard deviation, skewness, kurtosis, minimum, and maximum. As shown in the table, YSI ranges from 415.1 to 2743.41, and the mean is 1033.156. The abnormal YSI varies from a minimum of −0.563 to a maximum of 1.284.

3. Methodology

In this section, we discuss the main methods used in this paper, including mutual information (MI), DCCA cross-correlation coefficient, and multifractal detrended cross-correlation analysis (MF-DCCA).

3.1. Mutual Information. In information theory, the mutual information (MI) is a measure of the mutual dependence between the two time series [35, 36]. Specifically, MI quantifies the random dependency between two stochastic variables without making any hypothesis about the nature of the relationship [37]. To measure the correlation between two equal length time series $X = \{x_t\}$ and $Y = \{y_t\}$, $t = 1, 2, 3, \ldots, N$, we compute the Shannon entropy $H(X)$ (or $H(Y)$) as follows:

$$H(X) = -\sum_{x\in X} p_X(x)\log p_X(x), \tag{5}$$

where $p_X(x)$ (or $p_Y(y)$) is the probability density function of a random variable X (or Y).

For a bivariate case, the Shannon joint entropy is calculated as follows:

$$H(X;Y) = -\sum_{x\in X}\sum_{y\in Y} p_{X,Y}(x,y)\log p_{X,Y}(x,y), \tag{6}$$

where $p_{X,Y}(x,y)$ is the joint probability density function of two random variables X and Y.

If the random variable Y depends on the random variable X, conditional entropy can be used to measure the remaining uncertainly in X with given Y. The conditional entropy is defined as follows:

$$H(X\mid Y) = -\sum_{x\in X}\sum_{y\in Y} p_{X,Y}(x,y)\log p_{X,Y}(x\mid y). \tag{7}$$

Generally, the conditional entropy $H(X\mid Y)$ can also be presented in terms of joint entropy $H(X,Y)$.

$$H(X\mid Y) = H(X;Y) - H(Y). \tag{8}$$

To quantify the dependence between variables X and Y, the mutual information is wieldy used. The mutual information of two random variables X and Y is defined as follows:

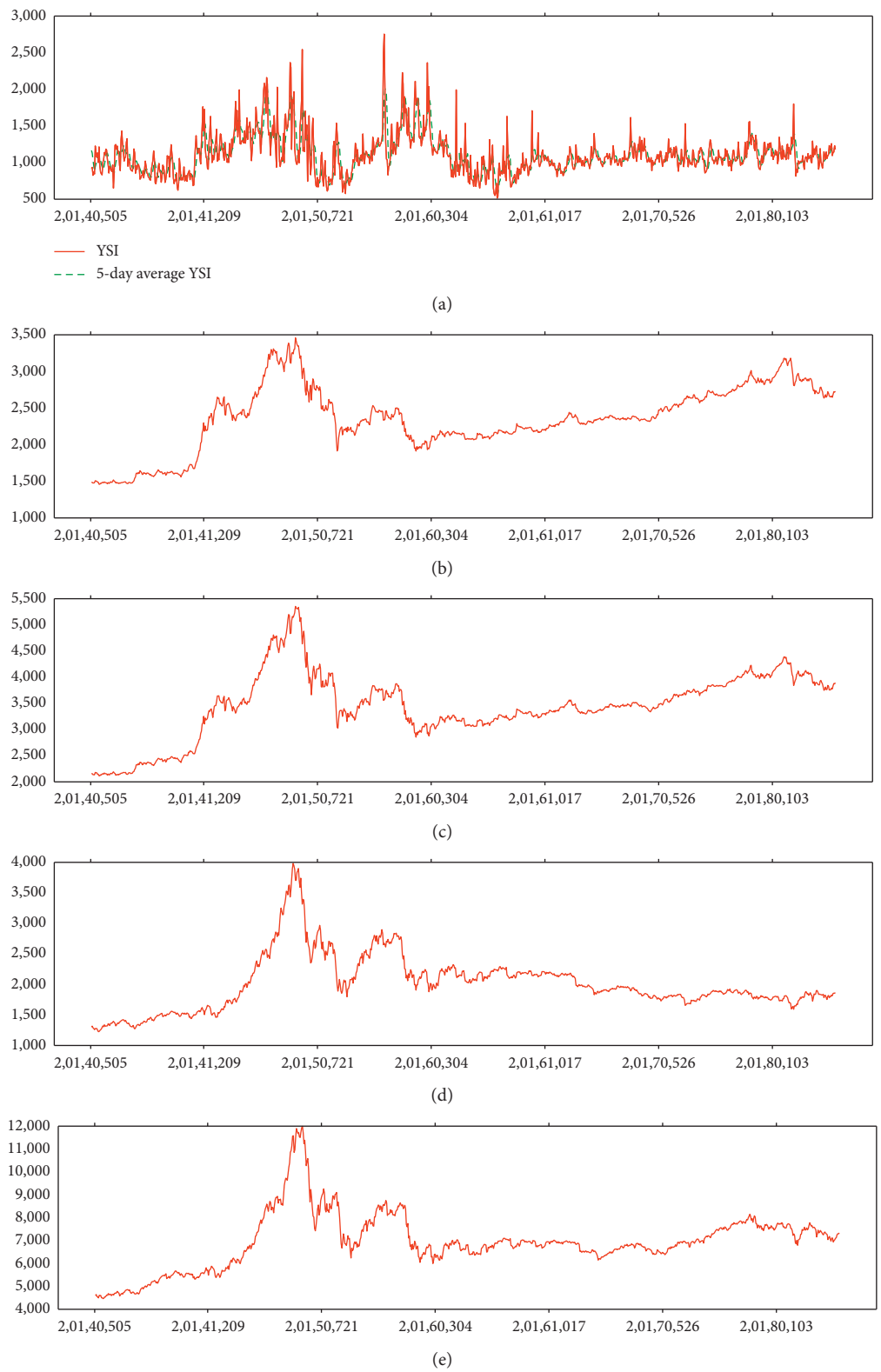

Figure 1: Time series of (a) YSI, (b) SSE50, (c) CSI300, (d) GEM, and (e) SME from May 1, 2014, to May 10, 2018.

$$\mathrm{MI}(X,Y) = \sum_{x\in X}\sum_{y\in Y} p_{X,Y}(x,y)\log\left(\frac{p_{X,Y}(x,y)}{p_X(x)p_Y(y)}\right). \quad (9)$$

Combining with Shannon's entropy, the mutual information $\mathrm{MI}(X,Y)$ can be expressed as

$$\mathrm{MI}(X,Y) = H(X) - H(X\mid Y). \quad (10)$$

Table 1: Summary statistics.

	Mean	Std. dev.	Skew.	Kurt.	Max	Min
(A) Yu'e Bao Sentiment Index						
YSI	1033.156	290.028	1.555	7.505	2743.41	415.1
Ab_YSI	0.00754	0.0457	1.169	7.064	1.284	−0.563
(B) Chinese stock market return						
SSE50	0.000266	0.00709	−0.839	10.336	0.0328	−0.0428
CSI300	0.000261	0.00691	−1.189	10.062	0.0282	−0.0398
SME	0.000211	0.00789	−1.042	7.507	0.0287	−0.0382
GEM	0.000165	0.00934	−0.669	5.835	0.0301	−0.0405
(C) Chinese stock market trade volume						
SSE50	0.0339	0.461	1.521	6.315	2.528	−0.752
CSI300	0.0254	0.351	1.189	5.257	1.968	−0.705
SME	0.0222	0.219	0.407	3.462	0.931	−0.758
GEM	0.0358	0.232	0.448	3.343	0.819	−0.767
(D) Chinese stock market volatility						
SSE50	0.000276	0.000362	2.506	9.999	0.00221	0.0000259
CSI300	0.000261	0.000343	2.441	9.240	0.00195	0.0000249
SME	0.000321	0.000331	1.819	5.489	0.00152	0.0000605
GEM	0.0004502	0.000439	1.659	4.928	0.00204	0.0000908

This table reports the mean, standard deviation (Std. dev.), skewness (Skew.), kurtosis (Kurt.), minimum (Min), and maximum (Max) of Yu'e Bao Sentiment Index (YSI and Ab_YSI), the return, volume, and volatility for four stock market indices: SSE50, CSI300, SME, and GEM. The sample period extends from May 5, 2014, through May 10, 2018.

By substituting equations (7) and (8), $\mathrm{MI}(X,Y)$ can be rewritten as

$$\mathrm{MI}(X,Y) = H(X) + H(Y) - H(X;Y). \tag{11}$$

Therefore, we can calculate mutual information between two random variables by estimating probability density functions $p_{X,Y}(x,y)$. In this paper, the probability density function is estimated by the method of equal distance histogram, which was proposed by Scott [38] to describe a one-dimensional or two-dimensional probability density function.

In equation (11), we have $0 \le \mathrm{MI}(X,Y) \le \infty$ [39]. We follow Granger and Lin [40] to use a standard measure for mutual information, which is defined as

$$I(X,Y) = \sqrt{1 - e^{-2\mathrm{MI}(X,Y)}}. \tag{12}$$

This measure ranges from 0 to 1 and can directly comparable with the linear correlation coefficient. Compared with traditional correlation coefficients, this function $I(X,Y)$ can capture the overall dependence, both linear and nonlinear, between two random variables.

3.2. Multifractal Detrended Cross-Correlation Analysis (MF-DCCA). The detrended fluctuation analysis (DFA) was proposed by Peng et al. [18] to explore the long-range correlations and multifractal features of a single nonstationary time series. Later, Kantelhard et al. [41] extended the DFA to multifractal system and proposed multifractal detrended fluctuation analysis (MF-DFA) to investigate the long-range auto-correlations of the financial time series.

Podobnik and Stanley [42] proposed a generalization of the DFA called detrended cross-correlation analysis (DCCA) method to explore the long range between two nonstationary time series. Based on MF-DFA and DCCA, Zhou [43] proposed multifractal detrended cross-correlation analysis (MF-DCCA) to detect the multifractal features of two nonstationary time series.

In this study, we adopt MF-DCCA to analyze the dynamic relationship between market participation willingness measured by YSI and Chinese stock market. Next, we will give a brief introduction to the methodology of MF-DCCA.

Consider any two equal length time series $\{x_i\}$ and $\{y_i\}$, $i = 1, 2, 3, \ldots, N$; the detailed steps of the MF-DCCA can be summarized as follows:

Step 1. Construct the profile of time series.

$$X_i = \sum_{k=1}^{i} (x_k - \overline{x}), Y_i = \sum_{k=1}^{i} (y_k - \overline{y}), \tag{13}$$

where $\overline{x} = (1/N)\sum_{k=1}^{N} x_k$ and $\overline{y} = (1/N)\sum_{k=1}^{N} y_k$.

Step 2. We divide the two profiles X_i and Y_i into $N_s = \mathrm{int}[N/S]$ nonoverlapping segments with the same length s. Consider that the length of the time series (N) is not always an integral multiple of the time scale s, and a short part segment at the end of each profile may remain. To make sure more information is contained in the time series, the same divided procedure is repeated starting from the end of each profile. So, we will get $2N_s$ nonoverlapping segments. In this paper, we set the scale s as $10 < s < N/4$.

Step 3. For each segment, we calculate the local trends by least-square fit of the series.

$$\widetilde{X}_{\lambda}(j) = \delta_k j^m + \cdots + \delta_1 j + \delta_0,$$
$$\widetilde{Y}_{\lambda}(j) = \gamma_k j^m + \cdots + \gamma_1 j + \gamma_0, \tag{14}$$

where
$j = 1, 2, \ldots; \lambda = 1, 2, 3, \ldots, 2N_s; m = 1, 2, 3, \ldots$.

Step 4. Calculate the detrended variances for each segment depending on the segment λ.

$$F^2(\lambda, s) = \frac{1}{s}\sum_{j=1}^{s}\left[X_{(\lambda-1)s+j} - \widetilde{X}_{(\lambda-1)s+j}\right]\left[Y_{(\lambda-1)s+j} - \widetilde{Y}_{(\lambda-1)s+j}\right], \tag{15}$$

where $\lambda = 1, 2, \ldots, N_s$; $\widetilde{X}$ and $\widetilde{Y}$ are the local trends.

$$F^2(\lambda, s) = \frac{1}{s}\sum_{j=1}^{s}\left[X_{N-(\lambda-N_s)s+j} - \widetilde{X}_{N-(\lambda-N_s)s+j}\right] \cdot \left[Y_{N-(\lambda-N_s)s+j} - \widetilde{Y}_{N-(\lambda-N_s)s+j}\right], \tag{16}$$

where $\lambda = N_s+1, N_s+2, \ldots, 2N_s$; $\widetilde{X}$ and $\widetilde{Y}$ are the local trends.

Step 5. Take the mean of the local trends of all detrended segments, and we get the qth-order fluctuation function:

$$F_q(s) = \left\{\frac{1}{2N_s}\sum_{\lambda=1}^{2N_s} F^2(s,\lambda)^{q/2}\right\}^{1/q}, \tag{17}$$

and for $q = 0$, this function can be defined as

$$F_0(s) = \exp\left\{\frac{1}{4N_s}\sum_{\lambda=1}^{2N_s}\ln\left[F^2(s,\lambda)\right]\right\}. \tag{18}$$

Step 6. By observing the plot of log-log plots of $F_q(s)$, we can analyze the scaling behavior of the fluctuations. If the two series are long-range cross-correlated, there is power-law relationship between them as follows:

$$F_q(s) \propto s^{h_{xy}(q)}. \tag{19}$$

This is equivalent to

$$\log F_q(s) = h_{xy}(q)\log(s) + \log C, \tag{20}$$

where $h_{xy}(q)$ denotes the slope of log-log plots of $F_q(s)$ versus s, which is computed by the method of OLS. And the value of $h_{xy}(q)$ indicates the cross-correlation of the two time series. In this paper, q varies from -10 to 10. If $q > 0$, $h_{xy}(q)$ reveals the scaling behaviors of the segments with large fluctuations; if $q < 0$, $h_{xy}(q)$ reveals the scaling behaviors of the segments with minor fluctuations; especially, when $q = 2$, the scaling exponent $h_{xy}(q)$ is the generalized Hurst exponent, and MF-DCCA reduces to DCCA. When $X(i)$ and $Y(i)$ denote the same time series, MF-DCCA reduces to MF-DFA.

Additionally, when $h_{xy}(q) > 0.5$, the cross-correlation between the two time series is persistent (positive), indicating that rise in one series is statistically likely to be followed by the increase of another; when $h_{xy}(q) < 0.5$, the cross-correlation between the two time series is antipersistent (negative), indicating that rise in one series is statistically likely to be followed by the decrease in another; and when $h_{xy}(q) = 0.5$, there are no cross-correlations between the two time series and the time series can be described as random walk.

Step 7. Following Shadkhoo and Jafari [44], we compute the multifractal scaling exponent $\tau_{xy}(q)$, called the Renyi exponent, to describe the multifractal property.

$$\tau_{xy}(q) = qh_{xy}(q) - 1. \tag{21}$$

If Renyi exponent $\tau_{xy}(q)$ is linear function of q, the cross-correlations of two series are monofractal. Otherwise, the relationships are multifractal.

Step 8. Through Legendre transform, we can obtain the multifractal spectrum $f(\alpha)$ as follows:

$$\alpha_{xy}(q) = H_{xy}(q) + qH'_{xy}(q), \tag{22}$$

and

$$f_{xy}(\alpha) = q\left[\alpha_{xy} - H_{xy}(q)\right] + 1, \tag{23}$$

where α_{xy} shows the degree of singularity of the time series and $f_{xy}(\alpha)$ reflects the fractal dimension of α.

Step 9. Calculate the multifractal intensity ΔH.

$$\Delta H = H_{\max}(q) - H_{\min}(q), \tag{24}$$

where the larger ΔH is, the higher the degree of multifractality is.

3.3. DCCA Cross-Correlation Coefficient. Zebende [45] proposed a new coefficient, namely, DCCA cross-correlation coefficient, to quantify the level of cross-correlation between nonstationary time series [46, 47]. The DCCA cross-correlation coefficient is defined in terms of the DFA method and the DCCA method, which is the ratio of the detrended covariance's function F^2_{DCCA} to the product of two detrended variance function F_{DFA}. This cross-correlation coefficient is widely used to measure the relations between two time series at different scales [48]. The function is defined as follows:

$$\rho_{\mathrm{DCCA}}(S) = \frac{F^2_{xy}(s)}{F_{xx}(s)F_{yy}(s)}, \tag{25}$$

where $F^2_{xy}(s)$ is the mean of the detrended covariance function. The functions F_{xx} and F_{yy} are, respectively, the root mean square fluctuation of each time series $\{x_t\}$ and $\{x_t\}$ separately. ρ_{DCCA} ranges from -1 to 1. A value of $\rho_{\mathrm{DCCA}} = 0$ means there is no cross-correlation. When $\rho_{\mathrm{DCCA}} = 1$, the two time series are completely antipersistent and positively correlated. When $\rho_{\mathrm{DCCA}} = -1$, the two time series are completely negatively correlated.

4. Empirical Results

4.1. Mutual Information Analysis. We start our analysis by investigating the overall dependence between the market participation willingness, measured by YSI, and Chinese stock market. Table 2 reports the mutual information ($I(X,Y)$) between market participation willingness and stock market returns, trading volume, and returns volatility, respectively. As shown in Table 2, $I(X,Y)$ between market participation willingness and Chinese stock market returns are all beyond 0.88. The mutual information between market participation willingness and Chinese stock market volume is beyond 0.89 and that between market participation willingness and Chinese stock market returns volatility is beyond 0.87. These results suggest that the market participation willingness contains much more dynamic information about Chinese stock market.

4.2. Cross-Correlation Test. To examine whether there is cross-correlation between market participation willingness and Chinese stock market, we refer to a cross-correlation test index $Q_{cc}(m)$ proposed by Podobnik et al. [49]. $Q_{cc}(m)$ is defined as

$$Q_{cc}(m) = N^2 \sum_{i=1}^{m} \frac{A_i^2}{N-i}, \tag{26}$$

where the cross-correlation function A_i^2 is given by

$$A_i^2 = \frac{\sum_{k=i+1}^{N} x_k y_{k-1}}{\sqrt{\sum_{k=1}^{N} x_k^2 \sum_{k=1}^{N} y_k^2}}, \tag{27}$$

where $\{x_t, t = 1, 2, \ldots, N\}$ and $\{y_t, t = 1, 2, \ldots, N\}$ are two time series.

The cross-correlation statistic $Q_{cc}(m)$ is approximately followed by $\chi^2(m)$ distributed with m degrees of freedom. The null hypothesis of cross-correlation is that there exists no cross-correlation between two time series. We set the critical values for the $\chi^2(m)$ distribution at 5% significance level for different degrees of freedom m. If the value of $Q_{cc}(m)$ exceeds the critical value of $\chi^2(m)$ distribution, the two time series have significant cross-correlations. Otherwise, no cross-correlations exist.

According to equations (26) and (27), we calculate the cross-correlation statistic $Q_{cc}(m)$ for the two time series with the degree of freedom varying from 1 to 800. The test results of market participation willingness and Chinese stock market returns are presented in Figure 2. The solid lines denote the critical value of $\chi^2(m)$ at 5% significance level. The dashed lines represent the value of $Q_{cc}(m)$. The cross-correlation statistic $Q_{cc}(m)$ for four market indices' returns, SSE50, CIS300, SME, and GEM, and market participation willingness is larger than the critical value for the χ^2 distribution at 5% level of significance, which means the Chinese stock market returns and market participation willingness are strongly cross-correlated. Figure 3 illustrates the cross-correlation statistic $Q_{cc}(m)$ for Chinese stock market volume and market participation willingness. The dashed lines in Figure 3 indicate that there is a long-range cross-correlation between Chinese stock market volume and market participation willingness. And we can also find that there exists a long-range cross-correlation between stock market returns volatility and market participation willingness in Figure 4.

4.3. DCCA Cross-Correlation Coefficient Analysis. The DCCA cross-correlation coefficient is quite different from the most popular measurement of the Pearson correlation coefficient and Spearman correlation coefficient, as these two measurements require the time-series to be stationary. However, the DCCA coefficient can measure the correlations between two nonstationary time series at different time scales. In this paper, we intend to apply the DCCA cross-correlation coefficient to investigate the cross-correlations between investors' market participation willingness (YSI) and stock market performance. Based on the different window size values s (n = 10, 50, 100, 150, 200, 250, 300, 350, 400), Table 3 presents calculation results for DCCA cross-correlation coefficient (ρ_{DCCA}). Our results show that all correlation coefficients are positive, meaning that investors' market participation willingness has positive correlation levels with the stock market, including stock returns, stock trading volume, and stock volatility. The results presented in Table 3 show that all of the ρ_{DCCA} fall within the interval at [0.4, 1], further verifying the cross-correlation test results.

4.4. Multifractal Detrended Cross-Correlation Analysis. As we show that there is serious long-range cross-correlation between market participation willingness and Chinese stock market, we can use the multifractal detrended cross-correlation analysis (MF-DCCA) to further investigate the cross-correlation between market participation willingness, measured by YSI, and Chinese stock market returns and trading volume, respectively.

Figure 5 illustrates the log-log plots of $F_{xyq}(s)$ versus s for market participation willingness and four major Chinese stock market indices' returns; the order q of lines decreases from top to bottom. As shown in Figure 4, for all series pairs, $F_{xyq}(s)$ increases linearly along with the scales s, implying that power-law behavior and long-range cross-correlations exist between market participation willingness and Chinese stock market returns. Additionally, Figure 6 illustrates the log-log plots for market participation willingness and four major Chinese stock market indices' trading volume, and Figure 7 illustrates the log-log plots for Chinese stock market returns volatility and market participation willingness. The linear log-log lines in Figures 6 and 7 both prove the existence of the power-law behavior and cross-correlations between market participation willingness and Chinese stock market trading volume and returns volatility, respectively.

Furthermore, we compute cross-correlation generalized Hurst exponents ($h_{xy}(q)$) based on equations (18)–(27). Figure 8 illustrates the cross-correlation generalized Hurst exponents between market participation willingness and Chinese stock market returns varying with q. As we can see, the cross-correlation generalized Hurst exponents are

Table 2: The mutual information between Chinese stock market and market participation willingness.

Market index	YSI and return	YSI and Ab_Volume	YSI and volatility
SSE50	0.884***	0.894***	0.879***
CSI300	0.885***	0.893***	0.879***
SME	0.891***	0.896***	0.889***
GEM	0.893***	0.898***	0.890***

This table reports the mutual information between Chinese stock market and YSI.

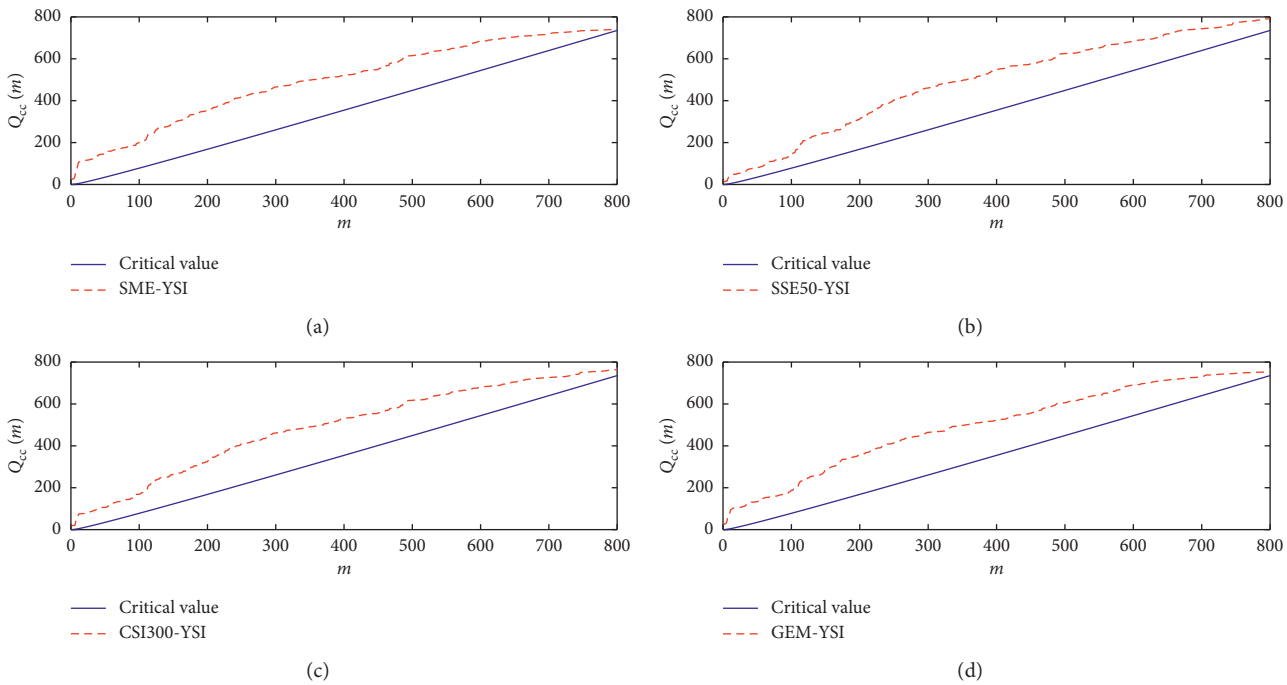

Figure 2: The cross-correlation statistic $Q_{cc}(m)$ for market participation willingness and Chinese stock market returns.

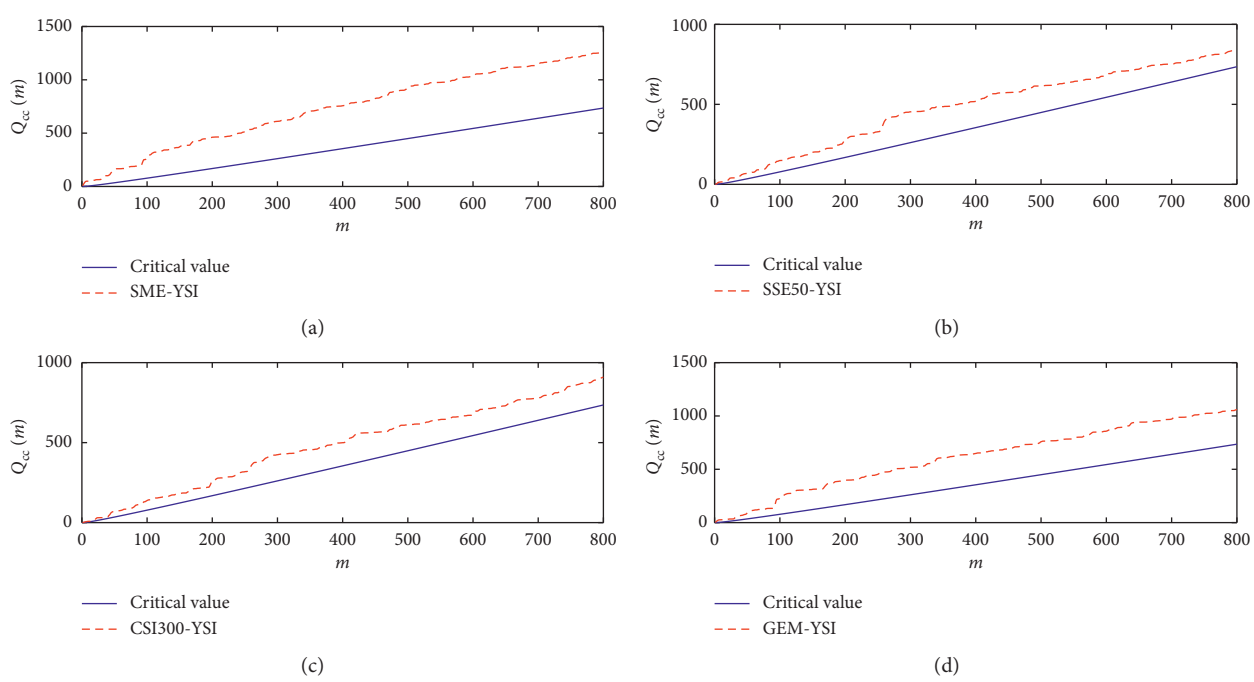

Figure 3: The cross-correlation statistic $Q_{cc}(m)$ for market participation willingness and Chinese stock market volume.

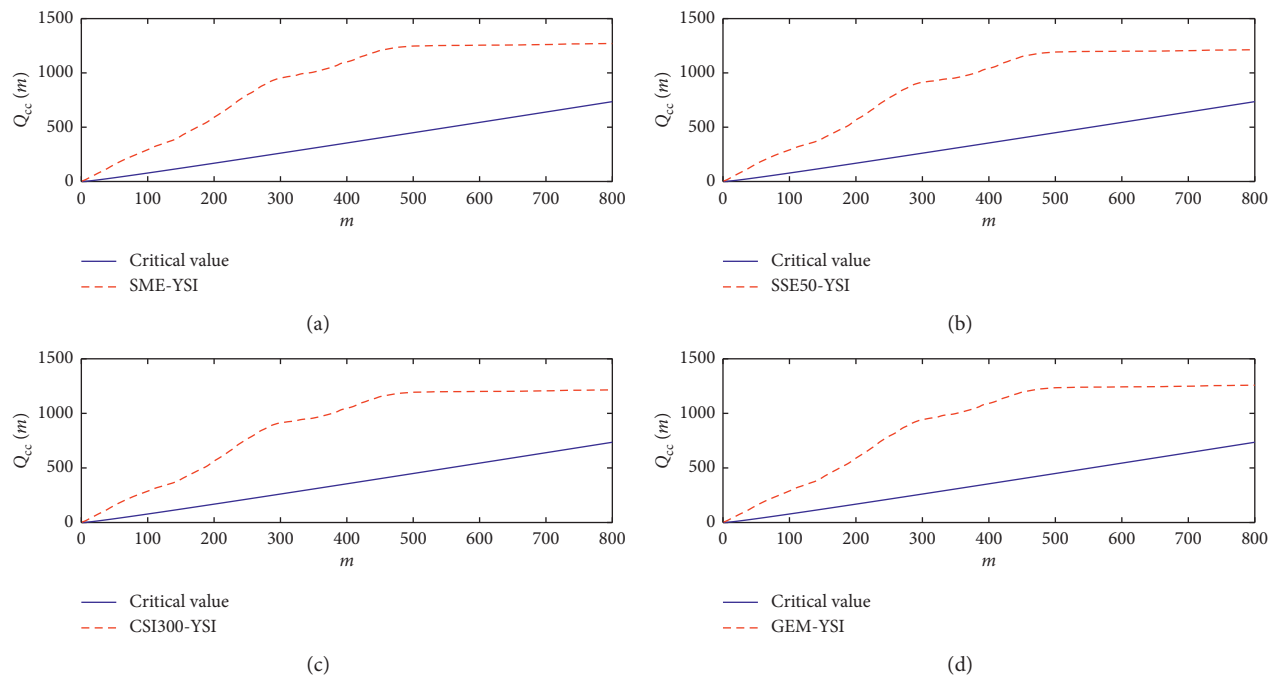

Figure 4: The cross-correlation statistic $Q_{cc}(m)$ for market participation willingness and Chinese stock market returns volatility.

Table 3: The detrended cross-correlation coefficient (ρ(DCCA)) for a given window size s.

Size (s)	10	50	100	150	200	250	300	350	400
(A) The detrended cross-correlation coefficient between YSI and market returns									
SSE50	0.618	0.630	0.657	0.652	0.649	0.673	0.677	0.639	0.634
CSI300	0.651	0.652	0.673	0.666	0.654	0.676	0.681	0.648	0.662
SME	0.671	0.670	0.698	0.668	0.646	0.642	0.637	0.615	0.663
GEM	0.661	0.682	0.693	0.672	0.659	0.661	0.660	0.632	0.658
(B) The detrended cross-correlation coefficient between YSI and market volume									
Size (s)	10	50	100	150	200	250	300	350	400
SSE50	0.548	0.574	0.544	0.567	0.557	0.574	0.584	0.637	0.589
CSI300	0.568	0.593	0.559	0.559	0.564	0.570	0.581	0.617	0.599
SME	0.619	0.608	0.621	0.615	0.638	0.642	0.648	0.627	0.656
GEM	0.599	0.614	0.614	0.605	0.610	0.644	0.629	0.631	0.647
(C) The detrended cross-correlation coefficient between YSI and market volatility									
Size (s)	10	50	100	150	200	250	300	350	400
SSE50	0.414	0.519	0.495	0.473	0.552	0.578	0.598	0.617	0.587
CSI300	0.424	0.518	0.506	0.529	0.556	0.559	0.586	0.648	0.558
SME	0.433	0.507	0.524	0.551	0.576	0.556	0.572	0.586	0.550
GEM	0.495	0.541	0.565	0.604	0.611	0.596	0.608	0.636	0.599

This table reports the detrended cross-correlation coefficient (ρ(DCCA)) between investors' market participation willingness (YSI) and stock market in function of time scale s. (A) reports ρ(DCCA) between the YSI and stock returns; (B) reports ρ(DCCA) between the YSI and stock trading volume; (C) reports ρ(DCCA) between the YSI and stock price volatility.

decreasing with q varying from −10 to 10. These results suggest that the cross-correlation of these two pairs is multifractal. Similar conclusions are also found in Figures 9 and 10, which shows the cross-correlation generalized Hurst exponents between market participation willingness and Chinese stock market volume and returns volatility, respectively.

Tables 4–6 report the value of cross-correlation Hurst exponents with q varying from −10 to 10 and the degree of multifractality ΔH_q. As shown in Table 4, when $q = 2$, the Hurst exponents of the cross-correlation between market participation willingness and four major stock market indices' returns, including SSE50, CSI300, SME, and GEM, are 0.486, 0.552, 0.553, and 0.457. The Hurst exponents of SSE50

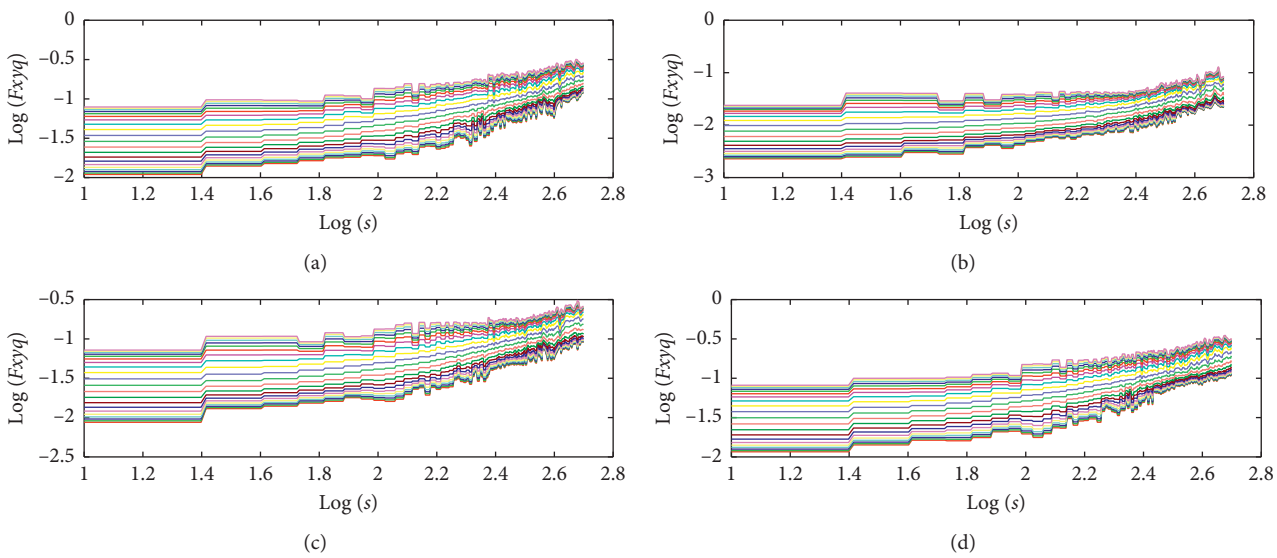

Figure 5: Log-log plots of cross-correlation fluctuation function versus time scale s for market participation willingness and Chinese stock market returns. (a) SME. (b) SSE50. (c) CSI300. (d) GEM.

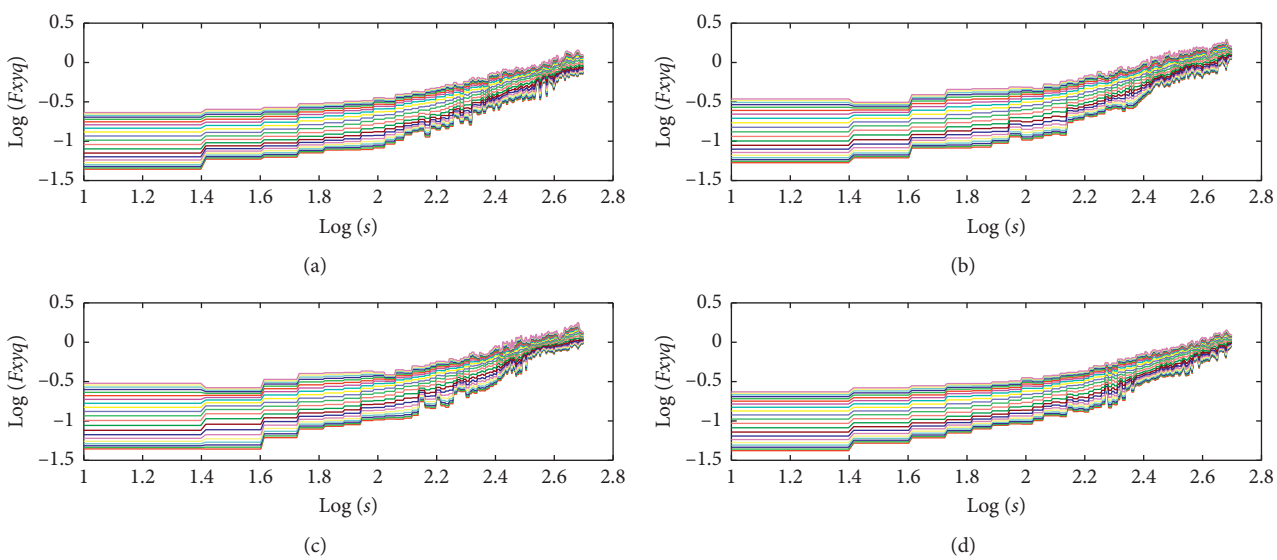

Figure 6: Log-log plots of cross-correlation fluctuation function versus time scale s for market participation willingness and Chinese stock market volume. (a) SME. (b) SSE50. (c) CSI300. (d) GEM.

and GEM are less than 0.5, implying that the cross-correlations between market participation willingness and SSE50 and GEM, respectively, are antipersistent; however, the Hurst exponents of CSI300 and SME are larger than 0.5, implying that the cross-correlations between CSI300 and SME, respectively, are persistent. However, when $q = 2$, all Hurst exponents of the cross-correlations between market participation willingness and Chinese stock market volume are larger than 0.5, indicating that the cross-correlations between market participation willingness and Chinese stock market volume are strongly persistent. For returns volatility, Table 7 reports that all degrees of multifractality for the small fluctuations ($q < 0$) are smaller than the large fluctuations ($q > 0$), suggesting that the cross-correlation between market participation willingness and Chinese stock market returns volatility is more stable when the fluctuation is large. Moreover, all the Hurst exponents of cross-correlation between Chinese stock market returns volatility and market participation willingness are larger than 0.5 when $q = 2$, indicating that the cross-correlations between Chinese stock market returns volatility and market participation willingness are significantly persistent.

Following Podobnik et al. [50], we can find turning points S^* in Figures 4–6 which indicate the fundamental change of the linear trend of the curves. There are two different behavior patterns in financial market: one is the short-term behavior which is easily influenced by the market

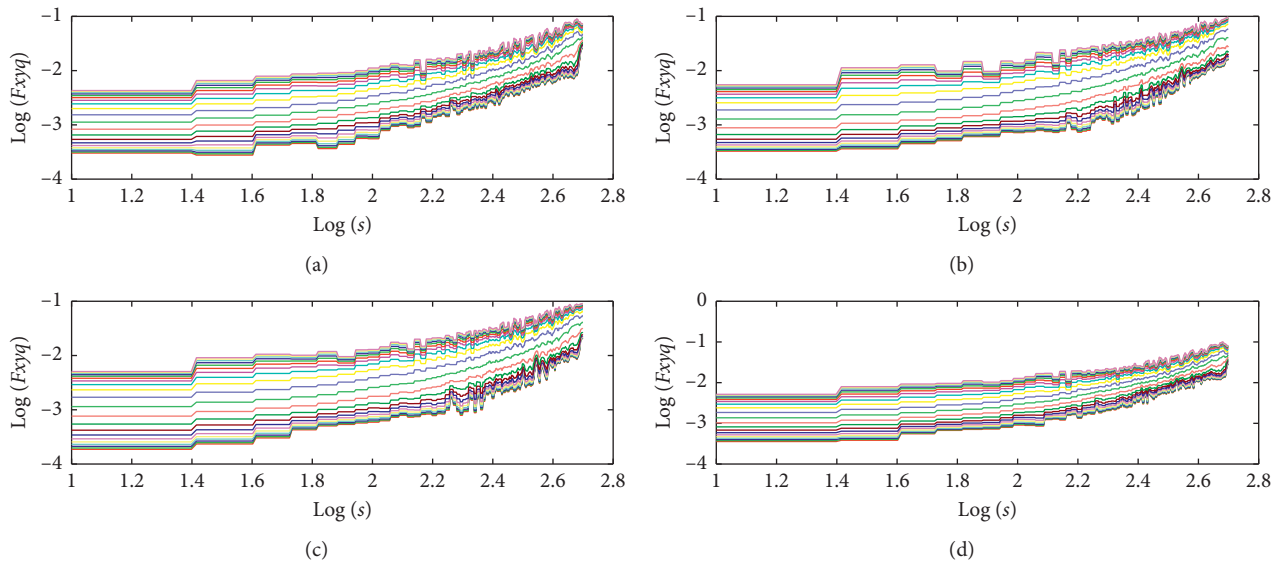

Figure 7: Log-log plots of cross-correlation fluctuation function versus time scale s for market participation willingness and Chinese stock market returns volatility. (a) SME. (b) SSE50. (c) CSI300. (d) GEM.

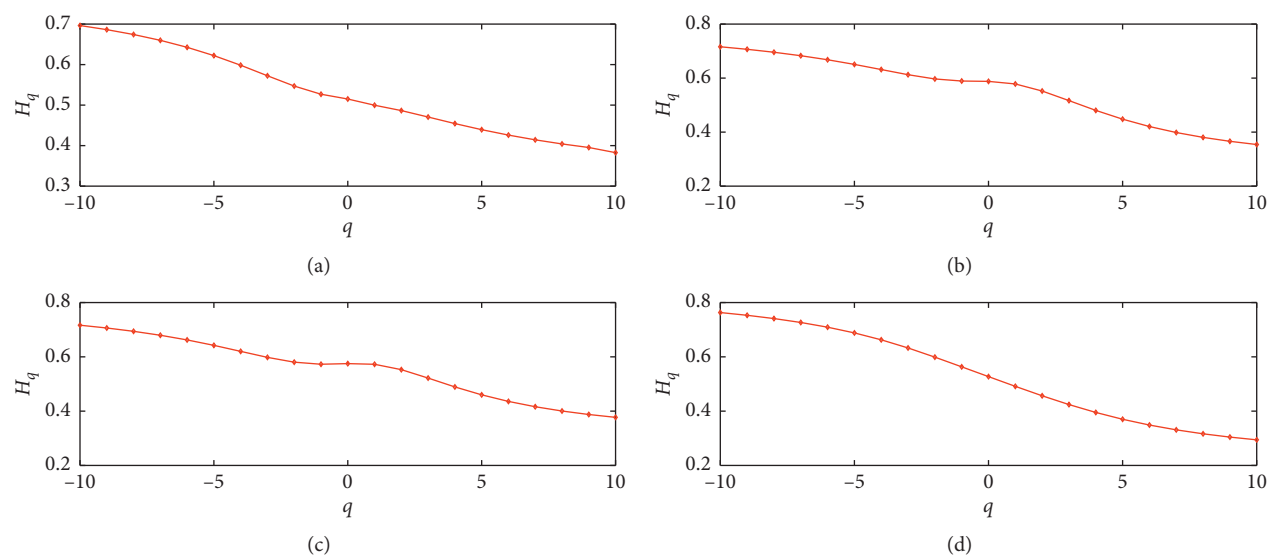

Figure 8: MF-DCCA scaling exponent for the market participation willingness and Chinese stock market returns. (a) SME-YSI. (b) SSE50-YSI. (c) CSI300-YSI. (d) GEM-YSI.

external factors and the other is the long-term behavior which is determined by the internal factors. The scaling exponents for $s < S^*$ can reflect the short-range correlation and imply the short-term behaviors, while the scaling exponents for $s > S^*$ imply the related behaviors in the long term. As observed from Figures 4–6, we can find the turning points at about $\log 10(S^*) = 2.3$ (about 200 days) for Chinese stock market returns, trading volume, and returns volatility. We provide the scaling exponents H_q with q varying from −10 to 10 in the short term ($s < S^*$) and long term ($s > S^*$) for Chinese stock market returns in Figure 11, trading volume in Figure 12, and returns volatility in Figure 13, respectively. Tables 7–9 report the values of the scaling exponents H_q with q. As shown in Table 7, the scaling exponents for $q = 2$ in the long term are all smaller than 0.5, indicating cross-correlated behaviors of large fluctuations are antipersistent in the long term for stock market return. In Table 8, we can find that all scaling exponents for $q = 2$ in the short term are larger than 0.5, implying the cross-correlated behaviors of large fluctuations are persistent in the short term for stock market volume, while the cross-correlated behaviors of large fluctuations are antipersistent in the long term for stock market volume. Table 9 reports that all the scaling exponents for $q = 2$ are larger than 0.5 both in

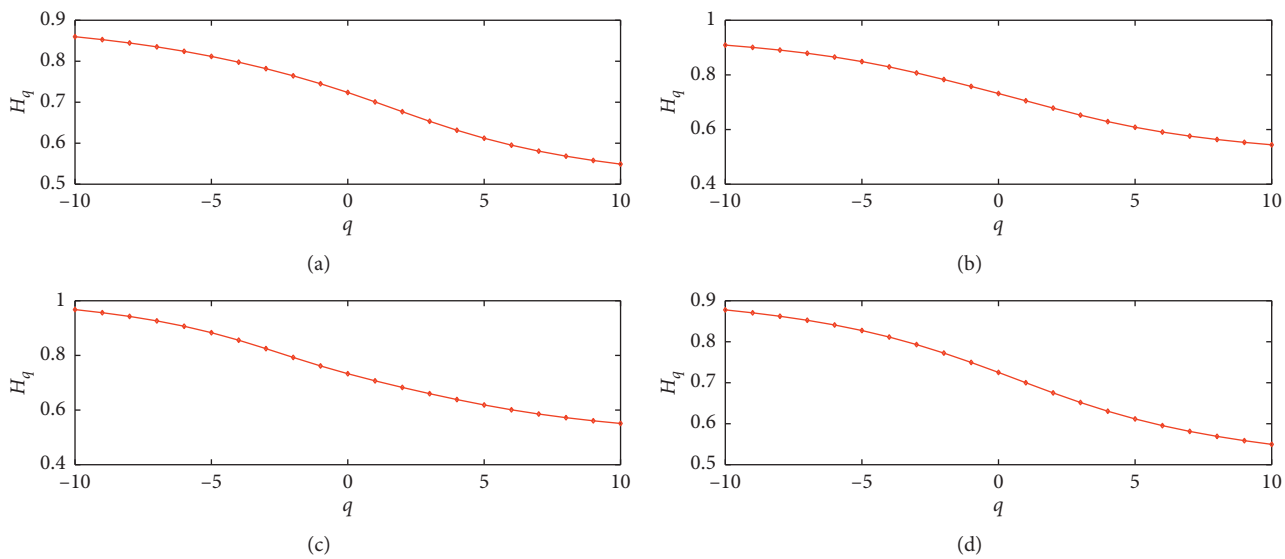

Figure 9: MF-DCCA scaling exponent for the market participation willingness and Chinese stock market volume. (a) SME-YSI. (b) SSE50-YSI. (c) CSI300-YSI. (d) GEM-YSI.

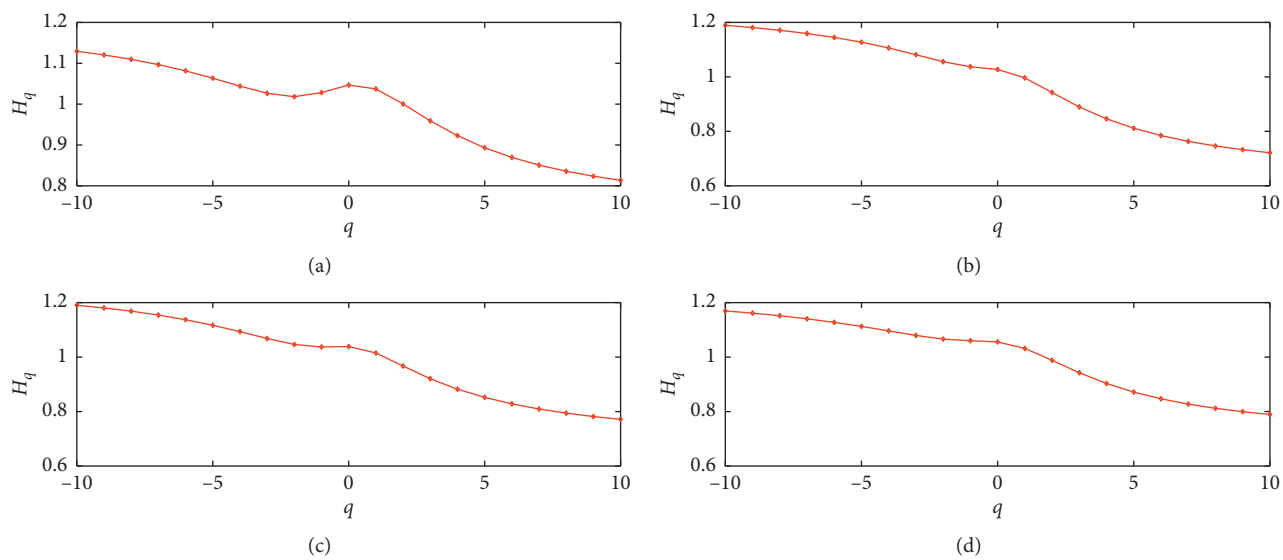

Figure 10: MF-DCCA scaling exponent for the market participation willingness and Chinese stock market returns volatility. (a) SME-YSI. (b) SSE50-YSI. (c) CSI300-YSI. (d) GEM-YSI.

the short term and long term, suggesting that the cross-correlated behaviors of lager fluctuations are persistent both in the short term and long term for Chinese stock market returns volatility. In addition, we find that the degrees of multifractality of the cross-correlation in the short term are smaller than those in the long term in Table 7. We can conclude that the cross-correlations between market participation willingness and Chinese stock market returns are more stable in the short term. Furthermore, the degrees of multifractality of the cross-correlation in the short term are larger than those in the long term in Tables 8 and 9, implying that the cross-correlations between market participation willingness and Chinese stock market trading volume and returns volatility, respectively, are more stable in the long term.

4.5. Rolling Window Analysis of Cross-Correlation. It is always a hot issue in the financial field to test or model structural breaks or regime switches in financial time series [20]. A number of these models, such as Markov switching ARCH [51] and Markov switching GARCH [52], are used to capture and depict regime shifts of low-frequency volatility dynamics. Later, the rolling window analysis, which is the approach of running a sequence of estimations over a moving window of data to analyze the evolving nature of time series, has been broadly adopted to explore dynamic features of scaling exponents and examine the impacts of external shocks and forecast trends.

Following Wang et al. [53], we set the window size to 250 trading days in this paper. Figure 14 illustrates the results of

Table 4: Results of the MF-DCCA scaling exponent for Chinese stock market returns.

q	SME-YSI	SSE50-YSI	CSI300-YSI	GME-YSI
−10	0.696	0.716	0.717	0.763
−9	0.686	0.707	0.706	0.753
−8	0.674	0.696	0.694	0.741
−7	0.659	0.683	0.679	0.727
−6	0.643	0.668	0.662	0.709
−5	0.622	0.651	0.642	0.688
−4	0.598	0.632	0.620	0.663
−3	0.572	0.613	0.598	0.633
−2	0.547	0.597	0.580	0.599
−1	0.527	0.589	0.573	0.563
0	0.515	0.587	0.575	0.527
ΔH_q	0.181	0.129	0.142	0.236
1	0.499	0.578	0.573	0.491
2	**0.486**	**0.552**	**0.553**	**0.457**
3	0.471	0.517	0.522	0.424
4	0.454	0.480	0.489	0.395
5	0.439	0.448	0.460	0.370
6	0.426	0.421	0.436	0.349
7	0.414	0.398	0.416	0.331
8	0.404	0.381	0.400	0.316
9	0.395	0.366	0.388	0.304
10	0.383	0.354	0.377	0.294
ΔH_q	0.116	0.224	0.196	0.197

This table reports the MF-DCCA scaling exponent between the returns of four stock market indices and market participation willingness with q varying from −10 to 10. The symbol ΔH_q denotes the degree of multifractality for the large and small fluctuations of the returns and YSI.

Table 5: Results of the MF-DCCA scaling exponent for Chinese stock market volume.

q	SME-YSI	SSE50-YSI	CSI300-YSI	GME-YSI
−10	0.859	0.909	0.968	0.878
−9	0.853	0.901	0.956	0.871
−8	0.845	0.891	0.943	0.862
−7	0.835	0.879	0.926	0.852
−6	0.824	0.865	0.907	0.841
−5	0.812	0.849	0.883	0.827
−4	0.798	0.829	0.856	0.812
−3	0.782	0.807	0.825	0.793
−2	0.764	0.783	0.792	0.772
−1	0.745	0.758	0.762	0.749
0	0.724	0.732	0.733	0.725
ΔH_q	0.135	0.177	0.235	0.153
1	0.701	0.705	0.707	0.700
2	**0.677**	**0.678**	**0.683**	**0.675**
3	0.653	0.653	0.659	0.652
4	0.632	0.629	0.638	0.631
5	0.612	0.608	0.619	0.612
6	0.595	0.591	0.601	0.595
7	0.581	0.576	0.585	0.581
8	0.568	0.563	0.572	0.569
9	0.558	0.553	0.561	0.559
10	0.549	0.544	0.551	0.549
ΔH_q	0.152	0.161	0.156	0.151

This table reports the MF-DCCA scaling exponent between the volume of four stock market indices and market participation willingness with q varying from −10 to 10. The symbol ΔH_q denotes the degree of multifractality for the large and small fluctuations of the returns and YSI.

the rolling window analysis for the cross-correlation between market participation willingness and Chinese stock market return. As observed from Figure 14, the cross-correlation exponents fluctuated violently around the level of 0.5 with exponents smaller than 0.5 accounting for the vast majority. These results imply the fact that mostly, the

Table 6: Results of the MF-DCCA scaling exponent for Chinese stock market returns volatility.

q	SME-YSI	SSE50-YSI	CSI300-YSI	GME-YSI
−10	1.129	1.189	1.190	1.169
−9	1.120	1.181	1.181	1.161
−8	1.109	1.171	1.169	1.152
−7	1.097	1.159	1.154	1.141
−6	1.081	1.145	1.137	1.128
−5	1.064	1.127	1.117	1.113
−4	1.044	1.106	1.093	1.096
−3	1.026	1.082	1.068	1.079
−2	1.018	1.056	1.046	1.066
−1	1.028	1.037	1.037	1.060
0	1.047	1.027	1.039	1.056
ΔH_q	0.082	0.162	0.161	0.113
1	1.037	0.996	1.015	1.032
2	**1.001**	**0.942**	**0.967**	**0.988**
3	0.959	0.889	0.920	0.943
4	0.923	0.846	0.882	0.903
5	0.893	0.812	0.852	0.872
6	0.869	0.785	0.828	0.847
7	0.851	0.763	0.809	0.827
8	0.836	0.746	0.794	0.812
9	0.824	0.733	0.782	0.799
10	0.814	0.722	0.771	0.789
ΔH_q	0.223	0.274	0.244	0.243

This table reports the MF-DCCA scaling exponent between the volatility of four stock market indices and market participation willingness with q varying from −10 to 10. The symbol ΔH_q denotes the degree of multifractality for the large and small fluctuations of the returns and YSI.

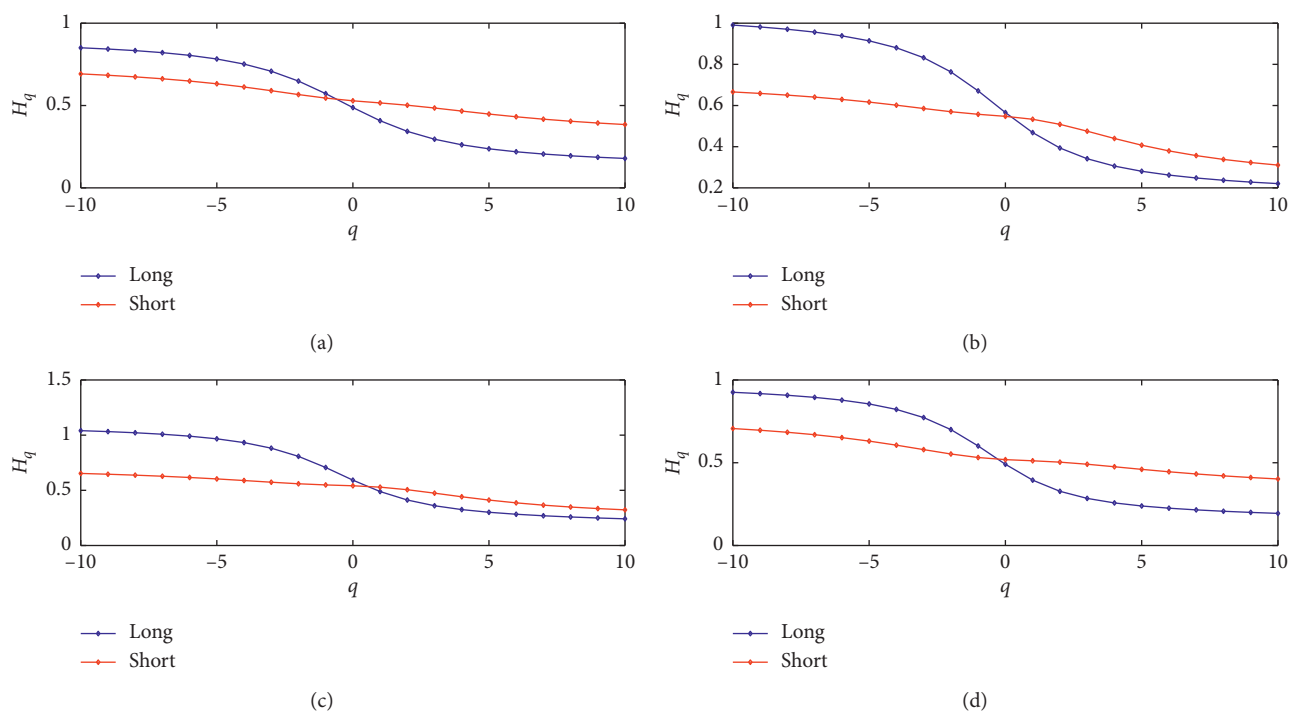

Figure 11: Short and long scaling exponents for Chinese stock market returns and market participation willingness. (a) SME-YSI. (b) SSE50-YSI. (c) CSI300-YSI. (d) GEM-YSI.

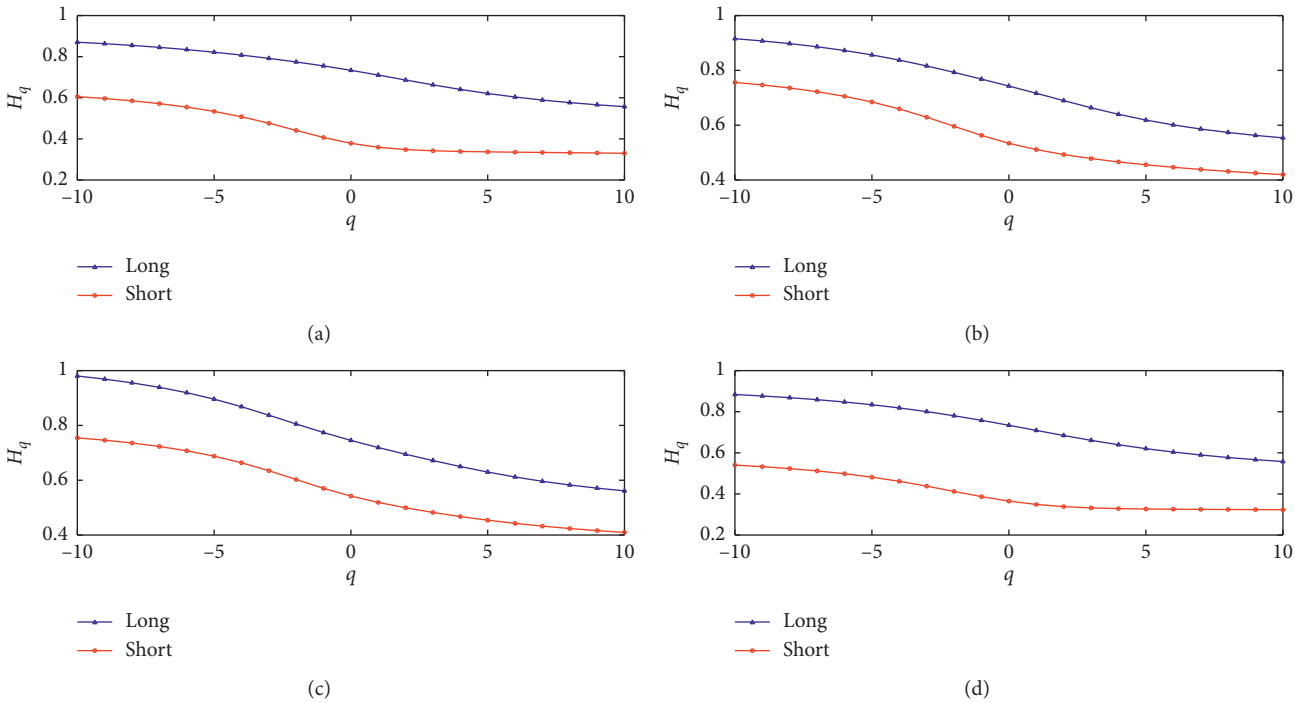

Figure 12: Short and long scaling exponents for Chinese stock market volume and market participation willingness. (a) SME-YSI. (b) SSE50-YSI. (c) CSI300-YSI. (d) GEM-YSI.

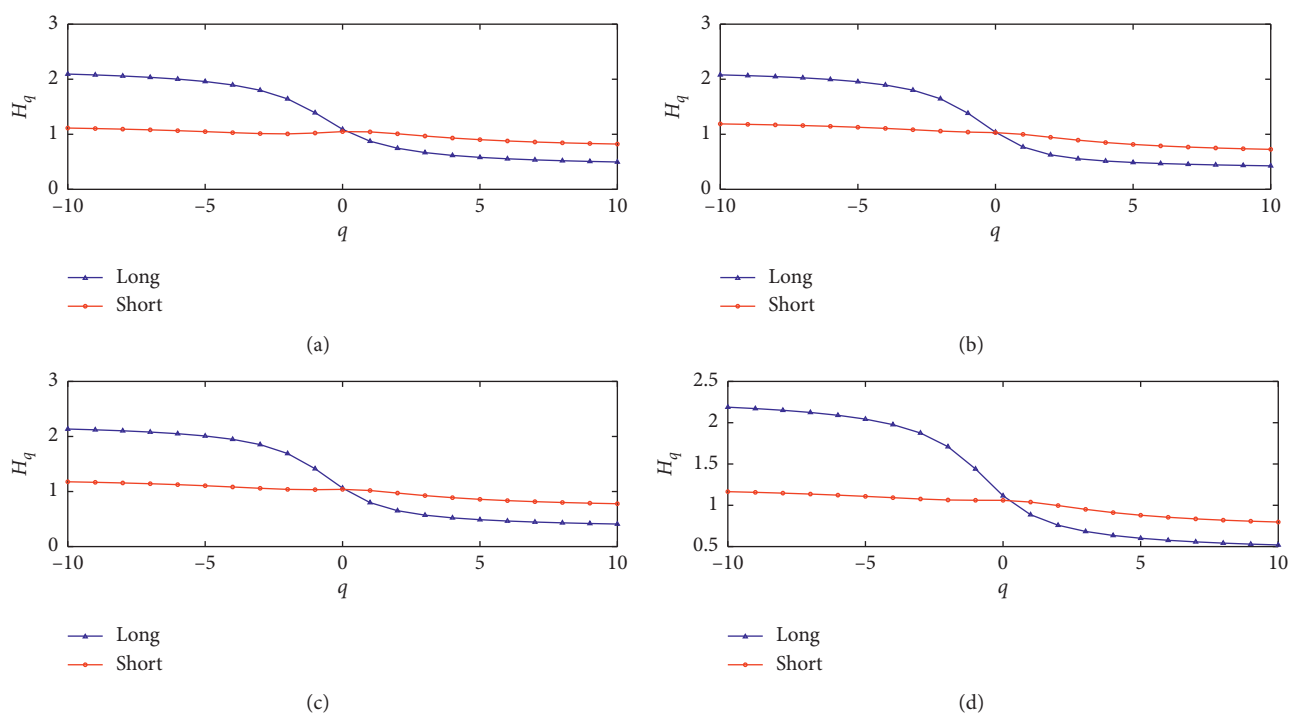

Figure 13: Short and long scaling exponents for Chinese stock market volatility and market participation willingness. (a) SME-YSI. (b) SSE50-YSI. (c) CSI300-YSI. (d) GEM-YSI.

cross-correlations between market participation willingness and Chinese market returns exhibit antipersistent features. Figure 15 illustrates the results of the rolling window analysis for the cross-correlation between market participation willingness and Chinese stock market trading volume. And we can observe that the cross-correlation exponents

Table 7: Results of the short-term and long-term scaling exponents for Chinese stock market returns.

q	SME-YSI		SSE50-YSI		CSI300-YSI		GME-YSI	
	Short	Long	Short	Long	Short	Long	Short	Long
−10	0.692	0.851	0.666	0.991	0.653	1.041	0.707	0.926
−9	0.684	0.843	0.659	0.982	0.646	1.032	0.696	0.918
−8	0.674	0.834	0.651	0.971	0.637	1.022	0.684	0.908
−7	0.662	0.821	0.641	0.957	0.628	1.008	0.669	0.895
−6	0.649	0.805	0.629	0.938	0.616	0.991	0.652	0.878
−5	0.632	0.783	0.617	0.914	0.603	0.967	0.631	0.855
−4	0.612	0.752	0.602	0.881	0.589	0.932	0.606	0.822
−3	0.590	0.708	0.585	0.832	0.573	0.882	0.579	0.773
−2	0.566	0.648	0.569	0.763	0.559	0.808	0.553	0.700
−1	0.545	0.572	0.557	0.671	0.549	0.707	0.531	0.601
0	0.528	0.487	0.547	0.565	0.541	0.592	0.519	0.491
1	0.516	0.408	0.533	0.468	0.529	0.4889	0.512	0.395
2	**0.502**	**0.343**	**0.509**	**0.394**	**0.506**	**0.412**	**0.504**	**0.327**
3	0.485	0.295	0.475	0.341	0.474	0.360	0.491	0.285
4	0.466	0.261	0.439	0.306	0.442	0.325	0.476	0.257
5	0.448	0.237	0.407	0.281	0.412	0.301	0.460	0.239
6	0.432	0.219	0.379	0.262	0.386	0.283	0.445	0.225
7	0.417	0.205	0.357	0.248	0.366	0.269	0.432	0.215
8	0.404	0.194	0.338	0.237	0.349	0.258	0.421	0.207
9	0.394	0.186	0.323	0.228	0.335	0.249	0.411	0.199
10	0.384	0.179	0.311	0.221	0.323	0.242	0.402	0.194
ΔH_q	0.308	0.672	0.355	0.770	0.330	0.799	0.305	0.732

This table reports the short-term and long-term scaling exponents between the returns of four stock market indices and market participation willingness with q varying from −10 to 10. ΔH_q is the multifractality degree. "Short" denotes $s < S^*$ and "Long" denotes $s > S^*$.

Table 8: Results of the short-term and long-term scaling exponents for Chinese stock market volume.

q	SME-YSI		SSE50-YSI		CSI300-YSI		GME-YSI	
	Short	Long	Short	Long	Short	Long	Short	Long
−10	0.870	0.606	0.916	0.756	0.980	0.755	0.884	0.541
−9	0.863	0.596	0.907	0.747	0.969	0.746	0.876	0.533
−8	0.855	0.585	0.898	0.736	0.955	0.736	0.868	0.523
−7	0.845	0.572	0.886	0.722	0.939	0.723	0.859	0.512
−6	0.834	0.555	0.872	0.705	0.919	0.707	0.847	0.498
−5	0.822	0.534	0.856	0.685	0.894	0.688	0.834	0.482
−4	0.808	0.507	0.838	0.659	0.868	0.664	0.818	0.461
−3	0.792	0.476	0.816	0.629	0.837	0.635	0.800	0.438
−2	0.774	0.441	0.793	0.596	0.805	0.602	0.780	0.412
−1	0.755	0.407	0.768	0.563	0.774	0.570	0.758	0.387
0	0.734	0.378	0.743	0.534	0.745	0.542	0.734	0.365
1	0.711	0.359	0.716	0.511	0.719	0.519	0.709	0.349
2	**0.686**	**0.348**	**0.689**	**0.493**	**0.695**	**0.499**	**0.684**	**0.338**
3	0.663	0.342	0.664	0.478	0.672	0.482	0.661	0.332
4	0.641	0.339	0.639	0.466	0.649	0.467	0.639	0.328
5	0.621	0.337	0.619	0.455	0.629	0.454	0.620	0.327
6	0.603	0.335	0.601	0.446	0.612	0.443	0.604	0.326
7	0.589	0.334	0.586	0.438	0.596	0.433	0.589	0.325
8	0.576	0.333	0.573	0.431	0.583	0.424	0.577	0.324
9	0.566	0.331	0.563	0.425	0.571	0.416	0.567	0.324
10	0.557	0.330	0.554	0.419	0.561	0.409	0.557	0.323
ΔH_q	0.313	0.276	0.362	0.337	0.419	0.346	0.327	0.218

This table reports the short-term and long-term scaling exponents between the volume of four stock market indices and market participation willingness with q varying from −10 to 10. ΔH_q is the multifractality degree. "Short" denotes $s < S^*$ and "Long" the $s > S^*$.

fluctuated violently all beyond the level of 0.5, indicating that the cross-correlations between market participation willingness and Chinese market volume exhibit persistent features in the whole period. Similar conclusions are also found in Figure 16, which illustrates the cross-correlation between market participation willingness and Chinese stock

Table 9: Results of the short-term and long-term scaling exponents for Chinese stock market returns volatility.

q	SME-YSI		SSE50-YSI		CSI300-YSI		GME-YSI	
	Short	Long	Short	Long	Short	Long	Short	Long
−10	2.094	1.113	2.079	1.188	2.135	1.177	2.188	1.165
−9	2.078	1.104	2.065	1.180	2.121	1.167	2.171	1.157
−8	2.059	1.093	2.048	1.170	2.103	1.156	2.151	1.147
−7	2.034	1.081	2.026	1.159	2.080	1.142	2.124	1.136
−6	2.002	1.065	1.996	1.145	2.050	1.125	2.089	1.123
−5	1.959	1.048	1.955	1.128	2.009	1.105	2.043	1.108
−4	1.896	1.029	1.895	1.107	1.948	1.083	1.977	1.092
−3	1.800	1.013	1.802	1.083	1.853	1.059	1.875	1.076
−2	1.643	1.007	1.645	1.058	1.690	1.039	1.709	1.064
−1	1.391	1.023	1.382	1.039	1.414	1.033	1.440	1.061
0	1.090	1.048	1.038	1.030	1.063	1.039	1.115	1.060
1	0.874	1.044	0.769	0.999	0.798	1.019	0.886	1.039
2	**0.746**	**1.009**	**0.627**	**0.945**	**0.652**	**0.972**	**0.758**	**0.997**
3	0.667	0.968	0.555	0.893	0.571	0.926	0.683	0.951
4	0.616	0.932	0.514	0.850	0.522	0.888	0.635	0.911
5	0.581	0.902	0.488	0.816	0.488	0.858	0.601	0.880
6	0.555	0.878	0.469	0.789	0.464	0.835	0.576	0.855
7	0.535	0.860	0.455	0.768	0.446	0.816	0.557	0.835
8	0.519	0.845	0.444	0.751	0.431	0.801	0.542	0.820
9	0.507	0.833	0.435	0.737	0.419	0.788	0.530	0.807
10	0.497	0.823	0.427	0.726	0.409	0.778	0.520	0.797
ΔH_q	1.597	0.290	1.652	0.462	1.726	0.399	1.668	0.368

This table reports the short-term and long-term scaling exponents between the returns volatility of four stock market indices and market participation willingness with q varying from −10 to 10. ΔH_q is the multifractality degree. "Short" denotes $s < S^*$ and "Long" denotes $s > S^*$.

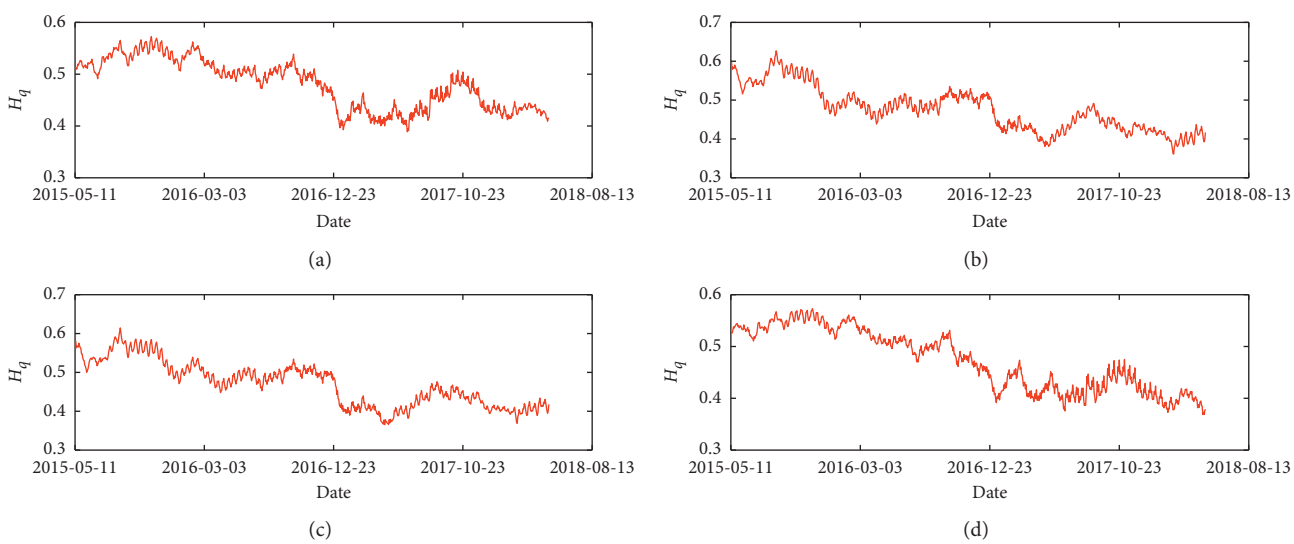

Figure 14: The time-varying scaling exponents for $q = 2$ for Chinese stock market returns and market participation willingness when window size is 250 days. (a) SME-YSI. (b) SSE50-YSI. (c) CSI300-YSI. (d) GEM-YSI.

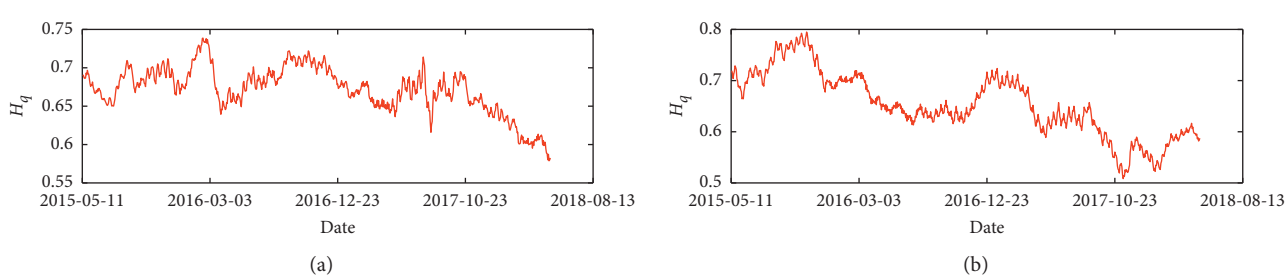

Figure 15: Continued.

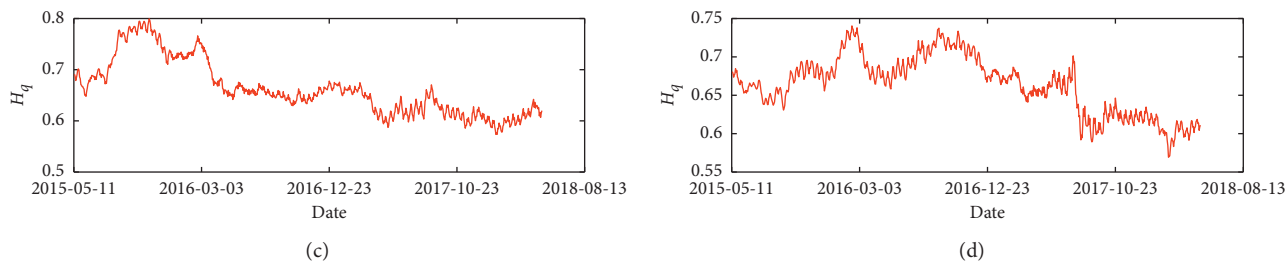

Figure 15: The time-varying scaling exponents for Chinese stock market volume and market participation willingness when window size is 250 days. (a) SME-YSI. (b) SSE50-YSI. (c) CSI300-YSI. (d) GEM-YSI.

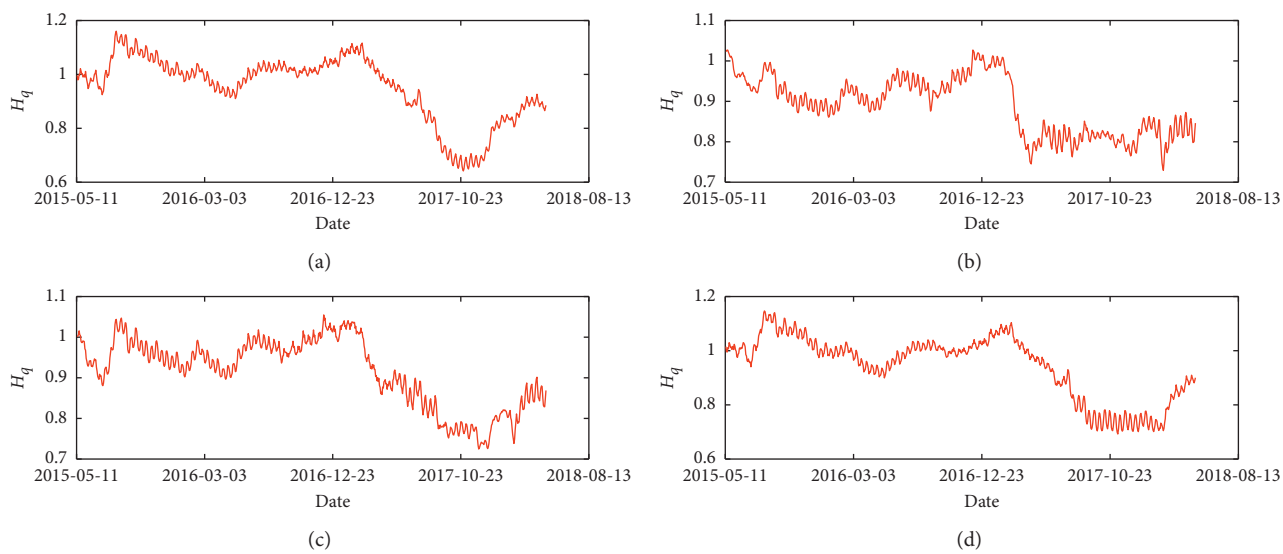

Figure 16: The time-varying scaling exponents for Chinese stock market volatility and market participation willingness when window size is 250 days. (a) SME-YSI. (b) SSE50-YSI. (c) CSI300-YSI. (d) GEM-YSI.

market returns volatility. The evolution of the cross-correlation exponents experienced erratic fluctuations and can be associated with financial events. For example, when Chinese stock exchanges introduced the circuit breakers in January 4, 2016, all cross-correlation exponents, both stock return and volume, were down.

5. Conclusions

In this paper, we investigate the nonlinear and dynamic relationship between market participation willingness, measured by Yu'e Bao Sentiment Index, and Chinese stock market performance. We utilize daily returns, trading volume, and returns volatility of SSE50, CSI300, SME, and GME to characterize the dynamic of Chinese stock market.

We employ mutual information to investigate the nonlinear dependence between the market participation willingness and Chinese stock market performance and find that there is overall dependence, both linear and nonlinear, between market participation willingness and Chinese stock market performance. Moreover, after cross-correlation test and DCCA cross-correlation coefficient analysis, we verify the existence of long-range cross-correlation between market participation willingness and stock market returns, trading volume, and volatility, respectively. We further employ MF-DCCA and find that there exists antipersistent cross-correlation between market participation willingness and Chinese stock market returns. We also find that there exists strong persistent cross-correlation between market participation willingness and Chinese stock market trading volume and returns volatility, respectively. Furthermore, we analyze the cross-correlation between market participation willingness and stock market in the short term and long term. We find that there is an antipersistent cross-correlation in the long term for market participation willingness and Chinese stock market returns and trading volume, respectively. And the cross-correlations between market participation willingness and Chinese stock returns volatility are strongly persistent both in the short term and long term. Moreover, cross-correlations between market participation willingness and Chinese stock market returns are more stable in the short term, but those between market participation willingness and Chinese stock market volume and returns volatility, respectively, are more stable in the long

term. Using the method of rolling windows, we find that the cross-correlation exponents between market participation willingness and Chinese stock market return are close to 0.5 over time and those between market participation willingness and stock market volume and returns volatility, respectively, are larger than 0.5. The evolution of cross-correlation exponents experienced erratic fluctuations.

Furthermore, several investment strategies and policy implications based on the findings can be derived. For investment managers, market participation willingness is an important factor to affect the stock market performance, which should be considered in investment portfolios. Moreover, regulators should take market participation willingness as an aspect of reflecting the market operation. Investors' market participation willingness should become an important reference of making or assessing the regulatory policies. For retail investors, market participation willingness can be considered as a valuable factor to predict stock market performance and help them make reasonable investment decision.

Data Availability

The data used to support the findings of this study are available from the corresponding author upon request.

Conflicts of Interest

The authors declare that they have no conflicts of interest.

Acknowledgments

This study was supported by the National Natural Science Foundation of China (71801136, 71771170, and U1811462) and the Fundamental Research Funds for the Central Universities (63202062).

References

[1] F. Allen and D. Gale, "Limited market participation and volatility of asset prices," *The American Economic Review*, vol. 84, no. 4, pp. 933–955, 1994.

[2] H. Guo, "Limited stock market participation and asset prices in a dynamic economy," *Journal of Financial and Quantitative Analysis*, vol. 39, no. 3, pp. 495–516, 2004.

[3] A. Vissing-Jorgensen, *Towards an Explanation of Household Portfolio Choice Heterogeneity: Non Financial Income and Participation Cost Structures*, National Bureau of Economic Research, Cambridge, MA, USA, 2002.

[4] P. J. Bayer, B. D. Bernheim, and J. K. Scholz, "The effects of financial education in the workplace: evidence from a survey of employers financial education in the workplace: evidence from a survey of employers," *Economic Inquiry*, vol. 47, no. 4, pp. 605–624, 2009.

[5] M. Grinblatt, M. Keloharju, and J. Linnainmaa, "IQ and stock market participation," *The Journal of Finance*, vol. 66, no. 6, pp. 2121–2164, 2011.

[6] J. Almenberg and A. Dreber, "Gender, stock market participation and financial literacy," *Economics Letters*, vol. 137, pp. 140–142, 2015.

[7] M. Van Rooij, A. Lusardi, and R. Alessie, "Financial literacy and stock market participation," *Journal of Financial Economics*, vol. 101, no. 2, pp. 449–472, 2011.

[8] P. Liang and S. Guo, "Social interaction, internet access and stock market participation-an empirical study in China," *Journal of Comparative Economics*, vol. 43, no. 4, pp. 883–901, 2015.

[9] Y. Bonaparte and A. Kumar, "Political activism, information costs, and stock market participation," *Journal of Financial Economics*, vol. 107, no. 3, pp. 760–786, 2013.

[10] Y. Rao, L. Mei, and R. Zhu, "Happiness and stock-market participation: empirical evidence from China," *Journal of Happiness Studies*, vol. 17, no. 1, pp. 271–293, 2016.

[11] S. Basak and D. Cuoco, "An equilibrium model with restricted stock market participation," *Review of Financial Studies*, vol. 11, no. 2, pp. 309–341, 1998.

[12] H. Guo, "Limited stock market participation and asset prices in a dynamic economy," *Journal of Financial and Quantitative Analysis*, vol. 39, no. 3, pp. 495–516, 2003.

[13] V. Polkovnichenko, "Limited stock market participation and the equity premium," *Finance Research Letters*, vol. 1, no. 1, pp. 24–34, 2004.

[14] L. Zhang, "Local equity market participation and stock liquidity," *The Quarterly Review of Economics and Finance*, vol. 63, pp. 101–121, 2017.

[15] Y. D. Wang, L. Liu, and R. B. Gu, "Analysis of efficiency for Shenzhen stock market based on multifractal detrended fluctuation analysis," *International Review of Financial Analysis*, vol. 18, no. 5, pp. 271–276, 2009.

[16] G. X. Cao, L. B. Xu, and J. Cao, "Multifractal detrended cross-correlations between the Chinese exchange market and stock market," *Physica A: Statistical Mechanics and Its Applications*, vol. 391, pp. 4855–4866, 2012.

[17] Y. H. Yang, W.-J. Xie, M.-X. Li, Z.-Q. Jiang, and W.-X. Zhou, "Statistical properties of user activity fluctuations in virtual worlds," *Chaos, Solitons & Fractals*, vol. 105, pp. 271–278, 2017.

[18] C. K. Peng, S. V. Buldyrev, S. Havlin, M. Simons, and A. L. Goldberger, "Mosaic organization of DNA nucleotides," *Physical Review E Statistical Physics Plasmas Fluids & Related Interdisciplinary Topics*, vol. 49, no. 2, pp. 1685–1689, 1994.

[19] S. P. Li, X. S. Lu, and X. H. Liu, "Dynamic relationship between Chinese RMB exchange rate index and market anxiety: a new perspective based on MF-DCCA," *Physica A: Statistical Mechanics and Its Applications*, vol. 541, Article ID 123405, 2020.

[20] X. S. Lu, X. X. Sun, and J. T. Ge, "Dynamic relationship between Japanese Yen exchange rates and market anxiety: a new perspective based on MF-DCCA," *Physica A: Statistical Mechanics and Its Applications*, vol. 474, pp. 144–161, 2017.

[21] G. X. Cao, Y. Han, Q. C. Li, and W. Xu, "Asymmetric MF-DCCA method based on risk conduction and its application in the Chinese and foreign stock markets," *Physica A: Statistical Mechanics and Its Applications*, vol. 468, pp. 119–130, 2017.

[22] Q. S. Ruan, H. Q. Yang, D. Y. Lv, and S. H. Zhang, "Cross-correlation between individual investor sentiment and Chinese stock market return: new perspective based on MF-DCCA," *Physica A: Statistical Mechanics and Its Applications*, vol. 503, pp. 243–256, 2018.

[23] M. Bonato, K. Gkillas, R. Gupta, and C. Pierdzioch, "Investor happiness and predictability of the realized volatility of oil price," *Sustainability*, vol. 12, no. 10, p. 4309, 2020.

[24] M. Bonato, K. Gkillas, R. Gupta, and C. Pierdzioch, "A note on investor happiness and the predictability of realized volatility of gold," *Finance Research Letters*, 2020.

[25] L. Bijl, G. Kringhaug, P. Molnár, and E. Sandvik, "Google searches and stock returns," *International Review of Financial Analysis*, vol. 45, pp. 150–156, 2016.

[26] N. Kim, K. Lučivjanská, P. Molnár, and R. Villa, "Google searches and stock market activity: evidence from Norway," *Finance Research Letters*, vol. 28, pp. 208–220, 2019.

[27] H. A. Aalborg, P. Molnár, and J. E. de Vries, "What can explain the price, volatility and trading volume of Bitcoin?" *Finance Research Letters*, vol. 29, pp. 255–265, 2019.

[28] J. Li and J. Yu, "Investor attention, psychological anchors, and stock return predictability," *Journal of Financial Economics*, vol. 104, no. 2, pp. 401–419, 2012.

[29] D. Andrei and M. Hasler, "Investor attention and stock market volatility," *Review of Financial Studies*, vol. 28, no. 1, pp. 33–72, 2015.

[30] N. Vozlyublennaia, "Investor attention, index performance, and return predictability," *Journal of Banking & Finance*, vol. 41, no. 4, pp. 17–35, 2014.

[31] X. Li, T. Qiu, G. Chen, L.-X. Zhong, and X.-F. Jiang, "Geography and distance effect on financial dynamics in the Chinese stock market," *Physica A: Statistical Mechanics and Its Applications*, vol. 457, pp. 109–116, 2016.

[32] R. Portes and H. Rey, "The determinants of cross-border equity flows," *Journal of International Economics*, vol. 65, no. 2, pp. 269–296, 2005.

[33] R. F. Engle, "Autoregressive conditional heteroscedasticity with estimates of the variance of United Kingdom inflation," *Econometrica*, vol. 50, no. 4, pp. 987–1008, 1982.

[34] P. H. Franses and D. Van Dijk, "Forecasting stock market volatility using (non-linear) garch models," *Journal of Forecasting*, vol. 15, no. 3, pp. 229–235, 1996.

[35] A. Q. Barbi and G. A. Prataviera, "Nonlinear dependencies on Brazilian equity network from mutual information minimum spanning trees," *Physica A: Statistical Mechanics and Its Applications*, vol. 523, pp. 876–885, 2019.

[36] M. Papapetrou and D. Kugiumtzis, "Tsallis conditional mutual information in investigating long range correlation in symbol sequences," *Physica A: Statistical Mechanics and Its Applications*, vol. 540, p. 123016, 2020.

[37] R. Steuer, J. Kurths, C. O. Daub, J. Weise, and J. Selbig, "The mutual information: detecting and evaluating dependencies between variables," *Bioinformatics*, vol. 18, no. 2, pp. 31–40, 2002.

[38] D. W. Scott, *Multivariable Density Estimation: Theory, Practice, and Visualization*, Wiley, New York, NY, USA, 1992.

[39] D. Andreia, R. Menezes, and D. A. Mendes, "Entropy-based independence test," *Nonlinear Dynamics*, vol. 44, no. 1–4, pp. 351–357, 2006.

[40] C. Granger and J.-L. Lin, "Using the mutual information coefficient to identify lags in nonlinear modelsficient to identify lags in nonlinear models," *Journal of Time Series Analysis*, vol. 15, no. 4, pp. 371–384, 1994.

[41] J. W. Kantelhardt, S. A. Zschiegner, E. Koscielny-Bunde, S. Havlin, A. Bunde, and H. E. Stanley, "Multifractal detrended fluctuation analysis of nonstationary time series," *Physica A: Statistical Mechanics and Its Applications*, vol. 316, no. 1–4, pp. 87–114, 2002.

[42] B. Podobnik, D. Horvatic, A. M. Petersen, and H. E. Stanley, "Cross-correlations between volume change and price change," *Proceedings of the National Academy of Sciences*, vol. 106, no. 52, pp. 22079–22084, 2009.

[43] W. X. Zhou, "Multifractal detrended cross-correlation analysis for two nonstationary signals," *Physical Review E Statistical Nonlinear & Soft Matter Physics*, vol. 77, no. 6, p. 66211, 2008.

[44] S. Shadkhoo and G. R. Jafari, "Multifractal detrended cross-correlation analysis of temporal and spatial seismic data," *The European Physical Journal B*, vol. 72, no. 4, pp. 679–683, 2009.

[45] G. F. Zebende, "DCCA cross-correlation coefficient: quantifying level of cross-correlation," *Physica A: Statistical Mechanics and Its Applications*, vol. 390, no. 4, pp. 614–618, 2011.

[46] X. Zhao, P. Shang, and J. Huang, "Several fundamental properties of DCCA cross-correlation coefficient," *Fractals*, vol. 25, no. 2, Article ID 1750017, 2017.

[47] U. Bashir, G. F. Zebende, Y. Yu, M. Hussain, A. Ali, and G. Abbas, "Differential market reactions to pre and post Brexit referendum," *Physica A: Statistical Mechanics and Its Applications*, vol. 5151, pp. 151–158, 2019.

[48] E. F. Guedes and G. F. Zebende, "DCCA cross-correlation coefficient with sliding windows approach," *Physica A: Statistical Mechanics and Its Applications*, vol. 527, Article ID 121286, 2019.

[49] B. Podobnik and H. E. Stanley, "Detrended cross-correlation analysis: a new method for analyzing two nonstationary time series," *Physical Review Letters*, vol. 100, no. 8, p. 84102, 2008.

[50] B. Podobnik, I. Grosse, D. Horvatić, S. Ilic, P. C. Ivanov, and H. E. Stanley, "Quantifying cross-correlations using local and global detrending approaches," *The European Physical Journal B*, vol. 71, no. 2, pp. 243–250, 2009.

[51] J. D. Hamilton and R. Susmel, "Autoregressive conditional heteroskedasticity and changes in regime," *Journal of Econometrics*, vol. 64, no. 1-2, pp. 307–333, 1994.

[52] F. Klaassen, "Improving GARCH volatility forecasts with regime-switching GARCH," *Empirical Economics*, vol. 27, no. 2, pp. 363–394, 2002.

[53] Y. Wang, Y. Wei, and C. Wu, "Cross-correlations between Chinese A-share and B-share markets," *Physica A: Statistical Mechanics and Its Applications*, vol. 389, no. 23, pp. 5468–5478, 2010.

Hindawi
Complexity
Volume 2020, Article ID 2757929, 15 pages
https://doi.org/10.1155/2020/2757929

Research Article

Digital Biomimetic Architecture between Art and Dynamic Structure: Case Study—Wings in Flight

Shi-Yen Wu,[1,2] **Felicia Wagiri**,[1] **Yen-Fen Huang**,[3] **and Shen-Guan Shih**[1]

[1]*Department of Architecture, National Taiwan University of Science and Technology, Taipei 10607, Taiwan*
[2]*Department of Architecture, National United University, Miaoli City 360, Taiwan*
[3]*Bartlett School of Architecture, University College London, London WC1E 6BT, UK*

Correspondence should be addressed to Shi-Yen Wu; sywu@mail.ntust.edu.tw

Received 2 September 2019; Revised 23 February 2020; Accepted 4 April 2020; Published 22 June 2020

Academic Editor: Dehua Shen

Architecture as a multirelated field is influenced and connected by many subjects. Among those subjects, the role of art and natural science is the most dominant frame without ignoring the development of advanced technology. By using technology, the impossible becomes possible such as to capture the body motion of humans as the subject of art and science at the same time. Body motion is a potential research of movement over the time. This does not only involve the aesthetic, but also even more the scientific aspect of a dynamic motion of an organism that can be investigated through a biomimetic approach. In order to understand the biomimetic term, we investigated the physical morphogenesis and geometrical principle of an organism. The term morphogenesis is a process in which the natural system produces and regulates the configuration of a material in space and over time. Based on that, we tried to design a dynamic structure using butterfly's motion as a subject of study with morphological and biomimetic approaches. Butterflies show a simultaneous aspect of movement over time characterized by fragmentation. This idea also summarizes many aspects of modern art such as portrayal of body movements by futurists, space-time continuum, cinematic freeze frame, and time-lapse photography. A futurist represents a movement that is emphasized on the factors of speed, technology, modernisms, and objects. This indicates an alternative position that may be relevant to the system of butterfly wings. This can only be achieved by utilizing a digital design and its parametric tools that help generate functions and form dynamic structures with high complexity and precision. Throughout the development of the system, there will be many changes to the form which will be constantly tested and evaluated using a series of prototype and visual digital design.

1. Introduction

Over the last 50 years, design and architecture have grown rapidly (and will continue to grow) to different phases and tried to break down their defined boundaries and started to integrate with other disciplines. Amongst many disciplines, visual arts and natural sciences such as physics, mathematics, chemistry, and social sciences, have constantly affected architectural thinking. The crossover results between these disciplines have resulted in a new form of collaboration and a new way of understanding the architectural context to promote a fresh perspective on design and architecture through the creative art processes and computer science that demonstrate reciprocal relationships.

The implementation of collaborative work was successful in generating a multidisciplinary attitude as well as achieving a new awareness of current technological advances. In this case, collaborative works discuss the potential partnerships between architects and artists in the creative interplay of Futurism and Dynamism. Futurism is an Impressionism of the mechanical world that uses advanced technology and urban modernity. It is committed to the new things, destroying older forms of culture and showing the beauty of modern life, machine, speed, and change [1]. The sensibility of the futurist is characterized by everything that is alive, which always responds and offers everything that moves, and whatever exists in motion (Dynamism and simultaneity).

There are many attractive works, ranging from Futurism and dynamics to creative applications in painting and art projects. The movement of the human body expresses mobility of space and sensibility of time and analyzes the potential for movement over time, involving many artistic activities such as dancing, theater, and spatial performing arts in both biological and psychological substances. The idea of motion is focused on the flux of memories and the sensations of what we remember, as well as the physical movement of what we see. The movement includes not only physical changes but also emotional and social changes. The artists are offered the possibility of motion visualization that not only featured the aesthetic aspect but also even more the scientific aspect of dynamic motion of body movement. The combination of physical movement of body, space, and time has been explored in another discipline that is chronophotography [2]. Dynamic motion can be seen from the artwork of cubists, where a story is formed by the movement of images with a painting. The overall transformations and positions are highly dependent on the physical motion of the body when one or more variables are changed within a given time frame.

Dynamic motions can also be found from morphological and biomimetical approaches with the goal of implementing into various dynamic structures in response to diverse backgrounds such as art, science, technology, and architecture. With a wide range of newly available tools, interdisciplinary collaboration makes it possible to investigate biomimetics. In order to understand the term of biomimetics, we can investigate the physical and geometrical principle of morphogenesis. Morphogenesis is known as the process by which the natural system produces and regulates the configuration of matter in space over time [3]. This movement is a great organizational pattern in a dynamic system. The same components can be configured differently to produce endless transformable structures depending on their positions and interconnections in space, and these can operate in two or three dimensions that form many possible shapes. Movement in this context refers to the physical motion of the organism. This refers to perceptions formed by spatial sequences, optical illusions, and composition changes that bring a feeling of movement, which may be experienced differently by each observer. On the other hand, time as a design element greatly enriched the possibilities in the development of this dynamic structure (see Figure 1). Structures can be designed by following coordinated movements and action of time, acting similarly to living organisms. In this case, movable elements can act on the rhythm, sequence, periodical, cyclical, repetitive, and diverse progressions. Furthermore, the dynamic structure involves consideration of abstract and qualitative issues concerning the awareness of technology, spatial experiences, and social engagements.

2. Technology in Science and Art

Technology and science sometimes "do art" and art "does science and technology" [2]. The borders between art and science have completely disappeared altogether. Technology and industrial products are always implemented into art creations that will always use the best newly available technology. Industrial products always use the best newly available technology to do art creations even in the past and yet still do today. Not only technology is being increasingly used, but the technology also becomes the creative art itself.

By using computer technology, it becomes possible to analyze the diversity and simulate the processes that occur in nature, structures from behavioral patterns, complex shapes that change over time, and habits that affect the environment and its physical form. Technology enables one to manipulate data through computer systems and machines that then make it into a three-dimensional object that has the potential to mimic the complex forms of nature that traditional construction cannot touch (see Figure 1). With the machine, it can grow a unique 3D shape that represents a new order in design evolution.

This dynamic field of computer technology tends to cooperate with art and science (based on Figure 1), trying to explore each new visualization possibilities with a new approach to the art process. Nowadays, computer is not only a tool, but also a cocreator because even though the artist has set and started certain algorithms, she/he cannot predict the end result of computer activity according to the algorithm. This technical invention has a major influence on art techniques and the creative process. Without it, there will be no graphic or photographic or digital media technique that opens up further possibilities of the related art discipline. In the dynamic technology, there are some basic approaches to visualize motion art, static (photography and images), or dynamic (movies and animations). Artists and dancers use cameras to catch their performance, whereby they have specific forms and types of photographs, which range start from artistic dance photography to the performance documentation and the study of movement.

The transformation of photography is an example of big invasion in technical applications of art which is naturally becoming an achievement of science and industry. Discipline like this can also be seen from the application of new media art, 3D printing, and computer visualization. However, examples of science and art can be found further in history that has discovered remarkable mathematical visualizations [4]. The principles of mathematics, geometry, and arithmetic are introduced not only to science and technology but also in art. When looking at the produced works throughout history, beauty is often associated with perfection of mathematical order, as Da Vinci frequently did. This order has been widely explored in nature, and artists seek to study it in detail to transfer it into painting, sculpture, and even architecture.

Neal Panchuk in "*An Exploration into Biomimicry and its Application in Digital and Parametric Architectural Design*" presented to the University of Waterloo, Canada, in 2006, said that by the rise of Postimpressionism, an improvement occurred, which in the development of science and technology embarked on a new paradigm of "being an imitation" to copy nature. Biomimicry is an applied science that derives inspiration from the study of nature. There is a relationship of nature with genetic coding. It is not to form a genetical code of an organism but rather the process of self-generation within the environment. Geometry has a subtle

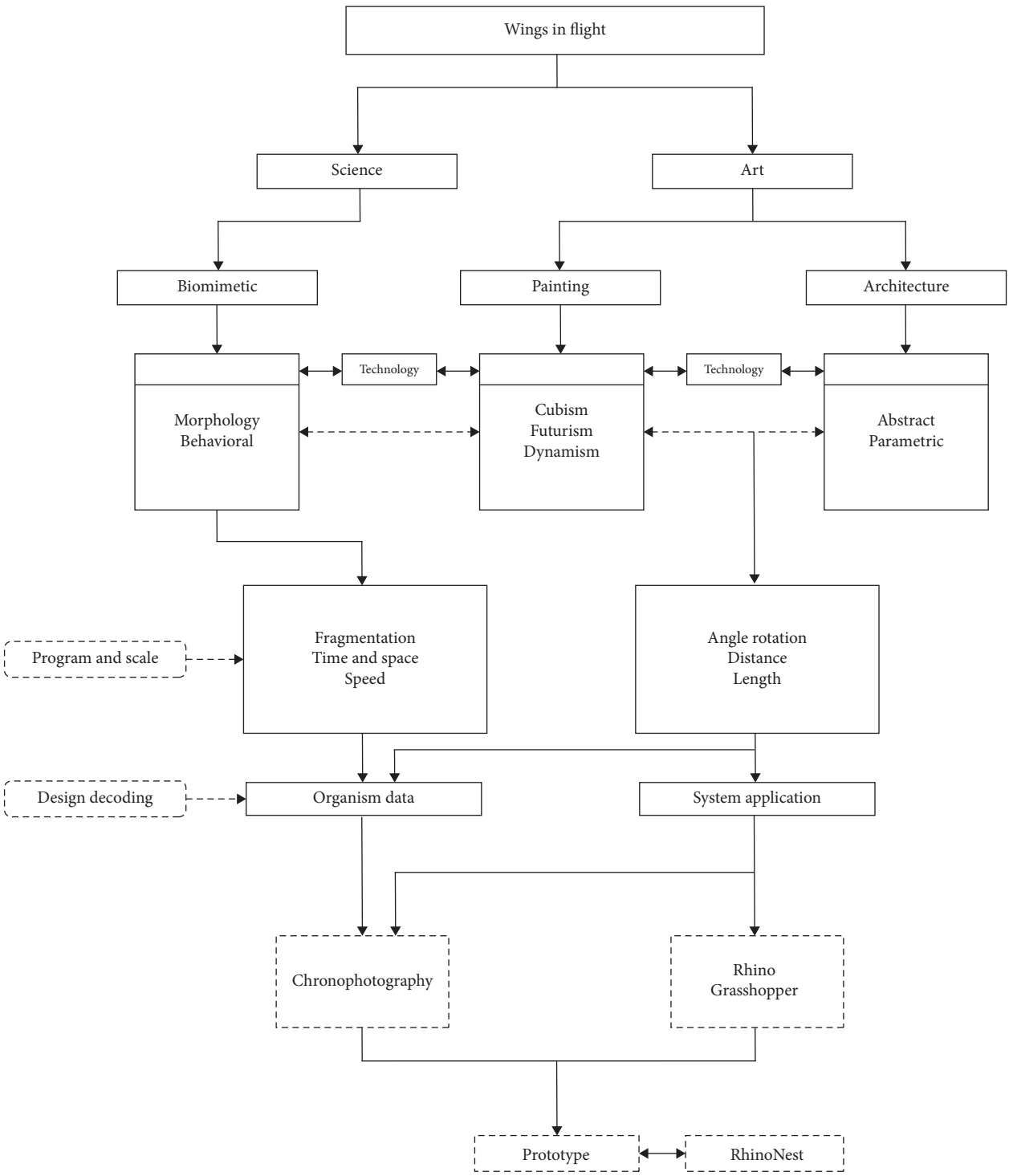

Figure 1: Diagram relationship between science and art (source: drawing by the research team).

role in morphogenesis [5]. It is necessary to think about biological geometry or computational forms not only as a description that is fully developed but also as a principle of local organization in self-organization during the process of morphogenesis.

2.1. Learning from Nature. In the book "*The Pulse Concept and the Study of Biomimicry*" published by the SCAD School of Design in 2014 cited Baumaister who said that biomimicry is the conscious emulation of nature's genius. It is an interdisciplinary approach that brings together two often

disconnected worlds, nature and technology, biology and innovation, and life and design [6]. This biomimicry seeks to bring the living wisdom of time tested and life practice into a design to inform humans in creating conditions that are conducive to sustainable living. In practical biomimicry, how to find sustainable solutions is to examine life's blueprints, chemical prescriptions, and ecosystem strategies. However, at the level of transformative biomimicry, it connects us with the most appropriate, aligns, and integrated way to the human species into the natural process of the Earth.

Biomimicry approach is seen as a design process that can be divided into two categories, namely, defining the human needs or design problems and seeing other organisms or ecosystems work as a solution to solve the problem. The so-called solution is design look for particular biology to identify its characteristics, its behavior, and its function in an ecosystem which is then translated into a human design that may affect biology [7].

When architecture is considered, there are many obvious distinctions between biomorphism and biomimicry at any level. Biomorphic design or architecture is rooted in the work of surrealists and Art Noveau. A surrealist, Grefory Grigson, coined the term "biomorphism" in 1936. Since then, the term of biomorphism has been combined with computation to replicate the visible free-form of nature because by looking at nature, we can create edges, surfaces, and volumes [8]. It is also possible to use this knowledge to find a form that resembles a living entity, but its function is not adapted. In this design approach, the results stay only at the visual level, not referring to functional and ecological levels.

Through the study of existing biomimetic technology that is still developing today, it is clear to see that there are three levels of mimicry, they are the organism, behavior, and ecosystem. The first level of biomimicry is to mimic the natural form of an organism. This type of mimicking is to copy the morphological attributes of an organism such as the visual form, component, material, or appearance. Design at this level can look fancy, but ecological and functional perspectives are not necessary at this level [8]. Morphology has been transformed from naturalism to schematic stylization in which an animal is formed abstractly, geometrically, and almost unidentified. Biomimicry at a deeper level, the second level, is mimicking the natural process. Imitating the natural process means imitating the behavioral pattern of an organism. This can be achieved by exploring and understanding how an organism relates among species within its own environment. It is possible to imitate relationships between organisms or how they behave. This requires a deeper understanding to make ethical decisions about the compatibility of what can be copied to the human context. This level is not suitable for all situations and contexts at all times. The third level is to imitate the natural ecosystem. This is a complex series of processes than the first and second levels. At this stage, the mimicking ecosystem should consider the designed objects and how those objects affect the environment explicitly and implicitly [9]. By extending the sphere of influence, the correct sustainable approach can be applied. In addition, the results are functional, sustainable, and also beautiful. Beauty is the most important part why biomimicry at any level resonates.

2.2. Art and Futurism. In the book "*History of Graphic Design, A Reference to Important Events*," it was mentioned that the future includes speed, technology, youth, and violence. Futurism influences many movements such as Constructivism, Surrealism, Art Deco, and Dadaism [1]. Futurism is practiced almost in every medium of art, such as sculpture, painting, ceramics, theater, film, fashion, graphic design, interior design, and architecture. Futurism is the Impressionism of the mechanical world. It uses the most advanced technology and considers urban modernity, refers to a new style, destroys the older forms of culture, and demonstrates the beauty of modern life-machine, speed, and changes. Unlike many other modern art movements such as Impressionism and Pointillism, Futurism is not easily recognized and understood because it is distinctive and influenced by Cubism.

The sensibility of the futurist is characterized by a passion for what is alive, which always moves and offers whatever in motion (Dynamism and simultaneity), in contrast to whatever in static. It is also dedicated to designs with high complexity which can only be achieved by machines and computers. Futurism requires interpretation precisely. The beauty of speed is the key element of Futurism. Futurists were influenced by new developments in visual technology, more specifically chronophotography, predecessors of animation and cinema that allow the movement of objects to be shown on a sequence of frames. Technology has an important influence on their approach to show movement, encouraging the abstract visual art with rhythm and pulsation.

Dynamism of a Dog on a Leash by Giacomo Balla in Figure 2 was fascinated by chronophotography, a technique in which movement changes are shown on several frames. This concept encouraged Balla to explore and discover new ideas to represent movement and rhythm in painting, and Dynamism became one of his most famous painting experiments.

Figure 2 shows a woman walking with a small black dog in which the movement melts into a single instant. It is showing a close-up of the feet. Balla articulated the action in a process by incorporating opaque and semitransparent shapes. This painting is a rapid-fire exposure that expressed the true dynamics of humans and animals in action and motion.

Chronophotography pioneer Eadweard Muybridge (1830–1904), an eccentric photographer, is famous all over the world for successfully photographing animal and human movements imperceptible to the human eye (see Figure 3). He was studying motion using several cameras from many angles once in a time, capturing essences and sensations of motion and speed. In 1872, Muybridge used photography to prove that there was a moment in horse's gallop, a time when all four hooves were off the ground at once (see Figure 3). In 1878, Muybridge has successfully photographed a horse in

Figure 2: Dynamism of a Dog on a Leash by Giacomo Balla using chronophotography [10].

Figure 3: The Horse in Motion (1872) by Eadweard Muybridge [4].

fast motion using a series of twenty four cameras. Muybridge used 12 stereoscopic cameras, 21 inches apart to cover the 20 feet taken by a single horse step, taking pictures in a thousand seconds.

The other great mind in the late 19th century was Etienne-Jules Marey. He is a scientist, a psychologist, and also at the same time a chronophotographist. His vision in motion and time is used to measure a beating heart and to capture birds in flight, resulting in technology leading to modern cinema. In Figure 4, he used such brilliant ideas to capture and record "The Man Walking" into several phases of movement in one photographic surface [4].

Some of the cubist artists, futurists, or readymade artists, e.g., Marcel Duchamp, were involved in various modern art movements and were responsible for excellent examples of futurist paintings that implied motion and time, titled Nude Descending the Staircase (1912) as shown in Figure 5. As can be observed, Duchamp offered his own interpretation of Muybridge's Woman Descending the Staircase. By using the abstract form of a naked woman who could be identified as she was moving down the stairs in the painting [4].

Motion is made much more explicit in nude paintings. Duchamp developed and refined the swirling lines and staccato arcs from points that describe the progress and displacement of the moving subject [11]. There is a relationship between Nude Descending a Staircase and Futurism. A futurist concerns on movement. By using popular chronophotography at the time, he was able to capture the movement of an organism over a period of time. The nude painting also leads us to Cubism in decomposing forms [12].

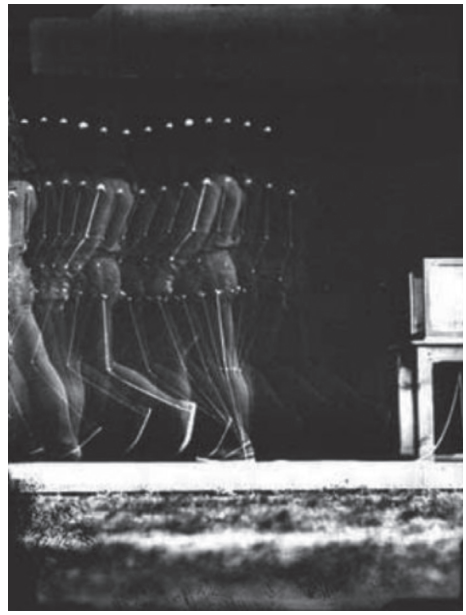

Figure 4: The man walking (1890) by Etienne-Jules Marey [4].

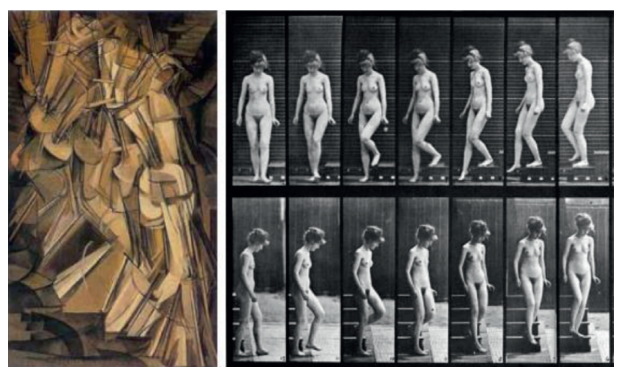

Figure 5: Nude descending the staircase (1912) by Marcel Duchamp; woman descending the staircase (1891) by Eadweard Muybridge [4].

3. When Science and Art Becomes One

In the modern era, science is aimed at applications, technical advancements, and mastery of nature. Art has no such purpose, its scope is symbolization, transmission of cultural meanings, human development, and self-interpretation in specific historical environments. To achieve these goals, art uses all the available advances that exist with exceptional ingenuity, including findings in various areas of expertise, scientific discoveries, and the invention of technological applications [4].

The examples listed above show that the production of contemporary art not only changes the boundaries between art and science but also redraws the line between the viewer and the creator. In many cases, viewers play an important role in the work, but in other cases, they are even able to inform the final form itself. The similarity is found in scientific and technological progress which does not only affect every aspect of our everyday life but also becomes a new art media that is often used in the process of art creation.

In every dynamic cultural development, art and science is known as a twin engine of creativity. Science tries to understand natural phenomena by using scientific methods including observation, experimentation, and testing, as well as formulating hypotheses. The field of science is focused not only on science itself but also extends to the realm of social and culture. Art, on the other hand, especially in the past, is characterized by the application of a respected time-honored media such as painting, graphic arts, and sculpture. They are created for the purpose of aesthetic experience. With the emergence of new artistic means and daring experiments with the latest technological advances, the boundaries between art and science have gradually disappeared. In the book with the title "*Art + Science*," Stephen Wilson refers to an institutional art theory with which he thinks the definition of art is dynamic and shaped by whatever network of art and artists, curators, historians, and critics consider to be accepted [2].

Although there are many theories that define the differences between the two entities, Stephen Wilson provides arguments based on the fact that the cave painters have become intensive investigators in the field of zoology, anatomy, and psychology. Their paintings reveal a sophisticated understanding of animal life processes. He further argues that by revealing the history of science or art, we will find prehistoric cave paintings the first important milestone in both. He points out that Leonardo Da Vinci and several others have the idea of "deep seeing," which means understanding the basic processes of the world (kind of what scientists do), and is seen as an essential tool for making art. For example, studying the flow dynamics can help an artist to paint water, studying flight mechanics can help artists while painting birds, and investigating anatomy and dissection allows the artists to become a better painter or a body sculptor [4].

3.1. Digital Biomimetic Architecture. In the last 20th century, architecture became the first art which is gradually used by designers who work with digital technology in the scope of arts. Architecture is also influenced by nature and living organisms. This includes a focused understanding not only on designing a better environment for humanity in the future in order to preserve ecological diversity, but also related to the concept of "Futurism" that provides interesting information and ideas in the creation of space and latest innovative designs with high complexity using computation technology. The focus of this concept will not only become the answer to sustainability, but more than that, it will also explore the process of a sustainable future and mobilize people to think of sustainability by mimicking the morphology of an organism [13].

Architectural morphology was introduced by Philip Steadman in his book entitled "*Architectural Morphology: An Introduction to the Geometry of Building Plan*." It focuses on geometric limitation primarily related to its boundaries, structure, and design. He often uses the phrase "morphology" which refers to the general science of potential forms such as natural forms, art forms, and architectural forms.

The emergence of the morphogenetic concept in its development shows the value of algorithms in pursuit of nonstandard and organic forms. Computation technology is considered as a new method of form-finding. One of the advantages of form-finding is the possibility of combining multidisciplinary research such as computational geometry and biomimetic patterns [13]. Conversely, in computational logic, the threshold depends on the Boolean value. The effectiveness of the algorithm calls for principle consideration. We must give the computer clear rules and orders to generate a form corresponding to the design ideology, in which it may be mathematical, biomimetical, or performative.

An author Leonardo in 2005 published a biology-based procedure to generate an experimental digital architecture. The text originated from Louis Sullivan's morphological design process articulated in the Architectural Ornament System. He said that the biomimetic architecture combines architectural paradigms with digital calculations, generative scripts, advanced fabrication, biomaterials, and nature that play an important role in the development of new systems, shapes, structures, aesthetics, and materials. This approach can integrate a procedure for understanding, visualizing, producing, and forming the architecture by studying the process in nature. For example, looking at seeds, diatoms, algae, shellfish, etc., can be a suitable biomimetic information to the possibility of new architectures. This new architecture considers how sustainable environments can become integral to new technical innovations and attitudes toward genetics, biomaterials, and science collaborations. The algorithm will also consider how the forms can follow some natural methods, such as those found in butterflies. Thus, biological growth determines body, behavior, and movement, resulting in a structure or a mechanical system that grows digitally for architecture.

Technology is one of the most important driving forces in the development of modern architecture. With technology focused on the digital computation design, it can provide flexibility in designs where it is possible to change the shape through parameters without having to change and redesign the entire form. Parametric design can be updated automatically through parameter changes. These systems are related to each other to inform the overall form. No one knows what will be the final outcomes because the result is unimaginable when using a computation program known as generation. By mimicking an organism, algorithmic and parametric designs show that the architecture can borrow from nature and generate the possibilities of infinite forms, defying previously set boundaries of knowledge. In the design parametric, everything can be manipulated from initial analysis and design process to the final form, materiality, fabrication, and construction, and control points are given to allow for a degree of flexibility [14]. The parametric design not only creates a generation of responsive forms for buildings, but also creates a space that can be adapted for future use. Architects now face a digital period that shifts from composition to generation.

3.2. Art and Dynamic Structure. Art is a kind of creativity that is communicated through visual, verbal, spatial, and audible aids, whether in the form of real phenomena or subjectively subjected experiences, abstract ideas, emotions (both in intellectual and aesthetic), and body sensations. To create a work of art, artists need at least a creative skill or competence in a particular field, but most artists in generative art leave some creative process to be done by a machine. By using computer technology, it is possible to analyze diversity as well as to simulate processes occurring in nature, ways of behavior, and complex shapes that can change over time (dynamic).

There are many exciting art works, ranging from various technology that uses human body motion as a subject through video simulation to creative applications in painting. The movement of the human body is a subject of research that has the potential to analyze movements over time as it involves many artistic activities such as dancing, theater, and performing arts that are inherently spatial in both their biological substance and psychological abilities. The artists are offered more possibilities of motion visualization, which not only display the aesthetic aspect, but also even more the scientific aspects of the dynamic movement. Digital motion tracking offers a broad field of investigation in Dynamism, continuing into ecological psychology, perception, memory studies, creativity studies, media studies, biomechanics, and the history of ideas.

In all ages, performers such as dancers and actors always use their bodies as the main elements of their creations and make their motion artwork recorded. In contrast to painters and sculptors, they use a physical form in their work to capture a "real-time" experience that cannot be repeated and only happens once; therefore, it is rare and unique in time. Petra Sobanova in his book titled "*Useful Symbiosis: Science, Technology, Art, and Education*" explained that the capture of elusive events with a particular media depends on the technical possibilities of a certain era of humans (drawings, paintings, chronological photography, cinematography, and video) [4]. This capture shows the dynamic movement as a set of fixed points in a movement continuum that explain the idea in every movement which can be captured graphically through different graphical representation techniques including drawing, 3D modeling, diagrams, and notation.

The movement developed in a dynamic motion as a new form of design derives interest in exploring its variables, testing its limits, and benefiting from its potential. This paper tries to design a dynamic movement of morphological and biomimetical approaches using butterflies as a study case with the goal of implementing it to various dynamic structures in response to a unique set of inputs from diverse backgrounds such as art, painting, science, technology, and architecture. Throughout the system development, it will continue to be tested and evaluated from a series of physical and digital prototypes.

While studying the morphology of dynamic structures, further elements have to be considered which are those related to the changes that may occur during the movement process. The morphological analysis takes a synergistic view in which a composite system of components is considered to achieve the overall transformation of its parts. Obvious variations are needed to be made between art and the dynamic structure to create motion and time that exist in space. This creates a dynamic space and space of movement, which represents the forces of life and produces a form of structure or architecture. Basically, architectural theories and practices have involved mobility in terms of physical movement of the inhabitants, the sensation of motion as a result of the visual effects of changes in lighting or even the presence of moisture, the existence of humidity, and the representation of movements with forms and structures that show Dynamism of the futurist art.

The futurist idea represents movement in a picture which struck the cubists, in which the painter seeks to capture coexistence of separate ideas or mental experience in an instant. Duchamp painted a picture that moves the world with the concept of Cubism. In a book entitled "*Cubism*" written by Guillaume Apollinaire and Dorothea Eimert, five movements of the movement of one person, descending a spiral staircase and captured on time lapse were mentioned [15]. For Marcel Duchamp, the goal of the personal style is fragmentation. Movement of fragmentation of this movement cultivates futuristic aesthetic. Fragmentation is a form of resistance to force destruction, to preserve the most important part of the whole and to reconfigure a difference in the future. Fragmentation often occurs during crisis times.

4. Case Study

The design is focused on biomimicry at the morphological and behavioral levels, where form and natural process will be studied further. The design is inspired by butterflies and related to the possible (interdisciplinary) future, where collaboration flows naturally in terms of architecture, biology, and technology. Milad Arkian in his research about butterfly, entitled "*Temperature Control Mechanism by Butterfly Wings*," stated that butterflies are known to live and survive under delicate environmental conditions with extreme weather changes. They are biologically cold blooded, and some form of basking is needed to raise their body temperature. They use their wings effectively to regulate body temperature. They require a heat-control mechanism to prevent overheating due to wing flapping, but body temperature must be high enough to be able to do a relief flight [16]. The purpose of this design is to investigate the biomimetic processes of the butterfly while regulating and maintaining their body temperature by modeling and understanding the principle pattern of wings' movement.

4.1. The Uniqueness of Butterfly's Aerial Feats. Birds and insects fluttering for a balanced flight in the air show taking off and landing vertically, alternately, and drift. A butterfly is a right model for describing the type of vehicle with an autonomous microaerial system because of the frequency of packing itself.

A research about the flying mechanism of a butterfly was done by three Japanese researchers, Masahiro Shindo, Taro

Fujikawa, and Koki Kikuchi, and successfully published by the international journal and publication named ATEAS (American Transactions on Engineering and Applied Sciences) in 2014. In that study, the position of the butterfly body is shown as in Figure 6 with symbols to illustrate the angle of roll, pitch, and yaw. Horizontal and vertical body planes symbolized by ZB and XB are defined as normal regulators. The angle rolled, depicted, and yaw are symbolized as follows: φ θ ψ. φ is the angle between the horizontal body plane and the Y axis, θ is the angle between the horizontal body plane and the X axis, and ψ is the angle between the vertical plane of the body and the Y axis [17].

4.2. Behavioral Thermoregulation. The flight parameters describing the state of the butterfly are selected as follows: the angle between the horizontal body plane and the front wing in a normal vector is defined as the flapping angle. The flapping cycle is divided into two phases, namely, the upper and lower strokes [17].

The three main postures shown in Figure 7 are typical butterfly postures for thermoregulation, and they are lateral, dorsal, and reflectance. Lateral basking is a state when wings are closed over the body and oriented perpendicular to the sun's rays. At the dorsal basking, the butterfly opens its normal wings into the sun rays so that it instantly heats the wings, thorax, and abdomen [16].

Photos in Figure 8 show behavioral illustrations when a butterfly is flapping its wings taken by a high-speed 3D camera system [17]. These pictures are designed to show how the butterfly's frame corresponds to loops and lines.

Butterflies body represent flying or flapping simultaneously in a terrible rush. The multiplication and motion effects allow forms to expand this movement. Figure 8(a) shows the streamlines around the wing caused by the flapping motion. The streamline color corresponds to the flow velocity, where the red line represents faster and the blue line represents slower [17]. The wake capture mechanism explains the increase in aerodynamic force during stroke reversal. Figure 8(b) shows the constant pressure surface on the wing as a stroboscopic image. The red and blue surfaces show positive and negative pressures. Positive pressure is on the upper side and negative underneath during the down stroke.

4.3. Implementation. Butterfly is an aspect of a simultaneous movement which is characterized by fragmentation and manipulation of the structure, which serves to distort and dislocate some elements. The design represents the aerodynamic characteristics during the roll rotation. This makes it possible to analyze flow fields that match the behavior when the butterfly is flying. Overlapping figures are used to increase the impact of flying motion to the viewer. Everything moves, everything runs, and everything changes rapidly. The figure is never stationary but appears and disappears constantly. Through the persistence of images on the retina, things in movement multiply and distort, succeeding each other like vibrations in the space through which they pass.

The structure is formed by the image of the butterfly motion exploring the techniques of mimicking, imitating, capturing, analyzing, deconstructing, and reconstructing the movement of butterflies in a dynamic spatial perspective. The entire structure is simply based only on repeating elements consisting of various slices of wings' movement and then represented together to imply their relationship to each other. The distance of each unit is different and floats separately. This can be seen as a time lapse from a higher interval to a lower interval. This design uses several different static positions creating a sense of motion and visual movement that a futurist has claimed. The idea of motion is focused on the flux of memories and the sensations of what we remember, as well as the physical body movements of what we see [18]. The movement does not only embrace the physical changes but also the emotional changes.

It has been concluded that the dynamic system which is involved in the production of forms differs fundamentally in biological and systematical. First, the dynamic form is the result of complex movements across scales and angles. Second, the model depends on the unit interacting in the dynamic way where everything depends on time lapse and interval. The connection between units and the overall shape is fundamental in relation to the dynamic system of the movement of a butterfly (Figure 9).

The movement of a butterfly is a great organizational pattern in dynamic systems. The same components can be configured differently to create transformable structures that are endless. Depending on their position in space and interconnection, they can operate in two or three dimensions that make up many possible shapes. Movements in this context indicate the physical motion of an organism. This refers to the perception of space formed by spatial sequences, optical illusion, and compositional changes that can bring a feeling of movement, which may be experienced differently by the observer [19]. Fly-free displays the importance of the time dimension in relation to space. Either it is invariant from space-time or a complete representation of objects. The time-space interval is constant because the length and time of the transformation are inversely related. The smaller the length of the unit, the greater the time. As a time interval increases, the length decreases, and as a length increases, the time interval decreases.

On the other hand, the introduction of time as a design element greatly enriches the possibilities in this dynamic structure. Structures can be designed to follow every script where movement and time are coordinated, acting similarly to living organisms. For this instance, moving elements can operate following rhythm, sequence, or progression, and movement can be periodical, cyclic, repetitive, and diverse. Furthermore, introducing dynamic systems into the design will involve consideration of abstract and qualitative issues concerning on awareness, spatial experience, social engagement, and user interactions [19].

Dynamic structure involves a setting of variable ranges and angles to change over a period of time. Variables must be modifiable and identified as length, angle, and position. The transformation and the overall position depend on the physical movement of the butterfly when one or more

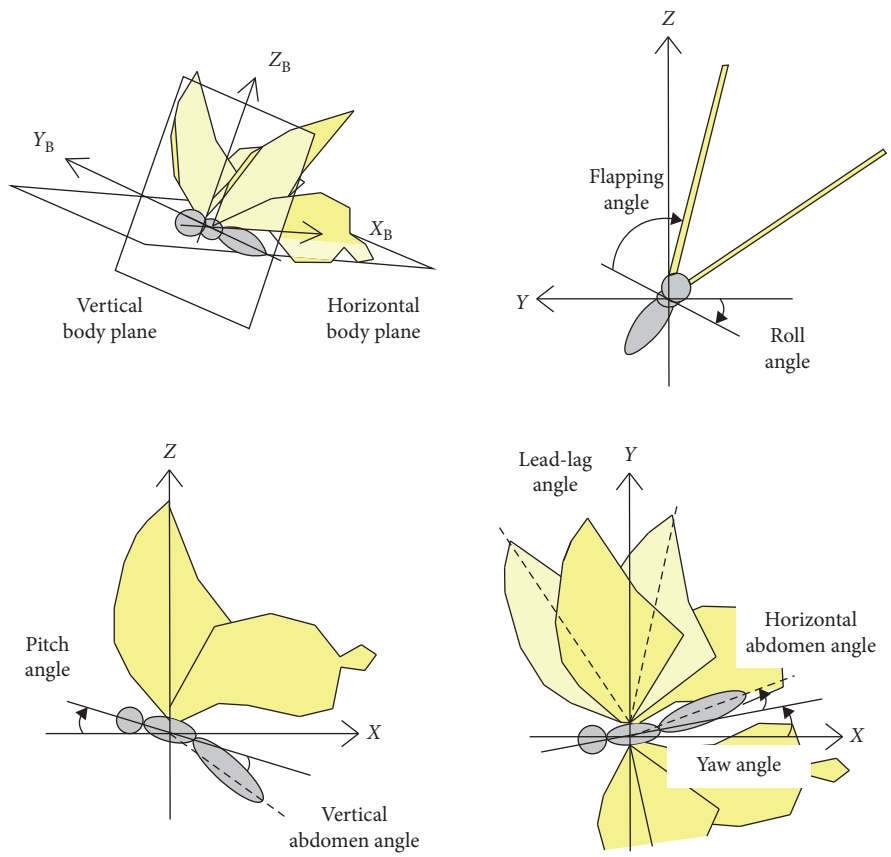

Figure 6: Definition of the butterfly frame, angles, and posture, picture from [17].

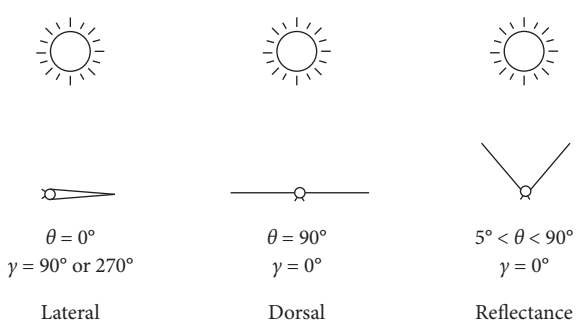

Figure 7: Basking postures: lateral, dorsal, and reflectance used by butterflies [16].

variables are changed within a specific time frame. These variables can be defined as different points that later define the form of the curve. Each curve serves in a different plane with different Graph Mapper as the controller (see Figure 10).

The fourth dimension is built from the similar geometry that we normally visualize [18]. As explained in Figure 10, it starts with a zero-dimensional point, and then by moving that point in any direction for any length creates a line (and an x-axis). Moving the line perpendicular to the x-axis creates a plane (and an x- and y-axis). Then, moving the plane perpendicular to both the x- and y-axis creates a space (an x-, y-, and z-axis).

This is the logical system that is used to easily understand the image of objects in a three-dimensional space system, regardless of how distorted it is because of its intuitive to the space perspective. As shown in Figure 11, by using the analogy of transformation, moving space perpendicular to the x-, y-, and z-axis creates the fourth dimension. However, being trapped in three-dimensional space, we cannot visualize the fourth dimension coordinate system, or what objects are in the fourth dimension. Two main methods for representing the fourth-dimensional objects, slicing methods and projection methods, have been developed as an attempt to make the invisible visible [18]. For a more complex design, not only as a sine curve, it is necessary to tweak the points in both planes, x and y points in the XY plane and x and z points in the XZ plane (see Figure 11).

Minkowski referred to his four-dimensional space-time formulation about the theory of relativity, "space by itself and time by itself are doomed to fade away into mere shadows, and only a kind of unity of the two will preserve an independent reality" [18]. Since three-dimensional geometry only relates to space, it cannot explain the implications of relativity. For a four-dimensional graph, that is what Minkowski and Einstein believe in our universe, in the field of the Cartesian plane, z-axis and y-axis must be released, and it is easier to see the two variables that are subject to change, x and t. Since time always flows through our universe and the contraction of length only affects x-axis, z-axis and y-axis can be taken out of consideration.

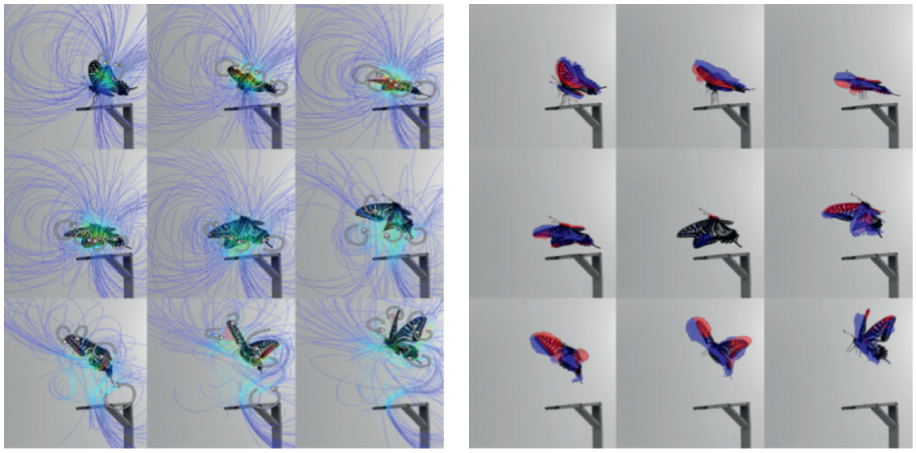

(a) (b)

Figure 8: Stroboscopic image pitch rotational flight picture from [17].

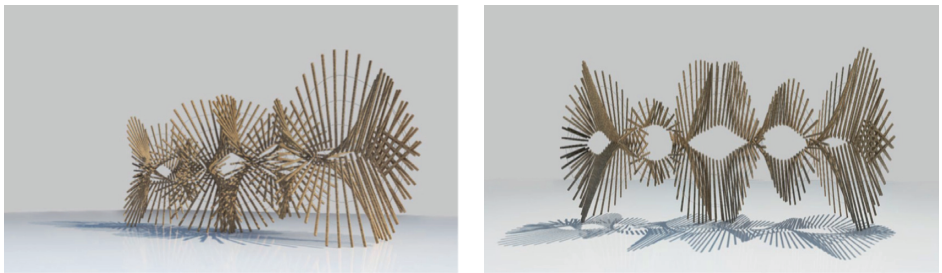

(a) (b)

Figure 9: Implementation structure of butterfly flying movement. Concept: wings in flight (source: drawing by the research team).

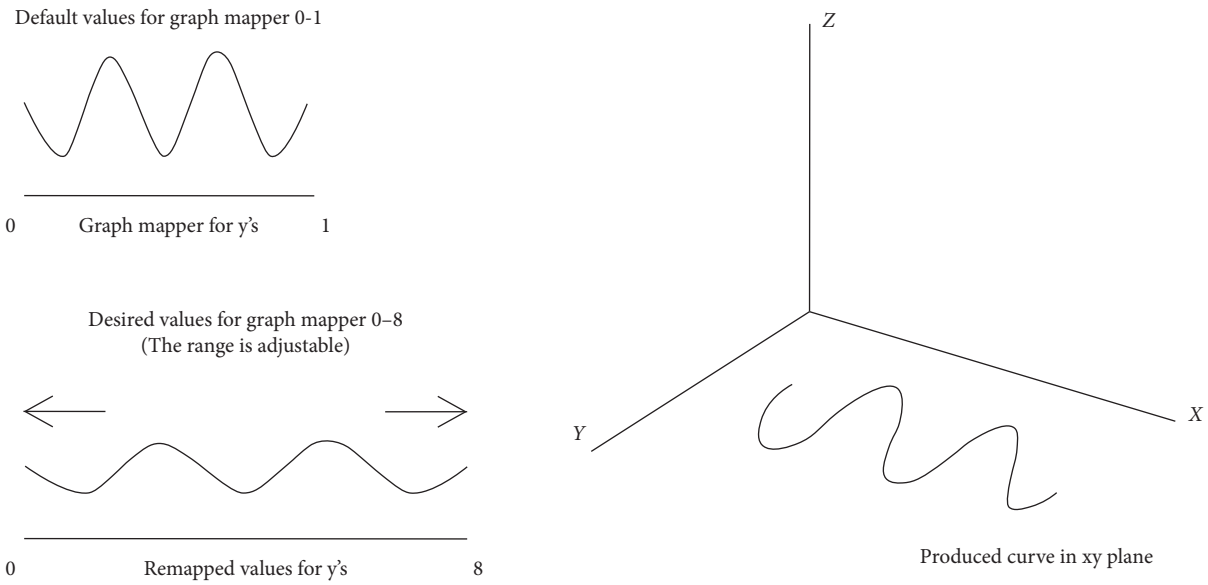

(a)

Figure 10: Continued.

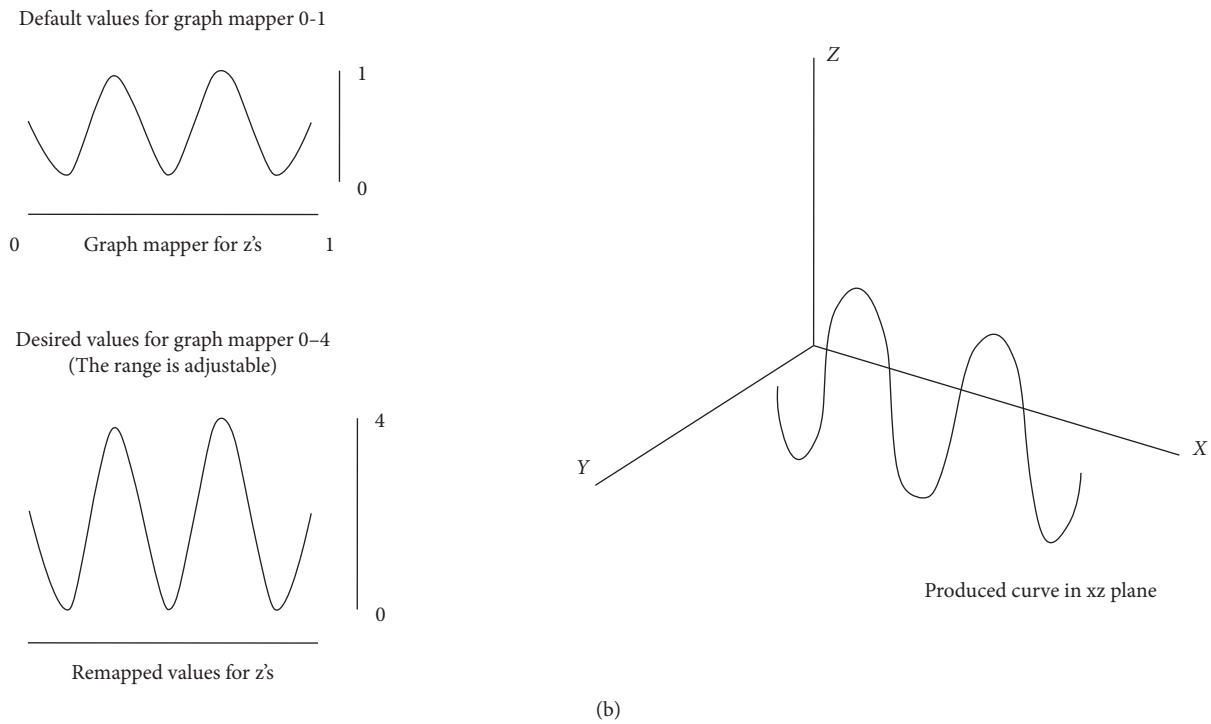

Figure 10: Logic static system of the model, inspired by the free movement angles (source: drawing by the research team).

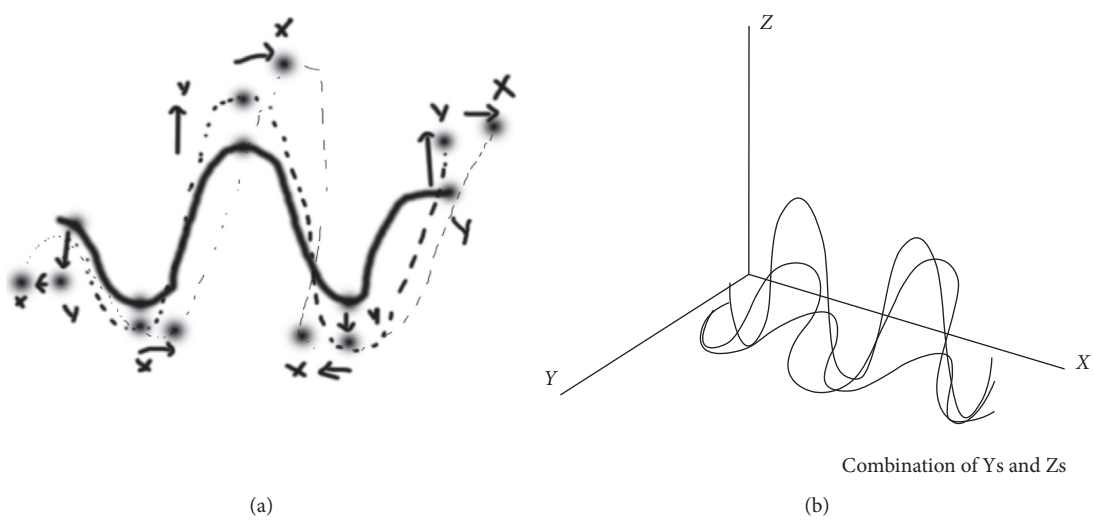

Figure 11: Curve on the combination of y and z planes (source: drawing by the research team).

Using that geometry principle, a graph of something would look like a vertical line, as time passes and the object length is constant at a single speed. The faster the something moves through space, the steeper the slope of the graph becomes. In Minkowski's mind, because space and time can both change shape or dilation or contraction, respectively, the only way to understand the true nature of an event is to incorporate two variable things into invariable space-time intervals.

The space-time interval is constant because according to Lorentz, the transformation between length and time is inversely related. The smaller the length of something, the larger the time. As the time interval increases, the length decreases, and as the length increases, the time interval will decrease, but the time interval remains the same since the ratio between the two is an inverse relation [18].

4.4. Fabrication from the Digital Data to the Real Object. To test the fabrication and assembly, prototype structures were built on a smaller scale 1 : 10 using 4×4 mm. Figure 12 shows the prototype image from various views. The model

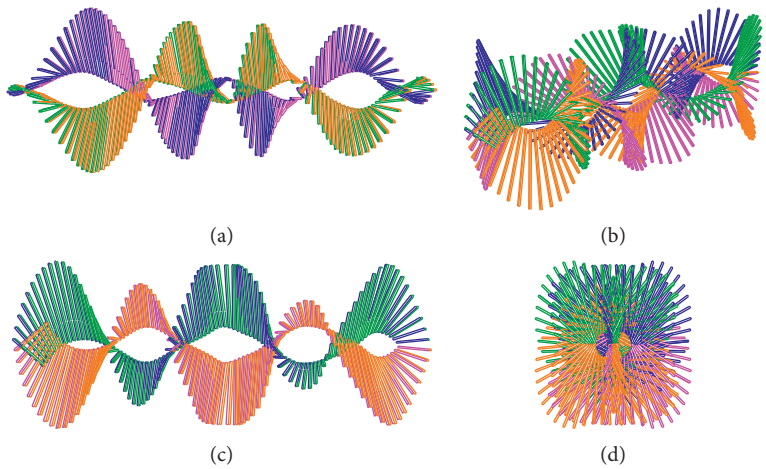

Figure 12: Case study of complex parametric model using the grasshopper logic system (source: drawing by the research team). (a) Top view_1 : 100. (b) Perspective view_1 : 100. (c) Front view_1 : 100. (d) Right view_1 : 100.

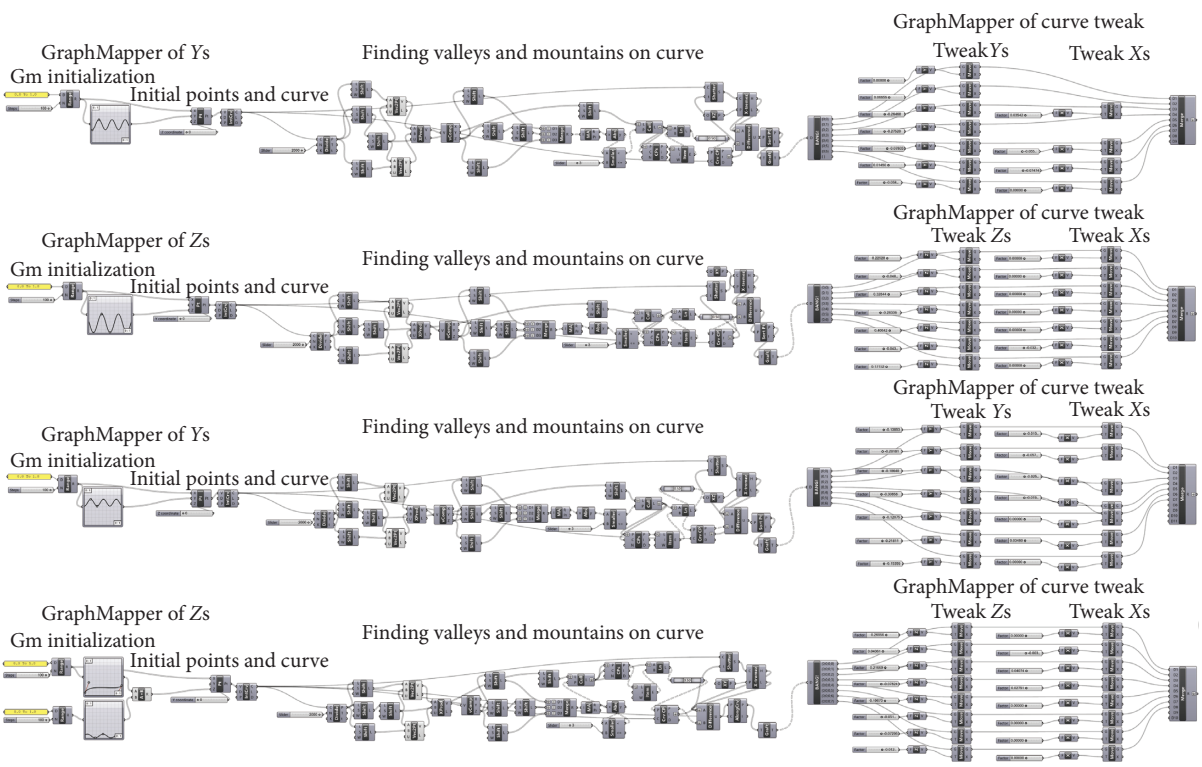

Figure 13: Case study of a complex parametric model using the grasshopper logic system (source: drawing by the research team).

consists of four parts identified by four different colors (blue, magenta, orange, and green). Each part consists of 34 pieces of wood. In total, there are 136 wood pieces connected by wires.

Using a computational genetic algorithm, the design starts with points and connects vertical points and then follows the arc pattern to illustrate the movement of the flying butterfly (see Figure 12). The surface is generated by the cross-linked wood elements with random angles along the structure with the aid of a genetic algorithm, which is then reflected through the XY plane to obtain a complex flight system fluidity. The angle represents the movement of a butterfly that flows in flight to regulate their body temperature.

The main algorithm produces a sine curve that has three mountains and two valleys. The initial points on each plane (either XY plane or XZ plane) are randomly determined by the Graph Mapper in Grasshopper (see Figure 13). In order to get a complex wood structure with cross-linked elements, a set of data for tweaking curves should be defined and merged to get one sine curve. For making other parts, sine curve can be mirrored horizontally and vertically (see Figure 14).

The second step after the outer curves have been determined is to generate the wood pieces. The size of the wood

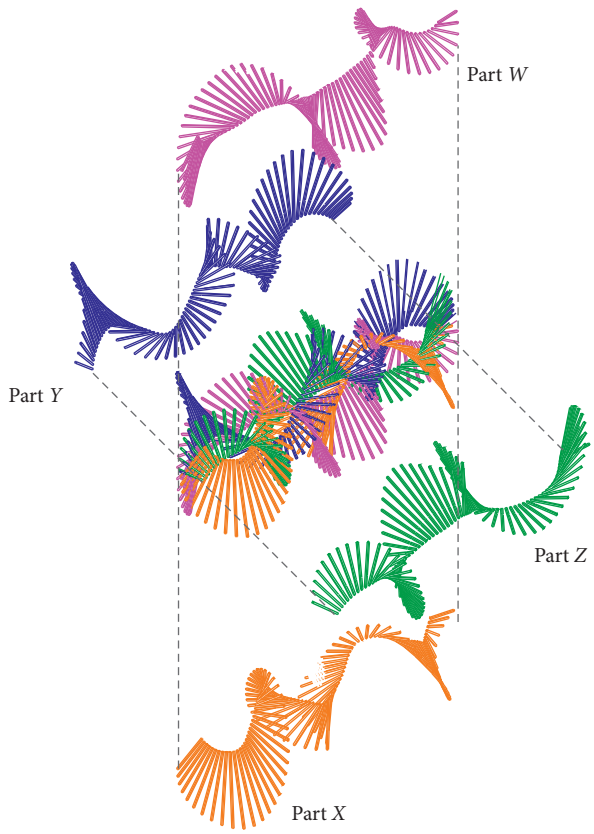

Figure 14: Making other parts by mirroring one part horizontally and vertically (source: drawing by the research team).

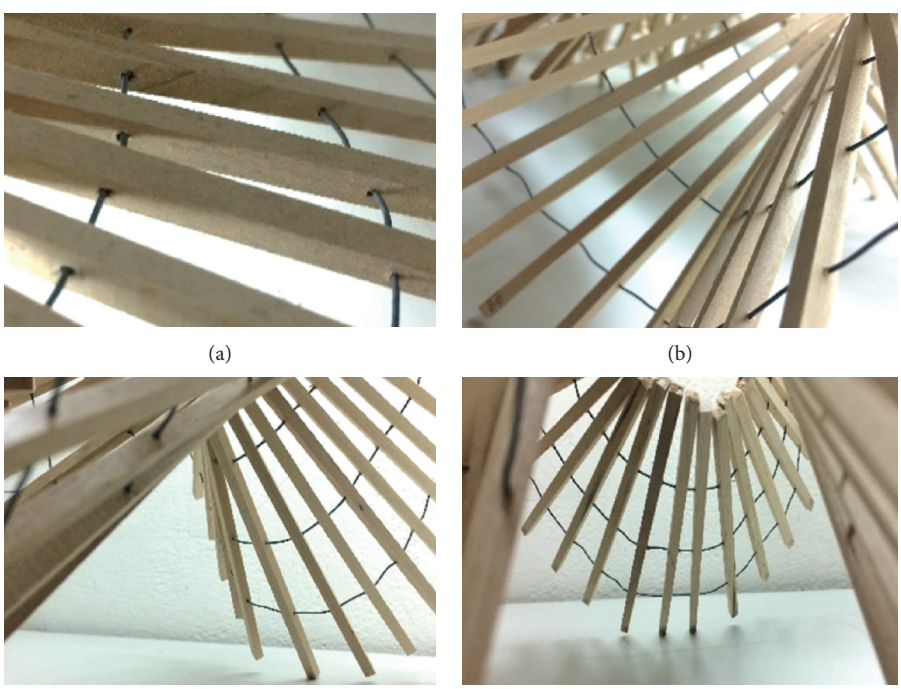

Figure 15: Wire connection of the complex parametric model (source: drawing by the research team).

(4 × 4 mm) is adjustable, but the length of the wood follows the outer curves that have been generated in the previous algorithm. The total amount of mountains and valleys depends on the total length of the prototype model for a stable structure. After the wood pieces are defined, the hole's marks for the wire connection can be created. In this prototype, three wires with different lengths were used (see Figure 15).

The part is assembled in an oblique position, inserting pieces connected by wires as shown in Figure 15. Between parts, the connection is very difficult because there is no general assembly direction that can be found to determine the distance between woods and the slope angle of each wood. At the full-scale structure, it is easier to use industrial robots for assembly.

Fabrication using industrial robots can produce more precise and accurate results because of their ability to perform an infinite number of nonrepetitive tasks, thus they are considered as the enablers for deeper transformations in the field of large-scale manufacturing systems. For this purpose, further research is needed, using an articulated robot for cost-effective and potential fabrication process. Only in this way, we can significantly expand our range in bio-inspired analysis, architectural design, and production aims, allowing the diversity and complexity of new materials to emerge.

5. Conclusion

When looking at architectural biomimetics made through digital design for Futurism, it connects traditional art (movement captured by painting) and new expressive science that allows us to analyze diversity and also simulate the processes that occur in nature through complex patterns of behavior that change from time to time. In order to achieve that, computers and industrial robots play an important role in defining and creating new complex architectural forms and spatial relationships. The relationship between art and science and their overlapping tendencies seems like a thought with postmodern influences and Cubism associated with mobility in terms of physical motion of the occupant, the sensation of motion as a result of visual effects. Representation of movements by forms and structures shows a Dynamism of the futurist art. Art should also be able to reflect the important phenomena of human existence and living organisms, as well as logical problems that science is completely indifferent.

The evolution of architecture from the traditional way to the modern era of computer-based design has really improved in various aspects such as designing, documenting, and idea communication and now stepping forward in integrating scripts, algorithms, and codes to provide a more efficient way of solving complicated problems in the design process, beyond the roots of representation of existing architectural forms in which it is limited by design techniques. In addition, it is important to emphasize that despite a much higher degree of flexibility and speed in generating possible outcomes in the realm of digital architecture, this situation must be considered very well, so that the existence of this technology means capable of serving and bridging the gap between humanity and complexity of the design process.

The design and construction process in this case study is a good reflection of computational methods that helps architects and designers to achieve innovative results and allows more design possibilities. There is always a need for changes in architectural methods when there is a change in human needs and human evolution, but the important thing is to learn the relationship between many fields which are interconnected to each other.

Data Availability

The data used to support the findings of this study are available from the corresponding author upon request.

Conflicts of Interest

The authors declare that they have no conflicts of interest.

Acknowledgments

The research case studies have been conducted in the Department of Architecture, National Taiwan University of Science and Technology, by the Ministry of Education, Taiwan. Additional expenses have been covered by authors' home research centres, namely, the D&A Lab, Department of Architecture, National United University, and the Department of Architecture, National Taiwan University of Science and Technology, in Taiwan.

References

[1] P. B. Meggs, *A History of Graphic Design, a Reference to Important Events*, Wiley, Toronto, Canada, 2016.

[2] S. Wilson, *Art + Science Now, How Scientific Research and Technological Innovation are Becoming Key to 21st Century Aesthetics*, Thames and Hudson, London, UK, 2010.

[3] P. Steadman, *Architectural Morphology an Introduction to the Geometry of Building Plans*, Moma Thames and Hudson, London, UK, 1983.

[4] P. Sobanova, *Useful Symbiosis: Science, Technology, Art, and Art Education*, Palacky University Olomouc, Olomouc, Czechia, 2016.

[5] P. Neal, *An Exploration into Biomimicry and its Application in Digital Parametric Architectural Design*, University of Waterloo, Ontario, Canada, 2006.

[6] N. Baker, *The Pulse Concept and Study of Biomimicry*, SCAD School of Design, Savannah, GA, USA, 2014.

[7] S. Virmani, "Architecture and nature: biomimicry as a tool for sustainable architectural design," Vastu Kala Academy, New Delhi, India, 2014.

[8] Y. Arslan, *Biomimetic Architecture a New Interdisciplinary Approach to Architecture*, Yeni Yuzyil University, Istanbul, Turkey, 2011.

[9] D. Baumeister and R. Tocke, *Biomimicry Resource Handbook A Seed Bank of Best Practices*, Create Space Independent Publishing Platform, Scotts Valley, CA, USA, 2013.

[10] Albright-Knox Art Gallery, *Dinamismo di un cane al Guinzaglio*, Albright-Knox Art Gallery, Buffalo, NY, USA, 1912, https://www.albrightknox.org/artworks/196416-dinamismo-di-un-cane-al-guinzaglio-dynamism-dog-leash.

[11] C. Tomkins, *The World of Marcel Duchamp*, Time Inc., New York City, NY, USA, 1966.
[12] J. Nelson, *Wisdom-Conversation with the Elder Wise Men of Our Day*, W. Norton & Co., New York, NY, USA, 1958.
[13] Harper Collins, *Innovation Inspired by Nature Work Book*, Harper Collins, New York, NY, USA, 2007.
[14] T. Fry, *Design Futuring: Sustainability, Ethics, and New Practice*, pp. 1–16, Berg, Oxford, UK, 2008.
[15] G. Apollinaire and D. Eimert, *Cubism. Art—History—Modern (Late 19th Century to 1945)*, Parkstone Press, New York, Ny, USA, 1st edition, 1980.
[16] M. Arkian, Temperature control mechanism by butterfly wings, 3rd year mechanical engineering initial report.
[17] M. Shindo, T. Fujikawa, and K. Kikuchi, "Analysis of roll rotation mechanism of a butterfly for development of a small flapping robot," in *Proceedings of the 3rd International Conference on Design Engineering and Science (ICDES2014)*, MM Publications, Pilsen, Czech Republic, August 2014.
[18] E. Bodish, *Cubism and the Fourth Dimension*, University of Montana, Missoula, MT, USA, 2009.
[19] C. M. Stevenson, "Morphological principal: current kinetic architectural structure," in *Proceedings of the International Adaptive Architecture Conference*, London, UK, March 2011.

Hindawi
Complexity
Volume 2020, Article ID 5205970, 11 pages
https://doi.org/10.1155/2020/5205970

Research Article

Application of Taiwan's Human Rights-Themed Cultural Assets and Spatial Information

Shuhui Lin

Department of Taiwan Culture, Languages and Literature, National Taiwan Normal University, Taipei, Taiwan

Correspondence should be addressed to Shuhui Lin; siokhui@gapps.ntnu.edu.tw

Received 6 December 2019; Revised 18 February 2020; Accepted 3 April 2020; Published 28 May 2020

Guest Editor: Shu-Heng Chen

Cultural assets preserve the traces of people's life history around the world. With an understanding of the historical context and meaning of cultural assets, people would cherish their value and then adopt appropriate cultural resource preservation strategies. Human rights as the universal value refer to the inalienable and basic rights of human beings. This article uses the National Cultural Assets Network to query Taiwan's human rights-themed cultural assets, and I apply the spatial information technology of the DocuSky digital humanities academic research platform to draw the maps with GIS and visualization tools. Also, I apply spatial information to the academic research of human rights-themed cultural assets, aiming to deepen local cultural identity and unveiling that human studies influence spatial practice. Tourism is an important experience economy. Based on the value of Taiwan's human rights-themed cultural assets, I plan to guide the human rights journey in Taipei to share Taiwan's experience of happiness with the world, as well.

1. Introduction

In recent years, the meaning of cultural and spatial information has been found out to explore the local cultural context and as well as the way to see the world. Calling the sense of locale from ancient to modern to attract the attention of international tourists has become an alternative way to promote Taiwanese culture. Due to the academic exchange and with the help of the visiting scholars, I personally experienced the Cultural Tour of Boston in the Freedom Trail. The tourists listened to the guides, who dressed in traditional costumes introduced the main scenes, and there were a number of visitors who made an on-the-spot inspection along the route paved by red bricks. A flock of tourists across the world visited the Anne Frank House in Amsterdam, Netherlands, and the United States Holocaust Memorial Museum, witnessing the historical significance and trauma as shown in the manuscript of Anne Diary and the museum display.

The landscape is shaped by the life experience of the people, and it is an ideographic system. Geography and literature are both the writings about place and space, and both are ideographic processes that impose meaning on a place in social media. With time flowing, the cultural assets preserve the traces of people's life history around the world and serve as the precious treasure of human society and culture in the world. Taiwan experienced multiple colonization, thus facing the problems of deep cultural grafting and transferring. Looking back at Taiwanese cultural tour activities, I find that they more often did not focus on individual historical site introduction; however, guided tours with themes and concepts can better highlight the ideological implication of Taiwan's diachronic character and reflect the universal value of the theme.

The identification principles of the world cultural heritage are mainly based on the universal value, rarity, and protection priority. According to the Law on the Preservation of Cultural Assets, which was amended and passed on July 12, 2016, the categories of monuments and historical sites were added, and cultural asset preservation education through the school education system was also implemented. The special measures for the cultural assets of indigenous peoples were specified, and the preservation of cultural assets of diverse ethnic groups was emphasized [1, 2]. Legal norms

are important all right, but there are more fundamental works to do to make people value their cultural assets. Accordingly, first people must be helped to recognize and love their culture. So, the study of space humanities becomes more urgent. What human rights-themed cultural assets do Taiwan own? How to apply spatial information to guided tours of human rights-themed cultural assets? This manuscript combines the cross-domain application of spatial information, hoping to present the theme of tangible cultural assets, highlighting it in Taiwanese culture.

2. Related Literature

Regarding the conceptualization of space, the French scholar Lefebvre's concepts of spatial practice, representation of space, and representational spaces are quite canonic. Spatial practice is to reflect the close connection between daily reality, affairs, and urban reality in the perceived space, involving various functional spaces from architecture to large-scale urban facilities. Representation of space involves conceptualized and conceived space, and furthermore, it is a space in which scientists, planners, and technical bureaucrats are engaged. As the dominant space in lifestyle, it identifies life and perception with concepts. The representational space is the space that is directly used for life through the related images and symbols. It is the space of the occupants and users, tending to be a system of coherent, nonverbal symbols and signs [3]. Wang pointed out that "place" is a meaningful location, a significant space created by human beings, who are attached to it in some way. The space to which the city refers is carved out by the interaction among specific institutions with historical and geographical features, social relations of production and reproduction, governmental actions, forms of communication, and media [4, 5]. Although the concept of space can be reflected in different levels, the texts related to cultural assets represent the process of so-called urban cultural changes, as well as the impact that such developments produced.

This manuscript points out that when the space constructed by cultural assets is accompanied by the accumulation of special experience, historical context, and a sense of identity, the meaning of place comes into being. These highly conceivable features and the meaningful realization about the place turn out to be people's emotional attachment to Taiwan, and thus express the meaning of locality. For the city dweller, each city is imaginable and is of consciousness associated with the atmosphere and taste of the environment, instead of a vague concept [6]. For example, literature contains rich social customs and habits, language and voice, agricultural and fishery products, dietary habits, landscapes, vegetation, residents' emotions, history, and culture, and other assets accumulated by conventional wisdom Literary works are impressively characteristic of local colors. I collect texts about cultural assets and read articles about imagery depiction in different places, which describes various spatial characteristics, impressions, and feelings. Also, they were integrated with geographic information systems to represent the memories and atmosphere of cultural assets in that era.

Backtracking to the maps drawn in the Japanese colonial period, such as the Taiwan Fort Map with a proportion of one to 20,000 in 1904 and the Taiwan Topographic Map with a proportion of one to 25,000 in 1926, it is seen that they mostly implied the planning, decision-making and management, statistics, investigation, and research about Taiwan, which had been conducted in the Japanese Empire, and these data are mostly based on maps. Therefore, the contents of the maps are all-encompassing, including natural resources, agriculture, forestry and fishery, urban planning, transportation, and tourism. A map is a representation of the distribution of surface space. Each map is the product coded by the drafter. In the coding process, the drafter inevitably incorporates his personal perspective [7, 8]. In recent years, scholars and some professional drafters have rewatched Taiwan from an alternative angle, and thus the maps have showcased a new perspective [9]. These examples are inclusive of Taiwan's proximity to Southeast Asia, its relative position with China, the value of eastern Taiwan, and how to ruminate Taiwan's interaction with the world. This manuscript is inspired in the remapping process, and the relevant maps of human rights theme present the association between Taiwan's cultural assets and social pulsations [10–12].

3. Main Data Sources

In the 19th century, European countries had started to formulate laws on the protection of historic sites and buildings on the cultural attractions and historical monuments constructed by the interaction between people and space. In 1922 (Taisho 11), the Governor's Office issued the Decree No. 521 (Act on the Preservation of Natural and Historical Monuments in Taiwan) and then designated prehistoric culture from the Qing Dynasty rule to the Japanese occupation and other cultural relics from different periods. Also, the content mainly focused on diversified cultural attraction resources. In the early postwar period, maintenance work was mainly made by craftsmen, and later the governmental authorities and folk craftsmen worked together to deal with the cultural assets. The Law on the Preservation of Cultural Assets was promulgated on May 26, 1982. Since then, it has been formulated and amended and has been the controversial social issue because of the preservation of historic sites. The broadly defined antiquities factors of prewar China and the local cultural asset elements of postwar Taiwan should be understood and blended with each other, creating a harmonization and transformation in concepts and keeping updating and adjusting the connotation of the prewar Cultural Assets Preservation Law to make it meet the local cultural and social needs of postwar Taiwan. This process of shaping the legal system means that the trajectory of the national identity axis flipped in the past [13]. As for the latest revision of the Cultural Assets Preservation Law in 2016, the so-called cultural assets refer to constructions with cultural values in history, art, and science and are designated or registered as tangible and intangible cultural assets. Among them, tangible cultural assets can be divided into historic sites, historical buildings, memorial buildings, settlement buildings, archeological sites, historical

sites, and cultural scenes [14]. The designation criteria for historic relics, repeal conditions, procedures for application and examination, assistance, and other measures to be followed shall be determined by the central competent authority [15]. Monuments include buildings and ancillary facilities with historical, cultural, and artistic values built by humans for their daily needs.

The concept of cultural scenery was proposed at the 16th session of the UNESCO World Heritage Committee in Santa Fe, New Mexico, in December 1992, and was included in the World Heritage List. In the current society, the sustainable landscape maintains a positive social role associated with traditional lifestyles, and its own evolution is still ongoing and witnessing historical evidence of evolution and development. Relevant cultural landscapes are characterized by their connection with natural factors, religion, art, or culture, rather than cultural evidence.

This article uses the National Cultural Assets Network (https://nchdb.boch.gov.tw/) to inquire about human rights-related persons, events, eras, locations, and cultural assets in Taiwan and sort them in Table 1.

The memorial locations related to the theme of human rights include the activists' residences, working place, and grave yards. For example, Qiu Xian-chia Cemetery, Tang Te-chang Memorial Park, Yin Hai-kuang's Residence, and Fenglin Principal's Dream Factory. Landscape was associated with human rights, as well. Take Wufeng Lin Family Mansion and Garden, for example. It was not only Lin's residence, a then gathering place of talents, but also the meeting place for literary men at the Taiwanese Culture Association.

The Qing Tanshui Camp had been established for the then authorities, who intended to contain aborigines and criminal gangs, chasing them out of the mountain after the Zhu Yi-kuei Event. The landscape witnessed the ruler's oppression and antihuman rights. Jen-Her Temple in Er-Lin was located where farmers gathered at the Mazu Temple (current Jen-Her Temple) and decided to organize "the group of farmers." As the protest had been hindered, many participants were put in jail. However, after that, the groups of farmers across Taiwan followed suit, lodging petitions, and holding mass protests. All of these were the historical events related to human rights. Other landscapes such as Remains of Taipei Prison Wall, Chiayi's Old Prison, Tainan District Court, and Taiwan Provincial Council Building showcased the historical development of Taiwanese human rights, as well.

At present, the practice of preserving cultural assets not only expands citizen participation, but also adds fresh categories such as monuments and historical sites to strengthen the connection between Taiwan's land and history. In addition, in the United Nations Conventions on World Cultural Heritage and Intangible Cultural Heritage, the definition of cultural asset classes and the principles of preservation have been described in the provisions of the bill, so that the preservation of Taiwan's cultural assets can be further in line with international standards. Because these monuments in Table 1 are mostly related to the spirit of freedom, representing the spirit of the age, the human rights-themed cultural assets are considered as the scope of research [16–22].

4. Methodology

In addition to the literature research method of collecting the outer background and text, the analysis of the collected cultural assets through geographic information system will help to represent the related context of cultural assets from the temporal axis and spatial dimensions. The main research methods are as follows.

4.1. Extensive Searching for Cultural Asset Classes by Database. In recent years, various institutions in Taiwan have collected Taiwanese historical materials through various channels, such as Taiwan postcards handed down from the Japanese rule period, old photos of diverse spots, ancient books, local chronicles, archaic documents, genealogies, rubbings from stone inscription, audiovisual materials, and digital video files of news [21, 21]. These Taiwanese historical documents and audio-visual records are archived with digital technology. It is hoped that through the establishment of the Taiwan Memory system, the historical documents associated with Taiwan will be stored in a digital archive, and the establishment of interpretation data through digital objects will achieve the purpose of data sharing and reusing [22–24]. Also, through the wide reach of the Internet, it is possible to expand the reading and research of historical materials in Taiwan to every corner of Taiwan and the whole globe.

In researching Taiwan's cultural assets, it often takes time to collect texts scattered all over the place, as well as the various long-term historical materials accumulated for a long time [25, 26]. If you use the database to search for related historical and historical files, you can save the time of searching for information and focus on the interpretation of the theme. However, the results of many databases searching often fail to show the relevant logic. If you do not know the context, when facing with complicated historical data, it is like needle hunting in the vast sea and makes people set back from the work. Many databases have functions such as Full Text retrieval and Metadata retrieval, providing humanities researchers with immediate and efficient assistance in the process of searching for references and interpreting historical data. Recently, some databases have been set up to provide subcategories of people's names, place names, ages, provenances, or word frequencies [24–30]. After categorizing the data, it really helps to inspire academic research. This manuscript uses the National Cultural Heritage Database Management System to screen human rights-related cultural assets in a thematic way. Also the form fields of the list are made according to type, administrative area, announcement number, announcement date, latitude, and longitude.

4.2. Application of Cultural Assets and Cartography. A landscape is a local surface of the Earth that we can deliberately view from a certain place. The landscape combines the physical topography of the local land (things that can be viewed) and the concept of vision (viewing modes). Scenery is a strong visual concept. In most of the definitions of scenery, the viewer is outside the scenery, which is the main difference

Table 1: Human rights-themed cultural assets in Taiwan.

Name	Category	Administrative division	Code of announcement	Date	North latitude	East longitude
Rose Historic Site-Tsai Jui-yueh Dance Research Institute	Historic site	Zhongshan Dist., Taipei City	8809036001	1999/12/31	25.055801	121.521987
Remains of Taipei Prison Wall	Historic site	Da'an Dist., Taipei City	8701538601	1998/3/25	25.033938	121.526848
Wufeng Lin Family Mansion and Garden	Historic site	Wufeng Dist., Taichung City	357272	1985/11/27	24.060856	120.703193
Jen-Her Temple, Er-Lin Cane Farmer Group	Historic site	Erlin Township, Changhua County	357272	1985/11/27	23.899129	120.368114
Tang Te-chang Memorial Park	Historic site	West Central Dist., Tainan City	09318507120	2004/4/30	22.992603	120.205019
Wistaria House	Historic site	Da'an Dist., Taipei City	860567701	1997/7/23	25.024631,	121.534325
Hai-Kuang's Residence	Historic site	Da'an Dist., Taipei City	09304427300	2004/2/9	25.024200	121.531994
National Taiwan Normal University	Historic site	Da'an Dist., Taipei City	09200513500	2003/8/12	25.025458	121.527349
Qiu Xian-chia Cemetery	Historic site	Beitun Dist., Taichung	0960147621	2007/7/13	24.15997	120.758974
Chiayi's Old Prison	Historic site	East Dist., Chiayi City	0940061286	2005/5/26	23.486155	120.458667
Strictly forbidden for artisans to transcend private monuments	Historic site	Meishan Township, Chiayi County	1030002735	2014/1/21	23.486180	120.458687
Tainan District Court	Historic site	West Central Dist., Tainan City	921648, 10330114152	1991/4/19	22.989654	120.201102
Qing Dynasty Tamshui Camp historic site	Historic site	Changzhi Township, Pingtung County	10530101300	2016/03/14	22.699449	120.538609
Lanyang coastline military barracks during the period of martial law	Historical building	Zhuangwei Township, Yilan County	1030001175B	2014/03/21	24.74026	121.816805
Fenglin principal's Dream Factory	Historical building	Fenglin Township, Hualien County	1020004845A	2013/01/10	23.747602	121.450369
Former Taiwan Provincial Council Parliament Building, Chaoqin hall, Parliament hall	Historic site	Wufeng Dist., Taichung City	0970009208	2008/12/25	24.053938	120.700203
Jing-Mei White Terror Memorial Park	Historical building	Xindian Dist., New Taipei	0960011931	2007/12/12	24.988133	121.532352
Cihlin Memorial Hall	Historical building	Wujie Township, Yilan County	2990	2001/6/29	24.708924	121.771214
The original site of Kaohsiung Service Office, Formosa Magazine	Historical building	Xinxing Dist., Kaohsiung City	0930020248	2004/4/9	22.629483	120.301412
Green Island White Terror Memorial Park	Cultural landscape	Ludao Township, Taitung County	1030010752	2014/1/27	22.675208	121.496317
Cemetery for political victims during the period of martial law	Cultural landscape	Xinyi Dist., Taipei City	10530402700	2016/6/4	25.017529	121.564446
Ooshen Event Memorial Park	Historic site	Ren'ai Township, Nantou County	1080148095	2019/7/11	24.02053	121.132593
Jing-Mei White Terror Memorial Park	Historical building	Zhongzheng Dist., Taipei City	10230334500	2013/6/11	25.032295	121.512074
Lo-Sheng Sanatorium	Cultural landscape /historical building	Xinzhuang Dist., New Taipei City	0980012321/ 09800123211	2009/09/07/ 2009/09/07	25.022329	121.409269
Chiang Wei-shui Memorial Park	Historical building	Xinyi Dist., Taipei City	10130329600	2012/6/1	25.022114	121.560002

Table 1: Continued.

Name	Category	Administrative division	Code of announcement	Date	North latitude	East longitude
National Taiwan Democracy Memorial Hall	Historic site	Zhongzheng Dist., Taipei City	0963132772-1	2007/11/9	25.036845	121.518217
Legislature	Historic site	Zhongzheng Dist., Taipei City	10630459200	2017/6/12	25.043900	121.519614
Hong Lou At Kaohsiung Municipal Kaohsiung Senior High School	Historical building	Sanmin Dist., Kaohsiung City	0920010663	2003/2/26	22.638069	120.298005
The Ke Qi-hua House	Historical building	Xinxing Dist., Kaohsiung City	0930020248	2004/4/9	22.636088	120.30001
Remains of Yilan Prison door	Historical building	Yilan City, Yilan County	2990	2001/6/29	24.753885	121.751533
Remains of Hualien Prison Wall	Historic site	Hualien City, Hualien County	1010020314A	2012/2/4	23.98423	121.604485
The Monument of Tianzhong	Historical building	Tianzhong Township, Changhua County	1010138438C	2012/5/23	23.851311	120.583393
The Yang Quan House	Historical building	Changhua City, Changhua County	1070131006A	2018/4/18	24.080784	120.542761
Former The Lin Zi Jin House	Historical building	East Dist., Taichung City	10701338451	2018/7/2	24.133626	120.688868
Ooshen Event Mahpo Ancient Battlefield -Butuc and Ancient Trail	Historic site	Ren'ai Township, Nantou County	1080148095	2019/7/11	24.015990	121.188638
The Castle of Jianshi tapung	Historic site	Jianshi Township, Hsinchu County	0950095754	2006/7/24	24.692815	121.303584

between scenery and place [31]. The link between spatial information and humanities research focuses on tracking and naming from the perspective of microobjects as well as exploring the significance of local historical moments. Objective data were used to collect maps and texts in a historical and scientific way and examine the location of cultural assets.

The DocuSky digital humanities academic research platform was applied, and the maps were drawn with "GIS and Visualization 5" and "DocuSky Geographic Information Tools," and the base map uses modern base map Pioneer, and the "reference layer" was used to draw lines and arrow directions to visualize the "text layer" [32]. Through the common participation and the interaction between people, most of Taiwan's cultural assets can be accumulated into assets with rich cultural connotation. Although the research on cultural assets is becoming more and more popular, there are few studies on the development of related academic topics combined with databases and geographic information systems. In particular, the application of the map information system is an aspect that requires urgent consideration of deepening the related researches, and demonstrating Taiwan's multicultural characteristics and the overlapping nature.

5. Results

The cultural landscapes contained in databases such as the Taiwan People's Daily during the Japanese rule period or the Taiwan digital Library built by the National Taiwan Library provide information on spatial imagery [33, 34]. The image conveys the message in which time and space were interwoven. The theme images were collected from the "Taiwan Old Photo Database" of the Digital Humanities Research Center of Taiwan University. This database collects digitized photos of Taiwan-related illustrations and "Taiwan Photo Posts" from the collected publications, generating more than 37,000 interpretation materials and providing subcategories of person names, place names, ages, and provenances. You can search for interpretation data and meanwhile download interpretation data and digital images within the academic fair use range. The indigenous cultural data contained in the database can also be compared with tribal field surveys. In applying these images, attention must be towards exploring the perspective of the author, painter, or photographer. On the other hand, it is appropriate to search for and interpret old photos such as the scenery of Taipei City that will strengthen the functions of cultural imagination and augmented reality.

In order to extensively collect background information on the subject of tourism and understand the historical trauma of Taiwan, the oral history or biographies and the National Human Rights Museum's oral documentaries related to political suppression were taken as references, by which we can imagine a series of tortures experienced by the victims. Some relatives of the victims converted the scars into words expressing their opaque and unspeakable emotions; however, in this vagueness, their depressed mood becomes more apparent. Field investigations or oral information reading can help understand the historical trauma in Taiwan.

Figure 1: Map of human rights-themed cultural assets in Taiwan.

The GIS Special Center of the Humanities and Social Sciences Center of Academia Sinica uses Google base maps and combines the online query function of online maps to develop systems such as the Taiwan's century-old historical map [30]. As for the TGOS map collaboration platform, the API and Responsive Web Design platform of the Ministry of the Interior's Land Surveying and Mapping Center are used to integrate the government's open source base map resources and cross-platform interface. It not only allows the users to create themes themselves, but also edit or modify collaborative data with other people. Recently, the thought about combining the application of spatial information in the teaching of guided cultural landscapes came into mind. In order to make young students understand the relationship between the text and context of the times, they are first guided to read important texts and establish their ability for analysis and interpretation and in turn broaden students' international views from a local perspective. Cloud mapping and geographic information systems are also applied to develop thematic cultural tours. For example, stories based on the Taipei Human Rights Road combine texts, photos, and videos to present the context of places, events, issues, or geographic changes. Also, in conjunction with the course, students are led to a guided cultural tour, take photos or videos on the spot, and then use the Taiwan Fort map and the topographic layers, city street maps, aerial images, and satellite images of each period to make a comparison. An online collaborative Web GIS and a TGOS map collaboration platform were used to create the theme of the map material. Creating and sharing maps, scenes, layers and data, and story maps to combine Taiwan's historical maps were used. At the same time, mobile devices such as smartphones and tablets can also be used to combine historical positioning functions to browse historical map information.

Cultural memory is a method of preserving cultural continuity of a society, coupled with the collective knowledge passed down from generation to generation, and it is also a cultural behavior that helps with the cultural memory and helps future generations construct their own cultural identity. When monuments are set in a public open space with convenient transportation, it reminds the visitors of the impact of this event. In order to show the spatial location of human rights-themed cultural assets, DocuGIS is used to draw Figure 1.

For example, the 228 Incident occurrences spot Monument, which is one of the sites reminiscent of the historical event, is located at the entrance of No. 185, Nanjing West Road, Taipei. As a spot for memory, it helps people to understand the historical context of the city and by deepening the interpretation of the historical event, it fully serves the cultural function of space. Another example is the former residence of Yin Hai-kuang, located at Alley 16, Lane 18, Wenzhou Street. Yin Hai-kuang moved from China to Taiwan in 1949, and then he translated and introduced Hayek's famous book "The Road to Slavery" to

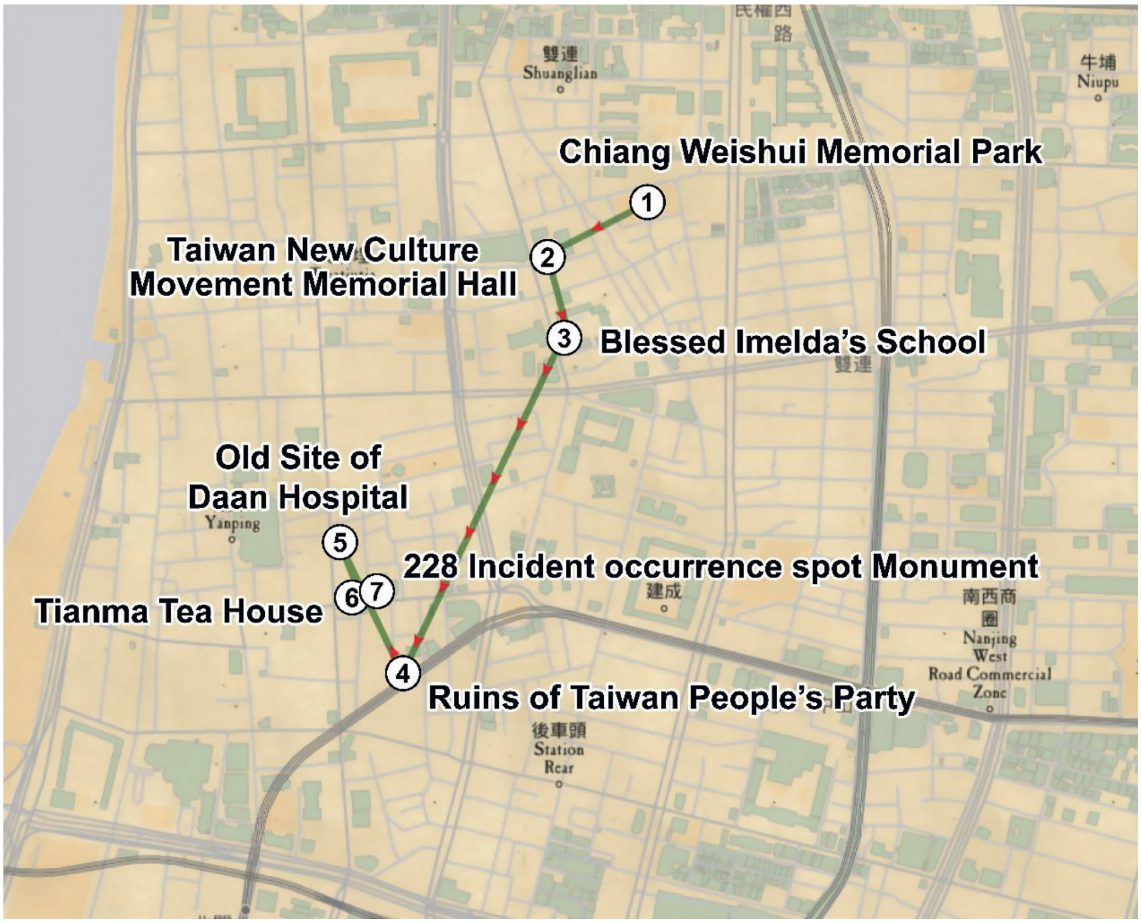

Figure 2: Taipei freedom route (A).

Taiwan. He upheld for life the spirit of "Would rather die than live in silence." He had taught at the Department of Philosophy of Taiwan University and wrote political commentaries for "Free China." He countered the prohibition of speech and thought with his pen and pointed out the errors of political affairs and offered advices in a philosophical way. Yin Hai-kuang reported customs of overseas countries in his travel writings, in order to criticize the party-state education in Taiwanese society at that time, and he analyzed the significance of freedom and democracy and published comments on cultural malady under Taiwan's totalitarian rule [36, 37]. This former residence is a space metaphor under the authoritarian system of Taiwan, and it also signified the worldly way of the intellectuals under the oppression of the party-state system. Chen Wencheng Memorial Plaza in preparation is being set up on the campus of National Taiwan University in honor of the 31-year-old Chen Wencheng. The Chen Wencheng incident has made the international community aware of Kuomintang's covert actions and the whistleblowing habits of campus agents, and it was a real case of Taiwanese people's suffering in their struggle for democracy.

Considering that guided tours within two hours will be better for general tourists [31, 32], Taipei Freedom Route is planned: one is Chiang Weishui Memorial Park (Taiwan Cultural Association, Taiwan People's Party member monument) ⟶ Taiwan New Culture Movement Memorial Hall (formerly Taipei Police Administrative Office) ⟶ Blessed Imelda's School (Taiwan Culture Association), Ruins of Taiwan People's Party ⟶ Old Site of Daan Hospital (Taiwan People News, Culture Publishing House) ⟶ Tianma Tea House ⟶ 228 Incident occurrence spot Monument (Figure 2).

Another route in the vicinity is planned: National Taiwan University (Chen Wencheng Memorial Plaza, the April 6th Incident) ⟶ Wisteria House ⟶ Yin Hai-kuang Former Residence ⟶ National Taiwan Normal University (Taipei High School Student Movement, the April 6th Incident) ⟶ Taipei Prison Wall Remains (Figure 3).

The Taipei Criminal Office established a prison outside the east gate of Taipei City during the Japanese rule period. In 1904, the city walls were torn down and then converted into a western style prison [33]. The postwar Kuomintang government continued to use it until 1963, known as the Taipei Prison. This prison witnessed the Miaoli incident in 1913, the Xilaiyan incident in 1915, and the police incident in 1923. On June 19, 1945, 14 captured American pilots were charged for "bombing civilians" and thus executed inside the prison's North Gate; after Japan announced its surrender, 11 foreign pilots held in prison were released and returned to their hometowns. After the war, witnessing the 228 incidents and White Terror, it

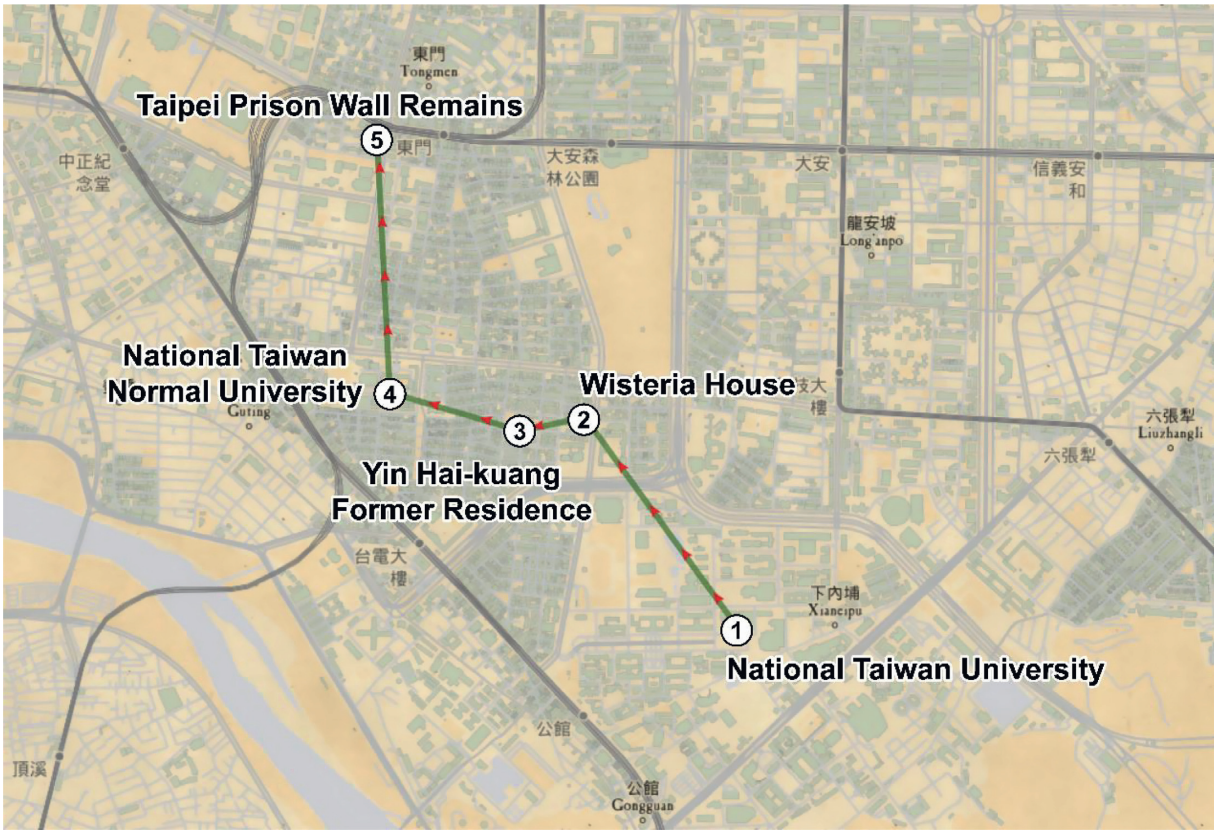

Figure 3: Taipei freedom route (B).

(a) (b)

Figure 4: The remains of the Taipei prison wall. Source: Photos by Shuhui Lin; time: December 2, 2017; location: Lane 44, Section 2, Jinshan South Road.

turned out be an international-level historical spot as well as an important human rights event spot in Taiwan. Professor Zhuang once stated in the newspaper: "South Korea could preserve the Seodaemun Prison in Seoul and establish a historical and cultural park. Couldn't Taiwan?" [34] He urgently and actively participated in the social movement to establish the "Taipei Prison Memorial Cultural Park." However, only hundred meters long and about 4 meters high prison wall was left. One part of the walls was a stone arched door, and was intentionally sealed with red bricks. According to legends, it was the location for the family to get back the body of the executioner at that time. The wall stones were the old stones of Taipei City Wall, and they were andesite and Qillian quartz arenite mined from Neihu and Dazhi during the Qing Dynasty, and each stone was 30 cm thick. Figure 4 shows what these stones look like today:

There are many other scenes related to the theme of freedom, and it is advisable to plan cultural corridors in the future such as Zheng Nanrong Memorial Hall, Cai Ruiyue

Figure 5: Human rights-themed cultural corridor in Taipei.

Dance Research Institute, Kongding culture lecture, Taipei Public Hall, Taipei 228 Peace Memorial Park, Machangding Memorial Park, and Jing-Mei White Terror Memorial Park, as shown in Figure 5.

Among them, the "Jing-Mei White Terror Memorial Park," one of the National Museum of Human Rights, was used as a detention center for the interrogation and detention of military, political, and public security cases from 1968 to the termination of the martial law. Its name was changed to "Jing-Mei White Terror Memorial Park" on December 10, 2007. This commemorative museum retains the historical building and space of the "Jing-Mei Military Detention Center," which represents the historical scene during the period of White Terror, and it functioned as a place for investigation and research, preservation of archives, display and publication, and promotion of human rights education [35]. In the past, since many real stories in the era of White Terror could not be revealed and transmitted, it was difficult to terminate tragedies and clarify misunderstandings. However, today it is possible to imagine the atmosphere of the martial law period by visiting important places known for prosecutions, trials, and executions due to political cases.

6. Discussion and Conclusion

By collecting information on Taiwan's cultural history, the multiple looks of the themed landscape are interpreted, guiding visitors to understand the context of Taiwan's cultural changes [36]. From Table 1, it is known that among cultural assets related to human rights themes, the number of historic sites is 19, the most, followed by 14 historical buildings, and the era spans the Qing Dynasty, Japanese rule, and the postwar period [44, 45, 46]. The geographical distribution is mostly in Taipei area, and then less in the middle, and least in the south and east. Relevant historical events include ethnic issues between the Han and indigenous peoples during the Qing Dynasty, the anti-Japanese movement of Han and indigenous people during the Japanese rule period, and related human rights topics covered the postwar 228 event and human rights-related events during authoritarian rule, as well as monuments and historic buildings featuring human rights symbols such as prisons and courts and memorial characters.

The manuscript uses a digital humanities methodology to examine cultural assets and their place in the "human rights journey" in Taipei. In particular, the DocuSky tools can deal with a real-world topic. The findings include the maps that effectively convey visual information regarding human rights-themed cultural assets in Taiwan and two Taipei freedom routes inspired by a similar route in Boston, USA. I also suggest additional possible routes. The discussion provides additional examples of the interaction between cultural assets, especially within the DocuSky database. I hope to make contributions to the digital humanities community.

In addition, the application of databases in related fields can help collect data on the interactive relationship of Taiwan's multiculturalism. Looking back at the humanities research with the help of spatial information technology, it is discovered that its resources not only transcend the limits of institutions, national borders, domains, etc., but also further reveal the multiple contexts implicit in the data. Thus, a location-based service platform is setup to make a

comprehensive analysis of cultural landscapes, provide a reference for planning tours to cultural landscapes, or enhance the humanism quality and emotional connection with the land, and promote the quality of cultural tourism for international tourists. For example, the Berlin Wall is the iconic scenery for tourists traveling to Germany, for it has a deep cultural significance. As for the Taipei Criminal Law Office, if the public can only see the remains of an old wall, how can they imagine its cultural implication. It is necessary to explain the story of the change of the Taipei Criminal Affairs Office, or through the public reports such as newspapers, readers' submissions and debates, or elites discussions about the process of planning ranging from the wall to the cultural park; it could then be made an example of cultural asset education. If combined with the stories of "Policy Incident," Lin Youchun, Jiang Weishui, Lai He, Wang Minchuan, and other human rights fighters who were detained at the Taipei Prison and interpreted the "Prison Literature" works, then the universal value will be manifested in this place. Tourism is a vital experience economy. Based on the value of Taiwan's human rights-themed cultural assets, the human rights journey in Taipei is guided to share Taiwan's happiness experience with the world. The application of innovative spatial information on the display of cultural assets is combined to reinterpret cultural understanding of the public and to give full play to the influence of humanities and public discourse on space practice.

Data Availability

The data used to support the findings of this study are available from the corresponding author upon request.

Conflicts of Interest

The author declares that there are no conflicts of interest.

Acknowledgments

This study was supported by the Ministry of Science and Technology of Taiwan (106-2410-H-003-116-MY3) and subsidized by the National Taiwan Normal University (NTNU), Taiwan.

References

[1] H.-Y. Tang, "Government support and authentication: the new tradition of city god folk festival in jinmen," *Journal of Chinese Ritual*, vol. 196, pp. 85–145, 2017.

[2] S.-H. Lin, "The Road to freedom: the universal value of Taipei's theme tourism," in *Collection Of Taiwan's Cultural Path: Zhuang Wanshou and His Cultural Academia*, pp. 152–158, Wu Sanlian Taiwan Historical Materials Foundation, Taipei, Taiwan, 2019.

[3] H. Lefebvre and Donald Nicholson-Smith trans, *The Production of Space*, pp. 1–9, Blackwell, Oxford, UK, 1991.

[4] C.-H. Wang, "Dialectics in multitude an exploration into/beyond henri lefebvre's conceptual triad of production of space," *Journal of Geographical Science*, vol. 55, pp. 1–24, 2009.

[5] C.-H. Wang, "Cultural production of imaged cities and urban meanings: an analysis of the Taipei pictorial," *City and Design*, vol. 13/14, pp. 303–340, 2003.

[6] W.-C. Chuang and S.-C. Chiou, "The study of urban spatial image," *Journal of Design Research*, vol. 4, pp. 116–127, 2004.

[7] J.-G Lay, Y.-W Chen, G. H. Yeh, and C.-C. Huang, "Research on taiwan map perspectives," *Journal of the Republic of China Map Society*, vol. 14, pp. 31–42, 2004.

[8] S.-H. Lin and S. Wang, "Configuration of american metropolises' image during the period of Japanese rule: according to Taiwanese elites' analysis," *Journal of Outdoor Recreation Study*, vol. 30, no. 2, pp. 1–20, 2017.

[9] J.-G. Lay, Y.-W. Chen, and K.-H. Yap, "Mapping Taiwan from an alternative angle," *Journal of Maps*, vol. 7, no. 1, pp. 244–248, 2011.

[10] B. Y. H. Liao, "Re-examining human rights in taiwan," *Taiwan Democracy Quarterly*, vol. 5, no. 4, pp. 235–245, 2008.

[11] F. F.-T. Liao, "Irish human rights commission-interaction between peace and human rights," *Tunghai University Law Review*, vol. 31, pp. 1–67, 2009.

[12] M. Huang, "Taiwan's human rights journey," *Taiwan Democracy Quarterly*, vol. 5, no. 4, pp. 181–187, 2008.

[13] H.-Yu Huang, "Early formation and development of Taiwan's cultural heritage preservation act 1945–1984," *Museum Quarterly*, vol. 31, no. 4, pp. 5–32+i, 2017.

[14] Ministry of Culture, "Cultural assets preservation act," Chapter I Article 3 of General Provisions, 2016.

[15] Ministry of Culture, "Cultural assets preservation act," *The Law on the Preservation of Cultural Assets*, Chapter 2 Article 17 of Historic Sites, Historic Buildings, Memorial Buildings and Settlements, 2016.

[16] C.-F. Wei, "The development and limitation of human rights of Taiwan in post-martial law-compares with other Asian countries," *Thought and Words: Journal of the Humanities and Social Science*, vol. 46, no. 4, pp. 1–103, 2008.

[17] V. Y.-C. Weng, "Dialogue and bargain: mapping the international human rights law to understand the implementation of universal human rights conventions in taiwan," *National Taiwan University Law Journal*, vol. 46pp. 1115–1201, S, 2017.

[18] M. Zembylas, P. Charalambous, S. Lesta, and C. Charalambous, "Primary school teachers' understandings of human rights and human rights education (HRE) in Cyprus: an exploratory study," *Human Rights Review*, vol. 16, no. 2, pp. 161–182, 2015.

[19] J. A. Roy, "Labor rights are human rights," *Working USA*, vol. 3, no. 2, pp. 72–77, 1999.

[20] S.-H. Lin, "The memory of medical pilgrimage: Dr. Tsungming Tu's strategy of travel writings about Europe and the United States during the Japanese colonial period," *Journal of Taiwan Literary Studies*, vol. 21, pp. 1–38, 2015.

[21] Y.-c. Fan, "Caught between imperial medicine and colonial medicine: beriberi in colonial Taiwan," *Taiwan Historical Research*, vol. 25, no. 4, pp. 75–118, 2018.

[22] S.-H. Lin, "The application of the Taiwan history digital library (THDL) to the research of poetry and prose regarding customs in the earlier qing-governed period," in *Digital Humanities: New Approaches to Historical Studies*, J. Hsiang, Ed., National Taiwan University Press, Taipei, Taiwan, 2011.

[23] S.-C. Lin, "The social constructing process of village place-name and landmark place-name in the tai-ping of shuang-xi, new Taipei city: the application of taiwan history digital library (THDL)," *Journal of Geographical Research*, vol. 57, pp. 23–48, 2012.

[24] D. Germano, "The relationship of buddhist studies and area studies: new perspectives from humanities computing," *The Journal of Chinese Buddhist Studies*, vol. 20, pp. 331–348, 2007.
[25] S.-P. Chen, Y.-M. Huang, J. Hsiang, H.-C. Tu, H.-I. Ho, and P.-Y. Chen, "Discovering land transaction relations from land deeds of Taiwan," *Literary and Linguistic Computing*, vol. 28, no. 2, pp. 257–270, 2013.
[26] J. Hsiang, S. P. Chen, H. I. Ho, and H. C. Tu, "Discovering relationships from imperial court documents of qing dynasty," *International Journal of Humanities and Arts Computing*, vol. 6, no. 1-2, pp. 22–41, 2012.
[27] A. Burdick, J. Drucker, P. Lunenfeld, T. Presner, and J. Schnapp, Eds., *Digital Humanities*, MIT Press, Boston, MA, USA, 2012.
[28] J. Hsiang, S.-P. Chen, and H.-C. Tu, "On building a full-text digital library of land deeds of Taiwan," in *Digital Humanities*, pp. 85–90, University of Maryland, College Park, MY, USA, 2009.
[29] S. P. Chen, J. Hsiang, H. C. Tu, and M. C. Wu, "On building a full-text digital library of historical documents," in *Asian Digital Libraries. Looking Back 10 Years and Forging New Frontiers*, D. Goh, T. Cao, I. Sølvberg, and E. Rasmussen, Eds., vol. 4822Springer, Lecture Notes in Computer Science, , pp. 49–60, Springer, 2007.
[30] T.-K. Ling, "Legislative yuan architecture analysis," *Taiwan Natural Science*, vol. 31, no. 2, pp. 18–23, 2012.
[31] T. Cresswell, *Place: A Short Introduction*, Wiley, NJ, USA, 2004.
[32] H.-C. Tu, "DocuSky: a platform for constructing and analyzing personal text databases," *Journal of Digital Archives and Digital Humanities*, vol. 2, pp. 71–90, 2013.
[33] S.-H. Lin, "Viewing landscapes to observe change: travel narratives in diaries during the japanese colonial period in Taiwan," *Bulletin of Taiwanese Literature*, vol. 32, pp. 23–52, 2018.
[34] P.-H. Hsu, "Common school graduates and Taiwanese society during the middle period of the Japanese occupation," *Bulletin of Academia Historica*, vol. 41, pp. 136–156, 2014.
[35] I.-C. Fan, H.-M. Liao, Ta-C. Chan, and L.-F. Chang, "Past, present and future of historical GIS in academia Sinica," *Journal of Asian Network for GIS-Based Historical Studies*, vol. 1, pp. 7–11, 2013.
[36] P.-H. Liao, "Print culture and the emergent public sphere in colonial Taiwan, 1895–1945," in *Taiwan Under Japanese Colonial Rule, 1895–1945*, D. D.-W. Wang and P.-H. Liao, Eds., History, Culture, Memory, Columbia University Press, New York, NY, USA, 2006.
[37] J. C.-h. Lin, "The personal is political: revisiting "English" and "Homeland" by reading shirley Geok-lin Lim's Hong Kong poetry," *Translocal Chinese: East Asian Perspectives*, vol. 13, no. 2, pp. 167–181, 2019.
[38] B. Curtis and C. Pajaczkowska, "Getting there: travel, time, and narrative," in *Travelers' Tales: Narratives of Home and Displacement*, G. Robertson and M. Mash, Eds., Routledge, London, UK, 1994.
[39] P. Barry, *Beginning Theory: An Introduction to Literary and Cultural Theory*, Manchester University Press, Manchester, UK, 2006.
[40] D. Botsman, *Punishment and Power in the Making of Modern Japan*, Princeton University Press, Princeton, NJ, USA, 2005.
[41] W.-S. Zhuang, *Don't Let History Get Into the Black Prison*, The Liberty Times, Taipei, Taiwan, 2014.
[42] C.-W. Lin, "Initial challenges and missions of the preparatory Office of the national human rights museum," *Museology Quarterly*, vol. 28, no. 3, pp. 111–126, 2014.
[43] C. Thompson, *Travel Writing*, Routledge, New York, NY, USA, 2011.
[44] S.-H. Lin, "The cultural cold war code of moving narration in today's world," *Literature and Philosophy*, vol. 32, pp. 433–458, 2018.
[45] S.-H. Lin, "An analysis of narrative strategies in border-crossing travel notes published by free China," *The Journal of Taiwan Historical Association*, vol. 20, pp. 116–152, 2016.
[46] Y.-J. Chen, "Dependence and competition: the dairy industry in Taiwan during the post-war and US-aid period (1945–1965)," *Journal of Chinese Dietary Culture*, vol. 13, no. 1, pp. 35–73, 2017.

Hindawi
Complexity
Volume 2020, Article ID 6152017, 13 pages
https://doi.org/10.1155/2020/6152017

Research Article

Monetary Incentives in Italian Public Administration: A Stimulus for Employees? An Agent-Based Approach

Linda Ponta,[1] **Gian Carlo Cainarca**,[2] **and Silvano Cincotti**[2]

[1]*LIUC-Cattaneo University, Corso G. Matteotti 23, I-21053 Castellanza, VA, Italy*
[2]*DIME-DOGE, University of Genoa, Via Opera Pia 15, I-16145 Genova, Italy*

Correspondence should be addressed to Silvano Cincotti; silvano.cincotti@unige.it

Received 7 February 2020; Accepted 22 April 2020; Published 23 May 2020

Academic Editor: Dehua Shen

The paper, focusing on the context of Public Administration (PA), addresses the effects of monetary incentives in employees' performance. In the Italian PA, the monetary incentives are distributed according to the D.L.150/09 (i.e., the monetary incentives are divided among the employees according to the employees' performance) which is based on the rank order tournament. The paper investigates if this mechanism has positive and sustainable impacts on the employees' performance in the short, middle, and long term. The employees' performance has been modeled as a function of ability and motivation. The results of the computational experiments show a positive impact of the monetary incentives, distributed according to merit criteria, on the employees' performance in the short, middle, and long term.

1. Introduction

Starting from the late 1970s many European countries have experienced a period of reforms in the public sector. The reforms regarded different fields and in particular from one side the management system, introducing control and planning system, and from the other the performance appraisal and the reward systems, fostering technical and cultural changes in the public sector [1–8]. In Italy, since the early 1990s, numerous reforms have been succeeded with the purpose of reaching a better use of the resources and a better quality of services given to citizen. It is worth noting that reforms in Italy are characterized by a "top-down" approach, i.e., by regulation, and the most important are D. Lgs. 29/1993 and Law n. 59/97 (so called Legge Bassanini). These reforms tried to adopt new managerial instruments usually used in the private sector, but the results were a failure because the transferability of these instruments to the bureaucracy of the Public Administration (PA) is not always effective. The main causes of the failure were the constraints of PA, such as the possibility to make change only by means of laws and the uncertainty of the amount of resources. The last attempt of reform is the "Decreto Legislativo 27 ottobre 2009, n. 150," "Attuazione della legge 4 marzo 2009, n. 15, in materia di ottimizzazione della produttività del lavoro pubblico e di efficienza e trasparenza delle pubbliche amministrazioni. (09G0164)," also called Brunetta reform, where a virtuous circle able to induce behaviors more efficient to overcome the previous failure is initiated giving instruments extremely concrete and ready to use. Following the New Public Management theory (NPM), the Brunetta reform considers the PA as firms and borrows from the firm context the key concepts of efficiency, efficacy, productivity, and transparency. In particular, the efficiency connects the resources used (input) with the results (output); the transparency means the possibility of the citizen to access to the activity of PA; the efficacy considers the measure of the action of the PA on the external environment; and finally the productivity means the performance of the employees and of the organization. In fact, according to NPM, performance management based on objectives, monitoring, and incentives must be introduced in public sector organizations [6]. Focusing on the incentives and in particular on the monetary incentives given to the employees, according to D.L. 150/09 the incentives are no more divided equally among the employees but they are distributed only to the employees

that perform better, ranking them according to merit criteria. In fact, as stated in [9, 10], pay-for-performance systems are less efficient than the promotion tournaments in public organizations.

The main goal of the paper is to verify the effects of the new incentives mechanism introduced with D.L.150/09 in the Italian PA and to observe its sustainability over time. In order to address such investigation, the paper presents an agent-based model and simulation based on empirical data collected by questionnaires. Simulation is a useful tool to investigate complex systems in many different fields such as engineering, physics, mathematics, and economics and is also becoming an increasingly significant methodological approach in organizations and strategy and public management field [11–16]. Among the different simulation models, the agent-based approach is very useful to investigate complex systems and networks characterized by a large number of simple interacting units [17–26]. An agent-based model provides a computational laboratory very suitable to make classical what-if analysis by means of experiments [27–33]. In organizations, field agent-based models (ABMs) are particularly well suited to study processes where heterogenous interacting entities are involved [34–37]. Thus, they represent a useful tool to investigate the effects of new policies such as new incentive mechanisms. In the following, Section 2 presents the literary review and the research gap, Section 3 the questionnaire data, Section 4 the simulation model, Section 5 the computational experiments, and Section 6 the empirical analysis. Finally, Section 7 provides the discussion and conclusions of the study.

2. Literature Review and Research Question

In the literature, many studies about the increasing of efficiency and performance of the PA have been presented [38]. Usually, the organizational performance is considered directly related to the performance of employees, and how to evaluate the performance of employees in the public sector is an interesting and difficult field of research [39–42]. The main theories consider jointly the "capacity to work" and the "will to work" to determine the employees' performance [43, 44]. The "capacity to work" has been formalized as ability, whereas the "will to work" as motivation [45]. Some years later, to improve the effective evaluation of the employees' contribution, the Ability, Motivation, and Opportunity model (AMO model), which adds the "opportunity to perform" to the "capacity to work" and "will to work," has been defined [46, 47]. According to this theory, Human Research (HR) system is viewed as a composition of employee skills, motivation, and opportunity to contribute in working life [46, 48–52].

2.1. Monetary Reward. It is already known that the economic motivation is one of the most used stimuli to improve the firm performance [53, 54]. Focusing on the relation between monetary incentives and employees' performance, one of the most important theories is Performance Related Pay (PRP) theory, derived from the principles of Weberian bureaucracy, see [55], for further details. With respect to a system that grants a bonus based on seniority, PRP is a mechanism able to quickly increase work motivation and improve the performance of employees [56]; in fact employees work harder if they, valuing the monetary rewards, trust that those awards are related to their increased efforts [57, 58].

In the literature, the use of financial incentives and in particular of monetary incentives is based primarily on the theoretical propositions of reinforcement theory [59] and expectancy theory [60]. Reinforcement theory, premised on the principles and techniques aimed at modifying organizational behavior, investigates the connection between the target behavior (e.g., performance) and the motivational tool (e.g., pay for performance) [61–63], whereas expectancy theory is an analytical tool to study how a reward system motivates the employees [64].

Other theories useful to investigate the link between incentives and motivation are the equity theory and the distributive justice. According to the equity theory, each employee compares her/his contribution to the organization with the reward gained by her/his job [65] and with the one obtained by other coworkers. Instead the idea of distributive justice is connected to the one of procedural justice. According to procedural justice, individuals evaluate the mechanism that the organization introduces to distribute rewards [66].

Several studies in the literature state that the efficacy of monetary incentives is connected to specific conditions of organizations. In particular, they argue that individual economic incentives are not so useful in the traditional public sector, if the medical and educational contexts are excluded [54, 59, 67–71].

In particular, a study focused on public managers reports that financial rewards had no significant effect on the managers' effort [72]. It is worth noting that the relationship between incentive and performance in public and private sector has different peculiarities mainly due to specificity of cultural dimension, market relations, bonus size, and nonexpandable business constraints [67, 73]. Finally, in the PA, the link between incentive and performance is not straightforward because it is difficult to identify the contribution of each employee. In fact, in private firms, this is easier because the results of operations are quantitatively measurable, whereas in the public sector, where profit is not the primary target, this is more difficult. Thus, an evaluation schemes, designed to capture the different levels of competence and predisposition of individuals to make a greater effort in the workplace, can be adopted.

2.2. Research Gap. In this paper, the employees' performance is evaluated focusing on their abilities and motivations. Many mechanisms can be used to detect the abilities of employees [74], but all of them can be attributed to two fundamental models: the subjective evaluations, that consider the individual organizational behavior, and the objective evaluations, that directly take into account the feedback of one or more superior or all of the colleagues.

Focusing on the objective evaluation, the network analysis, mainly focused on the links among the employees, allows to evaluate the importance and relevance of each employee, with respect to her/his colleagues. Indeed, the relationships, in the informal network, reflect the recognition given to a single employee from their colleagues for her/his skills and her/his opportunities to participate in working life.

The ability is also a measure of employees to make themselves available by their colleagues [75, 76].

The motivation is reflected considering a model with different levels of stimuli that depend on the employees' strength and successes. They are represented by the achievement of a predetermined threshold that leads to different monetary rewards [77]. This model is based on the expectancy theory of motivation, a process theory that provides an explanation of individual criteria used to choose among different behaviors. According to this theory, the work motivation depends on the perceived association between performance and outcomes. Employees modify their behavior based on their estimation of anticipated outcomes [78]. According to [79], the motivation for work is related to a series of causes and effects: first of all persons should trust that their increased efforts will translate into a better performance; secondary, a satisfactory performance should lead to a wanted reward; thirdly, the reward should fulfill a significant need for the individual. Finally, the desire to fulfill this need should be strong enough to make the initial efforts worthwhile.

So far, in the PA, the financial incentives are distributed among the employees following a hierarchical mechanism, without considering the performance of each employee. Specifically, the incentives are first uniformly distributed among the business units and then subdivided among individual employees. The portion of incentives received by each employee is proportional to its tenure, i.e., related to the role in the organization, not determined by its performance.

As mentioned in the introduction, the Italian D.L.150/09 tried to introduce a merit logic in the distribution of monetary incentives in the PA. According to the D.L.150/09, the bonus is evaluated with a merit logic, which is formalized by the closed rank tournament theory, which means that the employees are ranked and only a subset takes the monetary incentives according to the employees' performance. According to this law the employees are divided in three sets, called set A, B, and C, and receive a different amount of monetary incentives according to the set. In particular, 25% of the total employees is collocated in set A, 50% in set B, and 25% in set C. The total amount of monetary incentives is divided as follows: 50% to set A, 50% to set B, and 0% to set C. Thus, people in set C do not receive any kind of monetary incentives.

The main research question of the paper is to investigate if the monetary incentives, distributed according to merit criteria, i.e., according to D.L. 150/09, are a stimulus for better performance in the short, middle, and long term. The effect of the introduction of D.L.150/09 is investigated considering the sustainability of the new rules for the distribution of incentives along time using the agent-based simulation. The simulation verifies if the monetary incentives distributed with merit criteria have positive or negative effect after the introduction of the rule. In detail, the sustainability of the merit criteria in the distribution of monetary incentives is investigated considering how many employees every year are in the same set and how many employees change set trying to improve their performance.

3. The Data

A series of interviews has been arranged in order to explore the connection between the performance of the employees and the allocation of economic incentives: in February 2011, 131 employees were interviewed, and in January 2013, the arranged interviews were 126. The interviews consisted of one hour face-to-face sessions composed of 57 questions, to which the employees had to respond with a value between 1 and 7, according to the Likert scale [80]. The employees interviewed belong to five different organizational areas. In order to minimize misunderstandings, the research team directly administered the questionnaires. The questionnaires were anonymous, the provided data were only used for private purposes, and the people were interviewed in agreement with the trade unions. In February 2011, 126 questionnaires were collected out of 131 (four employees were absent in that period, and one was hired as a temporary secretary). In 2013, interviewees were 123 out of a total of 126. The total number of employees decreased because there have been a few retirements, and, due to the financial crisis, the assumption rate was lower than the retirement rate. The questionnaires were composed of four different sections:

(i) Personal data (gender and age)

(ii) Position (tenure and organizational area)

(iii) Skills (problem solving, teamwork, determination, customer oriented, and self-organization)

(iv) Intraorganization relationship

The resultant set of data provides information on both employee characteristics (occupied position, knowledge, skills, and background) and the organizational model (the relationships maintained between employees of the same organization and between different organizations). In addition to this data, the HR department provided the salary information of employees for the three years from 2010 to 2012. Specifically, this information included

(i) The uniformly distributed portion of the bonus granted to every employee

(ii) The portion of the bonus based on the criteria of merit

(iii) The salary-level: there are 12 levels, 8 of which are reserved for employees having nonexecutive positions

It is worth noting that, in 2010, the total amount of incentives distributed equally among the business units was 47% and the one distributed according the merit criteria was 53%, whereas in 2011, the allocation was 36% and 64%, respectively. Thus, the monetary incentives distributed according the merit criteria increases from 53% to 64%.

4. The Model

4.1. The Network. The employees in the model are organized as a directed graph, where the employees are the nodes and the arrows represent the interactions among employees. The total number of employees is N and each employee is characterized by an identification number id. An employee is linked to a set of other employees whose number and strength (of the connection) g_{ij} depends on the real data. The connections among the employees have been determined ignoring the vertical relation among supervisors and employees and considering the informal network created by means of the information obtained with the administered questionnaire. In fact, employees were asked with whom and how many times they need to interact to perform the given task. In particular, they had to indicate up to ten members of the organization they need to relate more directly and more frequently with, in order to improve or facilitate the execution of their activities. In order to quantify the frequency of the connection, i.e., the strength, a Likert scale that ranges from 1 (contacts infrequent, some once a month) to 7 (several times per day) has been used. With the collected information, an adjacency, squared, and not symmetrical matrix has been built and shown in the informal network of Figure 1. It is worth remarking that only the connections between employees in the same level have been considered, to find out only the "horizontal" relationships.

The interactions in the graph are assumed to be unidirectional (i.e., if employee j influences employee i, it does not necessarily mean that employee i influences employee j) and characterized by a weight g_{ji}, assumed a positive real number in the range [0, 1] proportional to the Likert scale. As a directed graph is used, both an output and input node degrees are defined. The output node degree is associated to the output branches of a given node, whereas the input node degree is related to the input arrows.

Furthermore, each employee is characterized by her/his rank r and her/his performance P.

At each time step h, the performance of employee i is evaluated and the rank r_i^h is updated. The agent's rank r is an integer number between 1 and 3 depending on the set to which the employee belongs. Employees in set A have rank $r_i^h = 1$, in set B have rank $r_i^h = 2$, and in set C have rank $r_i^h = 3$. According to their performance, in descending order, the employees are divided in three set: A, B, and C. Set A is formed by the top 25% of the total employees, set B by the next 50%, and set C by the last 25% (see D.L. 150/09, for more details). It is worth remembering that employees belonging to different sets receive a different fraction of monetary incentives. In particular, half of the total amount of monetary incentives is divided among employees in set A, half among employees in set B, and 0 among employees in set C.

The graph is responsible for the changes in employees' rank. In fact, at each time step, employees depending on their rank change a fraction of his/her connections in order to improve the performance.

4.2. The Performance. As already stated in Section 2, the performance is a function of Ability and Motivations and quantitatively the performance is measured as the production of ability and motivation [43]. In formulas,

$$\text{Performance} = \text{Ability} \times \text{Motivation}. \tag{1}$$

4.2.1. Ability. As already stated in Section 2, in order to detect the abilities of employees, the objective evaluations have been considered by using the network analysis approach. Generally speaking, the influence of an individual regarding other individuals within a network is indicated by his/her centrality [81].

Centrality in the advice network means the recognition given to a single employee from her/his colleagues for the availability in exchanging advices and in problem solving. A central individual can increase knowledge about different problems over the years, and as more and more colleagues become dependent on her/him for some help, she/he gains power and authority [82, 83]. There are many definitions of centrality, but the most common are the Degree, the Closeness, the Betweenness, the Coreness, and the Bonacich centrality [84–87].

In this paper, among the others the degree centrality is chosen and the centrality is measured by means of the number of connections among the employees, defining the centrality index.

The centrality index of employee i, CI_i, indicates the relationship between employee i and the other employees and, in particular, quantifies how employee i is involved in the activities of the other employees:

$$\mathrm{CI}_i = \frac{\mathrm{TAC}_i}{c_{\max}}, \tag{2}$$

where TAC_i is the task advice centrality of employee i and $c_{\max}$ is the maximum number of input connections among all the employees. The task advice centrality for each node, i.e., the centrality of the individual in the social consulting network, is the sum of all incoming arrows (input node degree) multiplied by their weights. As mentioned above, the employee's centrality in the intraorganizational network reflects her/his skills to participate in working life and, in particular, indicates how a node is necessary to perform the employees' activities. Thus, it is a proxy of the employees' ability. In the formula, the task advice centrality of employee i (TAC_i) is

$$\mathrm{TAC}_i = \sum_j c_{j,i} g_{j,i}, \tag{3}$$

where $c_{j,i}$ are the incoming arrows of employee i and $g_{j,i}$ are the respective weights.

4.2.2. Motivation. As stated in Section 2, the expectancy theory of motivation has been considered. According to this theory, employees can be motivated if they believe that there is a positive correlation between efforts and performance. This behavior has been schematized defining the motivation

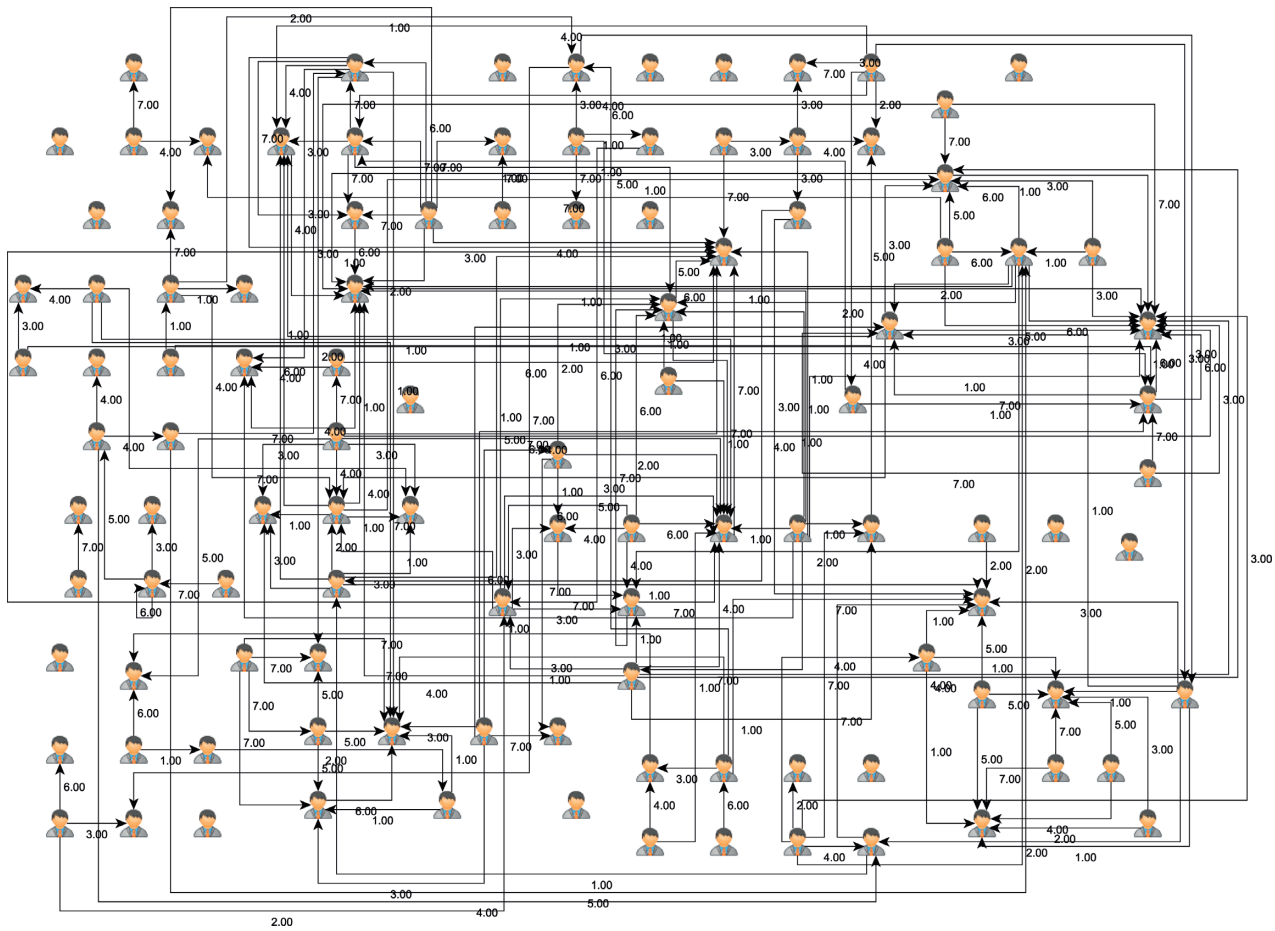

Figure 1: Network of employees at time $t = 0$.

index MI. In particular, the motivation of employee i is quantified with the motivation index MI_i. According to D.L. 150/09, the employees are ranked and divided in three sets A, B, and C and receive a different fraction of monetary incentive. In particular, 25% of the total employees is collocated in set A, 50% in set B, and 25% in set C, respectively, whereas half of the total amount of monetary incentives is divided among employees in set A, half among employees in set B, and 0 among employees in set C. The motivation index quantifies the motivation of each employee to do better in order to receive more monetary incentive. According to the deprivation-satiation proposition, the more often in the recent past a person has received a major award, the less he will confer a value to any further reward. Following this proposition, for employees in set A (corresponding to high incentives), the motivation decreases, increasing the performance evaluation, and conversely, for employees in set C, the motivation increases if performance evaluation increases. In particular, the employees near the upper bound of set A and the lower bound of set C are not motivated to do better [88]. In the formula, the motivation index MI_A in set A is

$$\mathrm{MI}_A = \frac{|E_s - P|}{(E_s - T_a)}, \tag{4}$$

where E_s is the maximum value of performance in set A, T_a the minimum value of performance in set A, P is the employee performance, and the motivation index in set C, and MI_C is

$$\mathrm{MI}_\mathrm{C} = \frac{|P - E_i|}{(T_b - E_i)}, \tag{5}$$

where E_i is the minimum value of rank in set C and T_b the maximum value of rank in set C. For employees in set B, the motivation is high when the employee is near the two bounds of the range and decreases in the middle. This is in line with the theory that while choosing among different actions, an employee chooses the one for which the results multiplied by the probability of getting it is greater [88]:

$$\mathrm{MI}_\mathrm{B} = \frac{|T_{mb} - P|}{(T_a - T_b)/2}, \tag{6}$$

where T_{mb} is the middle value of rank in set B. Table 1 summarizes the parameters abbreviations.

Figure 2 shows how the motivation index MI ranges along the set A, B, and C.

Employees in set A increase their motivation moving their level of assessment from E_s (maximum level of assessment) to T_a. Employees in set C decrease their motivation moving their level of assessment from T_b to E_i

Table 1: Description of the simulation model's parameters.

Abbreviation	Parameter
CI	Network centrality index
MI	Motivation index
E_s	Upper bound of set A
T_{ma}	Middle value of set A
T_a	Lower bound of set A and upper bound of set B
T_{mb}	Middle value of set B
T_b	Lower bound of set B and upper bound of set C
E_i	Lower bound of set C
P	Performance

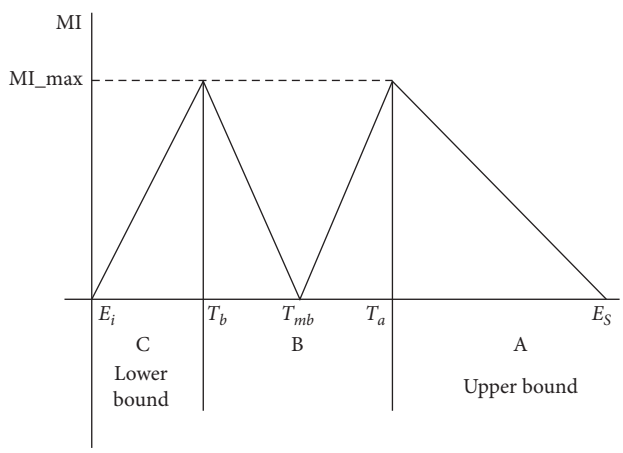

Figure 2: Motivation index.

(minimum level of assessment). Finally, in set B, employees' motivation tends to increase as their level of assessment is close to T_a and T_b and is minimum at the midpoint of the range T_{mb}.

Then, employee i has a motivation $\mathrm{MI}_{\mathrm{A},i}$ if his rank value belongs to set A, $\mathrm{MI}_{\mathrm{B},i}$ if it belongs to set B, and $\mathrm{MI}_{\mathrm{C},i}$ if it belongs to set C.

4.2.3. Performance Calculus. In the model, the ability is approximated quantitatively with the centrality index (CI), which considers the relations among the employees, i.e., the informal network, whereas the motivation with the motivation index (MI).

Thus, the performance of employee i is evaluated as follows:

$$P_i = \mathrm{CI}_i \times \mathrm{MI}_i, \tag{7}$$

where CI_i is the centrality index and MI_i the motivation index. It is worth remarking that the performance is considered as the product of centrality index (that is a proxy of ability) and motivation index (that is a proxy of motivation).

5. Computational Experiments

In the computational experiments, the number of agents considered is 110. Figure 1 shows the network of employees at time $t = 0$, which corresponds to the empirical data, whereas Figure 3 zooms the connections of employee 61 at time $t = 0$.

The simulation duration is twenty years ($T = 20$), in order to consider the short, middle, and long term. According to the empirical data, the number of ranks is three. The strength of each connection $g_{i,j}$ between two employees is a real number in the range [0, 1]. The number of employees in set A is fixed to 35, in set B to 70, and in set C to 5, whereas the total amount of incentives is divided in 47% for employees in set A, 52% for employees in set B, and 1% for employees in set C. It is worth noting that these values are different from the ones defined by D.L.150/09 because in the computational experiments the used values correspond to the empirical data. Table 2 summarizes the parameters used in the simulations.

At each time step that corresponds to a year, employees with rank 1, 2, and 3 change randomly from a uniform distribution 10%, 20%, and 30% of their connections, respectively. This assumption mimics the realistic behavior of employees; in fact, employees in set C change more connections than employees in set A and B because in order to improve the performance they contact new employees, whereas employees in set A change very few connections because they do not need to contact new employees to improve their performance. Figures 4–7 show in the top the rank story and in the bottom the performance of agent 9, 103, 119, and 108 during the simulation, exhibiting the different behaviors of employees.

Figure 4 shows an employee who does not change his/her rank during the twenty years. In this case, the monetary incentives system does not work as stimulus to improve his/her performance. Figure 5 shows the rank behavior of an employee that is not able to improve his/her performance, i.e., the performance worsens, and also in this case, the incentives' systems does not work, whereas Figure 6 shows the rank behavior of an employee who is able to improve his/her performance, and therefore in this case, the incentives' systems work. Finally, Figure 7 shows the rank behavior of an employee with positive and negative changes. Also, in this case, the incentives' systems work as stimulus to improve the employees' performance.

Figure 8 shows the percentage of employees with different behaviors during the simulation.

In particular, the blue circle line represents the percentage of employees who are in set A, the red dashed line the ones in set B, and the black stair line the ones in set C who did not change set during the twenty years. The green triangle line represents the percentage of employees who during the twenty years worsened or not improved their rank position, whereas the cyan diamond line represents the ones who have improved or not worsened. Finally, the magenta continuous line represents the percentage of employees who during the simulation time improved or worsened their position. It is worth noting that the percentage of employees who did not change set along the twenty years decreases, whereas the number of employees who did not improve and the ones who did not worsen is constant. Instead, the percentage of employees who sometime improved and sometime worsened their rank increases

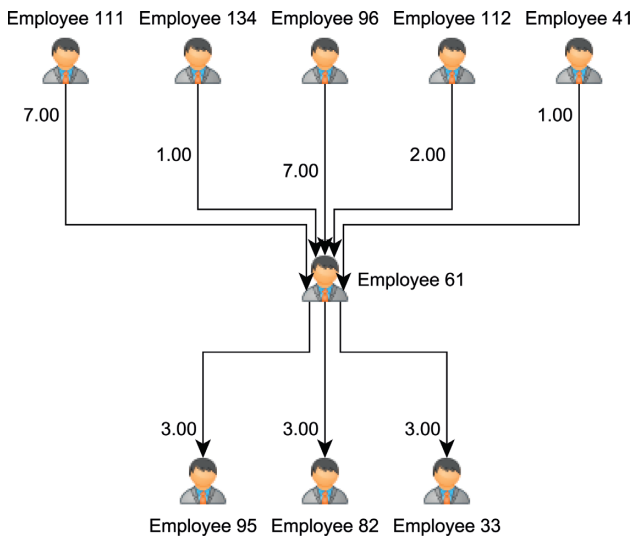

Figure 3: Zoom of connections of employee 61 at time $t = 0$.

Table 2: The most relevant parameter values used in the simulation.

Symbol	Description	Value
N	Number of employees	110
N_A	Number of employees in set A	35
N_B	Number of employees in set B	70
N_C	Number of employees in set C	5
T	Duration of simulation (years)	20
R	Number of rank	3
$g_{i,j}$	Strength of connections	[0, 1]

along the twenty years. This means that, in the short term, people think that changes in the PA cannot be possible, as shown by the number of employees fixed in a set, whereas in the middle and long term the incentive system works because employees who try to improve their performance increase and the number of employees who are fixed in a set decreases.

Table 3 underlies the rank story of the employees in the simulation analysis $T = 20$.

Figure 9 shows the percentage of employees for which the monetary incentives' mechanism works and did not work during the twenty years. The blue circle line represents the employees who are fixed in a set and the one that worsen their rank position. For these employees, the incentives' system does not work. The red stair line represents the employees who increase or increase and decrease their rank position. For these employees, the incentives' system works. It is worth noting that starting from year 12 (middle term) the percentage of employees which believes in the incentives' mechanism is larger than the one which does not. Moreover, this result confirms that the incentives distributed according to a merit approach bring to a better performance of employees and then of the firm in the middle and long term.

Finally, Figure 10 shows the analysis in the very short term, considering the behavior of employees rank and performance from year $t - 1$ and t.

Figure 10(a) shows that, from year $t - 1$ and t, the percentage of employees which does not change rank is between 85% and 95%, whereas the number of employees which improves and the one which worsens rank is between 5% and 15% in both cases, whereas Figure 10(b) shows that the percentage of employees which does not change their performance is between 1% and 15% whereas the number of employees which improves and the one which worsens their performance is around 50% in both cases. This means that even if, in the short term, the number of employees which does not change rank is very large, the number of employees which does not change their performance is very few, showing that the employees try to improve also in the short term even if the results is visible only in the middle and long term. In the very short term employees move their performance, but this is not visible from the rank.

Finally, the analysis shows that the monetary incentives distributed according to a merit logic and the performance are linked in particular in the middle and long term simulation. In fact, in the middle and long term, the number of employees which does not change their rank decreases, confirming the positive effect of the incentives distributed with merit criteria. This means that the employees consider the incentives a good motivation for better performing. Moreover, in the short and very short term, the results suggest that, from a macropoint of view the employees think that changes in the PA are very difficult, but a deeper analysis shows that the employees' performance changes meaning which they try to improve in order to get a larger incentive. It is worth noting that the incentives distributed with merit logic bring the employees to a better individual performance and then to a better firm's performance. Thus, the hypothesis is confirmed in fact after n-step people continue to try to improve their performance.

6. Empirical Analysis

The computational results are confirmed in the short term by the empirical analysis on real data. Table 4 shows the same analysis performed for the computational experiments for the real data. In particular, the number of employees which is always in set A, B, or C and the ones which always worsens or improves or worse/improve their rank in year 2010/2011 and 2010/2012 are reported.

The results confirm the decreasing number of employees in a fixed set and the increasing number of the employees which improves and worsens their rank position. The number of employees which always improves or worsens remain more or less constant.

Concerning the very short term, Tables 5 and 6 show the employees' rank and performance in the period 2010/2011 and 2011/2012. The results confirm the computational experiments results.

7. Discussion and Conclusions

In this paper, the distribution of monetary incentives in the PA through a rank order tournament has been addressed. The relationship between the monetary incentives and

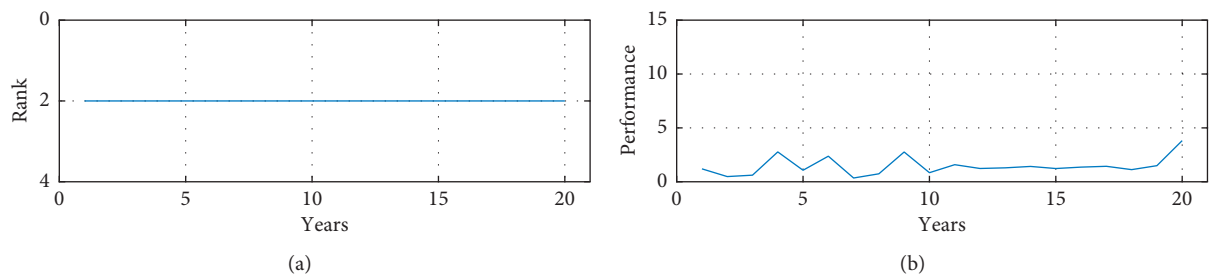

Figure 4: Rank history (a) and performance (b) of agent 9. During the simulation the employee 9 does not change his/her rank.

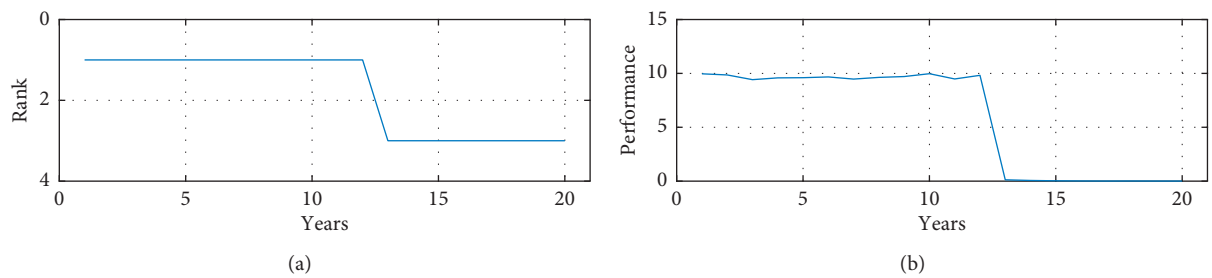

Figure 5: Rank history (a) and performance (b) of agent 103. During the simulation the employee 103 worsens his/her rank.

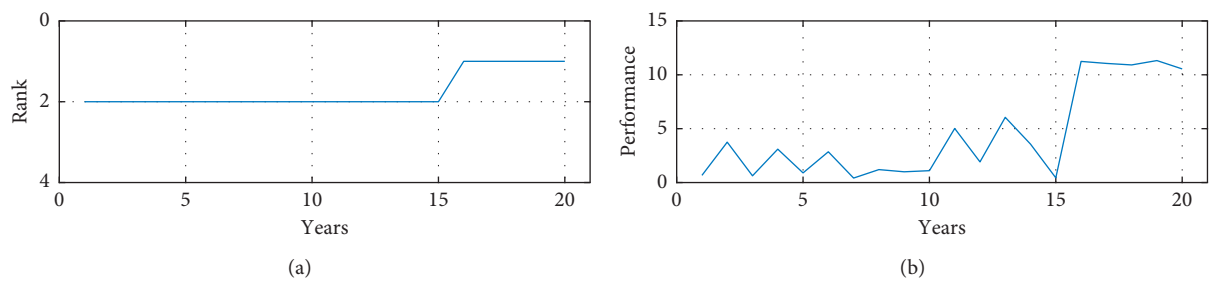

Figure 6: Rank history (a) and performance (b) of agent 119. During the simulation the employee 119 improves his/her rank.

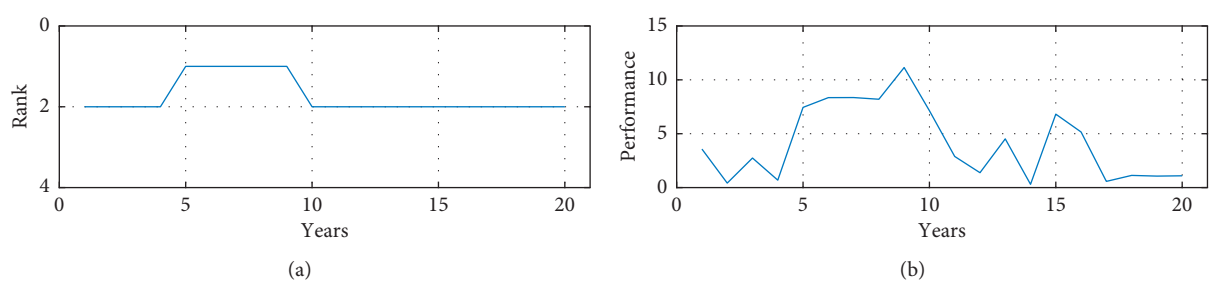

Figure 7: Rank history (a) and performance (b) of agent 108. During the simulation the employee 108 changes his/her rank.

performance of employees has been studied by mean of an empirical and computational approach. According to the classical literature, the proposed model incorporates two variables: the motivation and the ability. In particular, the employees' performance has been evaluated multiplying the motivation and the ability components, and the incentives have been distributed according to D.L.150/09 (the monetary incentives are divided among the employees with a logic that consider the employees' performance). The design of both employees' performance evaluation and monetary incentives distribution have been presented and discussed according to the theoretical and computational aspects.

The results have shown a modification of the employee's behavior according to both the theoretical foundations and the results discussed in [89, 90]. Both the empirical and computational results show that the monetary incentives work as stimulus for employees to reach the maximum incentive and the mechanism is suitable during the years. It

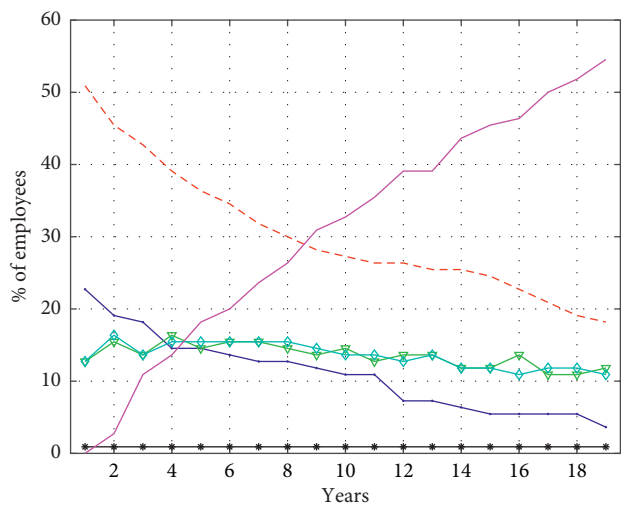

Figure 8: Percentage of employees with different behaviors during the simulation. The blue circle line represents the percentage of employees who are in set A, the red dashed line represents the ones in set B, and the black stair line represents the ones in set C who did not change set during the twenty years. The green triangle line represents the percentage of employees who during the twenty years worsened or not improved their rank position, whereas the cyan diamond line represents the ones who improved or not worsened. The magenta continuous line represents the percentage of employees who during the simulation time improved or worsened their position.

Table 3: Rank story of the employees. Number of employees who changed or did not change their rank during the twenty years simulation.

Employees' set	$T=1$	$T=2$	$T=3$	$T=4$	$T=5$	$T=10$	$T=15$	$T=19$
A	33	31	30	30	29	26	23	21
B	68	66	65	65	64	58	56	54
C	5	5	5	5	5	2	2	2
Worsening rank	2	4	5	5	6	12	14	16
Improving rank	2	4	5	5	6	12	13	15
Worsening/improving	0	0	0	0	0	0	2	2

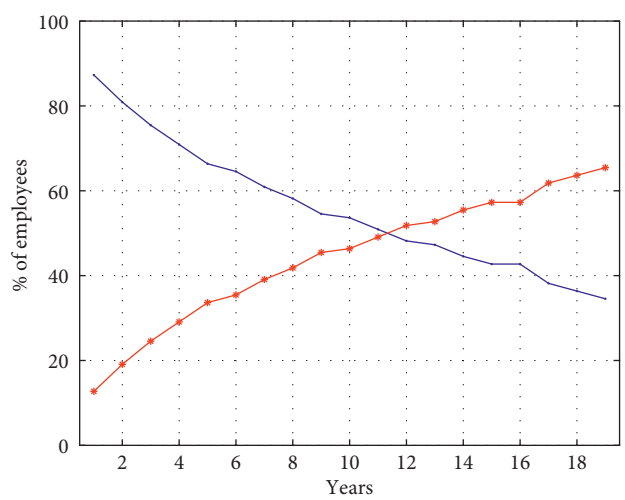

Figure 9: Percentage of employees for which the incentives' mechanism works in red star line and does not work in blue circle line.

is worth noting that, with the use of a rank order tournament mechanism, that is an ordinal system, to evaluate the performance of single employees, the result of the evaluation is known only at the end. This meritocratic system increases employee reactivity to managers' incitation, as suggested by the theory of social exchange [88]. Moreover, as discussed in [91, 92], the model implemented fits the fundamentals of a virtuous use of monetary incentives, such as the legitimacy of the appraisal, the objectivity of the criteria, and the possibility to achieve the initial goals at each repetition of the

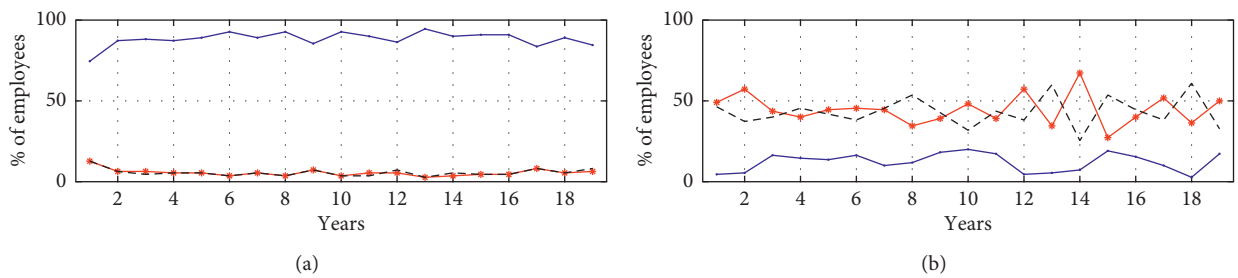

Figure 10: (a) % of employees which does not change rank from $t-1$ to t in blue circle line, % of employees which improves rank position from $t-1$ to t in black dashed, and % of employees which worsens rank position from $t-1$ to t in red star line. (b) % of employees which does not change their performance from $t-1$ to t in blue circle line, % of employees which improves their performance from $t-1$ to t in black dashed, and % of employees which worsens their performance from $t-1$ to t in red star line.

Table 4: Rank story of the employees in the real case. Number of employees which changes or does not change their rank during the periods 2010/2011 and 2010/2012.

Employees' set	2010/2011	2010/2012
A	26	23
B	60	53
C	3	3
Worsening rank	11	14
Improving rank	12	12
Worsening/improving	0	7

Table 5: Rank story of the employees (real data). Number of employees which changes or does not change their rank during years 2010/2011 and 2011/2012.

Employees' rank	2010/2011	2011/2012
Fixed rank	89	95
Worsening rank	11	10
Improving rank	12	7

Table 6: Performance story of the employees (real data). Number of employees which changes or does not change their performance during years 2010/2011 and 2011/2012.

Employees' performance	2010/2011	2011/2012
Fixed performance	31	42
Improving performance	44	46
Worsening performance	37	24

tournament. Furthermore, a study about various public companies in Britain has confirmed that employees' motivation is reduced if performance-based pay does not operate fairly [93]. Finally, results have shown that the monetary incentives distributed with a merit logic impact positively the firm performance in the short, middle, and long term. The main limitation of the study is that only one local PA has been considered to calibrate the model. In the near future, other PA will be considered to enrich the analysis and the simulation model. The developed agent-based model and simulator, where agents represent the employees, are one of the first attempts to provide a suitable tool to make managerial analysis. In particular, policy makers can use the developed tool to experiment different monetary incentives mechanisms in order to find the most convenient policy that allows to enhance the employee performance. In the end, it is worth remembering that the developed simulator is a useful tool not only for Public Administrations but also for private companies.

Data Availability

Personnel questionnaire data are subject to NDA and cannot be provided. Simulation data can be provided upon request.

Conflicts of Interest

The authors declare that there are no conflicts of interest regarding the publication of this paper.

Acknowledgments

The authors gratefully acknowledge Camera di Commercio di Genova for useful discussions.

References

[1] C. Pollitt and G. Bouckaert, *Public Management Reform: A Comparative Analysis*, Oxford University Press, Oxford, UK, 2004.

[2] M. Barzelay, *Breaking through Bureaucracy: A New Vision for Managing in Government*, University of California Press, Berkeley, CA, USA, 1992.

[3] N. Flynn, *Public Sector Management*, Sage, Thousand Oaks, CA, USA, 2007.

[4] W. J. Kickert, E.-H. Klijn, and J. F. M. Koppenjan, *Managing Complex Networks: Strategies for the Public Sector*, Sage, Thousand Oaks, CA, USA, 1997.

[5] C. Hood, "A public management for all seasons?" *Public Administration*, vol. 69, no. 1, pp. 3–19, 1991.

[6] C. Hood, "The "new public management" in the 1980s: variations on a theme," *Accounting, Organizations and Society*, vol. 20, no. 2-3, pp. 93–109, 1995.

[7] G. Gruening, "Origin and theoretical basis of new public management," *International Public Management Journal*, vol. 4, no. 1, pp. 1–25, 2001.

[8] J. Valasek, "Dynamic reform of public institutions: a model of motivated agents and collective reputation," *Journal of Public*, vol. 168, pp. 94–108, 2018.

[9] A. B. Whitford, "Incentives and tournaments in public organizations," 2006, https://ssrn.com/abstract=873488.
[10] T. Eriksson and M. C. Villeval, "Performance-pay, sorting and social motivation," *Journal of Economic Behavior & Organization*, vol. 68, no. 2, pp. 412–421, 2008.
[11] L. Ponta, A. Carbone, and M. Gilli, "Resistive transition in disordered superconductors with varying intergrain coupling," *Superconductor Science & Technology*, vol. 24, no. 1, Article ID 015006, 2011.
[12] A. Teglio, A. Mazzocchetti, L. Ponta, M. Raberto, and S. Cincotti, "Budgetary rigour with stimulus in lean times: policy advices from an agent-based model," *Journal of Economic Behavior & Organization*, vol. 157, pp. 59–83, 2019.
[13] M. Raberto, B. Ozel, L. Ponta, A. Teglio, and S. Cincotti, "From financial instability to green finance: the role of banking and credit market regulation in the Eurace model," *Journal of Evolutionary Economics*, vol. 29, no. 1, pp. 429–465, 2019.
[14] J. P. Davis, K. M. Eisenhardt, and C. B. Bingham, "Developing theory through simulation methods," *Academy of Management Review*, vol. 32, no. 2, pp. 480–499, 2007.
[15] D. C. Smith, "Making management count: a case for theory- and evidence-based public management," *Journal of Policy Analysis And Management*, vol. 28, no. 3, pp. 497–505, 2009.
[16] L. Iandoli, E. Marchione, C. Ponsiglione, and G. Zollo, "Learning and structural properties in small firms' networks: a computational agent-based model," *Research in Economics and Business: Central and Eastern Europe*, vol. 1, 2013.
[17] L. Fraccascia, I. Giannoccaro, and V. Albino, "Efficacy of landfill tax and subsidy policies for the emergence of industrial symbiosis networks: an agent-based simulation study," *Sustainability*, vol. 9, no. 4, p. 521, 2017.
[18] T. Wu, S. Huang, J. Blackhurst, X. Zhang, and S. Wang, "Supply chain risk management: an agent-based simulation to study the impact of retail stockouts," *IEEE Transactions on Engineering Management*, vol. 60, no. 4, pp. 676–686, 2013.
[19] M. A. Zaffar, R. L. Kumar, and K. Zhao, "Impact of inter-organizational relationships on technology diffusion: an agent-based simulation modeling approach," *IEEE Transactions on Engineering Management*, vol. 61, no. 1, pp. 68–79, 2014.
[20] A. F. de Toni and F. Nonino, "The key roles in the informal organization: a network analysis perspective," *The Learning Organization*, vol. 17, no. 1, pp. 86–103, 2010.
[21] S. Pastore, L. Ponta, and S. Cincotti, "Heterogeneous information-based artificial stock market," *New Journal of Physics*, vol. 12, no. 5, Article ID 053035, 2010.
[22] L. Ponta, S. Pastore, and S. Cincotti, "Information-based multi-assets artificial stock market with heterogeneous agents," *Nonlinear Analysis: Real World Applications*, vol. 12, no. 2, pp. 1235–1242, 2011.
[23] L. Ponta, M. Raberto, and S. Cincotti, "A multi-assets artificial stock market with zero-intelligence traders," *EPL (Europhysics Letters)*, vol. 93, no. 2, p. 28002, 2011.
[24] L. Ponta, E. Scalas, M. Raberto, and S. Cincotti, "Statistical analysis and agent-based microstructure modeling of high-frequency financial trading," *IEEE Journal of Selected Topics in Signal Processing*, vol. 6, no. 4, pp. 381–387, 2012.
[25] L. Ponta and S. Cincotti, "Traders' networks of interactions and structural properties of financial markets: an agent-based approach," *Complexity*, vol. 2018, Article ID 9072948, 9 pages, 2018.
[26] L. Ponta, S. Pastore, and S. Cincotti, "Static and dynamic factors in an information-based multi-asset artificial stock market," *Physica A: Statistical Mechanics and Its Applications*, vol. 492, pp. 814–823, 2018.
[27] B. Vermeulen and M. Paier, *Innovation Networks for Regional Development: Concepts, Case Studies, and Agent-Based Models*, Springer, Berlin, Germany, 2016.
[28] R. Axelrod, *The Complexity of Cooperation: Agent-asedModels of Competition and Collaboration*, vol. 3, Princeton University Press, Princeton, NJ, USA, 1997.
[29] R. Axelrod, "Chapter 33 agent-based modeling as a bridge between disciplines," *Handbook of Computational Economics*, vol. 2, pp. 1565–1584, 2006.
[30] J. M. Epstein, *Generative Social Science: Studies in Agent-Based Computational Modeling*, Princeton University Press, Princeton, NJ, USA, 2006.
[31] N. Gilbert and P. Terna, "How to build and use agent-based models in social science," *Mind & Society*, vol. 1, no. 1, pp. 57–72, 2000.
[32] A. Pyka and T. Grebel, *Agent-Based Computational Modelling*, Springer, Berlin, Germany, 2006.
[33] M. Wooldridge, "Agent-based computing," *Interoperable Communication Networks*, vol. 1, pp. 71–98, 1998.
[34] D. Helbing, *Social Self-Organization: Agent-Based Simulations and Experiments to Study Emergent Social Behavior*, Springer, Berlin, Germany, 2012.
[35] B. J. L. Berry, L. D. Kiel, and E. Elliott, "Adaptive agents, intelligence, and emergent human organization: capturing complexity through agent-based modeling," *Proceedings of the National Academy of Sciences*, vol. 99, no. 3, pp. 7187-7188, 2002.
[36] J. Grundspenkis, "Agent based approach for organization and personal knowledge modelling: knowledge management perspective," *Journal of Intelligent Manufacturing*, vol. 18, no. 4, pp. 451–457, 2007.
[37] G. Fioretti, "Agent-based simulation models in organization science," *Organizational Research Methods*, vol. 16, no. 2, pp. 227–242, 2013.
[38] R. D. Behn, "The big questions of public management," *Public Administration Review*, vol. 55, no. 4, pp. 313–324, 1995.
[39] P. M. Wright, T. M. Gardner, and L. M. Moynihan, "The impact of HR practices on the performance of business units," *Human Resource Management Journal*, vol. 13, no. 3, pp. 21–36, 2003.
[40] M. A. Youndt, S. A. Snell, J. W. Dean, and D. P. Lepak, "Human resource management, manufacturing strategy, and firm performance," *Academy of Management Journal*, vol. 39, no. 4, pp. 836–866, 1996.
[41] T. Boland and A. Fowler, "A systems perspective of performance management in public sector organisations," *International Journal of Public Sector Management*, vol. 13, no. 5, pp. 417–446, 2000.
[42] S. Brignall and S. Modell, "An institutional perspective on performance measurement and management in the "new public sector"" *Management Accounting Research*, vol. 11, no. 3, pp. 281–306, 2000.
[43] C. A. Mace, "Incentives. Some experimental studies," Industrial Health Research Board Report, Medical Research Council, London, UK, 1935.
[44] M. S. Viteles, *Motivation and Morale in Industry*, NYC Norton, Jersey City, NJ, USA, 1953.
[45] N. R. F. Maier, *Psychology in Industry: A Psychological Approach to Industrial Problems*, Houghton Mifflin, Boston, MA, USA, 1955.

[46] E. Appelbaum, *Manufacturing Advantage: Why High-Performance Work Systems Pay Off*, Cornell University Press, Ithaca, NY, USA, 2000.
[47] J. Paauwe, "HRM and performance: achievements, methodological issues and prospects," *Journal of Management Studies*, vol. 46, no. 1, pp. 129–142, 2009.
[48] P. Boxall and J. Purcell, "Strategy and Human Research Management. Management, Work and Organisations Series," *Palgrave Macmillan*, Basingstoke, UK, 2008.
[49] J. E. Delery and J. D. Shaw, "The strategic management of people in work organizations: review, synthesis, and extension," in *Research in Personnel and Human Resources Management*, vol. 20, pp. 165–197, Emerald Group Publishing, Bingley, UK, 2001.
[50] H. C. Katz, T. A. Kochan, and M. R. Weber, "Assessing the effects of industrial relations systems and efforts to improve the quality of working life on organizational effectiveness," *Academy of Management Journal*, vol. 28, no. 3, pp. 509–526, 1985.
[51] D. P. Lepak, H. Liao, Y. Chung, and E. E. Harden, "A conceptual review of human resource management systems in strategic human resource management research," in *Research in Personnel and Human Resources Management*, vol. 25, pp. 217–271, Emerald Group Publishing, Bingley, UK, 2006.
[52] A. H. Brayfield and W. H. Crockett, "Employee attitudes and employee performance," *Psychological Bulletin*, vol. 52, no. 5, pp. 396–424, 1955.
[53] M. Bannò and F. Sgobbi, "Firm participation in financial incentive programmes: the case of subsidies for outward internationalisation," *Journal of Policy Modeling*, vol. 32, no. 6, pp. 792–803, 2010.
[54] L. B. Andersen, "Professional norms, public service motivation and economic incentives: what motivates public employees?" in *Proceedings of the EGPA Conference 2007*, Department of Political Science, University of Aarhus, Madrid, Spain, September 2007.
[55] C. Dahlström and V. Lapuente, *Organizing Leviathan: Politicians, Bureaucrats, and the Making of Good Government*, Cambridge University Press, Cambridge, UK, 2017.
[56] E. Chang, "Motivational effects of pay for performance: a multilevel analysis of a Korean case," *The International Journal of Human Resource Management*, vol. 22, no. 18, pp. 3929–3948, 2011.
[57] T. Lah and J. L. Perry, "The diffusion of the Civil Service Reform Act of 1978 in OECD countries: a tale of two paths to reform," *Review of Public Personnel Administration*, vol. 28, no. 3, pp. 282–299, 2008.
[58] J. E. Salzman, "Labor rights, globalization and institutions: the role and influence of the Organization for Economic Cooperation and Development," *SSRN Electronic Journal*, vol. 21, pp. 769–975, 2000.
[59] R. F. Durant, R. Kramer, J. L. Perry, D. Mesch, and L. Paarlberg, "Motivating employees in a new governance era: the performance paradigm revisited," *Public Administration Review*, vol. 66, pp. 505–514, 2006.
[60] J. L. Pearce and J. L. Perry, "Federal merit pay: a longitudinal analysis," *Public Administration Review*, vol. 43, no. 4, pp. 315–325, 1983.
[61] B. F. Skinner, "Contingencies of reinforcement," *Encyclopedia of Pain*, Springer, Berlin, Germany, 1969.
[62] F. Luthans, "The contingency theory of management," *Business Horizons*, vol. 16, no. 3, pp. 67–72, 1973.
[63] A. D. Stajkovic and F. Luthans, "A meta-analysis of the effects of organizational behavior modification on task performance, 1975–1995," *Academy of Management Journal*, vol. 40, no. 5, pp. 1122–1149, 1997.
[64] W. Van Eerde and H. Thierry, "Vroom's expectancy models and work-related criteria: a meta-analysis," *Journal of Applied Psychology*, vol. 81, no. 5, pp. 575–586, 1996.
[65] J. S. Adams, *Advances in Experimental Social Psychology*, Vol. 2, Elsevier, Amsterdam, The Netherlands, 1965.
[66] J. Greenberg, "Organizational justice: yesterday, today, and tomorrow," *Journal of Management*, vol. 16, no. 2, pp. 399–432, 1990.
[67] J. L. Perry, T. A. Engbers, and S. Y. Jun, "Back to the future? Performance-related pay, empirical research, and the perils of persistence," *Public Administration Review*, vol. 69, no. 1, pp. 39–51, 2009.
[68] S. M. Davidson, L. M. Manheim, S. M. Werner, M. M. Hohlen, B. K. Yudkowsky, and G. V. Fleming, "Prepayment with office-based physicians in publicly funded programs: results from the Children's Medicaid Program," *Pediatrics*, vol. 89, no. 89, pp. 761–767, 1992.
[69] B. Dowling and R. Richardson, "Evaluating performance-related pay for managers in the national health service," *The International Journal of Human Resource Management*, vol. 8, no. 3, pp. 348–366, 1997.
[70] J. D. Shaw, M. K. Duffy, A. Mitra, D. E. Lockhart, and M. Bowler, "Reactions to merit pay increases: a longitudinal test of a signal sensitivity perspective," *Journal of Applied Psychology*, vol. 88, no. 3, pp. 538–544, 2003.
[71] J. Cilliers, I. Kasirye, C. Leaver, P. Serneels, and A. Zeitlin, "Pay for locally monitored performance? A welfare analysis for teacher attendance in Ugandan primary schools," *Journal of Public Economics*, vol. 167, pp. 69–90, 2018.
[72] N. Belle and P. Cantarelli, "Monetary incentives, motivation, and job effort in the public sector," *Review of Public Personnel Administration*, vol. 35, no. 2, pp. 99–123, 2015.
[73] G. J. Miller and A. B. Whitford, "The principal's moral hazard: constraints on the use of incentives in hierarchy," *Journal of Public Administration Research and Theory*, vol. 17, pp. 213–233, 2006.
[74] J. A. Marin-Garcia and J. M. Tomas, "Deconstructing AMO framework: a systematic review," *Intangible Capital*, vol. 12, no. 4, pp. 1040–1087, 2016.
[75] L. C. Freeman, "A set of measures of centrality based on betweenness," *Sociometry*, vol. 40, no. 1, pp. 35–41, 1977.
[76] P. Bonacich, "Power and centrality: a family of measures," *American Journal of Sociology*, vol. 92, no. 5, pp. 1170–1182, 1987.
[77] J. W. Atkinson, "Motivational determinants of risk-taking behavior," *Psychological Review*, vol. 64, no. 6, pp. 359–372, 1957.
[78] Y.-Y. Chen and W. Fang, "The moderating effect of impression management on the organizational politics-performance relationship," *Journal of Business Ethics*, vol. 79, no. 3, pp. 263–277, 2008.
[79] E. Lawler, L. Porter, and V. Vroom, *Motivation and management Vroom's expectancy theory. Value based management website*, https://www.valuebasedmanagement.net/methods_vroom_expectancy_theory.html, 2009.
[80] G. Albaum, "The Likert scale revisited," *Journal-Market Research Society*, vol. 39, pp. 331–348, 1997.
[81] D. J. Brass and M. E. Burkhardt, "Centrality and power in organizations," *Networks and Organizations: Structure, Form, and Action*, vol. 191, pp. 198–213, 1992.
[82] T. T. Baldwin, M. D. Bedell, and J. L. Johnson, "The social fabric of a team-based M. B. A. Program: network effects on

student satisfaction and performance," *Academy of Management Journal*, vol. 40, no. 6, pp. 1369–1397, 1997.

[83] K. S. Cook, R. M. Emerson, M. R. Gillmore, and T. Yamagishi, "The distribution of power in exchange networks: theory and experimental results," *American Journal of Sociology*, vol. 89, no. 2, pp. 275–305, 1983.

[84] R. Aalbers and W. Dolfsma, *Innovation Networks: Managing the Networked Organization*, Routledge, Abingdon, UK, 2015.

[85] L. Lü, T. Zhou, Q.-M. Zhang, and H. E. Stanley, "The H-index of a network node and its relation to degree and coreness," *Nature Communications*, vol. 7, no. 1, p. 10168, 2016.

[86] M. Kitsak, L. K. Gallos, S. Havlin et al., "Identification of influential spreaders in complex networks," *Nature Physics*, vol. 6, no. 11, pp. 888–893, 2010.

[87] J. Boissevain and J. C. Mitchell, *Network Analysis: Studies in Human Interaction*, Walter de Gruyter GmbH & Co KG, Berlin, Germany, 2018.

[88] G. C. Homans, *Social Behavior: Its Elementary Forms*, Revised, Ed., Harcourt, Brace and World, Inc., New York, NY, USA, 1974.

[89] G. C. Cainarca, F. Delfino, and L. Ponta, "The effect of monetary incentives on individual and organizational performance in an Italian public institution," *Administrative Sciences*, vol. 9, no. 3, p. 72, 2019.

[90] L. Ponta, F. Delfino, and G. C. Cainarca, "The role of monetary incentives: bonus and/or stimulus," *Administrative Sciences*, vol. 10, no. 1, p. 8, 2020.

[91] C. R. Knoeber and W. N. Thurman, "Testing the theory of tournaments: an empirical analysis of broiler production," *Journal of Labor Economics*, vol. 12, no. 2, pp. 155–179, 1994.

[92] S. Rosen, "Prizes and incentives in elimination tournaments," *American Economic Review*, vol. 76, no. 4, pp. 701–715, 1986.

[93] D. Marsden and S. French, "Performance pay in the United Kingdom," in *Paying for Performance: An International Comparison*, pp. 115–147, M.E. Sharpe, Armonk, NY, USA, 2002.

Hindawi
Complexity
Volume 2020, Article ID 4505064, 8 pages
https://doi.org/10.1155/2020/4505064

Research Article

On-Site Participation for Proto-Architectural Assemblies Encompassing Technology and Human Improvisation: "Fish Trap" and "Orchid" Architectural Interventions

Peter Buš,[1] Shi-Yen Wu,[2] and Ayça Tartar[3]

[1]*Digital Architecture Research Centre (DARC), Kent School of Architecture and Planning, University of Kent, Canterbury CT2 7NZ, UK*
[2]*Department of Architecture, National United University, 360 Miaoli City, Taiwan*
[3]*Department of Architecture (DARCH, Institute of Technology in Architecture), Swiss Federal Institute of Technology ETH, Zurich 8093, Switzerland*

Correspondence should be addressed to Shi-Yen Wu; sywu@mail.ntust.edu.tw

Received 2 September 2019; Revised 3 December 2019; Accepted 23 December 2019; Published 30 April 2020

Academic Editor: Dehua Shen

This research investigates the notion of builders' on-site engagement to physically build architectural interventions based on their demands, spatial requirements, and collaborative improvisation enhanced with the principles of uniqueness and bespoke solutions which are previously explored in computational models. The paper compares and discusses two physical installations as proto-architectural assemblies testing two different designs and building approaches: the top-down predefined designers' scenario contrary to bottom-up unpredictable improvisation. It encompasses a building strategy based on the discrete precut components assembled by builders themselves in situ. The paper evaluates both strategies in a qualitative observation and comparison defining advantages and limitations of the top-down design strategy in comparison with the decentralised bottom-up building system built by the builders themselves. As such, it outlines the position of a designer within the bottom-up building processes on-site. The paper argues that improvisation and builders' direct engagement on-site lead to solutions that better reflect human needs and low-tech building principles incorporated can deliver unpredictable but convenient spatial scenarios.

1. Introduction

The team of 16 self-builders, students of architecture from the Department of Architecture at the National United University in Taiwan, built two small-scale pavilions following the principles of decentralised discrete assemblies[1] to test the aspects of improvisation and collaborative negotiations in a crowd-driven assembly [2]. This activity was conducted at the Fabrication Festival, 2018, in London, established by the University of Westminster.

This research study aims to reveal limitations and to outline a position of a designer in collaborative building processes as well as a position of self-builders to investigate potentials to support productivity and efficiency in building and construction sectors. The built installations serve as a testbed for top-down design and building process in comparison with the improvisation and collaborative design strategies leading to two proto-architectural objects, possibly applicable as embedded urban interventions as artistic installations in a public space. The working hypothesis was outlined as follows: the building process based on bottom-up negotiations and improvisation of builders will lead to more flexible and open-ended design solutions adaptable to various conditions and with unique visual qualities and unpredictable design outcomes.

1.1. Rationale of On-Site Building Strategies by End-Users. There is an increasing trend in the construction strategies and building methods in which end-users build their built

scenarios by themselves. This applies especially in the cities with informal settlements, such as Rio de Janeiro, Medellín, or many other cities across the continents. The presence of informal settlements in cities is prevalent in many countries, especially those coping with increased population and urban growth, migration, and poverty where end-users, citizens, and urban communities have an urgent need to build a home or a shelter in a short period of time [3]. Architects, urban planners, stakeholders, and other parties involved in the design and planning processes within cities need to be able to react on such situations appropriately, providing guidelines, principles, and methods how to improve urban and spatial conditions for citizens—however, this is a complex task, not addressed in this article from all perspectives. One of the building methods where citizens and self-builders are involved within the building processes is application of kit-of-parts systems as discrete components, which are precut or prefabricated in the factory, delivered on-site, and assembled by self-builders themselves [4].

1.2. Expected Relation to the Real-World Practice. Participatory construction and building methods from predefined elements and built by self-builders address urban environment-related issues mentioned above in a more efficient and consistent manner and generally facilitate decision-making processes in building activities. Further, these methods tend to increase production efficiency in the construction sector and beyond. Urban communities' values, knowledge of local conditions and current urgent demands and spatial needs embed additional characteristics into the environment, preserving a unique local urban identity and memory-related characteristics in urbanised areas. As such, the strategy of kit-of-parts architecture build by self-builders can bring a new model of circular economy and business strategies to facilitate urban and economic growth within the specific local urban conditions, especially in high-densely populated areas [5]. Therefore, a need to investigate such models is necessary also in the context of contemporary architectural and urban design educational processes to prepare future experts for such challenges.

2. Methodological Approaches of the Conducted Study

This research study aims to explore and investigate the notion of building strategies based on contribution of self-builders, testing two methodological approaches—the predefined scenario from precut kit-of-parts system to assemble predesigned pavilion in contrast with more improvised, nonplanned, stochastic, bottom-up, and open-ended approach to assemble a structure from predefined discrete components. The first method applied in the investigation is a standard kit-of-parts assembly where the builders follow predefined manual and building scenario according to architect's instructions and outlined scenario. Usually such a strategy is based on a graphic manual or project drawings, which are predefined and prepared in advance before any building process starts. In contrast to top-down approach, the bottom-up principle lies on an immediate negotiations and collaborative activation of builders, improvising on-site to deliver demanded scenario, following the present and current interactive process. Within this process, the architect or a designer may give general instructions, which builders may follow as well but without any deeper perspective or a final goal to be achieved.

For the educational purposes, the intention is to understand such a process from the perspective of a builder, how such a process can be perceived, and what the builders can learn from it as well as to reveal limitations of such an approach in order to avoid future difficulties during the process of designing the components and manipulating the assemblies.

3. State of the Art

3.1. On-Site Building Bottom-Up Strategies Conducted by Self-Builders. The research is built upon the idea of building strategies based on builders' improvisation. This was previously explored in proposals by Yona Friedman in Seraj et al. [2], incorporating simple manuals with instructions for builders leading to improvised three-dimensional structures. The concept articulated the importance of simplicity, irregularity, low-tech principles in an assembly process, and its participative nature [6]. Similarly, the open-source movement brings new ideas and building opportunities also to discipline of architecture based on open-sourced and shared data and drawings, such as Elemental studio provided drawings for incremental housing publicly [7]. The precut components or construction systems for self-builders, such as the Wikihouse [8] condensed in a hub, a database of open-source project Bricks [9]. As such, the entire neighbourhood or even a district can be built in such a way[2]. Architects Teddy Cruz and Fonna Forman investigate in a long-term manner a potential for precut building components delivered on-site to provide a kit for end-users' assemblies to cope with the social housing crisis, informal settlements, and migration issues related to wider political or environmental conditions around the Mexican border line with the US [4].

3.2. Pedagogical Approach. At present, educational tendencies in the discipline of architecture and urban design operate with the advent of digital technologies and their incorporation in the design processes, which enrich traditional techniques used in design, building, and testing operations for prototypes or assemblies. However, the importance of hands-on work and manual assemblies in connection with digital fabrication and participatory strategies in contemporary architectural higher educational institutions needs to be articulated stronger as most of the schools' educational processes are based on linear process of learning. The educational process is usually based on a proposal of the concept, development of design, model making, and production of drawings, and the process ends here as there is no 1 : 1 prototype being built, from which the students learn, apart from selected high-end institutions, e.g., the Architectural Association or the Bartlett School of

Architecture, both based in London. In particular, this article refers to Erdine and Kallegias' educational concept [10] to address innovative pedagogical tendencies in architectural education mostly relying on practical hands-on working methods, generative design, spontaneity, user feedback, participation, and human interaction "enabling more seamless transition from design to fabrication and from academia to profession" [10]. Collaborative aspects in the design studios have been explored and investigated by Cabrinha [11] as a platform to discover relationships "between representation, simulation, and physical material in a digitally mediated design education," revealing "underlying principle to form relationships of teaching architecture through digital tools, rather than simply teaching the tools themselves." As such, an active engagement of students in a production and representation based on a "discovery" approach through making, building, and processes-oriented model of design was applied in the following case studies as a main pedagogical driver to activate and motivate the students.

4. Case Studies: Component-Based Pavilions

Following the strategy of previously explained architecture from discrete components and assemblies, the two case studies were built based on the logic of additive material assemblies and aggregative components [12]. The idea of installations was based on aspects of participatory design and building strategies to address potentials for customisation of urban spaces by interacting with the components, as previously explored by Bondin and Glynn [13], using a component device as a building block. Two ideas for the pavilion are introduced in this paper, addressing the component-based building strategy and a participatory experiment for an assembly without any predefined scenario to be built, purely relying on self-builders themselves to test two different methods and possibly reflecting real-world conditions, where builders need to solve any occurring problems in situ.

4.1. Fish Trap Pavilion. Our approach in the first example is based on a strategy without any use of manuals or predefined instructions for builders. The first case study, a Fish Trap (Figure 1), focuses on real-time engagement of builders in a building process dealing with predefined building blocks, deployable through the participatory design activity on-site. Our intervention, an abstract representation of a "fish trap" as a decentralised system of modules assembled together in a nonhierarchical manner, enables the possibilities of spatial aggregations into more complex morphologies based on mutual negotiations between the builders. The general idea was based on a predefined object in the form of an irregular polyhedron, a building block, which allows the builder to combine, assemble, and aggregate objects into various spatial variations creating customised architectural and urban space according to spatial necessities and aesthetic preferences.

The components were attached to each other, creating a self-supporting structure, which can grow in time and space, following the logic of diffusing and aggregating components. The polyhedron component has a variety of possibilities of face or edge connections. This brings an endless amount of open-ended spatial and structural solutions, which can be speculatively considered as either artistic installations, interior design elements, or urban interventions in a given public space. The possibilities for occupancy will depend on the scale and the context.

The components were precut from two-sided cardboard material utilising a laser cutter. The cut and unfolded sheets with the components were delivered on-site and handed over to self-builders. There were three leading designers present on-site, and they moderated the builders to creatively react on given conditions, considering builders' skills and capacities to respond to specific tasks. The building process itself was based on an improvisation reflecting direct participants' design intentions, negotiated and interactively applied during the building process.

4.2. Orchid Pavilion. In the second intervention (Figure 2.), the overall space is displayed with constructions based on three-legged units, inspired by "Ding," a traditional ancient Chinese cooking utensil. Its purpose has evolved into a ceremonial device which symbolises the domination of the kingship and the endlessly offspring. Its form and image represent the permanence and inheritance of the Chinese culture. The rules of assembly in this case study were strictly predefined by the designer, leading to one possible and unique spatial solution. However, as the mode of an assembly is based on slotting and mounting techniques, and the material chosen allows customisation of the components, it was assumed that such assembling strategy could yield a variety of design solutions as well. As such, the strict top-down approach can be easily redefined and customised according to the spatial demands later on. The units are combined together, forming into pillars, and eventually, the pillars merged and formed a dome. The pavilion is intended to display a variety of heights, mesmerising visitors with a sense of traveling into an ancient street.

The form of the architecture was inspired by the three legs, which a ding stands on, and the final achievement was also complied with the rule of a triangle. The body parts of the pillars are resemblance of the supportive walls of a ding. Assembling in a trigonometric matter, the top of the pillars was extended to form a classic triangular dome, and the rest of the pillars extended in all directions was demonstrated intentionally as unfinished domes to echo the promising possibility of Chinese traditional architecture.

The design process led the builders to start from the bottom to the top through the 3D model, which served as an initial exploration in the computer. The model was simultaneously translated and explored through a variety of different design ideas with aspects of user-oriented scenarios. The ultimate goal was to create new construction forms and innovative solutions to replace existing architectural forms with simple thinking.

Figure 1: The Fish Trap installation consisting of predefined precut components. The intervention was built on-site based on improvisation and collaborative design strategies. The possible spatial scenarios had been simulated computationally using stochastic aggregation strategies. The designer designed the building block only, which allows builders to build an endless variety of outcomes.

In the current common form of construction, the general construction module usually uses the "Fragment Geometry" to construct the fragmented unit to a huge entirety, and finally groups the main type together to challenge a structural form [14], but a bolder approach in the thinking of The Orchid Pavilion design was taken. A large area and efficient structural unit modulus were expected to be completed. At the same time, a different functional form through cutting and fine-tuning was made in order to achieve an efficient structure. Considering the construction method, this approach still maintains the logical thinking of building of basic units of the column, bridge, and board as a structure to provide continuous expansion into real building forms in the future.

5. Evaluation and Observation

The following comparative criteria have been applied to evaluate the results: material efficiency conveyed on-site, aesthetic and spatial qualities, flexibility and adaptability of the assembly for different spatial scenarios, ability of the assembly to be scaled up or to grow, and immediate reaction of the builders on-site.

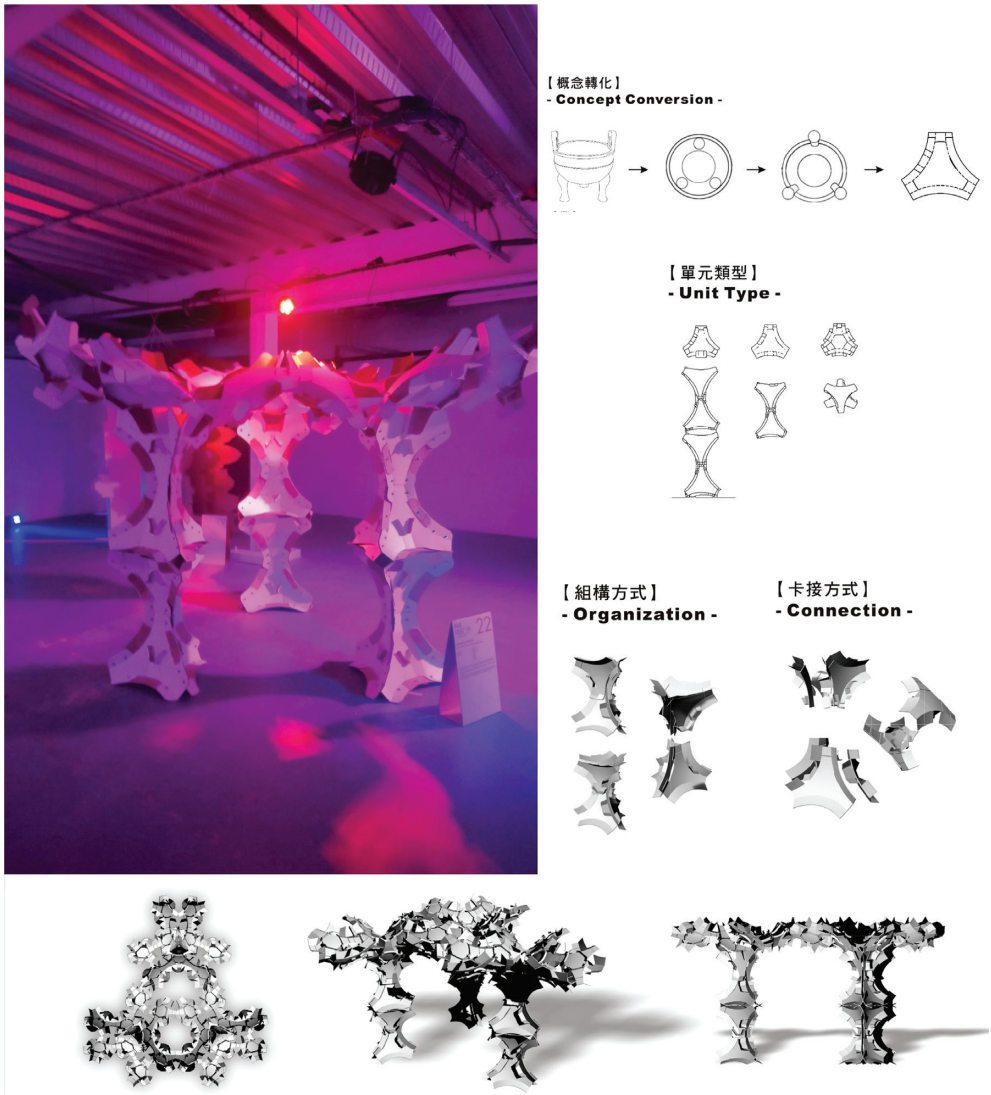

Figure 2: The orchid pavilion, a proto-architectural object assembled of discrete components and following more traditional form of Chinese architecture. The concept had been predefined by the designer with precise and specific means, computationally simulated, and visually analysed before the production and installation was made.

The results were evaluated by visual qualitative observations, following the above-mentioned criteria. The qualitative feedback from builders pointed how they were activated and collaboratively engaged in the process of an assembly. From the qualitative observations, the issues and limitations of the method and advantages or disadvantages during the building process were discovered and understood. It has been observed that the bottom-up assembly strategy was more difficult to conduct as there were no predefined rules, and the builders were improvising. The presence of the leading designer on-site was necessary in both cases.

A variety of spatial scenarios had been computationally simulated first, before the fabrication and assembly were made. As the Orchid pavilion has strict predefined rules of an assembly consisting of several types of components, this solution is more rigorous but not necessarily allowing more flexible spatial scenarios. On the contrary, the discrete component-based Fish Trap pavilion allows better flexibility in terms of different spatial solutions for an assembly. The stochastic computational model for an aggregation of components was tested in order to outline a variety of possible solutions for the assembly, although the final scenario did not follow any of those scenarios. This proves that using the decentralised approach of design and building strategy leads to unpredictable and endless variations of spatial solutions.

Aesthetic and spatial qualities are observable in both case scenarios, and more convincing and attractive pavilion was found which is the Orchid. However, the ability of the system to grow or be scaled up is present better in the Fish Trap pavilion as it encompasses open-ended solution for the assembly by means of discrete building blocks, only depending on the amount of the components. For the assembly, there were used 180 individually laser precut components.

5.1. General Observations. Based on a qualitative comparison, it was observed that the flexible and adaptive scenario based on the same discrete precut components is more convenient for improvisation and bottom-up assembly, but it brings another level of complexity into the building process which needs to be moderated by the designer. As such, although the improvisation on-site yields unexpected and unplanned results in unpredictable spatial scenarios, the presence of the designer on-site is still needed as he mentors and navigates the builders to deliver spatially convincing, meaningful, and architecturally and artistically appealing result. As such, the working hypothesis has been confirmed. However, this research did not reveal the potential and abilities of nonexperts possibly involved in the design and building process as the builders in this study were students of architecture. For that reason, the future research will test the engagement of nonexperts as builders in a real-world case scenario to outline the specific local demands for customisation and adaptation based on unique local requirements.

The installation of both pavilions was a test of the concept of on-site design participation, where the assemblies were delivered based on either top-down or bottom-up building strategies. Bottom-up negotiations of builders brought unpredictable form of a design solution. Predefined objects allowing open-ended configurations based on a simple rule-set proposed by the designer yield a variety of more complex aggregations with certain uniqueness in visual expression. Further, the results indicate that such a concept can grow and possibly be scaled up to wider spatial scenarios based on the uncontrolled decentralised approach by adding more components to the core agglomeration.

As it was expected in the assemblies' initial objectives and confirmed in the final forms of assemblies (especially in the case study of the Fish Trap), the outcomes seem more sculptural than architectural. However, there is a space for further speculation of possibilities of occupancy of such an intervention. As discussed above, such an assembly can be embedded within the urban context to activate and facilitate people's engagement to interact and physically manipulate with the objects.

5.2. Personal Conversations and Feedback

5.2.1. Feedback during Learning Process. Personal conversations with the builders were conducted during (i.e., July 2–6, 2018) and after the building processes (August 2018) between authors and student participants. The outcomes from these conversations which have been statistically involved in the production mainly aim to explore and discover potentials for the effective learning process. "The Orchid Pavilion 3.0" made the builders feel the stability, certainty of the design, and organization process during the learning activity. Especially, the time control and the level of completion led to decisions that are more confident during the building process in this case. This is also more evident in previous learning projects and study lists. Because of the features with timely adjustments and corrections, this is apparent that the learning projects fully demonstrate and reflect the practice, traditional learning, and consequently overall efficiency of the design studio learning activity.

The initial learning process of "The Fish Trap" made the builders feel at a loss because they could only confirm the shape of the unit and had no idea how the final group composition and type will be. This will lead to a conclusive statement that certain envision of the potential outcome which is going to be built is necessary to provide to builders at the beginning of the assembly process. Although the process was based on a random improvisation, however, the situation led the builders to the point when there was no choice for additional variations of an assembly, and they spent a lot of time digging the construction of the units and created some random type of an assembly, with no deeper consideration or an aim they should achieve.

5.2.2. Feedback Related to the Results. It was generally considered that "The Fish Trap" concept must spend more time on discussion and communication while following the notion of prosperity, meeting the common goal, and overall openness to further changes. The efficiency and the results are filled with uncertainty and unpredictability. People think this kind of operational mode seems to be more as an artistic creation rather than a design work following specific goals. However, the strategy was spontaneous, creative, and opens new possibilities to think about architecture from different perspectives, mostly relying on volumetric qualities and unique formal expression. This may serve as a public attractor in a given urban scenario. Contrary to the previous solution, "The Orchid Pavilion 3.0" obviously has quite significant design features, and the result is easy to be predicted because of its integrity and regularity. Although it maintains a stability and effective result above the standard, the operating process is not as easy as people think so. The whole process depends on the ability of design decision makers or the amount of builders. However, there is no doubt that the process is completely under control, and the results are significantly controllable.

5.3. Outcomes. As a result, two proto-architectural systems have been erected as installations, consisting of a set of simple predefined modules which can be assembled, reassembled, and assembled again in different configurations by the end-users on-site, leading to a diverse number of more complex spatial variants (Figure 3). These can be embedded within a public space as a demonstration of approaches taken during the process.

6. Overall Benefit and Contribution

There are two main contributing and beneficial aspects, discussed as follows.

6.1. Contribution to Pedagogy. The main benefit, which students can take from the study, is the experience-oriented learning through making. The students learnt how important is the negotiation, communication, interaction, team

Figure 3: Two proto-architectural interventions built on-site based on collaborative design strategies: top-down design process and bottom-up on-site interventions.

work and sharing the ideas, and knowledge acquired during and after the process. This may inform their further personal training in the discipline of architecture. Moreover, such a pedagogical strategy could be applied in educational processes more frequently in order to articulate hands-on working within the context of digital technologies, following the idea of spontaneity, participation, and predefined kits-of-parts component design and preparation. This strategy can be applied in all levels of learning in a vertical manner (lower level students can work with more experienced students and learn from them). The students participating in these two studies were undergraduate students. A model of learning through making will yield better-oriented experts in the discipline, capable to solve any particular problems more efficiently.

6.2. Potential Strategies for Real-World Participatory Construction Methods in the Future. This experiment confirmed that, for future participatory construction and building strategies, the self-builders need to be moderated by the designer or need to follow a predefined manual for an assembly unless there is no specific goal that needs to be achieved. The approach introduced in this paper, investigating a direct involvement and participation of users and utilising participatory kit-of-parts systems and components, will bring transparency and productivity-efficient building processes if applied in real-case scenarios. In addition, the participatory building method allows further postassembly and postactuation building processes to reconfigure and modify the given built solution. This approach is out of traditional scheme of client-contractor-supplier chains. Rather, it articulates values and knowledge of local urban communities, their skills, and with a prospective consideration of local resources and particular conditions only known to interacting participating parties. In that sense, the citizens themselves can improve the environmental conditions, liveability, production, and can contribute to the overall common improvement and efficiency of built environments.

Data Availability

The visual data used to support the findings of this study are included within the supplementary information files. The data used in this manuscript are based on qualitative observations, documented in photographs. The documentation is available in [15]. In addition, a supplementary video material is available in [16].

Conflicts of Interest

The authors declare that they have no conflicts of interest.

Acknowledgments

The research case studies have been conducted during the Fab Fest Festival, 2018, established by the University of Westminster in cooperation with Ambika P3 gallery in London. Additional expenses have been covered by authors' home research centres, namely, the Chair of Information Architecture DARCH ETH in Zurich and the Department of Architecture National United University in Taiwan. The article processing charge has been covered by the APC fund of the University of Kent, Canterbury.

References

[1] G. Retsin, "Discrete assembly and digital materials in architecture," in *Proceedings of the 34th eCAADe Conference*, vol. 1, pp. 143–151, University of Oulu, Oulu, Finland, August 2016.

[2] N. Seraj, Y. Friedman, and M. Orazi, *Yona Friedman the Dilution of Architecture*, Park Books, Zürich, Switzerland, 2015.

[3] R. Mehrotra, F. Vera, and J. Mayoral, *Ephemeral Urbanism: Cities in Constant Flux*, Harvard Graduate School of Design,

Centro de Ecologia Paisajey Urbanismo DesignLab Universidad Adolfo Ibáñez, Santiago, Chile, 2016.
[4] 2019, https://blog.ted.com/architect-teddy-cruz-shares-5-projects/.
[5] D. Hall, "Rethinking the business model for offsite constructions," in *Proceedings of the International Webinar from the Transforming Construction Network Plus N+*, London, UK, June 2019.
[6] G. Yan and E. Motisi, "Yona Friedman. Mobile Architecture. People's Architecture," in *Proceedings of the Public exhibition Maxxi Museum*, Rome, Italy, 2017.
[7] 2019, http://www.elementalchile.cl/en/.
[8] 2019, https://wikihouse.cc/.
[9] 2019, http://www.openbricks.io.
[10] E. Erdine and A. Kallegias, Edited by Thompson, Ed., "Reprogramming architecture—learning via practical methodologies," Edited by E. Mine, Ed., in *Proceedings of the Fusion-Proceedings of the 32nd eCAADe Conference*, vol. 1, pp. 373–380, Department of Architecture and Built Environment, Faculty of Engineering and Environment, Newcastle, UK, September 2014.
[11] M. Cabrinha, "Synthetic pedagogy in synthetic landscapes," in *Proceedings of the 25th Annual Conference of the Association for Computer-Aided Design in Architecture*, pp. 148-149, Louisville, KY, USA, 2006.
[12] D. Koehler, S. Abo Saleh, H. Li, C. Ye, Y. Zhou, and R. Navasaityte, Edited by A. Kepczynska-Walczak, Ed., "Mereologies—combinatorial design and the description of urban form," Edited by S. Bialkowski, Ed., in *Proceedings of the 36th eCAADe Conference-Computing for a Better Tomorrow*, vol. 2, pp. 85–94, Lodz University of Technology, Łódź, Poland, September 2018.
[13] W. Bondin and R. Glynn, "Fabricating behaviour: a problem, a solution, a prototype and a proposal," in *Proceedings of the Fabricate Conference*, pp. 280–287, ETH Zurich, Zurich, Switzerland, 2014.
[14] J. Sanchez and A. Andrasek, "Bloom the game. Design posters," in *Proceedings of the ACADIA 2013 Adaptive Architecture*, pp. 403-404, Riverside Architectural Press, Cambridge, Canada, October 2013.
[15] 2018, https://photos.app.goo.gl/13DhCFCvFvqwm3sX6.
[16] 2018, https://www.youtube.com/watch?v=aRgKCtFgJTE&;t=33s.

Hindawi
Complexity
Volume 2020, Article ID 6564731, 21 pages
https://doi.org/10.1155/2020/6564731

Research Article

An Anecdote of Investor Anxiety and Momentum in China

Hung-Wen Lin,[1] Kun-Ben Lin,[2] Jing-Bo Huang,[3] and Xia-Ping Cao[4]

[1]*Business School, Nanfang College of Sun Yat-Sen University, Guangzhou, China*
[2]*School of Business, Macau University of Science and Technology, Macau, China*
[3]*Lingnan College, Sun Yat-Sen University, Guangzhou, China*
[4]*College of Economics, Shenzhen University, Shenzhen, China*

Correspondence should be addressed to Xia-Ping Cao; jerrycao76@qq.com

Received 6 December 2019; Revised 28 February 2020; Accepted 7 March 2020; Published 25 April 2020

Academic Editor: Dehua Shen

We show the effect of investor anxiety on momentum in the Chinese stock market. In this market dominated by retail investors, we examine the momentum profits in 900 types of daily testing periods. We find prevalent price reversals in the long formation and holding periods in the Chinese A-share market. Compared to Goyal and Wahal (2015), Wang and Xie (2010), and Kang et al. (2002) who found no momentum, our novel finding from a daily basis is that the A-share market presents price momentum within the short formation and holding periods. We first test the momentum profits under different strengths of anxiety in the A-share market. The stocks held by the least anxious investors elicit the strongest price momentum, whereas the stocks held by the most anxious investors encounter much weaker price momentum in the A-share market. According to our empirical outcomes, the A-share market overall exhibits higher anxiety and weaker momentum, whereas the B-share market embodies milder anxiety and stronger momentum. From the results of single market and cross-market comparisons, the intrinsic anxiety of retail investors is an essential factor stimulating the Chinese stock market to be prone to price reversals.

"Anxiety arises from a transformation of the accumulated tension."

Sigmund Freud

1. Introduction

This paper investigates the relationship between investor anxiety and momentum in the Chinese stock market. Anxiety is an issue that has long been a concern in both psychology and finance. Compared to professional institutional investors, retail investors find it more difficult to grasp the essence of information due to information asymmetries, so that they are very easy to embody anxiety. Consequently, we focus attention on digesting the effect of investor anxiety on momentum.

To the best of our knowledge, there has not been momentum research throwing light on the effect of investor anxiety. A series of studies dissect the effect of negative investor sentiment or disposable panic (e.g., [1–15]). Although their endeavors on these topics have deepened our insights into the stock market, they do not directly detect the effect of anxiety. Hence, we dedicate to the effect of intrinsic and continuous anxiety from retail investors. In addition, the strength of anxiety will influence the behaviors of retail investors, thus activating considerable impacts on the stock market.

The appearance of severe anxiety is possible to provoke the investors to be tense and thus arouses overreactions when facing information asymmetries and uncertainties. On the contrary, when anxiety is weak, there may be underreactions or delayed reactions (e.g., [16–18]). Price momentum and price reversal are two essential characteristics of the stock price. According to Jegadeesh and Titman [19], price momentum depicts a pattern whereby past trends in stock prices will be maintained and will continue into the

future. This phenomenon originates from an underreaction or delayed reaction to firm-specific information. By contrast, price reversal implies that the past price trends of stocks will turn in opposite directions in the future, as the result of an overreaction to firm-specific information [20]. Hence, we would like to discuss how the changes in anxiety influence price momentum and reversal since these two characteristics of stocks come from underreaction and overreaction.

Psychologically, anxiety is a complex and mixed sentiment. When considered in more detail, anxiety is one type of negative sentiment regarding nervousness, tension, worry, and fear as faced by human beings (e.g., [21–25]). This type of sentiment will become a disorder once it persists for a period [26]. According to Peterson [27] and Passer and Smith [28], a panic disorder is one form of anxiety disorder that stems from terrifying attacks and that causes the agents to feel extremely tense. Therefore, we employ panic as a proxy for anxiety in this paper. To be precise, we use Lauterbach and Ben-Zion's [29] relative order imbalance (ROI) to represent the panic of investors, which is calculated on the basis of the standardized differences between the bid volume (BV) and ask volume (SV) (Spielberger [22] pointed out that anxiety is always accompanied by physiological arousal; bid volume and ask volume to some extent reflect investor trading behavior, whereby the relative order imbalance is a suitable proxy for anxiety given that it reflects the investor's panic).

China established its stock market in the 1990s and it grew rapidly, being comprised of the Shanghai stock exchange and Shenzhen stock exchange. However, the Chinese stock market is mainly characterized by violent price reversal rather than momentum (the stock markets in Europe and the US behave differently; in a one-month period, the stock markets exhibit a short-term price reversal; from two to twelve months, the stock markets are characterized by intermediate-term price momentum; moreover, in a three-to-five-year period, the markets tend to be trapped in a long-term price reversal (e.g., [30–33])). Under the dilemmas of high market volatilities and information asymmetries, the dominant retail investors may exhibit anxiety and thus overreactions, eliciting the emergence of reversal. In Figure 1, we present reversal ratios in various periods. We calculate percentage of the stocks having opposite price trends between formation and holding periods to obtain reversal ratios (in the construction of momentum portfolios, we must select winner and loser stocks in the formation period and then calculate the momentum profits in the holding period; the formation period is the period in which we select stocks based on the price growth rate and the holding period is the period in which we acquire momentum profit in the future; winner stocks are those with the highest price growth rate and loser stocks have the lowest price growth rate; each pair of formation and holding periods results in a momentum portfolio; please see Section 2.2 for more details). Among 900 reversal ratios for various periods, most of the ratios range from 40% to 75%, suggesting that at least 40% of stocks will reverse their past price trends in the future within a momentum portfolio. Even in the short formation and holding periods, there are still approximately

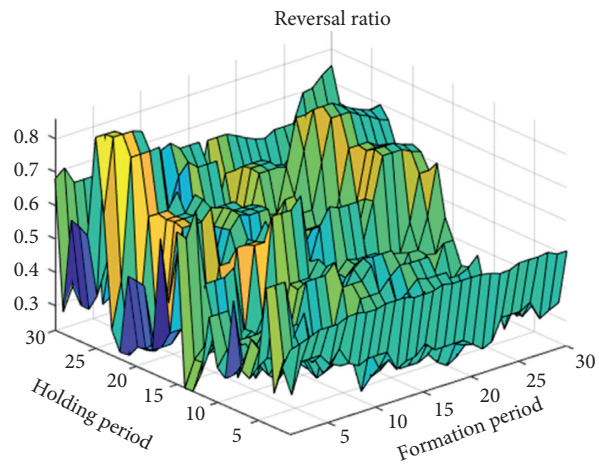

Figure 1: Daily reversal ratios in various periods. In the figure, the daily reversal ratios are plotted for various testing formation and holding periods. The maximum formation and holding periods are 30 days each, allowing 900 cases to come into being. We calculate the percentage of stocks that reverse their past price trends in the future. The reversal ratio is (#(REVS)/#(MOMS)), where #(REVS) denotes the number of stocks reversing their prices and #(MOMS) is the total number of stocks within a momentum portfolio.

half of stocks reversing their past price trends in the future. In the relatively long formation and holding periods, the reversal ratios all vary around 70%. These outcomes indicate that the Chinese stock market is a particularly special market in the world, thereby implying that it is very important for us to understand its in-depth structure.

The empirical analysis involves the following steps. First of all, following the conventional vein in terms of the momentum, the preliminary dissection relies on the conditional momentum portfolio. All stocks in the market are initially classified into several groups based on investor anxiety and subsequently sorted by the price growth rate within the groups according to the anxiety classifications. Second, the capital asset pricing model [34–36], Fama–French three-factor asset pricing model [37], and Chinese three-factor asset pricing model [38] come into their own to adjust the risks of momentum profits. Besides, we examine the momentum profits with different strengths of investor anxiety in the various testing periods.

What enables our study to stand out is that our momentum computations are based on a daily basis. If we make experiments on momentum profits in the Chinese stock market based on a monthly basis, it will be easy to find out significantly negative momentum profits, suggesting that price reversals prevail in the Chinese stock market (e.g., [30, 39–43]). However, in an actual stock market, transactions take place every day, and so tests conducted using monthly data may fail to capture the stocks' real price movements. Hence, we perform examinations every day and generate the corresponding daily momentum profits to address the possible price momentum.

From a multidimensional perspective, the influencing mechanism of anxiety has been documented by previous studies. Gao et al. [44] and Kaplanski and Levy [45] have

provided evidence that investor anxiety will negatively affect stock prices. Clearly, it is very likely that a great degree of anxiety will stimulate high fluctuations and dramatic declines in stock prices (e.g., [46–48]). In addition, Levy and Galili [49] hold that investors will engage in gambling activities in order to escape from the dilemma of anxiety. As for panic, due to it being one form of anxiety, it similarly exerts negative impacts on stock prices in the same manner (e.g., [50–52]). Based on the discussions above, anxiety is tightly related to stock price movements. Thus, it is reasonable for us to interpret how anxiety affects price momentum and reversal in China. The resulting findings will offer insights to both academia and industry.

We encode our story as follows. In the next section, the methodology and data descriptions in this paper are provided. Sections 3 and 4 report the empirical results of the A-share and B-share markets. The robustness checks are conducted in Section 5, and we conclude the paper in Section 6.

2. Methodology and Data

This section introduces the essence of investor anxiety, momentum profit, the conditional momentum portfolio, and asset pricing models used in this paper. We follow the approaches adopted by Jegadeesh and Titman [19] and Lauterbach and Ben-Zion [29] to measure momentum profit and investor anxiety, respectively. Consistent with past research on momentum, we derive the conditional momentum portfolio from a sequential classification. Furthermore, the capital asset pricing model, Chinese three-factor asset pricing model, and Fama–French three-factor asset pricing model are adopted to adjust risks.

2.1. Two Measures for Investor Anxiety. In psychology, anxiety consists of many negative sentiments, and thus it is difficult for us to construct a composite index for it. One possible way is to choose a proxy for a component of anxiety. Coon and Mitterer [53], Lahey et al. [24], and Peterson [54] all regard panic as one type of anxiety, and so panic is considered to be an appropriate representative of anxiety. According to Lauterbach and Ben-Zion [29], we measure the panic behavior based on a daily relative order imbalance. This variable implies instantaneous panic behavior on the part of investors.

$$\mathrm{ROI}_{i,d} = \frac{\mathrm{BV}_{i,d} - \mathrm{SV}_{i,d}}{\left(\left(\sum_{d=1}^{D}\left|BV_{i,d} - SV_{i,d}\right|\right)/D\right)}, \tag{1}$$

where $\mathrm{ROI}_{i,d}$ is the daily relative order imbalance of stock i on day d, BV is the bid volume, SV is the ask volume, and D is the number of days in a period. According to Lauterbach and Ben-Zion [29], a lower value of $\mathrm{ROI}_{i,d}$ indicates that a stock faces higher selling pressure, suggesting more severe anxiety.

We have already mentioned that anxiety will become a disorder if it persists for a period in Section 1. The quote from Freud also indicates the importance of accumulation in anxiety (e.g., [55–57]). According to their conceptions, we set up a proxy for the accumulation in anxiety. Our measure is as follows. The percentage of the negative relative order imbalance suggests the number of days with exceedingly severe anxiety, while the percentage of positive relative order imbalance represents the number of days with slight anxiety. Hence, the difference between them exactly indicates the accumulation in anxiety (a similar example can be seen in [58]).

$$\mathrm{ACCI}_{i,p} = \mathrm{neg}_{i,p}\% - \mathrm{pos}_{i,p}\%, \tag{2}$$

where $\mathrm{ACCI}_{i,p}$ is the accumulative relative order imbalance, $\mathrm{neg}_{i,p}\%$ denotes the percentage for the negative relative order imbalance in a period, and $\mathrm{pos}_{i,p}\%$ is the percentage for the positive relative order imbalance in the period. Note that a lower value of $\mathrm{ACCI}_{i,p}$ suggests a lower accumulation in terms of anxiety.

2.2. The General Algorithm of Momentum. Motivated by Jegadeesh and Titman [19], in what follows we describe a general model to calculate the momentum profit in various periods. In the field of momentum research, we must choose the formation and holding periods first, and so we let F denote the formation period and H the holding period. The formation period is the period in which we rank stocks based on the past price growth rate, and the holding period is the period for which we calculate the momentum profits in the future.

If we use different types of time length for the formation and holding periods, there will be different types of momentum portfolios according to the time length. Assuming that the length of the formation period ranges from 1 to M and that of the holding period from 1 to V, every pair of formation and holding periods results in a momentum portfolio. Hence, there will be total of $M \times V$ cases of momentum portfolios.

In the first period t_1, we use $P_{i,G} = (P_{i,f}^F - P_{i,1}^F / P_{i,1}^F)$ for each stock i to rank the stocks for the market as a whole, where $t_1 = F_1 + 1$, F_1 is the length of the formation period, $P_{i,G}$ is the price growth rate of each stock, $P_{i,f}^F$ is the price in the last period of the formation period, and $P_{i,1}^F$ is the price in the beginning period of the formation period.

The $(1/Q)$ stocks with the highest price growth rates constitute the winner portfolio and another $(1/Q)$ stocks with the lowest price growth rates form the loser portfolio. We create a long position for the winner portfolio and a short position for the loser portfolio, and so these positions constitute the first momentum portfolio. During the holding period H_1, we calculate the return spread between the winner and loser portfolios:

$$R_{t_1}^s = \overline{R_{H_1}^W} - \overline{R_{H_1}^L}, \tag{3}$$

where $\overline{R_{H_1}^W}$ is the average return of the winner portfolio during holding period H_1, $\overline{R_{H_1}^L}$ is the average return of the loser portfolio during holding period H_1, $H_1 = [\theta^{H_1,1}, \theta^{H_1,h}]$, $\theta^{H_1,h}$ is the last period of H_1, $\theta^{H_1,1}$ is the first period of H_1, and $\theta^{H_1,1}$ is equal to $t_1 + 1$. $H_1 = [\theta^{H_1,1}, \theta^{H_1,h}]$ means that H_1 extends from period $\theta^{H_1,1}$ to period $\theta^{H_1,h}$. Note that the

construction of the momentum portfolio is based on a rolling procedure.

Therefore, in the period $t_2\,(t_2 = (t_1 + 1))$, we proceed to use $P_{i,G}$ in F_2 to rank the stocks, where $F_2 = [\theta^{F_1,2}, (\theta^{F_1,f} + 1)]$, $\theta^{F_1,2}$ is the second period of F_1, and $\theta^{F_1,f}$ is the last period of F_1. In a similar vein to the above, $F_2 = [\theta^{F_1,2}, (\theta^{F_1,f} + 1)]$ suggests that F_2 ranges from period $\theta^{F_1,2}$ to period $\theta^{F_1,f} + 1$. During the holding period H_2, we calculate the return spread:

$$R^s_{t_2} = \overline{R^W_{H_2}} - \overline{R^L_{H_2}}, \tag{4}$$

where $\overline{R^W_{H_2}}$ is the average return of the winner portfolio during holding period H_2, $\overline{R^L_{H_2}}$ is the average return of the loser portfolio during holding period H_2, $H_2 = [\theta^{H_1,2}, (\theta^{H_1,h} + 1)]$, and $\theta^{H_1,2}$ is the second period of H_1.

After rolling n times, in period $t_n\,(t_n = (t_1 + (n-1)))$, we acquire the momentum portfolio by means of $P_{i,G}$ in F_n, where $F_n = [\theta^{F_{n-1},2}, (\theta^{F_{n-1},f} + 1)]$, $\theta^{F_{n-1},2}$ is the second period of F_{n-1}, and $\theta^{F_{n-1},f}$ is the last period of F_{n-1}. During H_n, the return spread is

$$R^s_{t_n} = \overline{R^W_{H_n}} - \overline{R^L_{H_n}}, \tag{5}$$

where $\overline{R^W_{H_n}}$ is the average return of the winner portfolio during holding period H_n, $\overline{R^L_{H_n}}$ is the average return of the loser portfolio during holding period H_n, $H_n = [\theta^{H_{n-1},2}, (\theta^{H_{n-1},h} + 1)]$, $\theta^{H_{n-1},2}$ is the second period of H_{n-1}, and $\theta^{H_{n-1},h}$ is the last period of H_{n-1}.

Finally, we have n return spreads, so the momentum profit (MP) is

$$\mathrm{MP} = \frac{1}{n}\sum_{q=1}^{n} R^s_{t_q}. \tag{6}$$

In addition, the signs of the momentum profit tell two stories. When the momentum profit is significantly positive, the market exhibits price momentum, suggesting that past price trends will continue in the future. By contrast, the market is characterized by price reversal if the momentum profit is significantly negative. In other words, past price trends will reverse in the future.

2.3. Conditional Momentum Portfolio. The effect of investor anxiety on the momentum profit is dissected by the conditional momentum portfolio in this paper (e.g., [59–61]). To be concrete, in the formation period, all the stocks for the market as a whole are first classified by investor anxiety into several groups. Subsequently, within each group generated from the anxiety classifications, the stocks are further classified by the formation price growth rate to construct winner and loser portfolios. Moreover, the momentum profits under various degrees of anxiety are obtained from the return spreads between the winner and loser portfolios with the same degrees of anxiety. To see the details of the conditional momentum portfolio, please refer to Appendix A.

2.4. Asset Pricing Models. We implement three asset pricing models to perform the risk adjustments for the momentum profit. The models include the capital asset pricing model (CAPM), Chinese three-factor asset pricing model [38], and Fama–French three-factor asset pricing model [37].

$$\begin{aligned}
\mathrm{WML}_{j,t} &= \alpha_j + \beta_j \mathrm{MKT}_t + \varepsilon_{j,t},\\
\mathrm{WML}_{j,t} &= \alpha_j + \beta_j \mathrm{MKT}_t + \sum_{z=1}^{2} \delta_{z,j} \mathrm{PF}^{\mathrm{CH}}_{z,t} + \varepsilon_{j,t},\\
\mathrm{WML}_{j,t} &= \alpha_j + \beta_j \mathrm{MKT}_t + \sum_{z=1}^{2} \lambda_{z,j} \mathrm{PF}^{\mathrm{FF}}_{z,t} + \varepsilon_{j,t},
\end{aligned} \tag{7}$$

where $\mathrm{WML}_{j,t}$ is the winner-minus-loser return spread under different degrees of investor anxiety, MKT_t is the market risk pricing factor of the CAPM, and $\mathrm{PF}^{\mathrm{CH}}_{z,t}$ represents the size and value pricing factors from Liu et al. [38]. In addition, $\mathrm{PF}^{\mathrm{FF}}_{z,t}$ denotes the size and value pricing factors obtained from Fama and French [37]. Following Celiker et al. [62], Chen and Zhao [63], and Garlappi and Yan [64], we utilize the regression intercepts of these models as risk-adjusted momentum profits. Appendix B shows the construction procedures of these pricing factors.

2.5. Data Descriptions. All the data in this paper are obtained from the China Stock Market and Accounting Research (CSMAR) database. The sample period ranges from the year 2007 to the year 2018 and encompasses both A-share and B-share stocks in China. To obtain the value pricing factor as in [38], we first compute the earnings-to-price ratio of each stock. Earnings is measured as net profit in excess of nonrecurrent gains and losses. As nonrecurrent gains and losses begin in the year 2007, we thus select this sample. Table 1 provides the descriptive statistics for the daily relative order imbalance and accumulative relative order imbalance of the A-share and B-share markets.

From Table 1, we can observe the mean values of daily relative order imbalance (ROI) and accumulative relative order imbalance (ACCI) for both A-share and B-share markets. The B-share market has a mean value in ROI of 0.2376, while the A-share market has a mean value in ROI of 0.1115, suggesting that A-share market has higher instantaneous anxiety than the B-share market. In addition, the A-share market acquires an ACCI of −0.0433, which is higher than that of the B-share market (B-share market has an ACCI of −0.1715), again implying that A-share market has higher anxiety from the perspective of accumulative relative order imbalance.

3. Empirical Results of the A-Share Market

This section examines how investor anxiety affects momentum profits through different avenues. First, we show the momentum profits of the A-share market as a whole in various periods. We then present the results for the 1-day, 2-day, 3-day, 30-day, and 180-day periods under different strengths of anxiety. Third, the outcomes for the extended periods under different strengths of anxiety are also depicted by several 3D figures.

Table 1: Descriptive statistics.

Mean	A-share market	B-share market
ROI	0.1115	0.2376
ACCI	−0.0433	−0.1715

This table presents the mean value of daily relative order imbalance (ROI) and accumulative relative order imbalance (ACCI) for the market as a whole. They are obtained based on a daily basis.

3.1. Momentum Profits of the A-Share Market in Various Periods. In this section, we draw a figure for the momentum profits of the A-share market as a whole. The formation and holding periods of momentum portfolios respectively range from 1 day to 30 days. Figure 2 shows the results.

From Figure 2, we can observe that most of the momentum profits from the A-share market are below 0 and related absolute t-statistics are all higher than 1.96. Although there are also significantly positive momentum profits, they just occur in the very short run. To be concrete, within 10 days, there are evident price momentum, but the results all turn to be price reversals if the periods are over 10 days. These outcomes show that the Chinese A-share market mainly embodies price reversals in most of the periods we adopt but presents price momentum in the very short run.

3.2. Investor Anxiety and Momentum Profits of the A-Share Market. In this section, we study how the daily relative order imbalance and accumulative relative order imbalance affect the daily momentum profits. Table 2 reports the effect of the daily relative order imbalance, while that of the accumulative relative order imbalance takes shape in Table 3.

3.2.1. Daily Relative Order Imbalance: Baseline Results. We dissect the effects of the daily relative order imbalance among Chinese A-share stocks. Table 2 presents the daily momentum profits and corresponding t-statistics for different levels of the daily relative order imbalance, which emphasizes the impact of instantaneous anxiety.

From Table 2, for the very short run of Panel A, we can see that the highest level of the daily relative order imbalance induces the most significantly positive momentum profit (the t-statistic is 24.2763) for the 1-day period. When we enter the 2-day and 3-day periods, this result is maintained. That is, the highest daily relative order imbalance still gives rise to the most significantly positive momentum profits (the t-statistics are 13.0337 and 8.9987, respectively). The highest daily relative order imbalance means that the stocks face the lowest selling pressure, implying the lowest instantaneous anxiety. This outcome suggests that the lowest instantaneous anxiety elicits the strongest price momentum in the very short run.

However, when we enter the 30-day and 180-day periods, we find that the result turns in a totally opposite direction. For the 30-day period, the discovery is that the highest daily relative order imbalance leads to the most significantly negative momentum profit with an absolute t-statistic of over 19, while the lowest daily relative order imbalance leads to the least significantly negative momentum profit and the absolute t-statistic is greater than 13. Moreover, in the case of the 180-day period, the highest daily relative order imbalance stocks still have the most significantly negative momentum profit with an absolute t-statistic of over 17, but the lowest one has a significantly negative momentum profit and the related absolute t-statistic is 10.7622. The results discussed above tell us that the lowest instantaneous anxiety gives rise to the most severe price reversal and the highest instantaneous anxiety activates the mildest price reversal in the long run.

Moreover, among Panels A, B, C, D, and E, there are significant differences in the momentum profits between the highest daily relative order imbalance group and the lowest daily relative order imbalance group since related absolute t-statistics are all over 5. We compute F-statistics to examine whether the changes in daily relative order imbalance significantly influence the momentum profits (average winner-minus-loser return spreads). The results show that the winner-minus-loser return spreads from various groups do not have the same mean values (p values are all smaller than 5%), suggesting that variations of daily relative order imbalance strongly affect momentum profits.

3.2.2. Accumulative Relative Order Imbalance: Baseline Results. Freud's quote shows the importance of accumulation in anxiety, and so we construct the accumulative relative order imbalance (ACCI) to study the accumulation of anxiety. In Table 3, we report the momentum profits and t-statistics among Chinese A-share stocks for different levels of the accumulative relative order imbalance.

In Table 3, we can find in the very short run for 1 day that the lowest accumulative anxiety (lowest ACCI) elicits the most significantly positive momentum profit (the t-statistic is 16.6676). This finding remains for the 2-day and 3-day period as the t-statistics are, respectively, 7.3361 and 4.8114 for the lowest accumulative anxiety stocks. Therefore, the lowest accumulative anxiety gives rise to the strongest price momentum in the very short run.

For the 30-day and 180-day periods, the phenomenon becomes wholly different. In Panel D and Panel E, the lowest accumulative anxiety stocks have the most significantly negative momentum profits because the absolute t-statistics are 20.4242 and 20.7767, respectively. Besides, the highest accumulative anxiety (highest ACCI) stocks result in the least significantly negative momentum profits with absolute t-statistics ranging from 7 to 8. These discoveries document that the lowest accumulative anxiety stocks are trapped in the most severe price reversal and the highest accumulative anxiety stocks suffer from much milder price reversal than the lowest one in the long run.

In addition, we perceive that significant differences in momentum profits (average winner-minus-loser return spreads) occur between the highest and lowest ACCI groups as absolute t-statistics are higher than 2 from Panels A, B, C, D, and E. We continue to use F-statistics to detect whether the winner-minus-loser return spreads from various groups grasp the same mean values. The outcomes

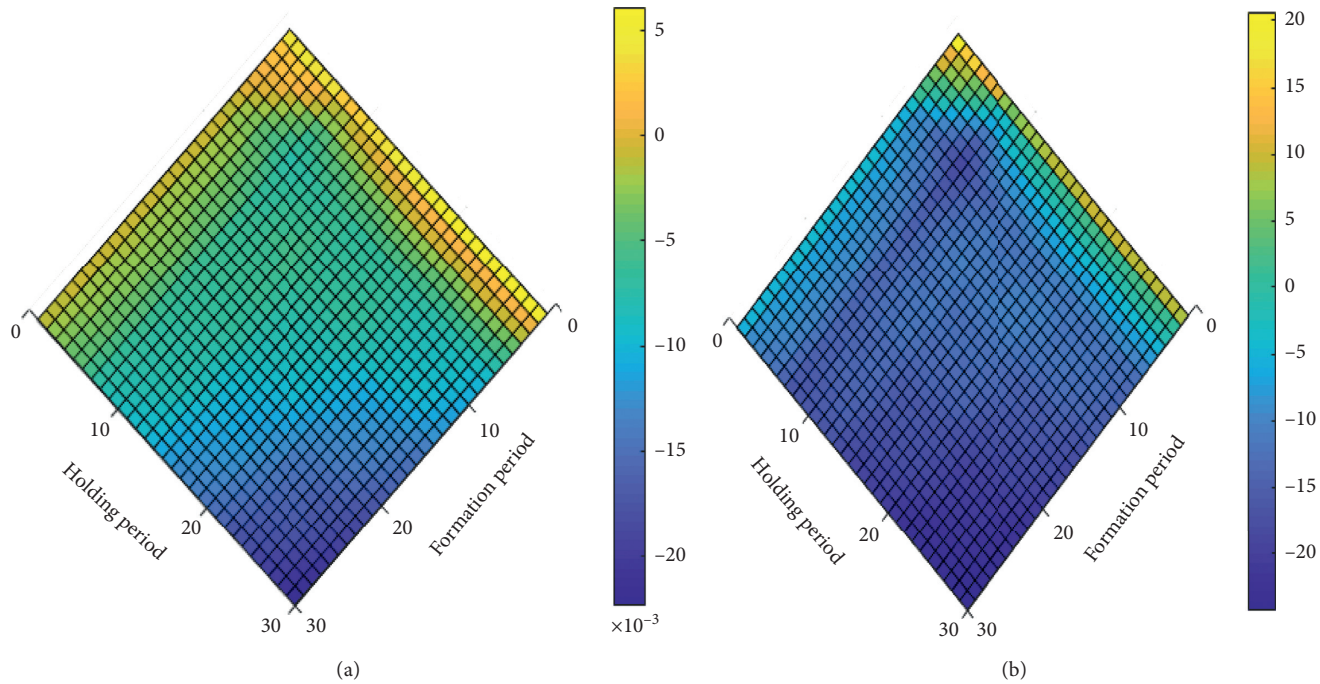

Figure 2: Momentum profits of the A-share market as a whole. This figure plots the momentum profits and related t-statistics of the A-share market in various periods. The formation and holding periods, respectively, range from 1 day to 30 days. (a) Momentum profit and (b) t-statistics.

document that the winner-minus-loser return spreads do not have the same mean values because the p values of F-statistics are all below 5%, implying that the changes in accumulative relative order imbalance significantly influence momentum profits.

3.2.3. Implications from the Baseline Results. In view of the instantaneous anxiety or accumulative anxiety, the empirical results are basically consistent with each other. In the very short run, the stocks held by the least anxious investors encounter the greatest price momentum, while the stocks held by the most anxious investors induce much weaker price momentum. However, in the relatively long run, the results change dramatically. That is, we all perceive strong price reversals regardless of the strength of anxiety.

The most intriguing point concerns why the lowest degree of anxiety behaves differently in the very short run and long run. With regard to the first, the lowest anxiety denotes extreme optimism. The majority of investors in the Chinese stock market are retail investors. This type of investor lacks sufficient knowledge and a decent information source compared to the institutional investors. The retail investors generally fail to make good decisions.

Our insights include that once the investors with poor decision making are characterized by extreme optimism, the stocks will be initially mispriced, but mispricing will be eventually corrected in the future. In the very short run, the retail investors do not have sufficient time to update their information. Due to their extreme optimism, they will not make any adjustments to their investments and will exhibit underreactions to information, exacerbating the price momentum of the stocks in which they invest. However, as time passes, the deviations from the fundamentals will not persist, suggesting that a price correction will finally come into being and a strong price reversal will also occur.

3.3. Risk Adjustments Using Asset Pricing Models of the A-Share Market. Section 3.2 reports the results of the baseline tests for anxiety and the momentum profits. In regard to momentum research, some may doubt whether the results are sufficiently robust after adjustments for risk using the asset pricing models. Hence, we answer this question below using the capital asset pricing model, Chinese three-factor asset pricing model [38], and Fama–French three-factor asset pricing model [37].

3.3.1. Daily Relative Order Imbalance: Risk Adjustments. Table 4 presents the outcomes of the risk adjustments for the momentum profits under different levels of instantaneous anxiety (represented by the daily relative order imbalance). From Table 4, after adjusting for the risks, the effect of instantaneous anxiety actually remains. In Panel A for the 1-day period, we can see that the lowest instantaneous anxiety (highest daily relative order imbalance) still generates the most significantly positive risk-adjusted momentum profits with t-statistics ranging from 23 to 23.2604 in spite of the asset pricing model's specifications. When we consider the 2-day and 3-day periods, the risk-adjusted momentum profits arising from the lowest instantaneous anxiety are also the most significantly positive (the t-statistics are over 12 and 8, respectively).

Table 2: The effect of the daily relative order imbalance of the A-share market.

Panel A: $F = H = 1$ day					
ROI	Highest	2	3	4	Lowest
MP	0.0093	0.0033	0.0015	0.0020	0.0041
t-stat	24.2763	10.7031	5.3008	7.3498	13.9771
		MP (H-L)		0.0052	
		t-stat		11.1713	
		F-stat (SFE)		99.0568	
		p value		0.0000	
Panel B: $F = H = 2$ days					
ROI	Highest	2	3	4	Lowest
MP	0.0064	0.0015	0.0009	0.0002	0.0022
t-stat	13.0337	3.8611	2.4428	0.4907	5.8371
		MP (H-L)		0.0042	
		t-stat		8.0401	
		F-stat (SFE)		36.3640	
		p value		0.0000	
Panel C: $F = H = 3$ days					
ROI	Highest	2	3	4	Lowest
MP	0.0051	0.0015	0.0009	0.0001	0.0018
t-stat	8.9987	3.1393	2.0881	0.2383	4.1545
		MP (H-L)		0.0033	
		t-stat		5.862	
		F-stat (SFE)		17.8774	
		p value		0.0000	
Panel D: $F = H = 30$ days					
ROI	Highest	2	3	4	Lowest
MP	−0.0283	−0.0248	−0.0227	−0.0213	−0.0179
t-stat	−19.6921	−18.2659	−17.4103	−16.3441	−13.4833
		MP (H-L)		−0.0104	
		t-stat		−6.2509	
		F-stat (SFE)		6.0864	
		p value		0.0001	
Panel E: $F = H = 180$ days					
ROI	Highest	2	3	4	Lowest
MP	−0.0529	−0.0485	−0.0438	−0.0413	−0.0307
t-stat	−17.4868	−16.5624	−14.8212	−14.2393	−10.7622
		MP (H-L)		−0.0222	
		t-stat		−6.9754	
		F-stat (SFE)		8.8145	
		p value		0.0000	

This table presents the daily momentum profits (MP) and related t-statistics (t-stat) of A-share stocks. F and H represent the length of the formation and holding periods, respectively. For each day, we calculate the daily relative order imbalance (ROI) of every stock and sort the stocks according to the daily relative order imbalance for that day. Within each group based on previous sorts, we select winner and loser stocks based on the past price growth rate in the formation period and then calculate the momentum profit (average winner-minus-loser return spread) for the holding period. In addition, we also calculate the momentum profit (average winner-minus-loser return spread) of the highest-minus-lowest ROI (H-L) group. According to Montgomery [65], our analyses for the effects of ROI on momentum profits are single-factor experiments (SFE), so we calculate F-statistics to test if the winner-minus-loser return spreads from different groups have the same average values. We first test the momentum profits in the very short run. The most natural choice is 1 day, and we also calculate momentum profits for 2 days and 3 days for robustness. In addition, we further test the momentum profits for 30 days and 180 days to see how they behave in the relatively long run. The sorts conducted for the daily relative order imbalance (ROI) are divided into 5 groups. Winner stocks are the one-fifth of stocks with the highest price growth rate, while loser stocks are the one-fifth of stocks with the lowest price growth rate. The formation and holding periods have the same length according to Verardo [66], Avramov et al. [67], and Hillert et al. [31]. The critical value of 5% significance of t-statistic is 1.96.

By throwing light on the 30-day and 180-day periods, the lowest instantaneous anxiety still induces the most significantly negative risk-adjusted momentum profits with absolute t-statistics of over 19 and 16, respectively. In addition, the highest instantaneous anxiety (lowest daily relative order imbalance) generates the least significantly negative risk-adjusted momentum profits as the absolute t-statistics only range from 9.9843 to 14.2392. Therefore, the effect of instantaneous anxiety is not sensitive to the pricing risks.

3.3.2. Accumulative Relative Order Imbalance: Risk Adjustments. In Table 5, we show the results for accumulative anxiety after adjusting for risk. Similar patterns appear

Table 3: The effect of the accumulative relative order imbalance of the A-share market.

Panel A: $F = H = 1$ day					
ACCI	Highest	2	3	4	Lowest
MP	0.0026	0.0029	0.0028	0.0037	0.0066
t-stat	9.3112	9.4786	8.5720	10.6619	16.6676
MP (H-L)				−0.004	
t-stat				−9.8863	
F-stat (SFE)				23.3471	
p value				0.0000	
Panel B: $F = H = 2$ days					
ACCI	Highest	2	3	4	Lowest
MP	0.0013	0.0017	0.0010	0.0010	0.0037
t-stat	3.4724	4.4059	2.4176	2.3579	7.3361
MP (H-L)				−0.0024	
t-stat				−4.662	
F-stat (SFE)				7.0371	
p value				0.0000	
Panel C: $F = H = 3$ days					
ACCI	Highest	2	3	4	Lowest
MP	0.0012	0.0017	0.0013	0.0003	0.0028
t-stat	2.7862	3.8181	2.7958	0.5068	4.8114
MP (H-L)				−0.0016	
t-stat				−2.6848	
F-stat (SFE)				3.6393	
p value				0.0057	
Panel D: $F = H = 30$ days					
ACCI	Highest	2	3	4	Lowest
MP	−0.0107	−0.0169	−0.0193	−0.0248	−0.0304
t-stat	−8.3662	−12.1924	−14.5438	−18.2731	−20.4242
MP (H-L)				0.0197	
t-stat				12.2662	
F-stat (SFE)				29.5456	
p value				0.0000	
Panel E: $F = H = 180$ days					
ACCI	Highest	2	3	4	Lowest
MP	−0.0222	−0.0281	−0.0310	−0.0484	−0.0682
t-stat	−7.6851	−8.9120	−10.6797	−16.4591	−20.7767
MP (H-L)				0.046	
t-stat				13.1039	
F-stat (SFE)				38.5732	
p value				0.0000	

This table presents the daily momentum profits (MP) and related t-statistics (t-stat) for A-share stocks. F and H represent the length of formation and holding periods, respectively. For each day, the accumulative relative order imbalance (ACCI = neg% − pos%) for every stock is acquired for the formation period and we initially classify the stocks based on ACCI. Then, for each group based on previous classifications, the stocks are sorted according to the past price growth rate in the formation period to identify the winner and loser stocks. Momentum profits (based on the average winner-minus-loser return spread) are thus calculated for the holding period. We also calculate the momentum profit (average winner-minus-loser return spread) of the highest-minus-lowest ACCI (H-L) group. According to Montgomery [65], our analyses for the effects of ACCI on momentum profits are single-factor experiments (SFE), so we calculate F-statistics to test if the winner-minus-loser return spreads from different groups have the same average values. We first test for the momentum profits in the very short run. The most natural choice is 1 day, and we also calculate momentum profits for 2 days and 3 days for robustness. In addition, we further test the momentum profits for 30 days and 180 days to see how they behave in the relatively long run. The sorts on ACCI are categorized into 5 groups. Winner stocks are those for the one-fifth of stocks with the highest price growth rate, while loser stocks are those for the one-fifth of stocks with the lowest price growth rate. The formation and holding periods have the same length according to Verardo [66], Avramov et al. [67], and Hillert et al. [31]. The critical value of 5% significance of t-statistic is 1.96.

once again. From Panel A, the risk-adjusted momentum profits are most significantly positive for the lowest accumulative anxiety (lowest ACCI) for the 1-day period (t-statistics are over 15). Moreover, for the 2-day and 3-day periods, the lowest accumulative anxiety is still characterized by the strongest significantly positive momentum profits due to the t-statistics varying from 4.4912 to 6.9145.

For the relatively long periods of 30 days and 180 days, the lowest accumulative anxiety produces the most significantly negative momentum profits owing to the absolute t-statistics all being over 19, but the highest accumulative anxiety (highest ACCI) results in the least significantly negative momentum profits (with the absolute t-statistics only varying from 6.6017 to 9.0809). Hence, the effect of accumulative anxiety is also not sensitive to the pricing risks.

3.4. Extended Periods of the A-Share Market. We further extend the formation and holding periods of the momentum profits in this section so that we can build up a clearer pattern of the effect of anxiety.

3.4.1. Daily Relative Order Imbalance in Extensions of the A-Share Market. The effects of the highest daily relative order imbalance and lowest daily relative order imbalance are studied in extensions. We depict the momentum profits and t-statistics in Figures 3 and 4.

Figure 3 shows that the momentum profits vary from −0.03 to 0.01 and large part of the surface of momentum profit is below 0. The daily momentum profits are only significantly positive in the very short run under the lowest instantaneous anxiety (highest daily relative order imbalance) because the t-statistics are all greater than 10 or even over 20. However, the results become significantly negative once the testing periods are extended (most of the absolute t-statistics are close to 10 or even equal to 20). These outcomes again document that the lowest instantaneous anxiety only produces price momentum in the short run but leads to severe price reversal in the long run.

While Figure 4 appears to be similar to Figure 3, there are obvious distinctions between the two. In Figure 4, most of momentum profits are also smaller than 0. The t-statistics of the significantly positive momentum profits under the highest instantaneous anxiety (lowest daily relative order imbalance) only change around 10 in the very short run. In the long run, although the highest instantaneous anxiety also induces significantly negative momentum profits, most of the absolute t-statistics only vary from 2.5 to 10. By contrast, many absolute t-statistics in Figure 3 change around 20. The absolute momentum profits in Figure 4 range from 0.004 to 0.02, but those in Figure 3 lie between 0.01 and 0.03, suggesting that the impacts of the lowest instantaneous anxiety on price momentum or reversal are always stronger than those for the highest instantaneous anxiety in extended periods.

3.4.2. Accumulative Relative Order Imbalance in Extensions of the A-Share Market. We examine the effects of the highest accumulative relative order imbalance and lowest accumulative

Table 4: The effect of the daily relative order imbalance after risk adjustments of the A-share market.

ROI	Highest	2	3	4	Lowest
Panel A: $F = H = 1$ day					
1F alpha	0.0090	0.0030	0.0014	0.0019	0.0041
t-stat	23.2604	9.8018	5.0059	6.7069	13.7079
CH-3 alpha	0.0090	0.0030	0.0014	0.0018	0.0041
t-stat	23.1289	9.7904	4.9579	6.6669	13.6641
FF-3 alpha	0.0090	0.0030	0.0014	0.0019	0.0042
t-stat	23.0065	9.7215	4.9283	6.6714	13.6330
Panel B: $F = H = 2$ days					
ROI	Highest	2	3	4	Lowest
1F alpha	0.0063	0.0014	0.0010	0.0002	0.0021
t-stat	12.6070	3.5199	2.6454	0.5100	5.4200
CH-3 alpha	0.0063	0.0014	0.0010	0.0002	0.0020
t-stat	12.5762	3.5225	2.6300	0.4821	5.3693
FF-3 alpha	0.0063	0.0014	0.0010	0.0002	0.0021
t-stat	12.4690	3.4930	2.5972	0.4690	5.4331
Panel C: $F = H = 3$ days					
ROI	Highest	2	3	4	Lowest
1F alpha	0.0052	0.0015	0.0010	0.0001	0.0016
t-stat	8.9597	3.0806	2.3848	0.1668	3.6955
CH-3 alpha	0.0052	0.0015	0.0010	0.00005	0.0016
t-stat	8.9300	3.0850	2.3652	0.1085	3.6304
FF-3 alpha	0.0051	0.0015	0.0011	0.0001	0.0016
t-stat	8.8141	3.0514	2.3829	0.1534	3.7256
Panel D: $F = H = 30$ days					
ROI	Highest	2	3	4	Lowest
1F alpha	−0.0285	−0.0251	−0.0236	−0.0222	−0.0192
t-stat	−19.3416	−18.0918	−17.6604	−16.5880	−14.1780
CH-3 alpha	−0.0285	−0.0250	−0.0236	−0.0222	−0.0193
t-stat	−19.3661	−18.0459	−17.6647	−16.5807	−14.2392
FF-3 alpha	−0.0284	−0.0250	−0.0235	−0.0221	−0.0191
t-stat	−19.2355	−17.9866	−17.5366	−16.4639	−14.0597
Panel E: $F = H = 180$ days					
ROI	Highest	2	3	4	Lowest
1F alpha	−0.0523	−0.0483	−0.0428	−0.0392	−0.0291
t-stat	−16.9308	−16.3887	−14.3305	−13.4320	−10.0824
CH-3 alpha	−0.0524	−0.0483	−0.0429	−0.0394	−0.0292
t-stat	−16.9177	−16.3102	−14.3240	−13.4106	−10.0567
FF-3 alpha	−0.0517	−0.0477	−0.0424	−0.0388	−0.0289
t-stat	−16.7266	−16.1821	−14.2409	−13.3209	−9.9843

This table presents the risk-adjusted daily momentum profits (MP) and related t-statistics (t-stat) for A-share stocks. F and H denote the length of the formation and holding periods, respectively. For each day, we calculate the daily relative order imbalance for every stock and sort the stocks according to the daily relative order imbalance for that day. For each group based on previous sorts, we select winner and loser stocks according to the past price growth rate in the formation period and then calculate winner-minus-loser return spreads in the holding period. We first test the momentum profits in the very short run. The most natural choice is 1 day and we also calculate momentum profits for 2 days and 3 days for robustness. In addition, we further test the momentum profits for 30 days and 180 days to see how they behave in the relatively long run. The sorts based on the daily relative order imbalance (ROI) are categorized into 5 groups. Winner stocks are based on the one-fifth of stocks with the highest price growth rate, while loser stocks are based on the one-fifth of stocks with the lowest price growth rate. The dependent variables are the winner-minus-loser return spreads for different levels of the ROI. 1F alpha denotes the regression intercept for the capital asset pricing model, CH-3 alpha is the regression intercept for the Chinese three-factor asset pricing model, and FF-3 alpha is the regression intercept for the Fama–French three-factor asset pricing model. The alphas are the risk-adjusted momentum profits. The t-statistics are based on White [68] heteroskedasticity-consistent standard errors according to Liu et al. [38]. The formation and holding periods have the same length according to Verardo [66], Avramov et al. [67], and Hillert et al. [31]. The critical value of 5% significance of t-statistic is 1.96.

relative order imbalance for extensions. The corresponding momentum profits and t-statistics are shown in Figures 5 and 6.

Figure 5 shows the effect of the highest accumulative relative order imbalance for extensions. The results for these extensions are very similar to those in our previous analysis. Overall, the momentum profits change from −0.01 to 0.002 but the major part of momentum profits is smaller than 0. The momentum profits are significantly positive in the very short run with the t-statistics lying between 2.5 and 10. When it comes to the long run, the surfaces of the momentum profits and t-statistics dramatically move down, implying that the highest accumulative relative order imbalance activates a price reversal. These outcomes suggest that the highest accumulative anxiety (highest accumulative

Table 5: The effect of the accumulative relative order imbalance after risk adjustments of the A-share market.

Panel A: $F = H = 1$ day					
ACCI	Highest	2	3	4	Lowest
1F alpha	0.0026	0.0028	0.0027	0.0035	0.0064
t-stat	8.9064	9.0696	8.1529	9.9282	15.6850
CH-3 alpha	0.0026	0.0029	0.0027	0.0035	0.0064
t-stat	8.8959	9.1000	8.1425	9.8894	15.6560
FF-3 alpha	0.0026	0.0029	0.0027	0.0035	0.0064
t-stat	8.8242	8.9779	8.0365	9.8559	15.4857
Panel B: $F = H = 2$ days					
ACCI	Highest	2	3	4	Lowest
1F alpha	0.0013	0.0017	0.0010	0.0009	0.0036
t-stat	3.3869	4.3199	2.2945	2.0152	6.9145
CH-3 alpha	0.0013	0.0017	0.0010	0.0009	0.0036
t-stat	3.3529	4.2977	2.2881	1.9869	6.8961
FF-3 alpha	0.0013	0.0018	0.0009	0.0009	0.0036
t-stat	3.3662	4.2934	2.2162	1.9870	6.8305
Panel C: $F = H = 3$ days					
ACCI	Highest	2	3	4	Lowest
1F alpha	0.0012	0.0018	0.0013	0.0002	0.0027
t-stat	2.7346	3.9028	2.6414	0.3550	4.5375
CH-3 alpha	0.0012	0.0018	0.0013	0.0002	0.0027
t-stat	2.6988	3.8771	2.6310	0.3066	4.5234
FF-3 alpha	0.0012	0.0018	0.0013	0.0002	0.0027
t-stat	2.7237	3.8698	2.5721	0.2961	4.4912
Panel D: $F = H = 30$ days					
ACCI	Highest	2	3	4	Lowest
1F alpha	−0.0117	−0.0181	−0.0203	−0.0263	−0.0315
t-stat	−9.0809	−12.7652	−14.8693	−18.8563	−20.8082
CH-3 alpha	−0.0117	−0.0181	−0.0203	−0.0263	−0.0315
t-stat	−9.0709	−12.7911	−14.9030	−18.8758	−20.8273
FF-3 alpha	−0.0116	−0.0181	−0.0202	−0.0262	−0.0315
t-stat	−8.9878	−12.7257	−14.7757	−18.6526	−20.7468
Panel E: $F = H = 180$ days					
ACCI	Highest	2	3	4	Lowest
1F alpha	−0.0199	−0.0251	−0.0290	−0.0471	−0.0667
t-stat	−6.7706	−7.8772	−9.9016	−15.5761	−19.7604
CH-3 alpha	−0.0201	−0.0251	−0.0289	−0.0470	−0.0667
t-stat	−6.7974	−7.8374	−9.8577	−15.5364	−19.6877
FF-3 alpha	−0.0193	−0.0246	−0.0286	−0.0464	−0.0663
t-stat	−6.6017	−7.7689	−9.7518	−15.3621	−19.5937

This table reports the risk-adjusted daily momentum profits (MP) and related t-statistics (t-stat) for A-share stocks. F and H represent the length of the formation and holding periods, respectively. On each day, the accumulative relative order imbalance (ACCI = neg% − pos%) of every stock is acquired in the formation period and the stocks are initially classified according to the ACCI. Then, for each group based on previous classifications, the stocks are sorted by their past price growth rates in the formation period in order to identify winner and loser stocks. Winner-minus-loser return spreads in the holding periods are then calculated. We first test the momentum profits in the very short run. The most natural choice is 1 day, and we also calculate the momentum profits for 2 days and 3 days for robustness. In addition, we further test the momentum profits for 30 days and 180 days to see how they behave in the relatively long run. The sorts on ACCI are categorized into 5 groups. Winner stocks comprise the one-fifth of stocks with the highest price growth rate, while loser stocks comprise the one-fifth of stocks with the lowest price growth rate. The dependent variables are the winner-minus-loser return spreads under different levels of ACCI. 1F alpha denotes the regression intercept of the capital asset pricing model, CH-3 alpha is the regression intercept of the Chinese three-factor asset pricing model, and FF-3 alpha is the regression intercept of the Fama–French three-factor asset pricing model. The alphas are the risk-adjusted momentum profits. The t-statistics are based on White [68] heteroskedasticity-consistent standard errors according to Liu et al. [38]. The formation and holding periods have the same length according to Verardo [66], Avramov et al. [67], and Hillert et al. [31]. The critical value of 5% significance of t-statistic is 1.96.

relative order imbalance) leads to price momentum in the short run but becomes restricted in terms of the price reversal in the long run.

We report the effect of the lowest accumulative anxiety (lowest accumulative relative order imbalance) in extensions as shown in Figure 6. Overall, although there are positive momentum profits, most of momentum profits are below 0. The absolute t-statistics in Figure 6 range from 15 to 20, and they are much larger than those in Figure 5 (the maximum absolute t-statistic is just 10). In addition, the absolute momentum profits vary from 0.005 to 0.03 in Figure 6, but those in Figure 5 lie only between 0.002 and 0.01. Regardless of the short run or long run, the absolute momentum profits under the lowest accumulative anxiety are higher than those under the highest accumulative anxiety. Consequently, the influences of the lowest

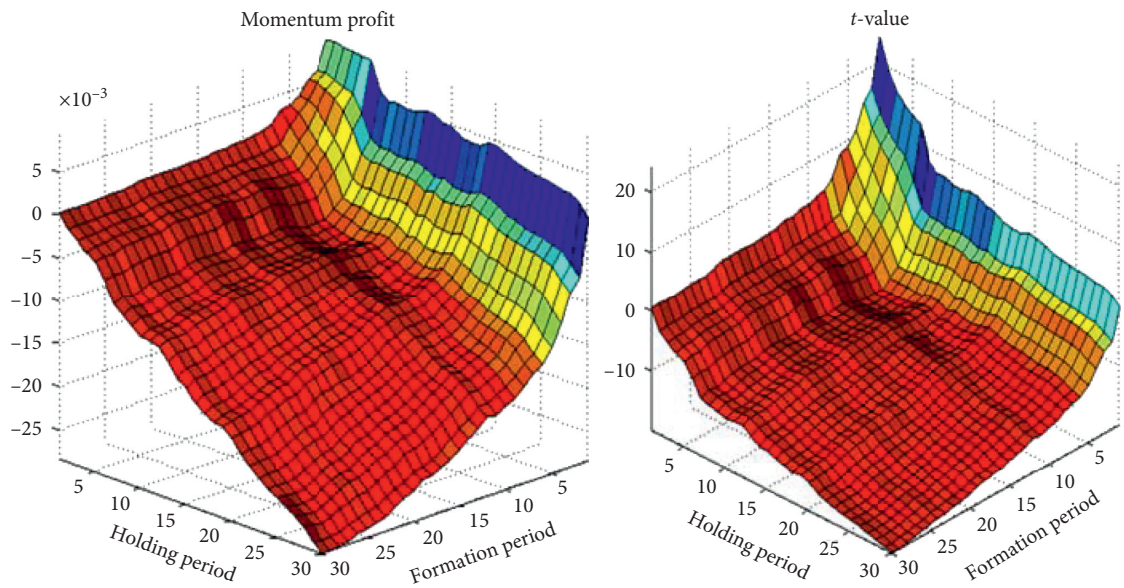

Figure 3: Highest daily relative order imbalance in extensions of the A-share market. This figure plots the daily momentum profits and their t-statistics under the highest daily relative order imbalance in A-share market. The formation and holding periods, respectively, range from 1 day to 30 days.

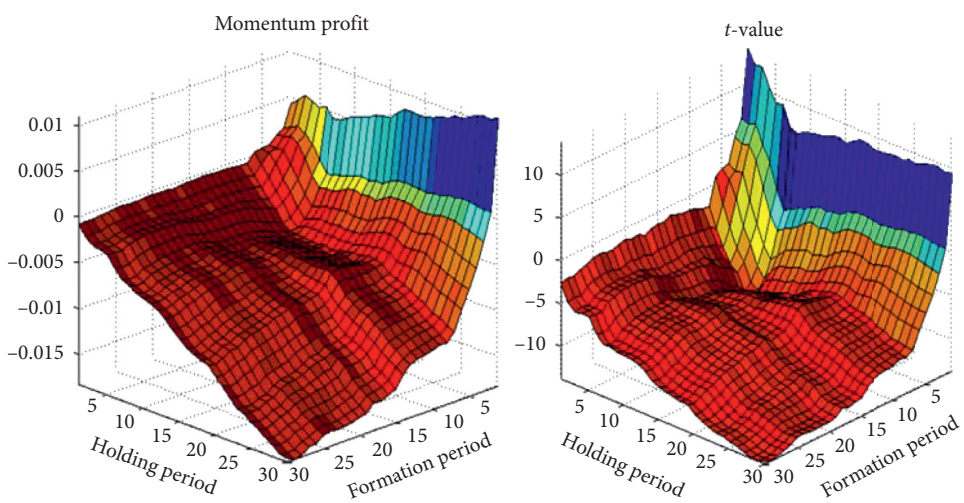

Figure 4: Lowest daily relative order imbalance in extensions of the A-share market. This figure plots the daily momentum profits and their t-statistics under the lowest daily relative order imbalance in A-share market. The formation and holding periods, respectively, range from 1 day to 30 days.

accumulative anxiety on price momentum or reversal are still stronger than the influences of the highest accumulative anxiety in extended periods.

4. Empirical Results of the B-Share Market

This section dedicates to settling the effects of anxiety on momentum profits in the B-share market from the perspectives of instantaneous and accumulative anxiety. We first test the momentum profits in 1 day, 2 days, 3 days, 30 days, and 90 days. In addition, we examine the momentum profits in extended periods. This section aims at comparing whether different investor structures of A-share and B-share markets have influences on the effects of anxiety on momentum profits. According to China Stock Market and Accounting Research, there are just 19.7156% of A-shares which are held by institutional investors, while there are still 23.3345% of B-shares belonging to institutional investors. It is obvious that the power of institutional investors in B-share market is stronger than that in A-share market. The detailed data of the proportion of institutional investors are given in Appendix C.

4.1. Momentum Profits of the B-Share Market in Various Periods. We present the momentum profits of the B-share market as a whole in this section. The formation and holding

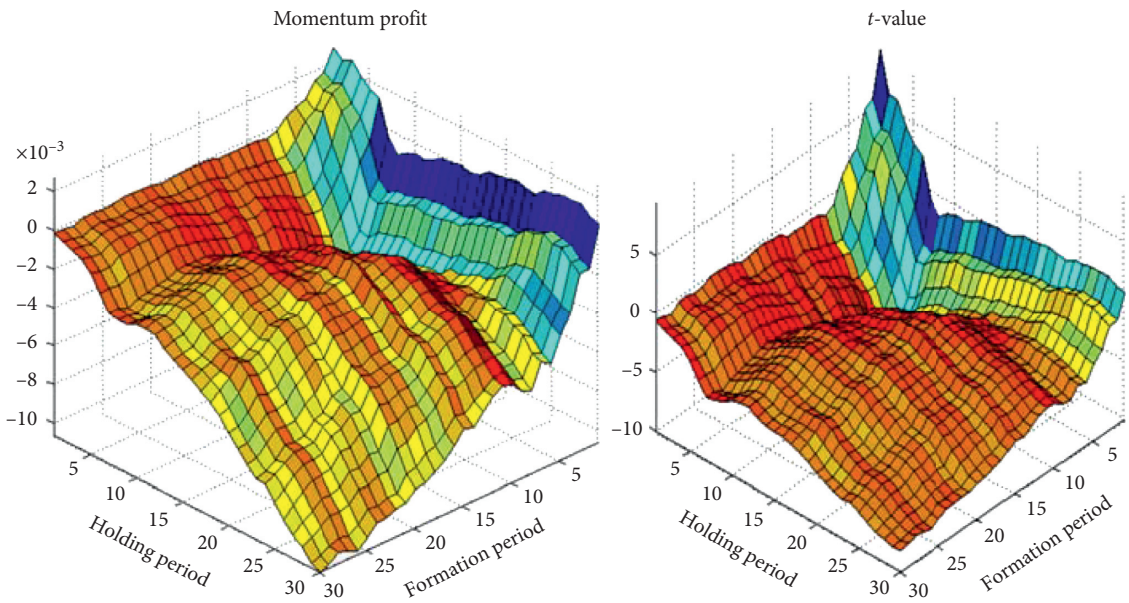

Figure 5: Highest accumulative relative order imbalance in extensions of the A-share market. This figure plots the daily momentum profits and their t-statistics under the highest accumulative relative order imbalance in A-share market. The formation and holding periods, respectively, range from 1 day to 30 days.

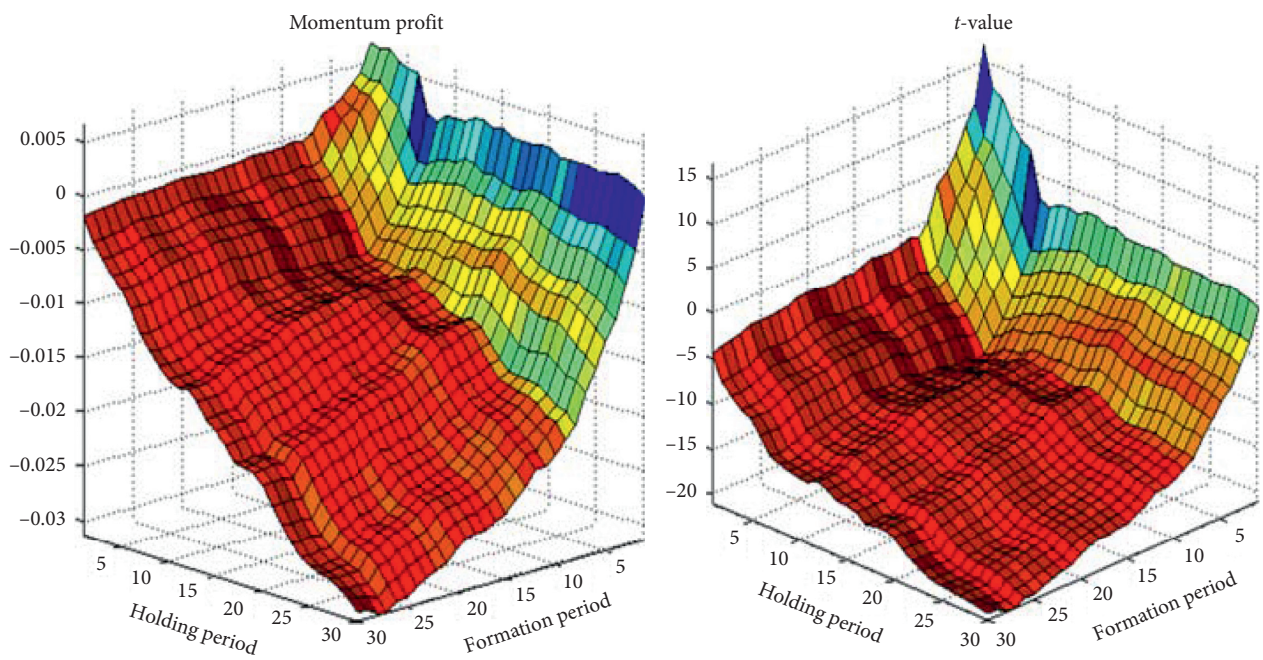

Figure 6: Lowest accumulative relative order imbalance in extensions of the A-share market. This figure plots the daily momentum profits and their t-statistics under the lowest accumulative relative order imbalance in A-share market. The formation and holding periods, respectively, range from 1 day to 30 days.

periods, respectively, vary from 1 day to 30 days. Figure 7 shows the results.

The momentum profits in Figure 7 show that the B-share market mainly embodies price momentum. Among many momentum profits we show above, they are significantly positive with absolute t-statistics higher than 2. Some of the positive momentum profits even have absolute t-statistics over 10 or 12. There are also significantly negative momentum profits in the figure, but they generally tend to be insignificant as presented in the blue part of the figure.

4.2. Investor Anxiety and Momentum Profits of the B-Share Market. We, respectively, analyze the effects of instantaneous and accumulative anxiety on momentum profits by

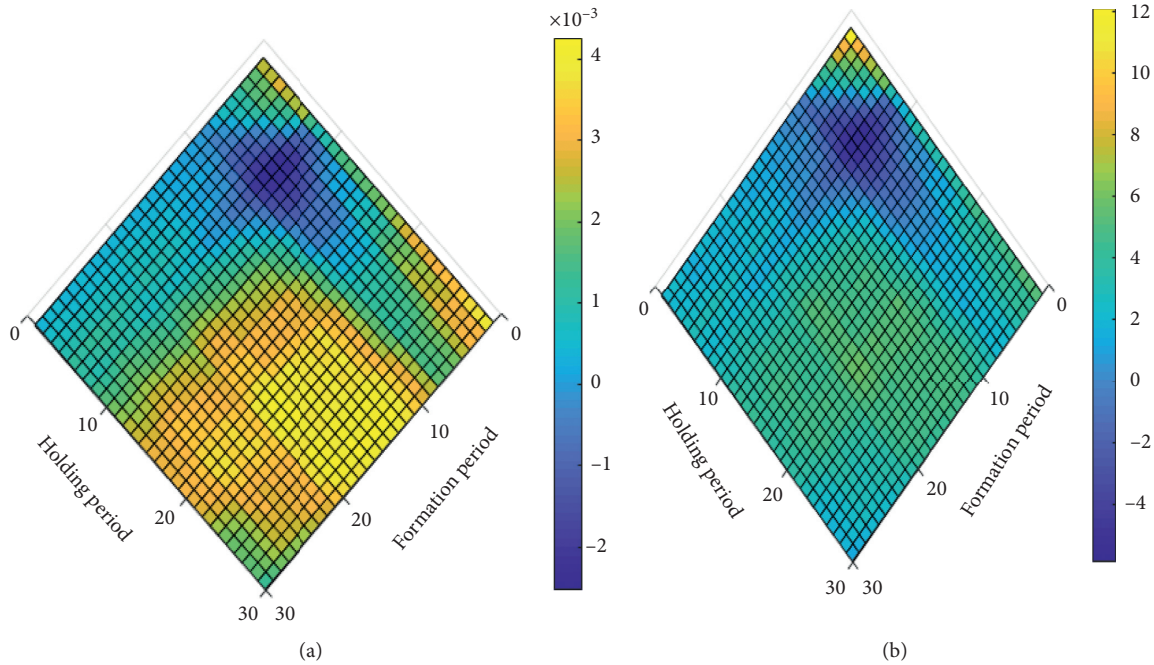

Figure 7: Momentum profits of the B-share market as a whole. This figure plots the momentum profits and related t-statistics of the B-share market as a whole. The formation and holding periods, respectively, range from 1 day to 30 days. (a) Momentum profit and (b) t-statistics.

daily relative order imbalance and accumulative relative order imbalance. Table 6 shows the results of daily relative order imbalance, whereas the results of accumulative relative order imbalance are given in Table 7.

As for B-share stocks in Table 6, instantaneous anxiety (daily relative order imbalance) does not appear to have any influence on momentum profits. In the very short run, most of the momentum profits are positive, but they are not very significant as many absolute t-statistics are below 1.96. However, when reaching the long run of 30 days and 90 days, the effect of instantaneous anxiety is also unclear and very weak. In 90 days, the momentum profits under the highest and the lowest daily relative order imbalance are all insignificant (absolute t-statistics are below 1.96), though those from 30 days are significant due to absolute t-statistics being higher than 1.96. Moreover, there is no sufficient evidence supporting that the changes in instantaneous anxiety affect the momentum profits since related p values of F-statistics are over 5%. Hence, based on the findings above, we can imply that instantaneous anxiety only affects the A-share stocks, while no sufficient evidence documents that B-share stocks fall under the shadow of instantaneous anxiety.

Similarly, from the viewpoint of accumulative anxiety (accumulative relative order imbalance), we do not find B-share stocks are influenced by anxiety in Table 7. For 1 day, 2 days, and 3 days, many absolute t-statistics are less than 1 regardless of the signs of the momentum profits. In addition, in the long run, many absolute t-statistics are still below 1.96. Furthermore, the p values of F-statistics are all higher than 5%, so there is no sufficient evidence supporting that the changes in accumulative anxiety affect the momentum profits in the B-share market. Therefore, regardless of the length of testing periods, the influence of accumulative anxiety is relatively strong for A-share stocks, but no strong evidence suggests that B-share stocks fall into the pitfall of the awful impact from anxiety.

4.3. Extended Periods of the B-Share Market. Like the manner of dissecting A-share market, we also investigate the effects of anxiety on momentum profits in B-share market in extended periods. The formation and holding periods of momentum portfolios vary from 1 day to 30 days. Section 4.3.1 shows the results of daily relative order imbalance and those of accumulative relative order imbalance emerge in Section 4.3.2.

4.3.1. Daily Relative Order Imbalance in Extensions of the B-Share Market. This section shows the momentum profits under the highest daily relative order imbalance and the lowest daily relative order imbalance in the B-share market. Figures 8 and 9 depict the outcomes.

From Figure 8, we can see that the momentum profits vary from −0.2 to 0.05 under the highest daily relative order imbalance in extensions of the B-share market. The t-statistics are between −6 and 1.8, but some of them are close to 0. However, most of t-statistics under the highest daily relative order imbalance from the A-share market lie between 5 and 20 or between −5 and −20. There is just very small number of t-statistics from the A-share market being close to 0, suggesting the effect of the highest daily relative order imbalance is stronger in A-share market than in B-share market.

In Figure 9, the momentum profits under the lowest daily relative order imbalance change from −0.15 to 0.05 in

Table 6: The effect of the daily relative order imbalance of the B-share market.

Panel A: F=H=1 Day				
ROI	Highest	2		Lowest
MP	0.008	−0.0006		0.02
t-stat	0.4765	−0.0544		1.56
F-stat (SFE)			0.9990	
p-value			0.4057	
Panel B: $F = H = 2$ days				
ROI	Highest	2		Lowest
MP	0.0057	0.0011		0.0164
t-stat	0.2126	0.0761		1.7463
F-stat (SFE)			0.3047	
p value			0.7446	
Panel C: $F = H = 3$ days				
ROI	Highest	2		Lowest
MP	−0.0145	−0.0244		0.0517
t-stat	−0.586	−1.0882		2.6181
F-stat (SFE)			1.7797	
p value			0.2232	
Panel D: $F = H = 30$ days				
ROI	Highest	2		Lowest
MP	−0.1396	−0.0481		−0.108
t-stat	−3.8853	−1.4117		−2.3744
F-stat (SFE)			0.4224	
p value			0.6649	
Panel E: $F = H = 90$ days				
ROI	Highest	2		Lowest
MP	−0.1405	−0.0965		0.0343
t-stat	−1.7508	−3.7581		1.0548
F-stat (SFE)			2.2867	
p value			0.1827	

This table presents the daily momentum profits (MP) and related t-statistics (t-stat) of B-share stocks. F and H represent the length of the formation and holding periods, respectively. For each day, we calculate the daily relative order imbalance for every stock and sort the stocks according to the daily relative order imbalance for that day. Within each group based on previous sorts, we select the winner and loser stocks according to the past price growth rate in the formation period and then calculate the momentum profit (average winner-minus-loser return spread) in the holding period. According to [65], our analyses for the effects of ROI on momentum profits are single-factor experiments (SFE), so we calculate F-statistics to test if the winner-minus-loser return spreads from different groups have the same average values. We first test the momentum profits in the very short run. The most natural choice is 1 day, and we also calculate the momentum profits for 2 days and 3 days for robustness. In addition, we further test the momentum profits for 30 days and 90 days to see how they behave in the relatively long run. The sorts based on the daily relative order imbalance (ROI) are classified into 3 groups. Winner stocks are the one-third of stocks with the highest price growth rate, while loser stocks are the one-third of stocks with the lowest price growth rate. The choices involving 90 days and one-third of the classifications are due to the small sample of B-share stocks (approximately 100 stocks). The formation and holding periods have the same length according to Verardo [66], Avramov et al. [67], and Hillert et al. [31]. The critical value of 5% significance of t-statistic is 1.96.

Table 7: The effect of the accumulative relative order imbalance of the B-share market.

Panel A: $F = H = 1$ day				
ACCI	Highest	2		Lowest
MP	0.0132	0.0124		0.0187
t-stat	0.9139	0.6781		0.9135
F-stat (SFE)			3.8613	
p value			0.0836	
Panel B: $F = H = 2$ days				
ACCI	Highest	2		Lowest
MP	0.0509	−0.0081		0.035
t-stat	2.0079	−0.2416		0.9545
F-stat (SFE)			2.8923	
p value			0.1320	
Panel C: $F = H = 3$ days				
ACCI	Highest	2		Lowest
MP	0.0592	−0.0237		0.0212
t-stat	8.627	−0.5423		0.5729
F-stat (SFE)			3.1636	
p value			0.1153	
Panel D: $F = H = 30$ days				
ACCI	Highest	2		Lowest
MP	−0.1317	−0.0748		−0.0787
t-stat	−2.3276	−1.4707		−1.8586
F-stat (SFE)			0.0976	
p value			0.9078	
Panel E: $F = H = 90$ days				
ACCI	Highest	2		Lowest
MP	−0.0757	0.0232		−0.1043
t-stat	−1.5088	0.7588		−2.1721
F-stat (SFE)			1.5604	
p value			0.2847	

This table presents the daily momentum profits (MP) and related t-statistics (t-stat) of B-share stocks. F and H represent the length of the formation and holding periods, respectively. On each day, the accumulative relative order imbalance (ACCI = neg% − pos%) for each stock is obtained in the formation period, and we initially classify the stocks based on ACCI. Then, in each group from the previous classifications, the stocks are sorted based on the past price growth rate in the formation period in order to identify winner and loser stocks. The momentum profits (average winner-minus-loser return spread) are thus calculated in the holding period. According to [65], our analyses for the effects of ACCI on momentum profits are single-factor experiments (SFE), so we calculate F-statistics to test if the winner-minus-loser return spreads from different groups have the same average values. We first test the momentum profits in the very short run. The most natural choice is 1 day, and we also calculate the momentum profits for 2 days and 3 days for robustness. In addition, we further test the momentum profits for 30 days and 90 days to see how they behave in the relatively long run. The sorts based on ACCI are categorized into 3 groups. Winner stocks consist of the one-third of stocks with the highest price growth rate, while loser stocks are made up of the one-third of stocks with the lowest price growth rate. The choices of 90 days and three group classifications arise due to the small sample of B-share stocks (approximately 100 stocks). The formation and holding periods have the same length according to Verardo [66], Avramov et al. [67], and Hillert et al. [31]. The critical value of 5% significance of t-statistic is 1.96.

the B-share market, which is similar to those from the highest daily relative order imbalance. In addition, the t-statistics are between −5 and 4, but many of them are close to 0. The momentum profits and t-statistics under the lowest daily relative order imbalance do not vary a lot from those under the highest daily relative order imbalance. Hence, no strong evidence shows the daily relative order imbalance affects the momentum profits in extensions of the B-share market. Moreover, there are just small number of t-statistics under the lowest daily relative order imbalance from A-share market being close to 0, so the effect of the lowest daily relative order imbalance is stronger in A-share market.

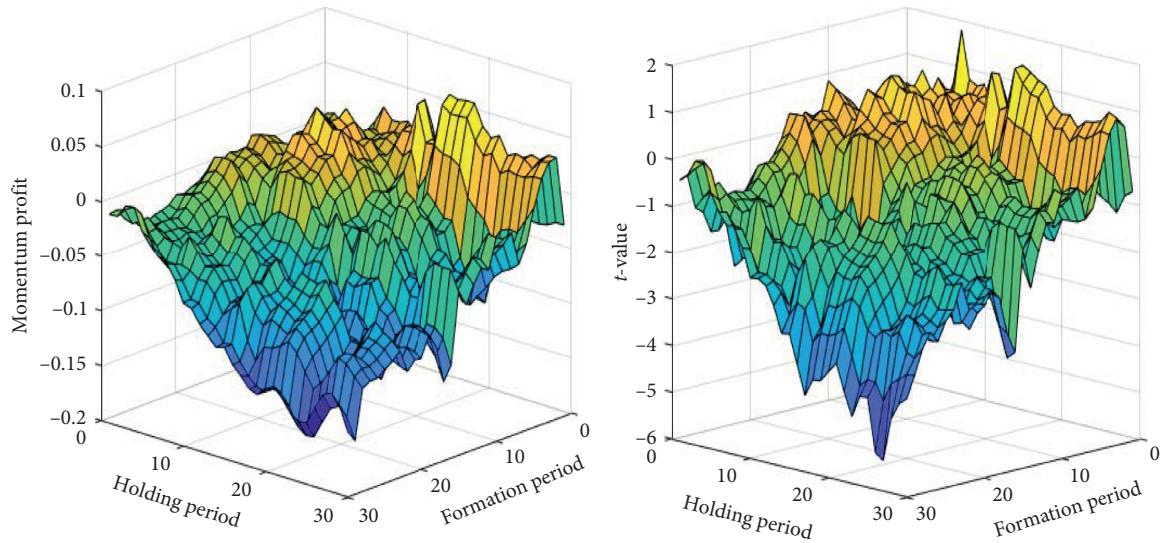

Figure 8: Highest daily relative order imbalance in extensions of the B-share market. This figure shows the momentum profits and t-statistics under the highest daily relative order imbalance in extensions of the B-share market. The formation and holding periods, respectively, range from 1 day to 30 days.

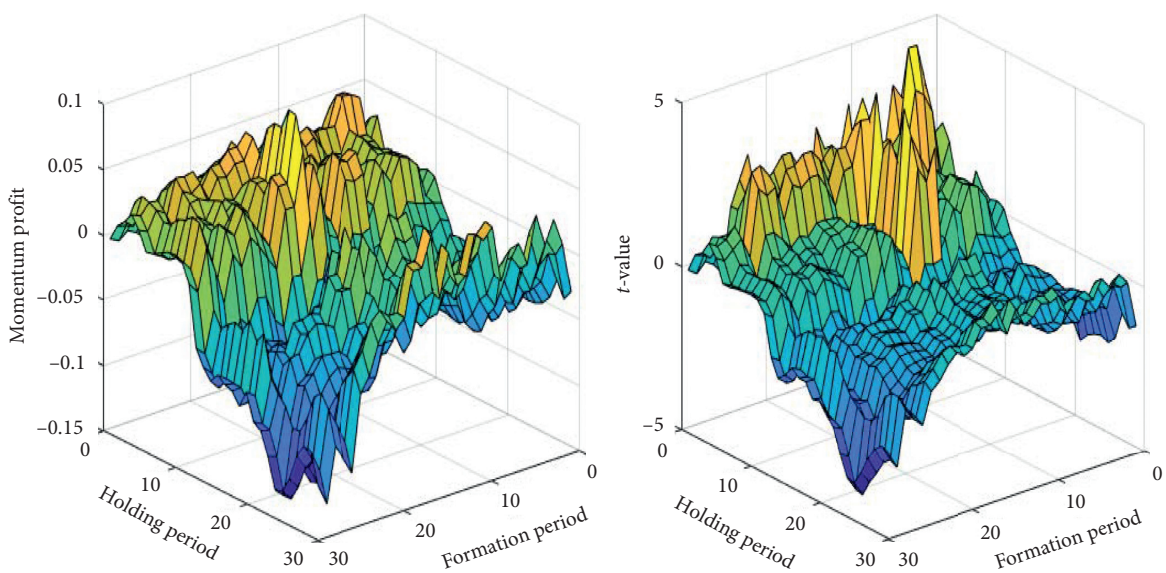

Figure 9: Lowest daily relative order imbalance in extensions of the B-share market. This figure shows the momentum profits and t-statistics under the lowest daily relative order imbalance in extensions of the B-share market. The formation and holding periods, respectively, range from 1 day to 30 days.

4.3.2. Accumulative Relative Order Imbalance in Extensions of the B-Share Market. In this section, we show the momentum profits and t-statistics under the highest accumulative relative order imbalance and the lowest accumulative relative order imbalance in extensions of the B-share market. Figures 10 and 11 contain the outcomes.

We can see that the momentum profits vary from −0.15 to 0.05 under the highest accumulative relative order imbalance from Figure 10. In addition, the t-statistics lie between −4 and 8. The majority of absolute t-statistics changes around 2, but some of them are close to 0. However, the counterpart of t-statistics from A-share market varies from −10 to 10, which is much higher than the B-share market. In addition, just a small number of t-statistics in A-share market approaches 0. Overall, the effect of the highest accumulative relative order imbalance is stronger in A-share market than in B-share market.

From Figure 11, we know that the momentum profits are between −0.2 and 0.06 under the lowest accumulative relative order imbalance, which is similar to those from the highest accumulative relative order imbalance. Moreover, most of absolute t-statistics under the lowest accumulative relative order imbalance are over 2 and some of them are close to 0, which is also similar to those under the highest

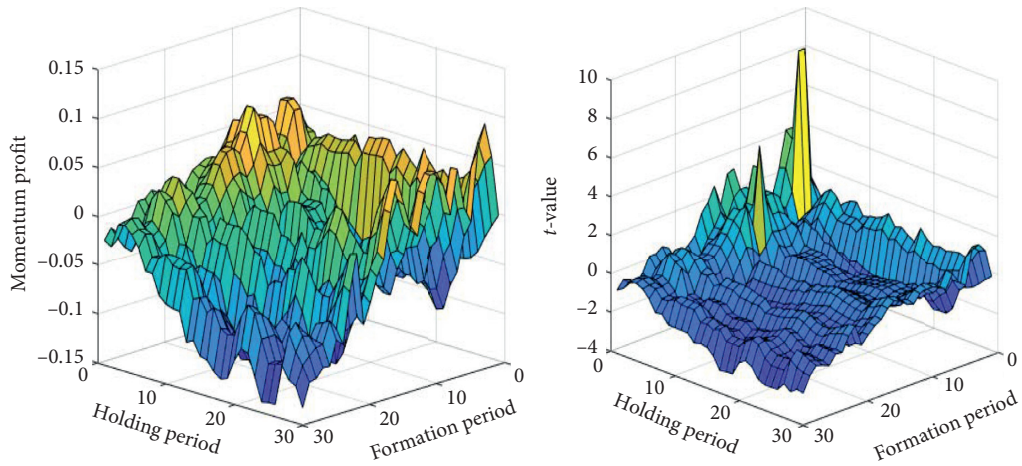

Figure 10: Highest accumulative relative order imbalance in extensions of the B-share market. This figure shows the momentum profits and t-statistics under the highest accumulative relative order imbalance in extensions of the B-share market. The formation and holding periods, respectively, range from 1 day to 30 days.

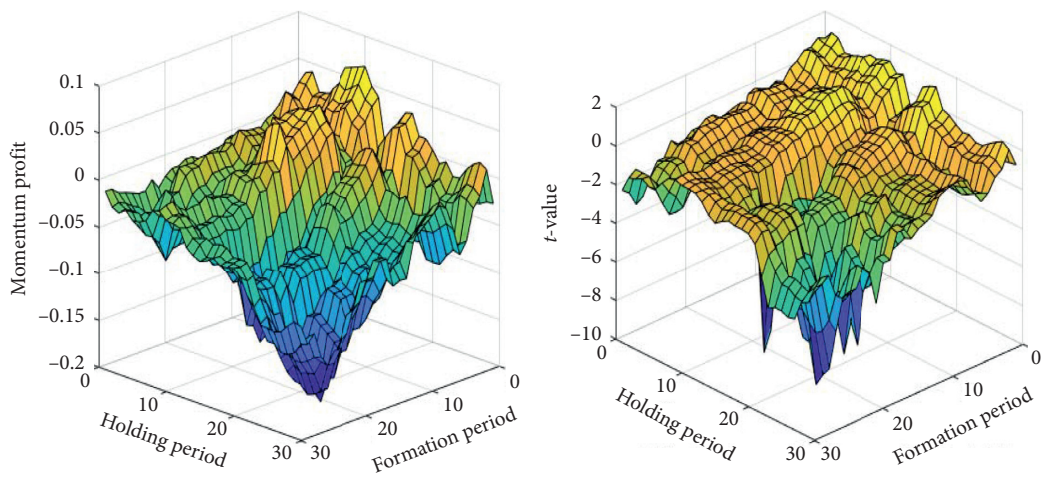

Figure 11: Lowest accumulative relative order imbalance in extensions of the B-share market. This figure shows the momentum profits and t-statistics under the lowest accumulative relative order imbalance in extensions of the B-share market. The formation and holding periods, respectively, range from 1 day to 30 days.

accumulative relative order imbalance. These outcomes suggest that no evidence proves accumulative relative order imbalance affects momentum profits in the B-share market. Furthermore, the counterpart of absolute t-statistics from A-share market is mainly over 5 and there is just very small number of them reaching 0, implying that the effect of the lowest accumulative relative order imbalance is also stronger in A-share market than in B-share market.

5. Robustness Checks

In Section 3, our analyses for the effects of anxiety on momentum profits in the A-share market are based on a 5-group basis, so we retest the effects of anxiety on momentum profits by 3-group analyses. Because no effect of anxiety on momentum profits is observed in all testing periods by 3-group analyses in the B-share market, we do not check the results here. Table 8 detects instantaneous anxiety (the daily relative order imbalance), and Table 9 investigates accumulative anxiety (the accumulative relative order imbalance).

From Table 8, it can be seen that the results for the Chinese A-share stocks are totally consistent with prior findings. The lowest instantaneous anxiety (highest daily relative order imbalance) generates the most significantly positive momentum profits in the very short run (the t-statistics are 18.116, 8.7766, and 5.0269, respectively, for the 1-day, 2-day, and 3-day periods). In the relatively long run comprising 30 days and 90 days, the lowest instantaneous anxiety turns to generate the most significantly negative momentum profits (the absolute t-statistics are 23.6567 and 28.479, respectively). The highest instantaneous anxiety (lowest daily relative order imbalance) stocks have the least significantly negative momentum profits with absolute t-statistics no higher than 22. These outcomes again prove that the lowest instantaneous anxiety most violently

Table 8: The effect of the daily relative order imbalance: three groups.

Panel A: $F = H = 1$ day			
ROI	Highest	2	Lowest
MP	0.0043	0.0010	0.0025
t-stat	18.1160	5.1436	12.0772
Panel B: $F = H = 2$ days			
ROI	Highest	2	Lowest
MP	0.0027	0.0001	0.0009
t-stat	8.7766	0.4354	3.3701
Panel C: $F = H = 3$ days			
ROI	Highest	2	Lowest
MP	0.0018	0.0000	0.0006
t-stat	5.0259	0.0732	2.0503
Panel D: $F = H = 30$ days			
ROI	Highest	2	Lowest
MP	−0.0218	−0.0177	−0.0153
t-stat	−23.6567	−19.6732	−16.5390
Panel E: $F = H = 90$ days			
ROI	Highest	2	Lowest
MP	−0.0422	−0.0353	−0.0306
t-stat	−28.4790	−24.1903	−21.3626

This table presents the daily momentum profits (MP) and related t-statistics (t-stat) of the A-share stocks. F and H represent the length of the formation and holding periods, respectively. For each day, we calculate the daily relative order imbalance for every stock and sort the stocks according to the daily relative order imbalance for that day. Within each group based on previous sorts, we select the winner and loser stocks according to the past price growth rate in the formation period and then calculate the momentum profit (average winner-minus-loser return spread) in the holding period. We first test the momentum profits in the very short run. The most natural choice is 1 day, and we also calculate the momentum profits for 2 days and 3 days for robustness. In addition, we further test the momentum profits for 30 days and 90 days to see how they behave in the relatively long run. The sorts based on the daily relative order imbalance (ROI) are classified into 3 groups. Winner stocks are the one-third of stocks with the highest price growth rate, while loser stocks are the one-third of stocks with the lowest price growth rate. The formation and holding periods have the same length according to Verardo [66], Avramov et al. [67], and Hillert et al. [31]. The critical value of 5% significance of t-statistic is 1.96.

Table 9: The effect of the accumulative relative order imbalance: three groups.

Panel A: $F = H = 1$ day			
ACCI	Highest	2	Lowest
MP	0.0021	0.0019	0.0029
t-stat	10.2420	8.4455	11.9803
Panel B: $F = H = 2$ days			
ACCI	Highest	2	Lowest
MP	0.0011	0.0006	0.0011
t-stat	4.3076	2.1889	3.4861
Panel C: $F = H = 3$ days			
ACCI	Highest	2	Lowest
MP	0.0012	0.0004	0.0003
t-stat	3.8767	1.3551	0.8205
Panel D: $F = H = 30$ days			
ACCI	Highest	2	Lowest
MP	−0.0110	−0.0152	−0.0237
t-stat	−12.2302	−17.1343	−25.3270
Panel E: $F = H = 90$ days			
ACCI	Highest	2	Lowest
MP	−0.0255	−0.0338	−0.0438
t-stat	−17.8584	−23.1833	−29.6983

This table presents the daily momentum profits (MP) and related t-statistics (t-stat) of the A-share stocks. F and H represent the length of the formation and holding periods, respectively. On each day, the accumulative relative order imbalance (ACCI = neg% − pos%) for each stock is obtained in the formation period and we initially classify the stocks based on ACCI. Then, in each group from the previous classifications, the stocks are sorted based on the past price growth rate in the formation period in order to identify winner and loser stocks. The momentum profits (average winner-minus-loser return spread) are thus calculated in the holding period. We first test the momentum profits in the very short run. The most natural choice is 1 day, and we also calculate the momentum profits for 2 days and 3 days for robustness. In addition, we further test the momentum profits for 30 days and 90 days to see how they behave in the relatively long run. The sorts based on ACCI are categorized into 3 groups. Winner stocks consist of the one-third of stocks with the highest price growth rate, while loser stocks are made up of the one-third of stocks with the lowest price growth rate. The formation and holding periods have the same length according to Verardo [66], Avramov et al. [67], and Hillert et al. [31]. The critical value of 5% significance of t-statistic is 1.96.

induces price momentum in the very short run but results in price reversals in the long run (we also run the linear regressions by regressing the momentum profit of the market as a whole on daily relative order imbalance of the market as a whole; we find that most of the absolute t-statistics of slopes from ROI are higher than 2 or even higher than 6).

In Table 9 on accumulative anxiety, the results remain basically same as what we discovered in Section 3. From the 1-day period in Panel A, for the lowest accumulative anxiety (lowest ACCI), the positive momentum profit obtains the highest value with a t-statistic of 11.9803. In the long run covering 30 days and 90 days, the lowest accumulative anxiety generates the most significantly negative momentum profits with absolute t-statistics of 25.327 and 29.6983, respectively. Although for the 2-day and 3-day periods, the lowest accumulative anxiety does not give rise to the most significantly positive momentum profits (the t-statistics are 3.4861 and 0.8205, respectively), the results for the 1-day, 30-day, and 90-day periods still support what we find in Section 3 (we also run the linear regressions by regressing the momentum profit of the market as a whole on the accumulative relative order imbalance of the market as a whole; we find that most of the absolute t-statistics of slopes from ACCI range from 4 to 9).

6. Conclusions

In this paper, we address the effects of investor anxiety on momentum in the Shanghai and Shenzhen stock exchanges from the perspectives of instantaneous anxiety and accumulative anxiety. The stocks held by the least anxious investors generate the strongest price momentum, while the stocks held by the most anxious investors stimulate much weaker momentum. However, when extending the examination periods, we perceive that price reversals prevail across various degrees of anxiety. Moreover, the risk adjustments by asset pricing models document the results are very stable. We infer that the impact of anxiety stems

Table 10: Institutional investors in the A-share and B-share markets.

Total Average	A-share market	B-share market
Investment fund	4.5718	0
Overseas investors	1.9041	2.8366
Brokers	1.8350	2.2429
Insurance corporations	2.2585	0
Security fund	1.6483	0
Entrust fund	2.6657	14.1800
Finance corporations	1.3673	0
Banks	3.4651	4.0750
Total proportion	19.7156	23.3345

This table presents the proportion (percentage) of shares held by institutional investors in the A-share and B-share markets from the year 2007 to the year 2018. The type of institutional investors includes investment fund, overseas investors, brokers, insurance corporations, security fund, entrust fund, finance corporations, and banks.

from the dominant role played by retail investors in the Chinese stock market.

The retail investors lack sufficient professional knowledge and good information sources compared to the institutional investors, so they always confront difficulties in decision making and anxiety behaves as one of their intrinsic characteristics. The lowest degree of anxiety denotes extreme optimism, with the result that the retail investors will not update their information in time in the short run, thereby initially letting mispricing come into being. This tendency implies an underreaction to information, forcing the stock prices to deviate from their fundamentals in the short run and thus price momentum turns to be evident. As time goes by, once the retail investors perceive the upcoming information is beyond expectations, they are possible to overreact to information and adjust past decisions. The initial mispricing will be corrected toward fundamentals and price reversals thus occur.

To the best of our knowledge, past studies detect disposable panic, but they do not devote to the discussions on the intrinsic anxiety from retail investors (e.g., [69–71]). Our experiments based on daily data exactly reflect the day-to-day anxiety from retail investors. Since the Chinese A-share market is tightly dominated by retail investors, the A-share market is very prone to the disturbance from anxiety, so we have no reason to neglect the role of anxiety. One of our notable contributions in this paper is that we discover price reversals of A-share market are derived from the overreactions induced by anxiety, enriching the perceptions on investor behaviors with respect to the effects of intrinsic anxiety from retail investors on momentum and reversal. Overall, we find that the A-share market is more likely to exhibit subtle momentum with higher anxiety, but the B-share market is easier to encounter considerable momentum with lower anxiety.

This research further reveals the behaviors of retail investors in the Chinese stock market. We have discussed instantaneous anxiety and accumulative anxiety in this paper, but an important issue is that how such anxiety transfers among investors. In addition, whether the resulting transfer releases an influence on the stock market should prove to be fruitful in future research.

Appendix

A. Details of the Conditional Momentum Portfolio

In the conditional momentum portfolio, the stocks are classified sequentially. Let ψ denote the investor anxiety of every stock in the formation period. First, all stocks are divided into Q groups via ψ. Second, in each group stemming from ψ, the stocks are further sorted into Q groups according to the formation price growth rate, P_G. The subscript Q denotes the highest level of the price growth rate or investor anxiety. These two classifications trigger Q^2 portfolios. The studies of Chang et al. [72], Kim and Suh [59], and Celiker et al. [62] implement the same portfolio.

$$\mathrm{Con}(\psi, P_G) = \begin{bmatrix} \Omega_t(P_{G,1} \mid \psi_1) & \Omega_t(P_{G,2} \mid \psi_1) & \cdots & \Omega_t(P_{G,Q} \mid \psi_1) \\ \Omega_t(P_{G,1} \mid \psi_2) & \Omega_t(P_{G,2} \mid \psi_2) & \cdots & \Omega_t(P_{G,Q} \mid \psi_2) \\ \vdots & \vdots & \vdots & \vdots \\ \Omega_t(P_{G,1} \mid \psi_Q) & \Omega_t(P_{G,2} \mid \psi_Q) & \cdots & \Omega_t(P_{G,Q} \mid \psi_Q) \end{bmatrix}. \tag{A.1}$$

From the matrix above, Q momentum profits are obtained as

$$\begin{aligned} \mathrm{MP}_{\psi_1}^{\mathrm{Con}} &= \frac{1}{n}\sum_{q=1}^{n}\left[\overline{R_{H_q}^{\Omega_t(P_{G,Q}\mid\psi_1)}} - \overline{R_{H_q}^{\Omega_t(P_{G,1}\mid\psi_1)}}\right], \\ \mathrm{MP}_{\psi_2}^{\mathrm{Con}} &= \frac{1}{n}\sum_{q=1}^{n}\left[\overline{R_{H_q}^{\Omega_t(P_{G,Q}\mid\psi_2)}} - \overline{R_{H_q}^{\Omega_t(P_{G,1}\mid\psi_2)}}\right], \\ &\vdots \\ \mathrm{MP}_{\psi_Q}^{\mathrm{Con}} &= \frac{1}{n}\sum_{q=1}^{n}\left[\overline{R_{H_q}^{\Omega_t(P_{G,Q}\mid\psi_Q)}} - \overline{R_{H_q}^{\Omega_t(P_{G,1}\mid\psi_Q)}}\right]. \end{aligned} \tag{A.2}$$

B. Constructions of the Pricing Factors

The capital asset pricing model, Chinese three-factor asset pricing model [38], and Fama–French three-factor asset pricing model [37] are used in this paper to adjust risks. We describe the construction procedures of these factors in this appendix.

MKT_t: the market risk factor of the capital asset pricing model is calculated as the daily value-weighted market return in excess of the daily risk-free rate.

$\mathrm{SMB}_t^{\mathrm{CH}}$ and $\mathrm{VMG}_t^{\mathrm{CH}}$: the Chinese size ($\mathrm{SMB}_t^{\mathrm{CH}}$) and value ($\mathrm{VMG}_t^{\mathrm{CH}}$) factors of Liu et al. [38] are calculated as follows. Following Liu et al. [38], in each month $t-1$, we delete the smallest 30% of stocks in the market based on market capitalization. The remaining 70% of stocks make up the sample for factor constructions. We sort the stocks into 2

groups denoted as the big and small groups based on market capitalization in month $t-1$. Independently, the stocks are sorted based on the most recent earnings-to-price ratios into 3 groups constituting the high, medium, and low groups. Besides, the intersections of these sorts give rise to 6 groups and we compute the daily returns of these groups in month t. The Chinese size factor is calculated by the simple average of the return spreads between the 3 small groups and 3 big groups (small minus big). The Chinese value factor is the simple average of the return spreads between 2 high groups and 2 low groups (high minus low). The earnings calculation follows the definition in Section 2.5, and so the earnings-to-price ratio is the ratio of earnings to market capitalization. Market capitalization is the product of the stock price and the number of shares.

$\mathrm{SMB}_t^{\mathrm{FF}}$ and $\mathrm{HML}_t^{\mathrm{FF}}$: the size ($\mathrm{SMB}_t^{\mathrm{FF}}$) and value ($\mathrm{HML}_t^{\mathrm{FF}}$) factors of Fama and French [37] are obtained as follows. According to Fama and French [37], in June of each year t, we classify all stocks into 2 groups based on the market capitalization of that month. Independently, all stocks are classified into 3 groups by the book-to-market ratio in December of each year $t-1$. From July of year t to June of year $t+1$, the daily returns of these 6 groups are generated. The Fama–French size factor is the simple average of the return spreads between the 3 small groups and 3 big groups (small minus big), while the corresponding value factor is the simple average of the return spreads between the 2 high groups and 2 low groups (high minus low). The book-to-market ratio is the ratio of book equity to market capitalization.

C. Proportion of Shares Held by Institutional Investors in the A-Share and B-Share Markets

This appendix shows the proportion of shares held by institutional investors in the A-share and B-share markets. The type of institutional investors includes investment fund, overseas investors, brokers, insurance corporations, security fund, entrust fund, finance corporations, and banks. The data are collected from China Stock Market and Accounting Research (CSMAR) database.

From Table 10, we can see the proportion of shares held by different types of institutional investors. Although all types of institutional investors hold the A-share stocks, the total proportion is 19.7156%. On the contrary, the total proportion of B-share market is 23.3345%, which is 3.6189% higher than the A-share market.

Data Availability

All data used to support the findings of this study were supplied by China Stock Market and Accounting Research (CSMAR) database under license and so cannot be made freely available. Requests for access to these data should be made to GTA corporation (e-mail: market@gtafe.com).

Conflicts of Interest

The authors declare that they have no conflicts of interest.

References

[1] C.-M. Cheng, A. YiHou Huang, and M.-C. Hu, "Investor attention and stock price movement," *Journal of Behavioral Finance*, vol. 20, no. 3, pp. 294–303, 2019.

[2] M. W. Uhl, "Reuters sentiment and stock returns," *Journal of Behavioral Finance*, vol. 15, no. 4, pp. 287–298, 2014.

[3] C. Antoniou, J. A. Doukas, and A. Subrahmanyam, "Cognitive dissonance, sentiment, and momentum," *Journal of Financial and Quantitative Analysis*, vol. 48, no. 1, pp. 245–275, 2013.

[4] L. Chi, X. Zhuang, and D. Song, "Investor sentiment in the Chinese stock market: an empirical analysis," *Applied Economics Letters*, vol. 19, no. 4, pp. 345–348, 2012.

[5] S. Akhtar, R. Faff, B. Oliver, and A. Subrahmanyam, "The power of bad: the negativity bias in Australian consumer sentiment announcements on stock returns," *Journal of Banking & Finance*, vol. 35, no. 5, pp. 1239–1249, 2011.

[6] M. Schmeling, "Investor sentiment and stock returns: some international evidence," *Journal of Empirical Finance*, vol. 16, no. 3, pp. 394–408, 2009.

[7] P. C. Tetlock, "Giving content to investor sentiment: the role of media in the stock market," *The Journal of Finance*, vol. 62, no. 3, pp. 1139–1168, 2007.

[8] M. Baker and J. Wurgler, "Investor sentiment and the cross-section of stock returns," *The Journal of Finance*, vol. 61, no. 4, pp. 1645–1680, 2006.

[9] A. Kumar and C. M. C. Lee, "Retail investor sentiment and return comovements," *The Journal of Finance*, vol. 61, no. 5, pp. 2451–2486, 2006.

[10] W. Y. Lee, C. X. Jiang, and D. C. Indro, "Stock market volatility, excess returns, and the role of investor sentiment," *Journal of Banking & Finance*, vol. 26, no. 12, pp. 2277–2299, 2002.

[11] K. L. Fisher and M. Statman, "Investor sentiment and stock returns," *Financial Analysts Journal*, vol. 56, no. 2, pp. 16–23, 2000.

[12] H. Hong and J. C. Stein, "A unified theory of underreaction, momentum trading, and overreaction in asset markets," *The Journal of Finance*, vol. 54, no. 6, pp. 2143–2184, 1999.

[13] R. J. Shiller, "Speculative prices and popular models," *Journal of Economic Perspectives*, vol. 4, no. 2, pp. 55–65, 1990.

[14] W. F. M. De Bondt and R. H. Thaler, "Further evidence on investor overreaction and stock market seasonality," *The Journal of Finance*, vol. 42, no. 3, pp. 557–581, 1987.

[15] R. J. Shiller, "Investor behavior in the october 1987 stock market crash: survey evidence," National Bureau of Economic Research Working Paper Series (w2446), 1987.

[16] S. A. Green and A. Ben-Sasson, "Anxiety disorders and sensory over-responsivity in children with autism spectrum disorders: is there a causal relationship?" *Journal of Autism and Developmental Disorders*, vol. 40, no. 12, pp. 1495–1504, 2010.

[17] R. A. Peterson and K. Plehn, "Measuring anxiety sensitivity," *Anxiety Sensitivity: Theory, Research, and Treatment of the Fear of Anxiety*, pp. 61–81, 1999.

[18] R. B. Malmo, "Studies of anxiety: some clinical origins of the activation concept," *Anxiety and Behavior*, Academic Press, Cambridge, MA, USA, pp. 157–177, 1966.

[19] N. Jegadeesh and S. Titman, "Returns to buying winners and selling losers: implications for stock market efficiency," *The Journal of Finance*, vol. 48, no. 1, pp. 65–91, 1993.

[20] W. F. M. De Bondt and R. Thaler, "Does the stock market overreact?" *The Journal of Finance*, vol. 40, no. 3, pp. 793–805, 1985.

[21] E. Gilbert and K. Karahalios, "Widespread worry and the stock market," in *Proceedings of the Fourth International AAAI Conference on Weblogs and Social Media*, Washington, DC, USA, 2010, May.
[22] C. D. Spielberger, "State-trait anxiety inventory," *The Corsini Encyclopedia of Psychology*, p. 1, 2010.
[23] P. Ekman, "Emotions revealed," *BMJ*, vol. 328, no. 5, Article ID 0405184, 2004.
[24] B. B. Lahey, S. A. Schneider, R. E. Landrum, and T. Landrum, *Psychology: An Introduction*, Brown & Benchmark Publishers, New York, NY, USA, 1995.
[25] W. K. Estes and B. F. Skinner, "Some quantitative properties of anxiety," *Journal of Experimental Psychology*, vol. 29, no. 5, pp. 390–400, 1941.
[26] D. G. Myers, *Psychology: Myers in Modules*, Worth Publishers, New York, NY, USA, 2001.
[27] R. L. Peterson, "Affect and financial decision-making: how neuroscience can inform market participants," *Journal of Behavioral Finance*, vol. 8, no. 2, pp. 70–78, 2007.
[28] M. W. Passer and R. E. Smith, *Psychology: Frontiers and Applications*, McGraw-Hill, Boston, MA, USA, 2000.
[29] B. Lauterbach and U. Ben-Zion, "Stock market crashes and the performance of circuit breakers: empirical evidence," *The Journal of Finance*, vol. 48, no. 5, pp. 1909–1925, 1993.
[30] A. Goyal and S. Wahal, "Is momentum an echo?" *Journal of Financial and Quantitative Analysis*, vol. 50, no. 6, pp. 1237–1267, 2015.
[31] A. Hillert, H. Jacobs, and S. Müller, "Media makes momentum," *Review of Financial Studies*, vol. 27, no. 12, pp. 3467–3501, 2014.
[32] C. S. Asness, T. J. Moskowitz, and L. H. Pedersen, "Value and momentum everywhere," *The Journal of Finance*, vol. 68, no. 3, pp. 929–985, 2013.
[33] S. Wahal and M. D. Yavuz, "Style investing, comovement and return predictability," *Journal of Financial Economics*, vol. 107, no. 1, pp. 136–154, 2013.
[34] J. Mossin, "Equilibrium in a capital asset market," *Econometrica*, vol. 34, no. 4, pp. 768–783, 1966.
[35] J. Lintner, "The valuation of risk assets and the selection of risky investments in stock portfolios and capital budgets," *The Review of Economics and Statistics*, vol. 47, no. 1, pp. 13–37, 1965.
[36] W. F. Sharpe, "Capital asset prices: a theory of market equilibrium under conditions of risk," *The Journal of Finance*, vol. 19, no. 3, pp. 425–442, 1964.
[37] E. F. Fama and K. R. French, "Common risk factors in the returns on stocks and bonds," *Journal of Financial Economics*, vol. 33, no. 1, pp. 3–56, 1993.
[38] J. Liu, R. F. Stambaugh, and Y. Yuan, "Size and value in China," *Journal of Financial Economics*, vol. 134, no. 1, pp. 48–69, 2019.
[39] Z. Chen and A. Lu, "Slow diffusion of information and price momentum in stocks: evidence from options markets," *Journal of Banking & Finance*, vol. 75, pp. 98–108, 2017.
[40] G. G. Booth, H. G. Fung, and W. K. Leung, "A risk-return explanation of the momentum-reversal "anomaly"" *Journal of Empirical Finance*, vol. 35, pp. 68–77, 2016.
[41] R. D. McLean, "Idiosyncratic risk, long-term reversal, and momentum," *Journal of Financial and Quantitative Analysis*, vol. 45, no. 4, pp. 883–906, 2010.
[42] C. Wang and L. Xie, "Information diffusion and overreaction: evidence from the Chinese stock market," *Emerging Markets Finance and Trade*, vol. 46, no. 2, pp. 80–100, 2010.
[43] J. Kang, M.-H. Liu, and S. X. Ni, "Contrarian and momentum strategies in the China stock market: 1993-2000," *Pacific-Basin Finance Journal*, vol. 10, no. 3, pp. 243–265, 2002.
[44] Z. Gao, H. Ren, and B. Zhang, "Googling investor sentiment around the world," *Journal of Financial and Quantitative Analysis*, vol. 55, no. 2, pp. 549–580, 2016.
[45] G. Kaplanski and H. Levy, "Sentiment and stock prices: the case of aviation disasters," *Journal of Financial Economics*, vol. 95, no. 2, pp. 174–201, 2010.
[46] G. Boyle and B. Walter, "Reflected glory and failure: international sporting success and the stock market," *Applied Financial Economics*, vol. 13, no. 3, pp. 225–235, 2003.
[47] A. Fostel and J. Geanakoplos, "Leverage cycles and the anxious economy," *American Economic Review*, vol. 98, no. 4, pp. 1211–1244, 2008.
[48] M. J. Kamstra, L. A. Kramer, and M. D. Levi, "Losing sleep at the market: the daylight saving anomaly," *American Economic Review*, vol. 90, no. 4, pp. 1005–1011, 2000.
[49] O. Levy and I. Galili, "Stock purchase and the weather: individual differences," *Journal of Economic Behavior & Organization*, vol. 67, no. 3-4, pp. 755–767, 2008.
[50] H.-H. Huang, M.-L. Chan, I.-H. Huang, and C.-H. Chang, "Stock price volatility and overreaction in a political crisis: the effects of corporate governance and performance," *Pacific-Basin Finance Journal*, vol. 19, no. 1, pp. 1–20, 2011.
[51] J. R. Nofsinger, "Social mood and financial economics," *Journal of Behavioral Finance*, vol. 6, no. 3, pp. 144–160, 2005.
[52] G. Barlevy and P. Veronesi, "Rational panics and stock market crashes," *Journal of Economic Theory*, vol. 110, no. 2, pp. 234–263, 2003.
[53] D. Coon and J. O. Mitterer, *Introduction to Psychology: Gateways to Mind and Behavior with Concept Maps and Reviews*, Cengage Learning, Boston, MA, USA, 2012.
[54] C. Peterson, *Psychology: A Biopsychosocial Approach*, Longman, New York, NY, USA, 1997.
[55] J. L. Valls, *Freudian Dictionary: A Comprehensive Guide to Freudian Concepts*, Routledge, London, UK, 2019.
[56] J. Webster, *Conversion Disorder: Listening to the Body in Psychoanalysis*, Columbia University Press, New York, NY, USA, 2018.
[57] B. B. Wolman, *Logic of Science in Psychoanalysis*, Columbia University Press, New York, NY, USA, 1984.
[58] Z. Da, U. G. Gurun, and M. Warachka, "Frog in the pan: continuous information and momentum," *Review of Financial Studies*, vol. 27, no. 7, pp. 2171–2218, 2014.
[59] B. Kim and S. Suh, "Sentiment-based momentum strategy," *International Review of Financial Analysis*, vol. 58, pp. 52–68, 2018.
[60] L. Menkhoff, L. Sarno, M. Schmeling, and A. Schrimpf, "Currency momentum strategies," *Journal of Financial Economics*, vol. 106, no. 3, pp. 660–684, 2012.
[61] R. Novy-Marx, "Is momentum really momentum?" *Journal of Financial Economics*, vol. 103, no. 3, pp. 429–453, 2012.
[62] U. Celiker, N. V. Kayacetin, R. Kumar, and G. Sonaer, "Cash flow news, discount rate news, and momentum," *Journal of Banking & Finance*, vol. 72, pp. 240–254, 2016.
[63] Y. Chen and H. Zhao, "Informed trading, information uncertainty, and price momentum," *Journal of Banking & Finance*, vol. 36, no. 7, pp. 2095–2109, 2012.
[64] L. Garlappi and H. Yan, "Financial distress and the cross-section of equity returns," *The Journal of Finance*, vol. 66, no. 3, pp. 789–822, 2011.
[65] D. C. Montgomery, *Design and Analysis of Experiments*, John Wiley & Sons, Hoboken, NJ, USA, 2017.

[66] M. Verardo, "Heterogeneous beliefs and momentum profits," *Journal of Financial and Quantitative Analysis*, vol. 44, no. 4, pp. 795–822, 2009.
[67] D. Avramov, T. Chordia, G. Jostova, and A. Philipov, "Momentum and credit rating," *The Journal of Finance*, vol. 62, no. 5, pp. 2503–2520, 2007.
[68] H. White, "A heteroskedasticity-consistent covariance matrix estimator and a direct test for heteroskedasticity," *Econometrica*, vol. 48, no. 4, pp. 817–838, 1980.
[69] M. Schaub, "Investor overreaction to going concern audit opinion announcements," *Applied Financial Economics*, vol. 16, no. 16, pp. 1163–1170, 2006.
[70] B. Hayo and A. M. Kutan, "IMF-related news and emerging financial markets," *Journal of International Money and Finance*, vol. 24, no. 7, pp. 1126–1142, 2005.
[71] A. Kutan and B. Sudjana, "Investor reaction to IMF actions in the Indonesian financial crisis," *The Journal of Policy Reform*, vol. 6, no. 3, pp. 181–190, 2003.
[72] R. P. Chang, K.-C. Ko, S. Nakano, and S. Ghon Rhee, "Residual momentum in Japan," *Journal of Empirical Finance*, vol. 45, pp. 283–299, 2018.

Hindawi
Complexity
Volume 2020, Article ID 5745916, 10 pages
https://doi.org/10.1155/2020/5745916

Research Article

Institutional Investor Information Sharing, Stock Market Extreme Risk, and Financial Systemic Risk

Xiao-Li Gong and Zhi-Qiang Du

School of Economics, Qingdao University, Qingdao, 266061, China

Correspondence should be addressed to Xiao-Li Gong; qdgongxiaoli@126.com

Received 3 December 2019; Revised 15 February 2020; Accepted 17 March 2020; Published 9 April 2020

Academic Editor: Dehua Shen

To analyze whether information sharing in the institutional investors plays the role of a market stabilizer or risk booster, this paper constructs the institutional investor information network employing the common holding stocks of the mutual funds as links. The information linkages between two funds with large positions in the same stock are hypothesized to be connected to each other. Then, we use the information sharing efficiency in the fund networks to study the effects of information transmission on stock market extreme risk and financial systemic risk. Especially, the speed of information diffusion in the network is characterized by the topology structures based on social network theory. Empirical research studies find that the Chinese fund information network exhibits small-world characteristics, which reflects rapid speed of information diffusion. Seen from the idiosyncratic risk of volatility, information sharing of institutional investors can improve the behavior consistency of fund managers, thus increasing the stock volatility via herd effects. Besides, it can be concluded that institutional investor information sharing can reduce the extreme risk by promoting the comprehensiveness of information flow and the market pricing efficiency of stocks, thereby reducing the degree of financial systemic risk. The obtained conclusions provide suggestions for decision-making of institutional investors. It can help the regulators to pay attention to the herd effects so as to control systemic risk.

1. Introduction

In recent years, the China Securities Regulatory Commission vigorously develops institutional investors. This strategy changes the situation in the Chinese capital market which is dominated by retail investors. In 2019, retail investors accounted for 31.4% of the market capitalization, and institutional investors accounted for 53.2% of the market capitalization. In the Chinese financial market, institutional investors are mainly based on securities investment funds. Due to its professional team and information advantages, institutional investors can easily trigger the herd effects of trading behavior through mutual learning and imitation in the same social ties [1]. Along with the booming development of institutional investors, China's stock market has become increasingly volatile. Also, the extreme risks of stock market occur more frequently. In addition to the subprime mortgage crisis in 2008, thousands of stocks fell in June 2015 due to the stock market crash in China. Hence, it led to the discussion that whether institutional investors play the role of amplifying market volatility due to herding behaviors [2], or stabilize the market with professional research teams [3].

Since the linkage between institutional investors has been strengthened, it means that there exists endogenous risk contagion in the stock markets. Therefore, it is meaningful to study the impact of information diffusion of institutional investor networks on stock market extreme risk and financial systemic risk. It can provide references for regulators to maintain financial stability and prevent financial crises caused by systemic risk contagion.

Investors often actively seek private information through social relationships when making decisions [4–6]. Fund managers in the same information network tend to display more obvious herd effects [7]. Information exchanges among investors can affect the stock price volatility [8–10]. In order to analyze the influence mechanism of institutional

investors on the financial risks, it is necessary to analyze the information dissemination features of this community. In recent years, financial networks have become an efficient tool in studying financial risk transmission as well as information dissemination [11, 12]. Networks play a vital role in the information flow through financial markets. Colla and Mele [13] found that closely related investor behaviors in the information networks are more likely to produce herd effects. Sharing private information among fund managers is the rational choice for maximizing their own interests [14]. Moreover, the topological structure characteristics of the social networks among fund managers can affect the effectiveness of information exchange and risk contagion [15]. According to Pareek [7], an information or stock ownership linkage between two mutual funds is defined by large positions in the same stock. The stock information network corresponds to the fund manager set amongst whom information concerning stock diffuses via word of mouth or via common sources of private information. Hence, this paper assumes that there exists private information exchange between the funds that have common holdings of stocks. Besides, previous studies have found that the formation of information networks is mainly based on social relationships and asset allocation [16]. Then, the institutional investor network can be constructed using the common holding stocks of the mutual funds as links. Further, we can analyze the impacts of information sharing efficiency in the network on stock price volatility and systemic risks.

Stock volatility cannot be directly observed, which needs to be extracted from the returns. The risk driven by the common components of economic fundamentals cannot be dispersed, while the idiosyncratic risk of individual stocks can be managed. Although the beta risk in the CAPM model or the Fama-French three-factor model can calculate the individual stock volatility, it does not examine the extracted idiosyncratic risk from the stock market when faced with common shocks. Especially, when calculating idiosyncratic risks, high-dimensional time series are prone to the "curse of dimensionality" problem. To tackle this problem, Barigozzi and Hallin [17] extended the generalized dynamic factor model (GDFM) based on Forni et al. [18] to decompose the stock volatility into the common shock-driven components and the idiosyncratic components. Then, it extracts the market volatility shock to investigate the volatility spillover effects. The advantage of GDFM is that it can achieve dimensionality reduction for high-dimensional data in the stock market without losing information. Therefore, we continue to employ this method for calculating idiosyncratic stock volatility.

Financial systemic risk denotes the risk that causes financial system damage and the financial service interruption, which will seriously harm the real economy. Adrian and Brunnermeier [19] proposed the notion of the conditional value at risk (CoVaR) based on VaR, which refers to the risk value of other institutions or the entire financial system when the particular institution is in a certain state. Rodríguez-Moreno and Peña [20] pointed out that ΔCoVaR can well capture the tail risk in extreme cases. Acharya et al. [21] proposed the concept of marginal expected loss (MES) based on ES, which represents the expected loss of single institution's returns when the entire financial market falls. Using CoVaR and MES to measure systemic risk has become the mainstream method for the current risk management, such as Karimalis and Nomikos [22]. The commonly used calculation methods for CoVaR include the quantile regression method, the GARCH-DCC model method, and the Copula method. As we all know, the volatility of financial returns shows stochastic volatility features. Hence, it is necessary to consider the clustering characteristic of financial returns when using financial data. Therefore, this paper utilizes the AR-GARCH-DCC-based method to calculate CoVaR and MES when calculating systemic risk.

At present, research studies on institutional investors mainly focus on the governance role [23, 24], paying less attention to their market behaviors. There are not yet researches on the relationship between information sharing efficiency and financial systemic risk from the perspective of institutional investor information networks. In this paper, we hypothesize that two fund managers allocating 5% or more of portfolio to the same stock are connected to each other. And, information about the same stock is likely to diffuse through common information sources. Then, it is significant to investigate the effect of information sharing in the institutional investor network on the financial risk in the stock market.

The innovative contributions of this study over the existing literature mainly include the following aspects. Primarily, the information network of institutional investors is constructed using the common holding stocks of fund as links. Specifically, we define the fund information network as all other funds which hold more than 5% of portfolio in any stock in which the fund has also invested at least 5% of its portfolio. The information linkages between two funds with large positions in the same stock are hypothesized to be connected to each other. Then, the network information diffusion features are characterized by the network topology structures. On this basis, we further analyze the relationship between the structure characteristics of the fund network and different financial risks (including idiosyncratic risk, extreme risk, and systemic risk). Secondly, concerning the volatility of individual stocks, the GDFM model is used to extract idiosyncratic volatility from high-dimensional data considering that the stock market will be affected by the common information flow. Thirdly, when calculating the financial systemic risk, the corresponding systemic risks are computed taking into account the clustering and stochastic volatility features of the stock data.

2. Model Framework

In this paper, we mainly focus on the trading behavior of transactional institutional investors, which are represented by the mutual equity investment funds. Institutional investors can directly exchange information and correct their cognitive bias through indirect social learning. The institutional investor network has an important impact on stock price volatility and stock market extreme risk, which further affects financial systemic risks. The extent of information

dissemination in the institutional investor network is related to the efficiency of information sharing. This paper employs the topological indicators reflecting the structure of the fund information network as the proxy variables of institutional investor information sharing efficiency. Specifically, the network centrality and network density indicators are mainly used to measure the efficiency of information sharing. Concerning the different sources of risks, it is divided into three levels, namely, the idiosyncratic risk of individual stocks, the extreme risk of the stock market, and the financial systemic risk.

2.1. Institutional Investor Information Network. In the institutional investor information network, if two funds hold common stocks with large position, then the two funds are defined to be in the same fund information network. The fund holding stocks with large position mean that the market value of the fund that hold the stock accounts for more than 5% of the total market capitalization of the shareholdings. Institutional investors need to rely on public information and private information in their decision-making processes. Public information refers to information obtained from the open market, such as historical transaction information, financial statement information, and the behavior of other investors. Private information mainly refers to the information disseminated by investors within a small scope and the unique information existing in the social relationships in which they are located. Due to the information sharing of private information, the herd effects of fund managers in the same information network are usually more obvious. Therefore, private information plays a vital role in the decision-making of institutional investors.

The information advantage of institutional investors' decision-making and trading behavior often comes from private information. Direct information exchange between institutional investors through social relations can verify the information they have. And through indirect social learning, they can correct their own cognitive biases. In the same information network, the sharing of private information improves the consistency of trading strategies, and the produced pseudoherding effects further affect the stock price volatility and financial risks. The fund information network is the collection of all other funds that are in the same information network. This paper uses the data of China's mutual funds to construct the institutional investor network model linked by the fund's common holding stocks. If institutional investors learn from each other through information networks, the structure of networks can help understand the process of information flow. The institutional investor network topology is utilized to characterize the information sharing efficiency, as well as the influence mechanism of institutional investor information sharing on the stock market extreme risk and financial systemic risk. Specifically, the information sharing efficiency of the investor network is characterized by the indicators including the degree of network centralization and the network density.

The degree of the centralization of the graph in the institutional investor network portrays the overall centrality of the network graph. It indicates how much the institutional investor network is constructed around certain special nodes, which can be calculated as follows:

$$\text{degree} = \sum_{k-1}^{N} \frac{\left(D\left(n_{\max}\right) - D\left(n_k\right)\right)}{(N-2)},$$
$$D\left(n_k\right) = \frac{d\left(n_k\right)}{(N-1)}, \tag{1}$$

where $d(n_k)$ represents the degree of node n_k in the network and $D(n_{\max})$ represents the maximum value of $D(n_k)$. The larger degree value means that there exist nodes that play critical roles in the propagation of network information, and these key nodes affect the speed of information diffusion in the network, accelerating the information spreading.

The network density in the institutional investor network denotes the ratio of the number of the actual edges E_i among the k_i neighbor nodes of node v_i and the total number of possible edges $M_{k_i}^2$, which is shown in formula (2). The network density of the node represents the closeness of the relationship between the node and its neighboring. The greater the network density of the node, the more obvious the clustering phenomenon in the network, which will hinder the comprehensive dissemination of information:

$$\text{density} = \frac{E_i}{M_{k_i}^2}, \tag{2}$$

in which the greater the value of the network density, the more "small groups" that are closely connected in the network. Such small groups often generate hindrance to the information transmission within the network for the sake of profit. Therefore, network density reflects the information transmission degree within the network.

Because of the strong social ties and effective information transmission channels between fund managers, the network formed by the interaction of institutional investors will produce herd effects within the community, which easily lead to extreme risks in the market. Furthermore, the financial systemic risk contagion can be analyzed by means of the network structure characteristics of information sharing among institutional investors.

2.2. Stock Market Extreme Risk and Financial Systemic Risk

2.2.1. Idiosyncratic Risk. Regarding the volatility of individual stocks, traditional methods such as the standard deviation, the GARCH model, and the CAPM model did not reasonably reflect the overall idiosyncratic risk of the stock market. However, the nonparametric generalized dynamic factor model can decompose the volatility sequence into the common factor-driven volatility component and the idiosyncratic volatility component.

When using high-dimensional data to calculate the idiosyncratic volatility risk in the stock market as a whole, it will face the "dimensional curse" problem.

Fan et al. [25] decomposed the covariance matrix of high-dimensional financial data into the sum of "low rank plus sparse" type, corresponding to the common components and the idiosyncratic components, respectively. Barigozzi and Hallin [17] proposed the two-stage GDFM method to decompose the overall volatility vector $\mathbf{Z}_n$ into the common volatility component and the idiosyncratic volatility component as shown in formula (3). Then, the idiosyncratic volatility of the stock market is extracted, and the decomposition of components is mainly based on the dynamic principal component concept of Brillinger:

$$\begin{aligned} \mathbf{Z}_{n,t} &= \mathbf{X}_{n,t} + \mathbf{Y}_{n,t} = \mathbf{B}_n(L)\mathbf{u}_t + \mathbf{Y}_{n,t}, \\ (\mathbf{I}_n - \mathbf{C}_n(L))\mathbf{Z}_{n,t} &= \mathbf{H}_n\mathbf{u}_t + (\mathbf{I}_n - \mathbf{C}_n(L))\mathbf{Y}_{n,t}, \end{aligned} \tag{3}$$

in which L represents the lag operator of the filter $\mathbf{B}_n$, the impact vector $\mathbf{u}_t$ represents the orthogonal white noise process, which is orthogonal to $\mathbf{Y}_{n,t}$ and can be loaded by the matrix load $\mathbf{H}_n$, $\mathbf{C}_n(L)$ denotes the block diagonal matrix of the filter, so that the VAR operator $\mathbf{I}_n - \mathbf{C}_n(L)$ has no characteristic roots in the unit circle and is square-addable, $\mathbf{H}_n$ denotes the full-rank matrix, and $(\mathbf{I}_n - \mathbf{C}_n(L))\mathbf{Y}_{n,t}$ represents the idiosyncratic volatility. Besides, the data-driven method is utilized to identify the number of factors q in $\mathbf{Z}_n$.

Through formula (3), the stock market volatility is decomposed into the volatility caused by the common market shock and the idiosyncratic volatility. And, the residuals of the common component $\mathbf{X}_n$ can be obtained via the method of Forni et al. [18], while the residuals of the idiosyncratic component $\mathbf{Y}_n$ can be obtained via univariate AR fitting. In addition, the shocks driving these two different types of volatility are mathematically orthogonal.

2.2.2. Extreme Risk. Financial risk measurement is the foundation of financial risk supervision, which requires efficient tools. Different from the idiosyncratic risk that reflects the idiosyncratic volatility component, the extreme risk mainly captures the tail risk of the stock market that is caused by an external tail event. The tail events that result in extreme risk are represented by the leptokurtosis and thick tail feature of return distribution as well as the stochastic volatility feature of returns. On this basis, the extreme risks caused by frequent tail events in the stock market can easily induce financial systemic risks. Then, the VaR and ES indicators are primarily employed to describe the extreme risk.

VaR is employed to determine the capital level that financial institutions need to retain in response to financial risks. Let r_{it} denote the returns of institution i at time t, $r_{it} = 100 \times (\ln P_{ti} - \ln P_{t,t-1})$. When the confidence level is $1-q$, VaR can be defined as $\Pr(r_{it} < \mathrm{VaR}^i_{q,t}) = q$. $\mathrm{VaR}^i_{q,t}$ can be understood as the q quantile of asset returns for institution i, whose value is generally negative. However, it mainly focuses on the risks of individual institutions and does not reflect the risks when the stability of the whole financial system is in distress.

ES represents the expected loss of individual institutions when the loss of asset returns exceeds VaR_α. Regarding the financial system in the crisis state as systemic events, and the threshold C which is used to define the stress event, then the expected loss ES of the financial system at time t can be defined as follows:

$$\mathrm{ES}_{m,t-1}(C) = E_{t-1}\left(r_{\mathrm{mt}} \mid r_{\mathrm{mt}} < C\right) = \sum_{i=1}^{N} w_{it} E_{t-1}\left(r_{it} \mid r_{\mathrm{mt}} < C\right). \tag{4}$$

2.2.3. Systemic Risk. When systemic risks accumulate to a certain degree, the release will cause a large number of institutions to be closed down. Then, it will cause the entire financial system to face systemic crisis. Conditional value at risk (CoVaR) refers to the risks that the overall financial system face when an institution is in crisis. It can be used to describe the risk spillover relationships between different institutions. It describes the risk degree that the entire financial system ultimately assumes from the information transmission through different channels. Assume that the $C(X^i)$ event occurs in institution i at time t, then CoVaR represents the VaR value of institution i at the confidence level of $1-q$. That is, the conditional risk value of the whole financial system if the loss of institution i is at the level of $\mathrm{VaR}^i_{q,t}$. Further, the CoVaR can also be defined as the q quantile of the probability distribution of asset returns:

$$\Pr\left(r_{jt} \le \mathrm{CoVaR}^{i|C(X^i)}_{q,t} \,\middle|\, C(r_i)\right) = q, \tag{5}$$

where $\mathrm{CoVaR}^i_{q,t}$ represents the VaR of the financial system when the institution i is at the $\mathrm{VaR}^i_{q,t}$ level, covering the systemic risk spillover effects of institution i on the whole financial system. When examining the systemic risk, the risk contribution degree from individual institution i to the whole financial system can be expressed as the difference between the conditional risk value of the whole financial system when the institution i is in financial distress and the conditional risk value of the system when the institution i is in the median state, which can be expressed in the following formula:

$$\Delta\mathrm{CoVaR}^i_{q,t} = \mathrm{CoVaR}^{C(r_i)}_{q,t} - \mathrm{CoVaR}^{\mathrm{Median}^i}_{q,t}, \tag{6}$$

where ΔCoVaR indicates the negative external spillover of risks that the individual institution generates on the whole financial system, quantifying the additional risks to the whole financial system when the single institution is under pressure. It captures the marginal contribution of institution i to the total systemic risk, reflecting the marginal risk contribution of the institutions in crisis to the system, with larger absolute values indicating higher degree of systemic risk.

The systemic risk MES represents the marginal contribution of the individual institution to the risk measured by the ES measure, which is the partial derivative of the system ES on the weight of institution i. It represents the amount of

change in the market risk indicator ES caused by the change in the weight of the i-th institution in the financial system by one unit. The higher the MES value, the greater the contribution of institution i to systemic risk. According to Scaillet [26], MES can be expressed as the first derivative of ES on weights for the i-th asset, which can be expressed as follows:

$$\mathrm{MES} = \frac{\partial E\,S_{m,t-1}(C)}{\partial w_i} = E_{t-1}\left(r_{it} \mid r_{\mathrm{mt}} < C\right). \tag{7}$$

MES measures all the losses exceeding the α quantile of the loss distribution. The marginal expected shortfall is the expectation of business risk level and profitability of the institution in crisis, which reflects the ability of an institution to resist market risks.

The AR-GARCH-DCC model method is employed to describe the nonlinear risk correlation and clustering property between variables in the stock market and calculates the risk contribution degree of an individual stock to the system. Specifically, the dynamic conditional correlation DCC model is employed to model the dynamic correlation between system returns and individual institution returns primarily. Then, we use the AR-GARCH (1, 1) framework to model the volatility and get the conditional volatility and standard residuals of the system and the individual institutions, respectively. The parameter estimation uses the quasimaximum likelihood estimation method to obtain a consistent, asymptotic estimator. Secondly, according to the independent and identical distribution properties of the innovation term of the volatility process, the nonparametric kernel estimation of the tail expectations is performed. Finally, the systemic risk is calculated according to the abovementioned CoVaR and MES risk measurement formulas.

2.3. Model Specification. Using the institutional investors' network topology structure features to characterize the information sharing characteristics, we further analyze the relationship between the information sharing of institutional investors network and different levels of risks. The corresponding risks include idiosyncratic risks, stock market extreme risks, and financial systemic risk. The model can be specified as follows:

$$\mathrm{risk}_{it} = \beta_0 + \beta_1\,\mathrm{density}_{it} + \beta_2\,\mathrm{degree}_{it} + \gamma\,\mathrm{control}_{it} + \varepsilon_{it}. \tag{8}$$

In order to control other factors that affect stock price risk, the following two types of control variables are introduced into the model: (1) valuation variables, including the standard deviation of stock returns (vari), company size (lncapi), ratio of returns to market value (retcap), asset-liability ratio (asslia), price earnings ratio (pe), and the shareholding ratio of major shareholders (holder); (2) the herd effect control variables, including the individual stock turnover (turnover), the price momentum (momen), and the sentiment indicator (willing). The specific definitions and computation methods of the variables are shown in Table 1.

3. Empirical Results

3.1. Institutional Investor Information Network. This paper uses the Chinese mutual security investment fund and the listed company stocks as samples. The sample data cover the period from the first quarter of 2007 to the second quarter of 2019, and the data come from the Wind database in China. We select the mutual funds that hold common stocks with large position for the type of ordinary stock funds, hybrid funds with partial stocks, and the balanced hybrid funds during the sample period. Especially, the top holding stocks refer to the stocks being the top ten stocks with the largest positions announced in the quarterly report of the fund, and the market capitalization of these stocks accounts for more than 5% of the market capitalization of the fund. According to the statistics, the quarterly average of the proportion of the funds with large position stocks in all funds is 41.4%, which indicates that the fund information network has important impacts on the stock volatility. Additionally, it has been found that the size of the fund information network is constantly increasing.

Primarily, based on the 2019 semiannual report data, the overview of the China mutual fund network is pictured, as shown in Figure 1. In Figure 1, the average path length of the network is 1.7049 and the clustering coefficient is 0.7455, indicating that the Chinese institutional investor network displays small-world features, which reflects rapid speed of information diffusion. In order to more clearly show the stock connection relationship in the fund information network, we take the China Inner Mongolia Yili Industrial Group (Yili) as an example, and the stock network built around Yili shares is shown in Figure 2. In Figure 2, Yili's shares are held by five mutual funds, and the code of these five funds are, respectively, 006429.OF, 004868.OF, 162107.OF, 001186.OF, and 090016.OF, and all these five funds have their own fund information network. Yili's stock network is the collection of the five funds holding its shares and their respective fund information networks.

3.2. Stock Market Extreme Risk and Financial Systemic Risk. Figure 3 shows the daily level of extreme risk measured by the VaR method using individual Chinese stock market data. Systemic events are defined as situations where the market returns exceed 5% risk threshold level. Judging from the market average value, the degree of extreme risk in the Chinese financial market is low, indicating that the extreme risk in China is generally controllable. In addition to the sharp increase in extreme risks in the Chinese stock market during the international financial crisis in 2008 and the Chinese stock market disaster in 2015, the degree of extreme risks in the Chinese stock market rose again in 2018. This is mainly due to the impact of credit events in China such as the Internet finance defaults, bond defaults, and the escalation of Sino-US trade frictions in 2018, which have increased the degree of systemic risk.

Figure 4 shows the daily level of financial systemic risk in China. Different from the extreme risk of the stock market measured by VaR, the systemic risks measured by ΔCoVaR

Table 1: Control variable name and meaning.

Control variable	Meaning and computation method
Asslia	Asset-liability ratio, total liabilities divided by total assets
Holder	Shareholding ratio of major shareholders, the sum of the shareholding ratios of the top five shareholders in the listed companies
Pe	Price earning ratio, stock price divided by earnings per share
Lncapi	Company size, natural logarithm of market capitalization
Retcap	Ratio of returns to market value
Turnover	Individual stock turnover, ratio of trading volume to the total number of shares issued
Vari	Standard deviation of returns, standard deviation of stocks relative to benchmark returns in the fund network
Momen	Price momentum, an indicator analyzing the trend of the stock price based on the variations of the speed of the stock price changes
Willing	Sentiment indicator, popular willingness

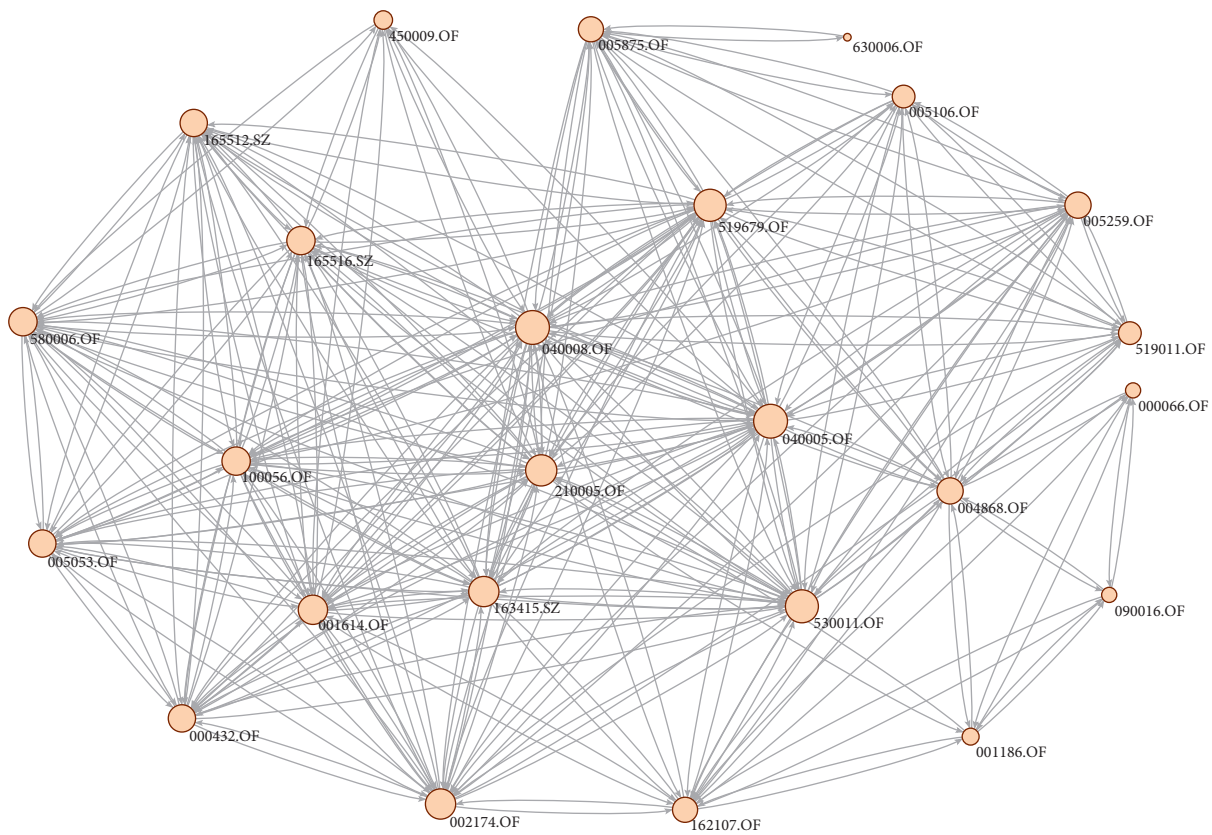

Figure 1: Mutual fund network based on the 2019 semiannual report in China.

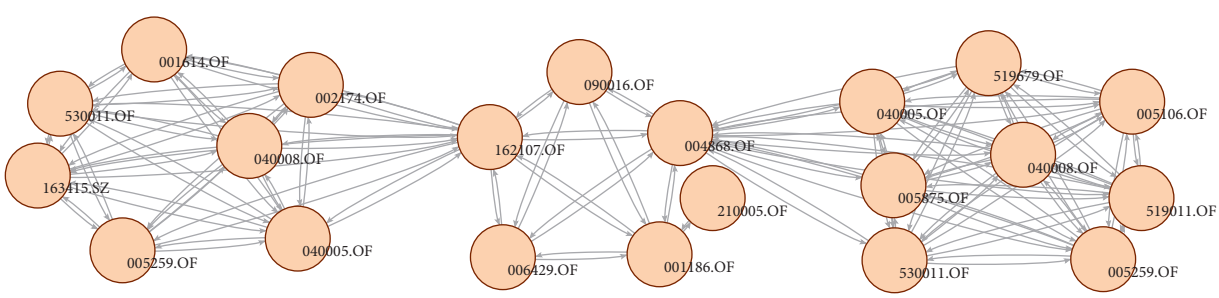

Figure 2: Stock network centered on Yili shares.

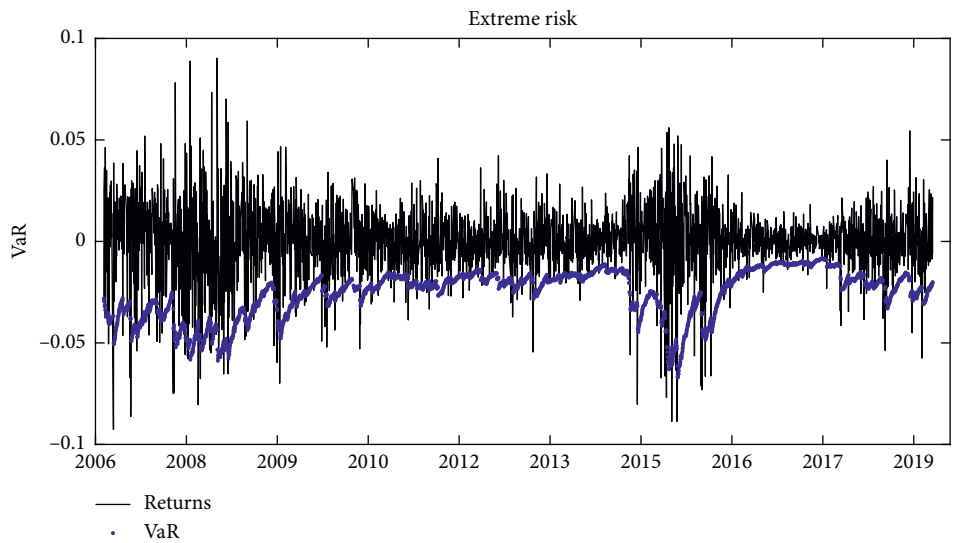

Figure 3: Stock market extreme risks in China.

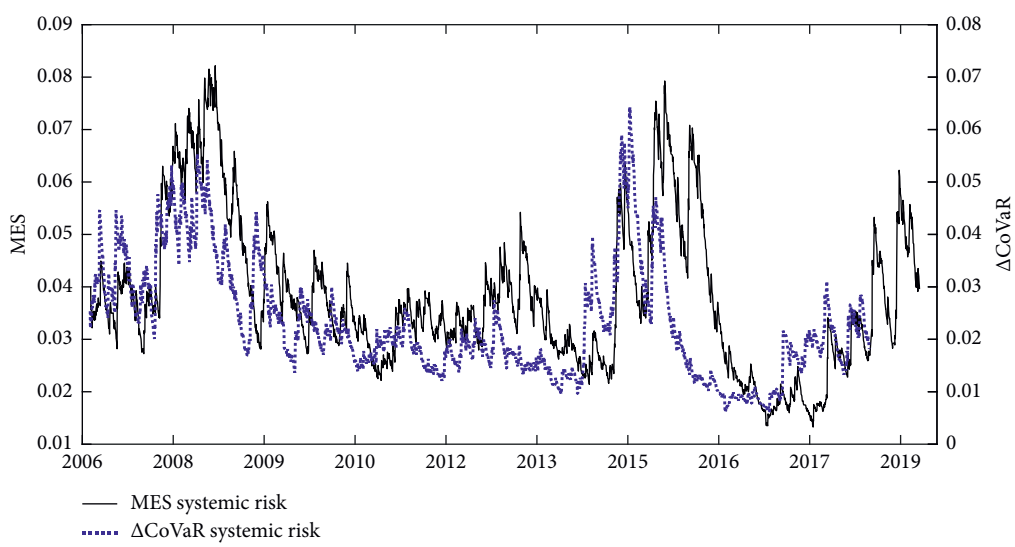

Figure 4: Financial systemic risk in China.

and MES not only identify the risk surge caused by the subprime crisis in 2008, the Chinese stock market disaster event in 2015, and the credit defaults in 2018, but also identify the risk surge caused by the money shortage incident in China in 2013. Moreover, the cyclical characteristics of systemic risk in China are obvious, and the systemic risk indicator values of ΔCoVaR and MES change significantly during the financial crisis. In 2013, due to the tighter interbank funding and higher interest rates, financial institutions and the related institutions were affected by the risk of money shortage. At the end of 2014, the systemic risk indicator showed gradual rise, and then the risk indicators reached a peak during the turbulent period with thousands of stocks dropping in 2015 subsequently. In 2018, the comprehensive effects caused by the Internet financial defaults, corporate bond defaults, and the escalation of Sino-U.S trade frictions impacted the stock markets, making the systemic risk rise sharply. This phenomenon also makes it necessary and urgent to prevent the cross-sectoral transmission of financial risks, so as to prevent the systemic risk occurring.

3.3. Institutional Investor Information Sharing with Extreme Risks and Systemic Risks. The topology structure of the fund network characterizes the efficiency of information sharing. The larger the degree of the network, the faster the propagation speed of the network information, with the efficiency of information sharing improved. The larger network density means that there are small groups of interests in the network, which will hinder the spread of information and reduce the efficiency of information sharing. According to the previous model specification, we analyze the influence of the centralization and network density of the fund

Table 2: The impact of fund information networks on idiosyncratic risks and extreme risks.

	Idio	t value	VaR	t value	ES	t value
Degree	0.1053**	(1.9316)	−0.0012*	(−1.7151)	−0.0011**	(−2.0967)
Density	−1.0104*	(−1.8456)	0.0462***	(2.6023)	0.0399**	(2.4270)
Asslia	6.4355	(1.4979)	0.0894**	(1.9548)	0.0999**	(2.3588)
Holder	−0.5845***	(−4.5066)	0.0003	(0.1748)	−0.0007	(−0.4429)
Pe	$-1.8E-04$	(−0.2297)	$-7.22E-05$	(−0.9398)	$-7.57E-05$	(−1.0635)
Lncapi	1.2795**	(2.4647)	−0.0142***	(−2.5991)	−0.0126***	(−2.4873)
Retcap	0.1062	(1.3946)	0.0017**	(2.1773)	0.0013*	(1.7379)
Turnover	−0.0111***	(−3.5202)	0.0002***	(3.6297)	0.0002***	(3.8499)
Momen	3.9483***	(3.0464)	−0.0337***	(−2.4880)	−0.030**	(−2.3859)
Willing	−0.1276	(−0.7351)	−0.0002	(−0.0654)	$-8.19E-04$	(−0.0518)
Vari			0.0269***	(3.7005)	0.0029*	(1.9466)
Adjusted R^2		0.36	0.61	0.69		

***, **, and * indicate statistical significance at 1%, 5%, and 10% level, respectively.

Table 3: The impact of fund information network on systemic risk.

	CoVaR	t value	MES	t value
Degree	−0.0011**	(−2.2873)	−0.0012*	(−1.9013)
Density	0.0385**	(2.3972)	0.0579***	(2.5451)
Asslia	0.0962**	(2.3279)	0.1139*	(1.9391)
Holder	−0.0005	(−0.3875)	0.0003	(0.1695)
Pe	$-7.5E-05$	(−1.0802)	−9.71E − 05	(−0.9854)
Lncapi	−0.0129**	(−2.6001)	−0.0189***	(−2.6887)
Retcap	0.0011*	(1.7113)	0.0021**	(2.1298)
Turnover	0.0002***	(3.5983)	0.0002***	(3.4348)
Momen	−0.0275**	(−2.2469)	−0.0416**	(−2.3984)
Willing	0.0005	(0.3683)	0.0005	(0.2371)
Vari	0.0025*	(1.6923)	0.0022	(1.0626)
Adjusted R^2		0.65	0.59	

***, **, and * indicate statistical significance at 1%, 5%, and 10% level, respectively.

information network on the idiosyncratic risk of stock volatility and the extreme risk in the stock market. Seen from the results shown in Table 2, it can be seen that the centralization degree of the fund information network has positive correlation with the idiosyncratic risk of individual volatility after controlling other related factors. However, the network density and the idiosyncratic volatility show negative correlation. In other words, institutional investor information sharing has exacerbated the idiosyncratic volatility of individual stock prices. This is mainly because institutional investors learn from each other, which results in similar investment decisions. Information sharing improves the consistency of the trading operation of fund managers and forms herd effects. The herd effects of institutional investors prevent information from being comprehensively incorporated into the stock price in a timely manner, which increases the stock volatility in the short term. As far as individual stock volatility is concerned, it is necessary to reduce the risk of stock market crashes caused by institutional investors imitating each other.

Seen from the consequences of extreme risks, the centralization degree of the fund information network displays negative correlation with the extreme risks of the stock market measured by VaR and ES methods after controlling other related factors. And, the network density and the extreme risks of the stock market measured by VaR and ES methods also display significant positive correlation. It indicates that information sharing between institutional investors can reduce extreme risks in the stock market. Besides, the effects of fund information networks on idiosyncratic risk and extreme risk are different. Specifically, the effects on individual stock volatility can be realized in the short period, while the effects on extreme risks need relative longer time to be fully transmitted to the market.

Furthermore, we analyze the influences of centralization and network density of the fund information network on systemic risks, with the results shown in Table 3. Judging from the consequences of systemic risk, the degree of centralization of the fund information network displays negative correlation with the systemic risk measured by CoVaR and MES indicators. However, the network density displays significant positive correlation with the systemic risk. It indicates that information sharing among institutional investors can reduce the systemic risks. This is mainly because the information sharing among institutional investors improves the comprehensiveness and accuracy of market information transmission, so that it can improve the market pricing efficiency of stocks. Through reducing the extreme risks in the stock market, it further reduces the degree of financial systemic risk. It implies that improving the quality of information disclosures of institutional investor helps reduce extreme risk and systemic risk.

4. Conclusion

This paper assumes that there exists private information sharing among funds that hold common stocks with large position. Then, we build the institutional investor information network using the common holding stocks of mutual funds as links. And, the impacts of information sharing efficiency represented by the network topology structure on the extreme risk of stock market and financial systemic risk are investigated. Based on the empirical analysis of China mutual fund and stock market data from 2007 to 2019, we reveal the inherent formation mechanism of fund herd behaviors. The studies find that the Chinese institutional investor network exhibits small-world characteristics, which reflects fast speed of information diffusion. After controlling other related factors, it can be found that from the idiosyncratic risk of individual volatility, institutional investor information sharing has increased the idiosyncratic risk. However, from the perspective of the effects on stock market extreme risk, there exists negative relationship between information sharing of the institutional investor network and the stock market extreme risk. That is, information sharing among institutional investors reduces extreme risk in the stock market. In addition, there exists a negative relationship between institutional investor information sharing and systemic risk, meaning that information sharing among institutional investors reduces financial systemic risk.

It indicates that in order to prevent the transmission of systemic risk, it is necessary to pay attention to the role of information flow of the fund manager in the social networks. Institutional investor information sharing reduces the probability of black swan incidents by improving the comprehensiveness of market information transmission and the market pricing efficiency of stocks. The conclusions of the study provide reference for regulators to stabilize the market and to prevent the manipulation of stock prices caused by the herd effects of investors. As far as individual stock volatility is concerned, it is necessary to reduce the risk of stock market crashes caused by institutional investors imitating each other. Concerning the extreme risk and systemic risk, improving the quality of information disclosures of institutional investor helps reduce these risks. The obtained conclusions are also instructive for regulators and investors in other financial markets. The use of the fund information network contributes to identifying important institutional investors so as to conduct targeted supervision and prevent manipulation of stock prices.

Data Availability

The Wind database data (Excel type) used to support the findings of this study are available from the corresponding author upon request.

Conflicts of Interest

The authors declare that they have no conflicts of interest.

Acknowledgments

The authors would like to acknowledge the financial support from the National Natural Science Foundation of China (nos. 71901130, 71532009, and 71790594), Shandong Social Science Planning Project (no. 19CJRJ21), and China Postdoctoral Science Foundation (2018M641653).

References

[1] W. Li, G. Rhee, and S. S. Wang, "Differences in herding: individual vs. institutional investors," *Pacific-Basin Finance Journal*, vol. 45, pp. 174–185, 2017.

[2] N. C. Brown, K. D. Wei, and R. Wermers, "Analyst recommendations, mutual fund herding, and overreaction in stock prices," *Management Science*, vol. 60, no. 1, pp. 1–20, 2013.

[3] P. Irvine, M. Lipson, and A. Puckett, "Tipping," *Review of Financial Studies*, vol. 20, no. 3, pp. 741–768, 2007.

[4] V. K. Pool, N. Stoffman, and S. E. Yonker, "No place like home: familiarity in mutual fund manager portfolio choice," *Review of Financial Studies*, vol. 25, no. 8, pp. 2563–2599, 2012.

[5] V. K. Pool, N. Stoffman, and S. E. Yonker, "The people in your neighborhood: social interactions and mutual fund portfolios," *The Journal of Finance*, vol. 70, no. 6, pp. 2679–2732, 2015.

[6] G. Cici, S. Jaspersen, and A. Kempf, "Speed of information diffusion within fund families," *Review of Asset Pricing Studies*, vol. 7, no. 1, pp. 144–170, 2017.

[7] A. Pareek, "Information networks: implications for mutual fund trading behavior and stock returns," in *Proceedings of the Atlanta Meetings Paper*, Atlanta, GA, USA, January 2012.

[8] J.-B. Kim, Y. Li, and L. Zhang, "Corporate tax avoidance and stock price crash risk: firm-level analysis," *Journal of Financial Economics*, vol. 100, no. 3, pp. 639–662, 2011.

[9] H. N. Ozsoylev, J. Walden, M. D. Yavuz, and R. Bildik, "Investor networks in the stock market," *Review of Financial Studies*, vol. 27, no. 5, pp. 1323–1366, 2014.

[10] J. Blocher, "Network externalities in mutual funds," *Journal of Financial Markets*, vol. 30, pp. 1–26, 2016.

[11] M. Billio, M. Getmansky, A. W. Lo, and L. Pelizzon, "Econometric measures of connectedness and systemic risk in the finance and insurance sectors," *Journal of Financial Economics*, vol. 104, no. 3, pp. 535–559, 2012.

[12] Z. Yang and Y. Zhou, "Quantitative easing and volatility spillovers across countries and asset classes," *Management Science*, vol. 63, no. 2, pp. 333–354, 2017.

[13] P. Colla and A. Mele, "Information linkages and correlated trading," *Review of Financial Studies*, vol. 23, no. 1, pp. 203–246, 2010.

[14] S. S. Crawford, W. R. Gray, and A. E. Kern, "Why do fund managers identify and share profitable ideas?" *Journal of Financial and Quantitative Analysis*, vol. 52, no. 5, pp. 1903–1926, 2017.

[15] A. Krause and S. Giansante, "Interbank lending and the spread of bank failures: a network model of systemic risk," *Journal of Economic Behavior & Organization*, vol. 83, no. 3, pp. 583–608, 2012.

[16] A. W. Butler and U. G. Gurun, "Educational networks, mutual fund voting patterns, and CEO compensation," *Review of Financial Studies*, vol. 25, no. 8, pp. 2533–2562, 2012.

[17] M. Barigozzi and M. Hallin, "A network analysis of the volatility of high dimensional financial series," *Journal of the*

Royal Statistical Society: Series C (Applied Statistics), vol. 66, no. 3, pp. 581–605, 2017.

[18] M. Forni, M. Hallin, M. Lippi, and P. Zaffaroni, "Dynamic factor models with infinite-dimensional factor spaces: one-sided representations," *Journal of Econometrics*, vol. 185, no. 2, pp. 359–371, 2015.

[19] T. Adrian and M. K. Brunnermeier, "CoVaR," *American Economic Review*, vol. 106, no. 7, pp. 1705–1741, 2016.

[20] M. Rodríguez-Moreno and J. I. Peña, "Systemic risk measures: the simpler the better?" *Journal of Banking & Finance*, vol. 37, no. 6, pp. 1817–1831, 2013.

[21] V. V. Acharya, L. H. Pedersen, T. Philippon, and M. Richardson, "Measuring systemic risk," *Review of Financial Studies*, vol. 30, no. 1, pp. 2–47, 2017.

[22] E. N. Karimalis and N. K. Nomikos, "Measuring systemic risk in the European banking sector: a copula CoVaR approach," *The European Journal of Finance*, vol. 24, no. 11, pp. 944–975, 2018.

[23] J. L. Callen and X. Fang, "Institutional investor stability and crash risk: monitoring versus short-termism?" *Journal of Banking & Finance*, vol. 37, no. 8, pp. 3047–3063, 2013.

[24] H. An and T. Zhang, "Stock price synchronicity, crash risk, and institutional investors," *Journal of Corporate Finance*, vol. 21, pp. 1–15, 2013.

[25] J. Fan, Y. Liao, and X. Shi, "Risks of large portfolios," *Journal of Econometrics*, vol. 186, no. 2, pp. 367–387, 2013.

[26] O. Scaillet, "Nonparametric estimation and sensitivity analysis of expected shortfall," *Mathematical Finance*, vol. 14, no. 1, pp. 115–129, 2004.

Hindawi
Complexity
Volume 2020, Article ID 7670382, 13 pages
https://doi.org/10.1155/2020/7670382

Research Article

Complexity to Forecast Flood: Problem Definition and Spatiotemporal Attention LSTM Solution

Yirui Wu,[1] **Yukai Ding**,[1] **Yuelong Zhu**,[1] **Jun Feng**,[1] **and Sifeng Wang**[2]

[1]*College of Computer and Information, Hohai University, Nanjing, China*
[2]*School of Information Science and Engineering, Qufu Normal University, Rizhao, China*

Correspondence should be addressed to Sifeng Wang; sfwang@qfnu.edu.cn

Received 30 November 2019; Revised 15 February 2020; Accepted 24 February 2020; Published 26 March 2020

Academic Editor: Dehua Shen

With significant development of sensors and Internet of things, researchers nowadays can easily know what happens in physical space by acquiring time-varying values of various factors. Essentially, growing data category and size greatly contribute to solve problems happened in physical space. In this paper, we aim to solve a complex problem that affects both cities and villages, i.e., flood. To reduce impacts induced by floods, hydrological factors acquired from physical space and data-driven models in cyber space have been adopted to accurately forecast floods. Considering the significance of modeling attention capability among hydrology factors, we believe extraction of discriminative hydrology factors not only reflect natural rules in physical space, but also optimally model iterations of factors to forecast run-off values in cyber space. Therefore, we propose a novel data-driven model named as STA-LSTM by integrating Long Short-Term Memory (LSTM) structure and spatiotemporal attention module, which is capable of forecasting floods for small- and medium-sized rivers. The proposed spatiotemporal attention module firstly explores spatial relationship between input hydrological factors from different locations and run-off outputs, which assigns time-varying weights to various factors. Afterwards, the proposed attention module allocates temporal-dependent weights to hidden output of each LSTM cell, which describes significance of state output for final forecasting results. Taking Lech and Changhua river basins as cases of physical space, several groups of comparative experiments show that STA-LSTM is capable to optimize complexity of mathematically modeling floods in cyber space.

1. Introduction

As more sensors are applied to acquire variant data from physical space, researchers try to build a corresponding cyber space to describe inherent mathematical relationship between sensor acquired factors and results, which provides users a great deal of convenience to find novel solutions for problems in the real world. However, mathematical and technical complexity and challenge rise in both procedures, i.e., transforming problem-related data from physical space to cyber space, and utilizing models to solve problems in cyber space. Inspired by data-driven and artificial intelligent idea to solve problem in physical space, we intend to smartly solve the problem of flood forecasting by means of complexity modeling and optimization.

Flood often occurs with sudden and devastating nature, causing huge life and economic losses to human society. Therefore, it is of significance to forecast flood disasters in advance. To minimize impacts brought by floods, researchers have proposed quantity of methods to accurate forecasting in the past decade [1, 2]. Based on core ideas to forecast, we divide their proposed methods into two categories: physical model [3, 4] and data-driven model [5, 6]. Physical model explains hydrological procedures with conceptual math equations, such as rain, evaporation, and flow concentration. Afterwards, a highly nonlinear function system is constructed to model complex flood process from hydrological clues to result of large run-off values. We can find carefully designed physical models in works of Fan et al. [7] and Pontes et al. [8, 9], where their models well fit in special areas to handle complexity of flood forecasting.

Data-driven model directly models mathematical interactions between different hydrological factors and run-off

values based on historical observations. In other words, data-driven models learn mapping between flooding cues and flow rates without considering detailed physical processes, which is the main difference between physical models and data-driven models [10]. Due to rapid development of machine learning technology, many novel data-driven forecasting methods have been proposed and practiced, including Bayesian network [1], SVM model [11], neural network [6], and their variations and integrations.

It is noted that both physical and data-driven models are sensitive to their internal parameters, which requires both quantity of convinced data and great deal of manual efforts from researchers to adjust. In other words, the main difficulty to apply models on small or medium river basins lies in the fact of insufficient data to support accurate forecasting. Moreover, small or medium river basins are generally short of special research in most developing countries, which leads to difficulties in designing appropriate physical models for forecasting. Based on all these discussions, we aim to optimize complexity to forecast flood in small or medium river basins by methods of data-driven models.

Recently, deep learning structures gained lots of attentions by their significant classification and regression results on visual tasks of text detection, object categorization, language translation, and so on. Following the big progress of deep learning technology on accuracy, we concentrate on LSTM network for the goal of more accurate flood forecasting results. Essentially, LSTM is developed on the basis of Recurrent Neural Network (RNN), which could handle long-time sequential data with special designs of gates. Based on its high potential property to forecast time-varying variables, we apply LSTM to model inherent and complex relationship between hydrological factors and run-off values.

Attention mechanism is widely used in prediction tasks, due to its novelty to borrow idea from human visual attention, namely, that humans purposely view parts of environment or picture with the context information or advanced semantic knowledge. Inspired by core ideas of attention mechanism, we study flood formation of small and medium river basins by firstly gathering related hydrological data of different locations and timings. Afterwards, a novel LSTM structure embedding a spatiotemporal attention module, named as STA-LSTM, is constructed to dynamically select hydrological features for accurate forecasting.

STA-LSTM takes advantages of original LSTM structure, which is capable to handle long-time time-varying data. Meanwhile, the embedded spatiotemporal attention module dynamically assigns spatial-wise weights for input hydrological factors acquired from different locations at first. After that, it allocates temporal-wise weights to hidden output of each LSTM cell, which is comprehended as context information in Liu et al. [12]. Such spatial- and temporal-wise weights result in capability to dynamically characterize significance of hydrological factors obtained at any timings and locations. According to case study experiments in Europe Lech and China Changhua river basins, STA-LSTM could realize accurate flood forecasting by constructing contexture-based weighting schemes.

We conclude two contributions of this paper as follows:

(i) Facing complexity of modeling cyber-physical interaction, a novel LSTM model embedding spatial-temporal attention module is proposed, which is capable of accurately predicting run-off values in cyber space based on hydrological data acquired from physical space.

(ii) We design a novel temporal attention module, which is built on contextual information to compute weights for each LSTM cell output. Incorporating with both spatial and temporal context information, the proposed attention module helps describe how hydrology factors interact to form flood in physical space and appropriately builds such process in cyber space by constructing weighting schemes in STA-LSTM.

2. Related Work

In this section, we introduce related methods with two categories, i.e., data-driven model for flood forecasting and introduction to attention model.

2.1. Data-Driven Model for Flood Forecasting. Early, Juliang et al. [13] propose an accelerated genetic algorithm (AGA). Their method utilizes a Back Propagation Neural Network (BPNN) to optimize initial parameters, which brings advantages of better and faster convergence performance. Inspired by development of support vector machine (SVM), Yu et al. [11] compare performance on flood forecasting between artificial neural network (ANN) and SVM. After performing a number of comparison experiments, they draw a conclusion that SVM is slightly better than ANN in forecasting floods. Later, Minghua et al. [14] emphatically compare experimental results achieved by Xinanjiang model (a famous physical model) and ANN model. Afterwards, they conclude that ANN could reflect time-varying characteristics of hydrological process, which is an advantage by comparing with abstract representation of hydrology process in Xinanjiang model.

After analyzing various flood forecasting models, Cheng et al. [15] utilize quantum particle swarm optimization method to solve complexity of defining parameters for ANN, which is later examined by experiments to forecast daily run-off values of reservoirs. Lima et al. [16] conduct flood frequency analysis with a hierarchical Bayesian framework, which estimates Generalized Extreme Value (GEV) distribution parameters in a local sense for explicitly modeling and uncertainties reduce. Recently, Wang et al. [10] proposed a Bayesian-based method, which establishes a posterior distribution for daily flow rate forecasts and uncertainty quantifications.

With the idea of coupling the strength of physical model and data-driven model, O'Connel et al. [17] use paleo hydrologic information constraints to effectively reduce the uncertainty during flood frequency analysis. Following such idea, Biondi et al. [18] firstly simulate the hydrologic response by a rainfall-run-off model named as Infiltration and Saturation Excess (RISE) and then utilize the extracted

hydrological information for later deterministic Bayesian Forecasting. Recently, Wu et al. [5] successfully transformed hydrological process described by Xinanjiang model into entities and connections of Bayesian network, which offers a solution to integrate expert knowledge in a data-driven model. In order to offer a task-specified computing service, data-driven models nowadays have been developed accompany with Internet of things [19, 20], cloud-edge computing [21–23], big data [24, 25], and other technologies [26–28].

2.2. Introduction to Attention Model. Core idea behind attention model is to select informative and significant information for task goal, which coincides with principle of human selective visual mechanism. Existing attention models for deep learning can be divided into two groups: hard and soft attention. Hard attention can be comprehended as spatial selection for salient regions, which leads the input areas to be processed as different parts with values of 0 (ignore areas) or 1 (concentrate areas). Meanwhile, soft attention assigns flexible weight values between 0 and 1 to parts of input data.

Mnih et al. [29] introduce general idea of hard attention by optimally selecting salient regions from input images based on pre-defined selection rules. Their proposed method performs recognition tasks on selected salient regions with a novel RNN structure. Following idea of hard attention, He et al. [30] propose a convolutional neural network, named as Text-CNN, to involve attention scheme for scene text detection. Specifically, their scheme not only extracts salient regions as informative parts of input images, but also particularly selects informative features from feature pools for more accurate detection.

Soft attention is flexible and efficient to be an additional and functional part for deep learning networks. For example, Song et al. [31] propose spatial attention module to accurately and robustly recognize human actions. Their proposed method firstly constructs a spatial-wise weight scheme to pay attention on informative joints in each RGB-D skeleton frame and then assigns spatial attention weights to guide the construction of feature map of the corresponding frame. To utilize global attention information for higher accuracy and robustness, a globally context-aware attention LSTM [12] is built, which successfully constructs and optimizes global attention information for each RGB-D human action sequence from dataset [32].

Most recently, Yeung et al. [33] utilize soft attention model to assign frame-wise weights for frames captured by a sliding window, which helps fuse multiframe information for recognition tasks. Chen et al. [34] build an attention model on the basis of a novel network architecture combining advantages of CNN and RNN, which successfully extracts informative and modality-specific feature for human activity recognition. They claim that their extracted feature is able to represent high-level visual information, even training with an imbalanced and limited size dataset. Anderson et al. [35] construct a bottom-up and top-down attention model on top of Faster R-CNN, which is capable of assigning weights in object or salient image region level. After conducting experiments on several public datasets, they have achieved state-of-the-art performance on image caption task. Inspired by above attention models, we designed the proposed spatial-temporal attention model to allocate attention weights for temporal and spatial dimensions.

3. The Proposed Method

We firstly introduce the experimental small river basins, i.e., Lech and Changhua river basin. Then, we introduce overall network structure of the proposed STA-LSTM model. Finally, a novel spatial-temporal attention module is proposed to show how context information is extracted.

3.1. Introduction to Experimental River Basins. We take two river basins, i.e., Lech and Changhua, as experimental areas, due to their small and complex nature for flood formation. Due to significant development of remote sensing and sensor technologies, we build our prediction model on data collected from remote sensing imageries and sensors. Specifically, data about Lech river basin are achieved from European Centre for medium-range Weather Forecasts (ECWMF), which is free to download worldwide weather and hydrological information. Meanwhile, we get hydrological data about Changhua river basin from cooperation China government.

Figure 1(a) refers to the map of Lech river basin, where we suppose latitude and longitude range for Lech river basin is from (10.68E, 47.65N) to (10.94E, 48.73N) with 0.01×0.01 radius precision. Originating from northwest slope of Lysitar mountain, Lech river finally flows into Danube river at 40 km north of Augsburg. Total length, basin area, and estuary average annual flow of Lech river are 263 km, 4126 km^2, and 120 m^3/s, respectively. Weather in Lech river basin areas is warm and humid throughout the year.

Figure 1(b) shows the map of Changhua river basin, where we can find that Changhua river originates from Jixi County and finally flows into Xinanjiang river. Total length, basin area, and estuary average annual flow of Changhua river are 96 km, 905 km^2, and 146.651 m^3/s, respectively. Daily run-off value of Changhua river could vary from 0.58 m^3/s to 2100 m^3/s.

Our goal for both river basins is to realize forecasting of surface run-off at their converge locations (represented as red circles at Figure 1) through the proposed STA-LSTM model. Specifically, the proposed model adopts multiple hydrological factors as inputs, including precipitation, evaporation, soil tension water, temperature, and wind.

3.2. Network Architecture Design. We firstly offer a brief introduction to mathematical theory of LSTM cell. Then, we explain how attention scheme improves accuracy of flood forecasting. Afterwards, we design a novel LSTM network architecture involving context information to complete task of flood forecasting. At last, we offer pseudocode of STA-LSTM for readers' convenience.

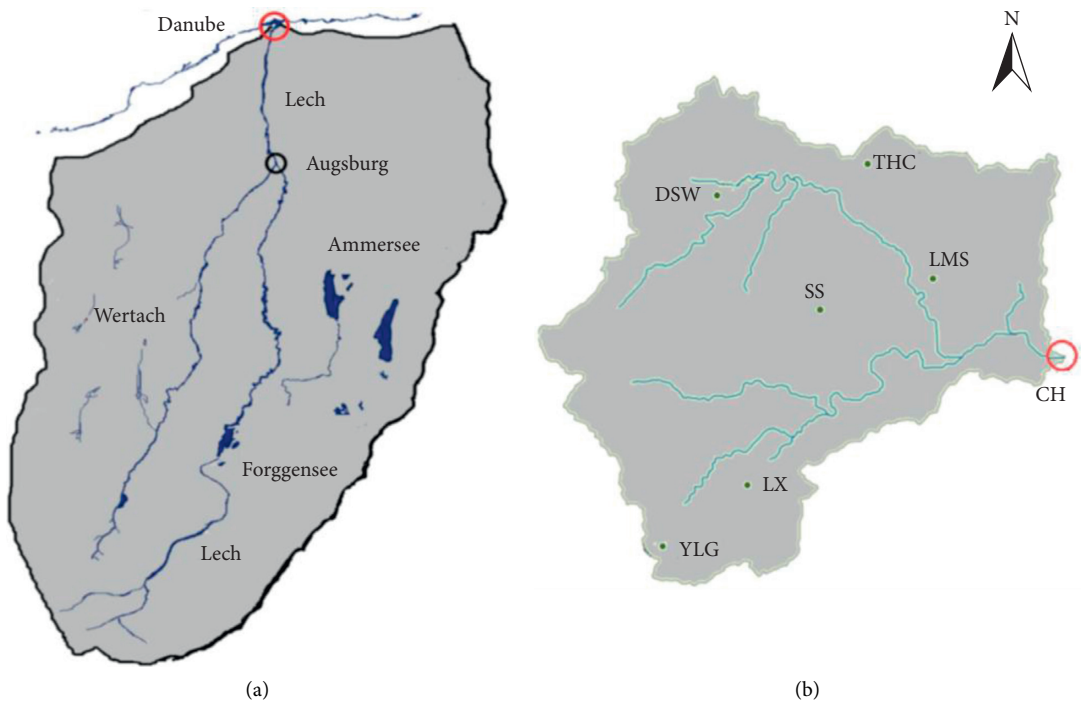

Figure 1: Illustration of Lech (a) and Changhua (b) river basins, where we need to predict flow rate values of converge locations labeled by red circles.

3.2.1. Mathematical Theory of LSTM Cell. Due to difficulty in maintaining long-distance dependency information, LSTM modifies RNN by designing gate structure to keep long-term state. Typical structure of a LSTM cell is represented in Figure 2, where we can observe input gate i, output gate o, input modulation gate g, forget gate f, and memory cell c. Each LSTM cell is responsible to update its hidden output representation h at each state t with the following function:

$$h_t = \sigma\left(W\begin{pmatrix} x_t \\ h_{t-1} \end{pmatrix}\right), \tag{1}$$

where x represents input signal and function $\sigma()$ refers to operation of Sigmoid.

LSTM introduces a long-term memory structure c to maintain long-term information for each cell. Furthermore, it decides whether to forget information inside memory based on the following equations:

$$\begin{pmatrix} i \\ f \\ o \\ g \end{pmatrix} = \begin{pmatrix} sigm \\ sigm \\ sigm \\ sigm \end{pmatrix}\left(W\begin{pmatrix} x_t \\ h_{t-1} \end{pmatrix}\right), \tag{2}$$

$$c_t = f \odot c_{t-1} + i \odot g, \tag{3}$$

$$h_t = o \odot \mathrm{Tan}\, h(c_t), \tag{4}$$

where $\odot$ refers to element-wise multiplication. From equation (3), we can notice that internal memory cell c_t would be updated, if forgetting gate f is activated. After activating f, c_t will be assigned with signal controlled by input gate i and input modulation gate g. Afterwards, LSTM cell will update hidden output h_t on the basis of output gate o and current memory cell c_t, which is described in equation (4). With above designs of memory cell and different gates, output of LSTM can be associated with previous input signals to memorize long-time sequential information [36].

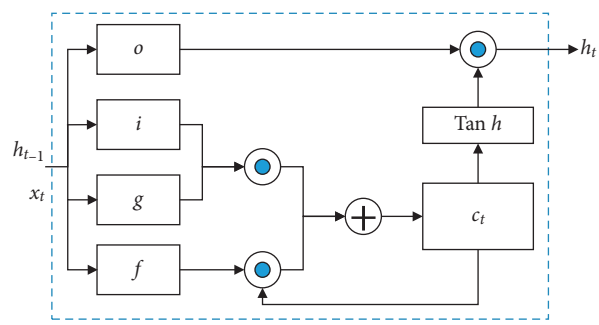

Figure 2: Structure of a typical LSTM unit.

3.2.2. Function of Attention Scheme in Flood Forecasting. After years of research on applying data-driven models to forecast flood, we find adopting all hydrological data for forecasting could not help achieve satisfactory forecasting results, since some hydrological features are useless or even independent with run-off predictions. For example, soil tension water is an important factor for initial state of floods in humid areas. When value of soil tension water increases and exceeds maximum amount that soil can maintain during raining, it would have no impact on variation of run-off

values. Furthermore, soil tension water does not affect river flow values in dry locations with sandy soil, due to bad capability to maintain water of sandy soil. All these facts can be found in hydrological simulation studies or physical models [37].

Due to high spatial and temporal variation of hydrological processes, it is highly recommended to collect hydrological factors by a dense network of hydrometeorological stations. Built on the basis of sufficient stations to collect hydrological features, modeling informativeness degrees of hydrological features would contribute to accurate forecasting. In other words, selectively utilizing informative factors acquired at significant timings and locations is the key idea to adopt attention scheme in flood forecasting. With the ability of focusing on key features and ignoring irrelevant features, data-driven models can appropriately integrate different factors to fit in process of floods, instead of expert knowledge used in physical models. Besides, irrelevant factors could bring in noise to decrease forecasting accuracy.

Based on above discussions, we thus establish a dynamic feature selection mechanism, i.e., attention mechanism, to describe informativeness degrees of flood factors, so that different combinations or weights can be applied on input hydrological features based on context information, i.e., inherent characteristics of river basin for flood formation. It is noted that there exists a trend in deep learning domain that researchers should design all functions by one single network, which brings advantages of less computation and high optimization efficiency. Following such trend, we aim to design a novel LSTM network, i.e., STA-LSTM, to complete task of choosing variables by attention module, which works with the same function of Principal Component Analysis (PCA) indeed.

3.2.3. Structure of STA-LSTM. Network structure of the proposed STA-LSTM is shown in Figure 3, where the proposed attention module allocates dynamic weights to both input and output of STA-LSTM cells for usage of selection on informative features. After building attention module, hidden outputs of all STA-LSTM cells would be concatenated to form F for prediction on increase or decrease in run-off values. It is noted that we prefer to predict based on all hidden outputs, since LSTM structure is restricted in preserving global contextual information by designing forgetting gate. Considering flood forecasting as a global regression problem, we thus prefer to perform forecasting on all hidden outputs, rather than hidden output for final state.

As shown in Figure 3, we firstly acquire hydrological raw data from a small or median river basin to construct input dataset $X = \{x^i \mid i = 1, 2, \ldots, n\}$, where i and n refer to index and total number of samples. There exists n flood records in input dataset X. Afterwards, raw sample x^i is normalized to construct corresponding hydrological feature set $\widehat{x^i}$:

$$\widehat{x^i} = f_{\text{norm}}\left(x^i\right) = \{I_t \mid t = 1, 2, \ldots, \tau\}, \text{ where } I_t \in R^{H \times W}, \tag{5}$$

where function $f_{\text{norm}}()$ represents normalization function, τ represents total number of states over the whole network, and $H \times W$ refers to the size of input feature for each state and is formed by variant hydrological factors.

At state t which refers to the part labeled by blue rectangle in Figure 3, the corresponding tth LSTM cell would compute hidden output of current state h_t with

$$h_t = f_{\text{lstm},t}\left(\widehat{I}_t, \widehat{h}_{t-1}\right), \tag{6}$$

where function $f_{\text{lstm},t}()$ represents processing of the tth LSTM cell to maintain long-term information, $\hat{I}_t$ represents weighted input feature computed by spatial attention module S, and $\hat{h}_{t-1}$ refers to weighted former hidden computed by temporal attention module T. It is noted that number of LSTM cells is the same with total number of states τ.

Specifically, weighted input feature $\hat{I}_t$ in equation (6) is processed by the proposed spatial attention module S with

$$\widehat{I}_t = \alpha_t \otimes I_t = \varphi_{t-1}^S\left(\widehat{h}_{t-1}\right) \otimes I_t, \tag{7}$$

where α_t refers to spatial attention weight for state t, $\otimes$ denotes element-wise operation, and function φ_{t-1}^S means operations inside $t-1$th spatial attention module to compute α_t. It is noted that number of either spatial or temporal attention module is $\tau - 1$.

Meanwhile, hidden output $\hat{h}_t$ is processed by the proposed temporal attention module T with

$$\widehat{h}_t = \beta_t \odot h_t = \varphi_{t-1}^T\left(I_{t-1}, I_t\right) \odot h_t, \tag{8}$$

where I_{t-1} and I_t are original input features for state $t-1$ and t, respectively, β_t refers to spatial attention weight for state $t-1$, $\odot$ operation represents element-wise multiplication, and function φ_{t-1}^T represents operations inside $t-1$th temporal attention module to compute β_{t-1}.

3.2.4. Pseudocode of STA-LSTM. After describing steps of building STA-LSTM network with mathematic functions, we provide detail pseudocode in Algorithm 1, where readers can easily understand the process of experiment and implementation details of STA-LSTM model.

3.3. Spatial-Temporal Attention Module. Structure of the proposed spatial-temporal attention module is shown in Figure 4. Compared with traditional physical models which rely on expert knowledge and experience to manually assign factor weights, the proposed attention model can automatically select informative factors to forecast based on inherent characteristics of collected data, which is more flexible for different application scenarios.

3.3.1. Spatial Attention Module. Acquired data from ECWMF sites is gathered with structure of grids ruled by latitude and longitude, which offers detailed information on spatial distribution of inputting hydrological factors. However, small radius precision, i.e., 0.01×0.01 radius, could greatly increase computation burden of the proposed model.

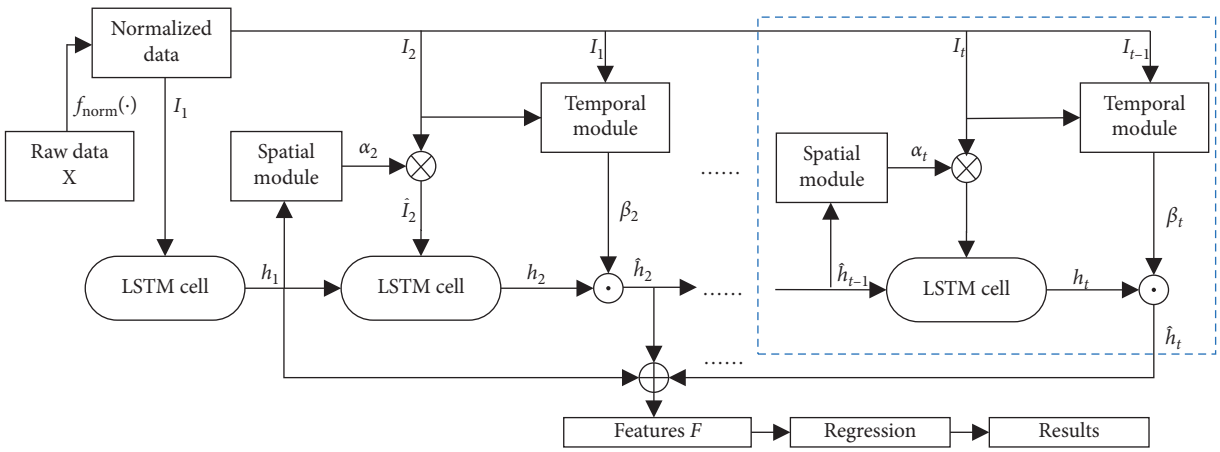

Figure 3: Network structure of the proposed STA-LSTM, which takes raw data as input and computes regression results to predict increase or decrease in run-off values. It is noted that we use blue rectangle to locate parts of STA-LSTM, which is described by equations and explanations in detail.

Input: Input dataset X with n samples, each sample refers to a hydrological feature set collected from total τ states, input initial super-parameters θ.
Output: Run-off value Prediction Y.
Initialize STA-LSTM model with initial super-parameters θ and random network weights W_1.
  Set sample index $i = 1$;
  for $i \leq n$ **do**
    Set current state $t = 2$, hidden output in the first state $h_1^i = f_{\text{lstm},1}(X_1^i)$, weighted hidden output in the first state $\widehat{h}_1^i = h_1^i$;
    for $t \leq \tau$ **do**
      Input $\widehat{h}_{t-1}^i$ into $t-1$th spatial attention module to calculate spatial attention weight by $\alpha_t = \varphi_{t-1}^S(\widehat{h}_{t-1}^i)$;
      Refine current input X_t^i with spatial attention weight α_t by $\widehat{X_t^i} = \alpha_t \otimes X_t^i$;
      Input $\widehat{X_t^i}$ and $\widehat{h}_{t-1}^i$ into tth LSTM cell to compute current hidden output by $h_t^i = f_{\text{lstm},t}(\widehat{X_t^i}, \widehat{h}_{t-1}^i)$;
      Input X_{t-1}^i and X_t^i into $t-1$th temporal attention module to compute temporal attention weight by $\beta_t = \varphi_{t-1}^T(X_{t-1}^i, X_t^i)$;
      Refine current hidden output h_t^i with spatial attention weight β_t by $\widehat{h_t^i} = \beta_t \odot h_t^i$.
      t++;
    end for
    Increase or Decrease value in Run-off $Y^i = \text{Outlayer}(\widehat{h_1^i}, \widehat{h_2^i}, \ldots, \widehat{h_\tau^i})$
    Calculate RMSE with Y^i and ground-truth value.
    if RMSE decreases **then**
      Update model weights with: $W_{i+1} = W_i - (\partial \text{loss}/W_i)$;
    else
      Continue;
    end if
    i++;
end for
End training process and Save model parameters.
Input testing samples to output corresponding prediction value Y.
Calculate RMSE, DC and MAPE for testing samples.

Algorithm 1: Pseudocode of STA-LSTM for implementation.

Therefore, we reconstruct organization form of the acquired data to keep balance on precision and effectiveness, where the reconstructed data structure is shown in Figure 5. We can notice that Figure 5(a) is abstracted from Figure 1 with flip operation and large spatial grids. After accumulating data from original and small grids into large grid, we finally achieve a novel and effective representation for input hydrological factors in Figure 5(b), where each factor can be viewed as a 3D dimension vector with feature, position, and time values inside.

Informativeness for input hydrological factors varies greatly in different locations. For example, regions near Lech river should be more important than regions far away, since rainfall near river can quickly be converged to increase run-off values. To utilize spatial property of input hydrological factors, a spatial attention module is constructed to assign weights for hydrological features acquired from different location grids. Essentially, spatial attention module explores interchannel relationship among features obtained from

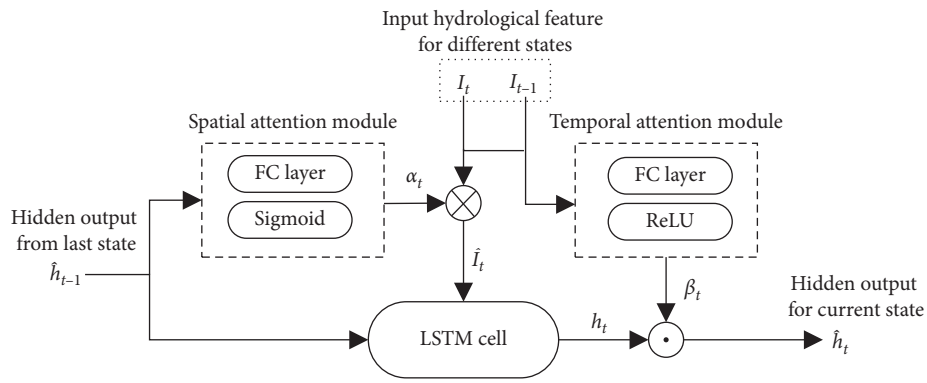

Figure 4: Architecture of the proposed spatial-temporal attention module.

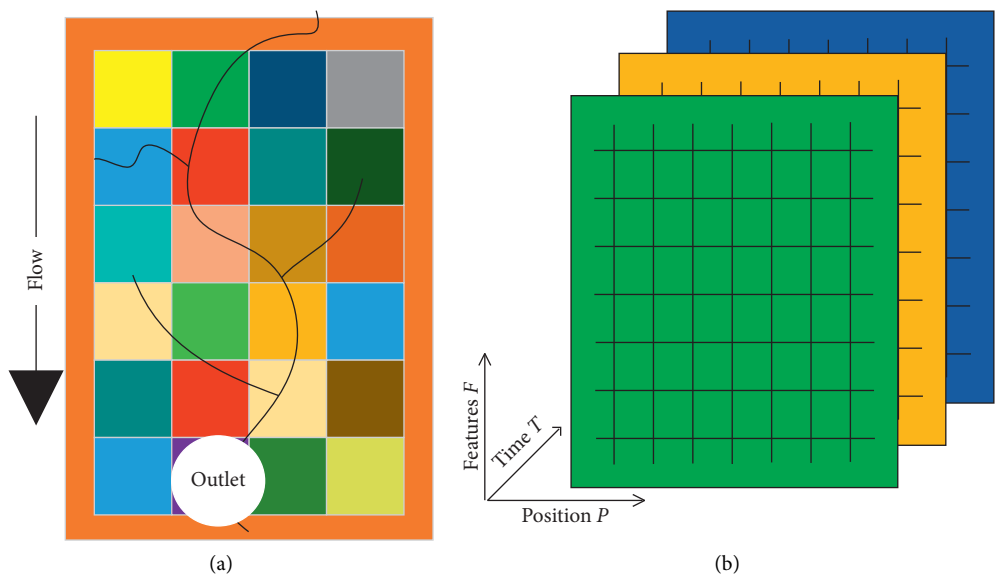

Figure 5: Illustration of the reconstructed data structure for information acquired from ECWMF: (a) abstract Lech river basin with large spatial grids and (b) data representation for input hydrological factors with three independent dimensions to represent feature, position, and time, respectively.

different locations, which help STA-LSTM to pay more attention on salient grids for accurate forecasting.

As shown in Figure 4, input feature I_t is processed by a fully connected layer and a sigmoid function to output spatial-wise weight α_t:

$$\alpha_t = f_s\left(W_S \tilde{h}_{t-1} + b_s\right), \tag{9}$$

where function $f_s()$ refers to sigmoid operation, W_S and b_s represent weighting matrix and bias parameters for fully connected network, respectively.

3.3.2. Temporal Attention Module. Considering that there generally exists a trend in sequential data, researchers design Holt-Winters double exponential smoothing filter to describe relationship between current and former observation values. Following such supposition and implementing it with a dynamically updating weight scheme, we utilize temporal attention module to assign weights for hidden output of STA-LSTM cells, which acts as a relation modeling function between observations at different timings.

As shown in Figure 3, we utilize hidden output of current state and former state to construct temporal attention module, which explores the difference between two states to decide whether current input is informative. The detailed structure of the proposed temporal module is shown in the right part of Figure 4, where we compute temporal weight β_{t-1} for state $t-1$ as

$$\beta_{t-1} = f_R\left(W_{t-1,t-2} I_{t-2} + W_{t,t-1} I_{t-1} + b_{t-1}\right), \tag{10}$$

where function $f_R()$ represents ReLU function, $W_{t-1,t-2}$ and $W_{t-1,t-2}$ refer to parameter matrix required to be defined during training, and b_{t-1} is the bias vector. In fact, temporal-wise weight is key to control information passing through network from former hidden output to next cell. Therefore, temporal attention module is a beneficial complementary to spatial attention module.

4. Experiments

In experiment section, we firstly introduce dataset and measurements. Then, we design two groups of ablation experiments to discuss sensibility of hydrological features and effectiveness of the proposed attention module. Afterwards, we conduct comparative studies with several flood forecasting methods to compare effectiveness. Finally, we offer implementation details of STA-LSTM.

4.1. Dataset and Measurement. We utilize two datasets to prove the effectiveness of STA-LSTM, i.e., Lech and Changhua river basins. It is noted that they have differences in features, since they are collected from ECWMF and cooperation government departments, respectively. Specifically, we utilize the tool provided by ECWMF to collect 7360 hydrological instances of Lech river basin varying from May 1, 2002, to January 1, 2018. These instances have shown significant increase of run-off values, which provide raw data to detect patterns of variation for run-off factor. Meanwhile, we collect 8555 samples varying from January 1, 1998, to December 31, 2010, which represent 40 floods and are manually recorded hydrological data from rainfall, evaporation, and gaging station in Changhua watershed. It is noted that Lech dataset contains sufficient information on adopted hydrological features, i.e., precipitation, evaporation, soil tension water, temperature, and wind. Meanwhile, Changhua dataset is short of information on temperature and wind. Shortage of these two minor hydrology factors does not have a great impact on accuracy of flooding results. Moreover, we achieve data of soil tension water according to calculation of Xinanjiang model (Short for XAJ model), which is a famous physical model to forecast flood in semihumid regions.

Table 1 offers descriptive statistics for flow and rainfall data collected from Lech and Changhua river basin, where we can observe that data representation for both datasets is different. This is due to their distinctive data collection operations, where Lech dataset is constructed from remote sensing imageries and data in Changhua Dataset is collected manually. From Table 1, we can notice obvious difference in data distribution between Lech and Changhua rivers, since characteristics of different river dataset varies greatly from one to another. This phenomenon brings large difficulty to accurately forecast river run-off values, since it requires models to describe relation function between input hydrological features and run-off values without overfit performance.

Due to the nature of ECWMF, i.e., they collect hydrological data every 3 hours, we refer each state in STA-LSTM as 3 hours for modeling. As represented in Figure 5, we utilize such 3D feature by defining time value (state value) as 6, which results in an input feature to describe hydrological factors in 18 hours. After training, we perform regression task with STA-LSTM on run-off values for next 1, 2, and 3 states based on input of hydrological features of former 6 states.

We use standard quality measures, i.e., Root Mean Square Error (RMSE), Mean Absolute Percent Error (MAPE), and Deterministic Coefficient (DC) to measure the quality of flood forecasting. These three measurements are formulated as

$$\begin{aligned} \mathrm{RMSE} &= \sqrt{\frac{1}{n}\sum_{i=1}^{n}\left(y_i - q_i\right)^2}, \\ \mathrm{MAPE} &= \frac{100}{n}\sum_{i=1}^{n}\left|\frac{y_i - q_i}{y_i}\right|, \\ \mathrm{DC} &= 1 - \frac{\sum_{i=1}^{n}\left(y_i - q_i\right)^2}{\sum_{i=1}^{n}\left(q_i - \overline{q}\right)^2}, \end{aligned} \tag{11}$$

where y_i and q_i refer to forecasting run-off values and corresponding ground-truth run-off values, $\overline{q}$ refers to average of ground-truth run-off values, and n is number of testing instances. It is noted that higher DC value implies more convinced flood forecasting results. Meanwhile, RMSE and MAPE are used to quantify similarity between forecasting results and groud-truth values, where smaller values in RMSE and MAPE indicate high accuracy on flood forecasting quality.

4.2. Performance Analysis. We design three comparative experiments to analyze performance of STA-LSTM. Specifically, the first experiment is designed to estimate sensibility of input hydrological features, the second one is used to compare the effectiveness of STA-LSTM with or without attention module, and the last experiment aims to compare performance of STA-LSTM with comparative methods. For all experiments in this paper, input time period is settled form T-5 to T, which makes input data contain hydrological features of 6 states before T.

4.2.1. Feature Sensibility Experiment. We show related experimental data on feature sensibility in Table 2. In each case of experiment, we eliminate one input hydrological feature and keep other inputs remain same, which could show sensibility of specifical feature in obtaining accurate forecasting results. Due to shortage of two hydrology features in Changhua dataset, we prefer Lech dataset to complete feature sensibility experiment. To better compare results, we offer two more statistics data in tables, i.e., mean and bias value represented with subscripts of A and σ, where the latter one calculates the difference value between result under current running condition and achieved by STA-LSTM.

From Table 2, we can notice smallest value in RMSE is achieved by Wo-Temperature, and the best performance in MAPE and DC are achieved by Wo-Wind. In other words, eliminating factors of either temperature or wind have a small impact on forecasting results. Based on this observation, we can conclude these two hydrological factors are less related with formatting of floods. Meanwhile, the worst performance in three measurements is all achieved by Wo-

Table 1: Descriptive statistics of daily flow and relevant data for Changhua and Lech dataset, where evaluation SD refers to standard deviation and p and R represent flow rate values and rainfall values, respectively. It is noted that subscripts c and l refer to gauging stations in Chuanghua and Lech River, respectively; subscript g refers to mean evaluation on basin areas of Lech river; subscripts DSW, THC, and other abbreviations represent names of rainfall stations for Changhua dataset. Note that unit for p is defined as m^3/s and units for R is settled as mm/h.

Evaluation	Changhua river basin								Lech river basin	
	p_c	R_{DSW}	R_{THC}	R_{LMS}	R_{SS}	R_{LX}	R_{YLG}	R_{CH}	p_l	R_g
Mean	146.651	0.596	0.618	0.704	0.786	0.712	0.822	0.631	433.395	0.931
SD	202.501	2.411	2.303	2.636	2.553	2.560	2.666	3.405	107.557	2.659
Median	80.320	0	0	0	0	0	0	0	48.780	0
Skewness	3.987	11.026	7.946	10.700	7.819	8.599	7.484	27.617	2.875	12.916
Kurtosis	24.388	198.996	89.910	190.660	104.110	120.549	100.293	1124.804	0.574	213.598

Table 2: Comparison experiments on Lech dataset to show sensibility of different input hydrological features, where Wo- refers to operation of eliminating one specifical hydrological feature, ST-Water is short for hydrological feature of soil tension water, subscripts A and σ represent mean value and bias value respectively, R, M and D represents measurements of RMSE, MAPE, and DC, respectively. Note that bold texts indicate best performance among comparative methods. We define unit for M as %.

Methods	R_{T+3}	R_{T+6}	R_{T+9}	R_A	R_σ	M_{T+3}	M_{T+6}	M_{T+9}	M_A	M_σ	D_{T+3}	D_{T+6}	D_{T+9}	D_A	D_σ
Wo-precipitation	117.0	121.3	145.3	127.9	61.88	29.61	31.96	36.31	32.63	16.12	0.35	0.33	0.28	0.32	0.49
Wo-evaporation	65.82	74.08	85.16	75.02	9.00	16.49	18.53	22.39	19.14	2.63	0.80	0.76	0.64	0.73	0.08
Wo-ST-water	80.44	74.74	77.92	77.70	11.68	19.91	18.92	19.64	19.49	2.98	0.71	0.80	0.73	0.75	0.06
Wo-temperature	63.38	68.51	75.50	69.13	**3.11**	15.94	17.18	19.04	17.39	0.88	0.82	0.79	0.74	0.78	0.03
Wo-wind	63.81	68.12	75.91	69.28	3.26	15.98	17.06	18.32	17.12	**0.61**	0.82	0.78	0.76	0.79	**0.02**
STA-LSTM	**60.94**	**65.56**	**71.56**	**66.02**	—	**15.24**	**16.39**	**17.89**	**16.51**	—	**0.84**	**0.81**	**0.77**	**0.81**	—

Precipitation, which proves that rainfall is the most significant factor to accurately forecast flood.

For experiment of Wo-Evaporation, we can notice bias values in three measurements increase with larger forecasting time. On the contrary, we can find bias values corresponding to Wo-ST-Water decrease with larger forecasting time. Based on this observation, we could know that importance of evaporation gradually becomes larger for long-time forecasting, while Wo-ST-Water mostly contributes to short-time forecasting. Essentially, ST-Water defines the initial state before formation of flood, which makes it significant to short-time forecasting. Meanwhile, evaporation affects the formation of flood throughout the whole process of flood. Last but not least, we should notice that both factors of evaporation and ST-Water are not major features for accurate prediction, when comparing with precipitation.

4.2.2. Ablation Experiment. Details of comparative experiment on effectiveness of attention modules are shown in Table 3. Specifically, we perform three cases of experiments with spatial attention module only, with temporal attention module only, and with both modules, respectively.

From Table 3, we can observe that measurement-related performance obtained by STA-LSTM is larger when comparing with spatial or temporal attention module only, which proves effectiveness of attention module to involve context information for hydrological feature enhancement. We can also notice that most cases of second best performance and best performance in bias value are achieved by method with temporal module, which proves that temporal attention information contributes more to forecasting than spatial attention information. Essentially, flood is a complex procedure of run-off generation, separation, and routing, which leads timing to be an important factor for flood forecasting. Therefore, temporal context information extracted from sequential data contributes more to accurate forecast flood.

4.2.3. Experiment with Comparative Methods. Tables 4 and 5 offer the detailed statistics by testing STA-LSTM and comparative methods on Lech and Chuanghua dataset, respectively. Specifically, we implement SVM, LSTM, and 10 layers FCN (fully connected network) to work as comparative methods. For fair comparisons, structure and parameters of LSTM are settled to be the same with STA-LSTM. Moreover, we implement XAJ model as a comparative study in Table 5 to offer data for comparing data-driven models with physical models. Reason to abandon usage of XAJ model on Lech dataset lies in the fact that XAJ model is specially designed for Changhua river basin or other semi-humid regions, which is not fit for Lech river basin under our supposition.

As proved by R_A, M_A, and D_A in Table 4, STA-LSTM achieves the best performance in Lech dataset. Meanwhile, Table 5 shows that STA-LSTM achieves the best performance in DC and second best performance in RMSE and MAPE after conducting experiments on Changhua dataset. By comparing between XAJ model and STA-LSTM in Table 5, we can notice that specifically designed physical model, i.e., XAJ model, is capable of obtaining a higher accuracy on flood forecasting, especially in long-time period forecasting. Such phenomenon can be explained by the truth that flood is a complex process for data-driven modeling under a limited

Table 3: Comparison experiments on Changhua dataset to test effectiveness of attention module. Note that bold and underline texts indicate best and secondary best performance among comparative methods, respectively. We define unit for M as %.

Methods	R_{T+3}	R_{T+6}	R_{T+9}	R_A	R_σ	M_{T+3}	M_{T+6}	M_{T+9}	M_A	M_σ	D_{T+3}	D_{T+6}	D_{T+9}	D_A	D_σ
With spatial	54.51	79.77	95.26	76.51	1.42	13.59	19.93	23.81	19.11	0.34	0.84	0.69	0.60	0.71	0.02
With temporal	54.33	78.46	94.61	75.80	**0.71**	13.55	19.64	23.67	18.95	**0.18**	0.84	**0.71**	0.61	0.72	**0.01**
STA-LSTM	**52.37**	**78.36**	**94.55**	**75.09**	—	**13.09**	**19.59**	**23.64**	**18.77**	—	**0.85**	**0.71**	**0.62**	**0.73**	—

Table 4: Comparisons on Lech dataset with several comparative methods. Note that bold texts indicate best performance among comparative methods.

Models	R_{T+3}	R_{T+6}	R_{T+9}	R_A	M_{T+3} (%)	M_{T+6} (%)	M_{T+9} (%)	M_A	D_{T+3}	D_{T+6}	D_{T+9}	D_A
FCN	**51.27**	82.54	123.4	85.74	**12.82**	20.64	30.85	21.44	**0.88**	0.70	0.32	0.63
SVM	63.99	79.98	92.49	78.82	16.00	20.00	23.12	19.71	0.82	0.72	0.62	0.72
LSTM	68.92	75.12	80.85	74.96	17.23	18.78	20.21	18.74	0.79	0.75	0.71	0.75
STA-LSTM	60.94	**65.56**	**71.56**	**66.02**	15.24	**16.39**	**17.89**	**16.51**	0.84	**0.81**	**0.77**	**0.81**

Table 5: Comparisons on Changhua dataset with several comparative methods. Note that bold texts indicate best performance among comparative methods.

Models	R_{T+3}	R_{T+6}	R_{T+9}	R_A	M_{T+3} (%)	M_{T+6} (%)	M_{T+9} (%)	M_A (%)	D_{T+3}	D_{T+6}	D_{T+9}	D_A
FCN	56.87	88.36	129.7	91.63	14.22	22.09	32.41	22.91	0.84	0.64	0.31	0.60
SVM	60.89	86.34	110.6	85.93	15.22	21.59	27.64	21.48	0.82	0.67	0.53	0.67
LSTM	66.11	84.49	109.2	86.60	16.53	21.12	27.30	21.65	0.79	0.68	0.54	0.67
XAJ model	77.30	**68.31**	**69.25**	**71.62**	19.26	**17.09**	**17.45**	**17.93**	0.65	0.70	**0.71**	0.69
STA-LSTM	**52.37**	78.36	94.55	75.09	**13.09**	19.59	23.64	18.77	**0.85**	**0.71**	0.62	**0.73**

size of data. Therefore, utilizing insufficient data to fit flood process without building inherent and knowledge-embedded relations could not work well for long-time period forecasting. Furthermore, errors and noise for data-driven are easy to accumulate without appropriate means of error optimization during forecasting process.

By comparing STA-LSTM with other data-driven models in Tables 4 and 5, we can notice that FCN performs better than STA-LSTM for forecasting at $T+3$ in Lech dataset. However, it fails to obtain consistent performance for long-time period forecasting, i.e., $T+6$ and $T+9$. In fact, ten layer structure of FCN with limited size of parameters makes it suitable to fit in cases of relatively simple short-time forecasting. However, complexity increases in a large degree with longer forecasting period, which results in worse performance with insufficient parameters of FCN to model and optimize complexity. SVM is widely used to handle cases of learning with limited size of data. However, traditional SVM is not appropriate to conduct regression inference based on complex and sequential data, which leads to worse performance achieved by SVM than STA-LSTM. Original LSTM performs worse than STA-LSTM in all cases, which proves that attention module is of significance in improving accuracy by focusing on informative hydrological factors and timings, especially in forecasting with small dataset.

It is evident to observe that all data-driven methods perform better for short-time forecasting, i.e., $T+3$, since core task of short-time forecasting for data-driven model is to fit data with suitable parameters and prevent over-fitting. Due to accumulations of uncertainty and errors sourced from models and input factors like weather forecast, there exist a decrease in performance with long-time forecasting. To deal with complexity of long-time forecasting, the proposed STA-LSTM is built on the basis of LSTM structure to resolve long-time dependencies, which designs cell memory to represent and memorize long-time dependencies. Moreover, STA-LSTM inherently models context information to better describe long-term memory and decreases impacts brought by noisy input. As a result, STA-LSTM is capable of forecasting flood with higher accuracy and longer time period than other data-driven models, which is proved by best performance at $T+6$ and $T+9$.

We adopt one instance in test datasets to compare forecasting performance on run-off values achieved by STA-LSTM and other comparative methods in Figure 6. According to plot for $T+3$, we can find that FCN performs best, performance of STA-LSTM is close to LSTM, and SVM achieves the worst forecasting result. Essentially, the forecasting curve obtained by SVM is too smooth to coincide with great time-varying characteristics of ground-truth run-off values, due to its inherent modeling supposition that output values should be smooth to a certain extent. Due to smooth output property, we could find that forecasting results of SVM are low in RMSE, but fail to coincide with time-varying run-off forecasting plot. By comparing forecasting curves between short-time and long-time forecasting, we can notice obvious distortions for $T+6$ and $T+9$ due to large increase in complexity and difficulty of forecasting task. Among methods for long-time forecasting, STA-LSTM performs best, LSTM and SVM achieves slightly worse results, and FCN performs worst. Above all, overall forecasting performance of STA-LSTM is much more accurate and consistent

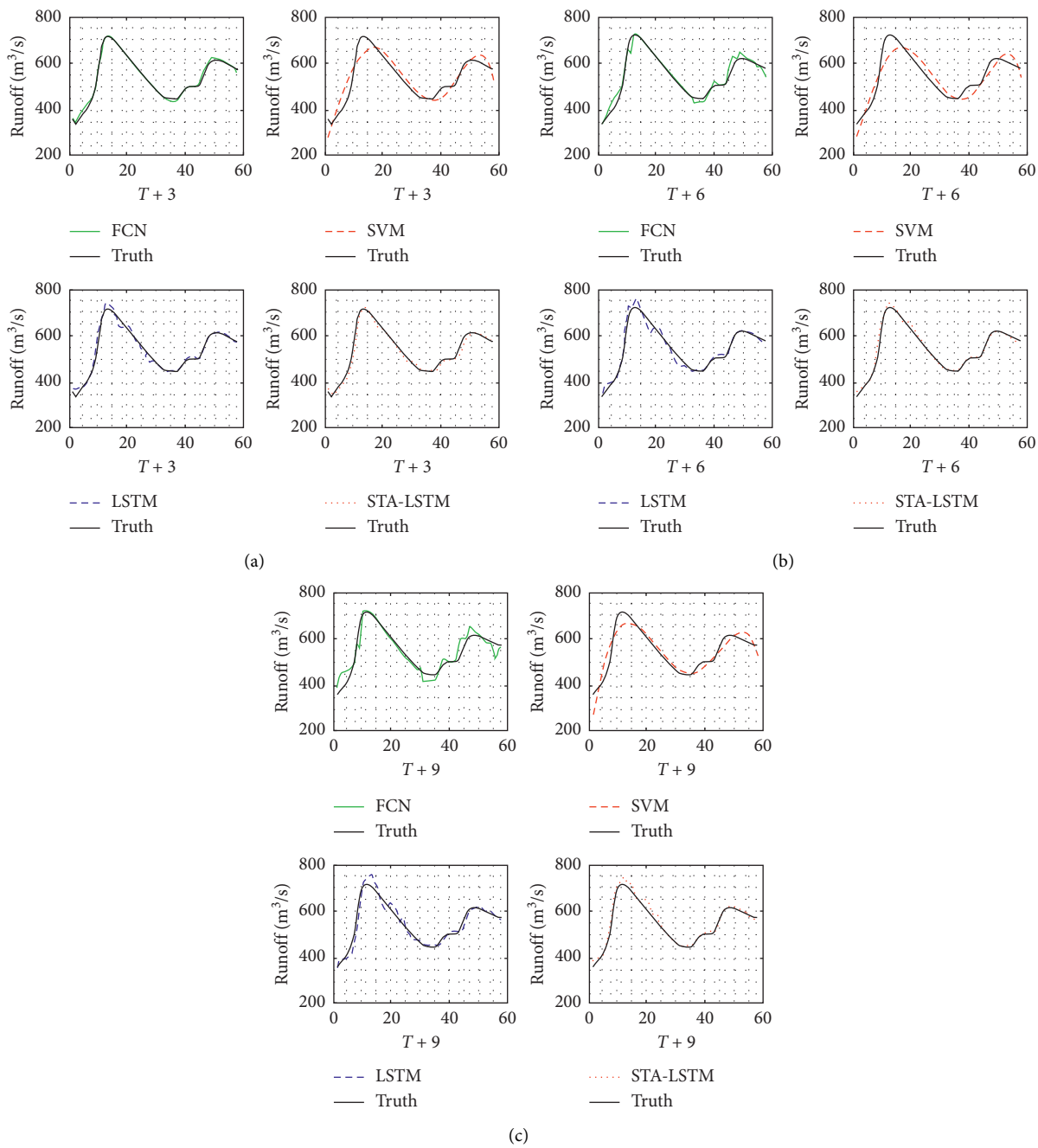

Figure 6: Comparisons in forecasting run-off values among STA-LSTM and other comparative methods, where three groups of plots refer to forecasting results performing for (a) $T+3$, (b) $T+6$, and (c) $T+9$, respectively.

than comparative methods in this case study. Meanwhile, plots achieved by SVM and LSTM are close in visual effects, where we could find a certain and obvious degree of distortion. Last but not least, FCN obtain forecasting plot with serious distortion and large deviation in several key timings.

4.3. Implementation. Experiments were performed on a server (2.4 GHz 6-core Xeon CPU, 60 GB RAM and one Nvidia GeForce GTX 1080 Ti card). For Lech and Changhua datasets, we utilize 4-folder cross validation to test STA-LSTM and other comparative methods. During network design, dimension of hidden state, and total state number of STA-LSTM network are defined as 128 and 32, respectively. During training, learning rate, weight decrease, and iteration times of STA-LSTM network are defined as 0.0025, 10^{-6}, and 500, respectively. We update the learning rate every 100 times, and the corresponding decrease rate is 0.01.

5. Conclusion

Facing difficulties in transforming problem-related data from physical space to cyber space and utilizing models to

solve problems in cyber space, we firstly define the problem of flood from views of both physical and cyber space, and then propose STA-LSTM by embedding spatial-temporal attention information for flood forecasting. STA-LSTM could selectively utilize informative hydrological features acquired from significant locations and timings. Experiments on Lech and Changhua river basins prove the effectiveness of STA-LSTM by comparing with several comparative studies. Our future work includes construction of a light-weight flood forecasting model by eliminating useless hydrological features, which not only boosts running speed of flood forecasting system, but also largely decrease complexity in collecting data and modeling feature relationship.

Data Availability

The image and acquired sensor data used to support the findings of this study were supplied by Yukai Ding under license and so cannot be made freely available. Requests for access to these data should be made to Yirui Wu (wuyirui@hhu.edu.cn).

Conflicts of Interest

The authors declare that they have no conflicts of interest.

Acknowledgments

This work was supported by National Key R&D Program of China under Grant 2018YFC0407901, Natural Science Foundation of China under Grant 61702160, and Natural Science Foundation of Jiangsu Province under Grant BK20170892.

References

[1] S. Han and P. Coulibaly, "Bayesian flood forecasting methods: a review," *Journal of Hydrology*, vol. 551, pp. 340–351, 2017.

[2] A. Kauffeldt, F. Wetterhall, F. Pappenberger, P. Salamon, and J. Thielen, "Technical review of large-scale hydrological models for implementation in operational flood forecasting schemes on continental level," *Environmental Modelling & Software*, vol. 75, pp. 68–76, 2016.

[3] W. Collischonn, R. Haas, I. Andreolli, and C. E. M. Tucci, "Forecasting river Uruguay flow using rainfall forecasts from a regional weather-prediction model," *Journal of Hydrology*, vol. 305, no. 1-4, pp. 87–98, 2005.

[4] V. A. Siqueira, R. C. D. Paiva, A. S. Fleischmann et al., "Toward continental hydrologic-hydrodynamic modeling in South America," *Hydrology and Earth System Sciences*, vol. 22, no. 9, pp. 4815–4842, 2018.

[5] Y. Wu, W. Xu, J. Feng, S. Palaiahnakote, and T. Lu, "Local and global Bayesian network based model for flood prediction," in *Proceedings of International Conference on Pattern Recognition*, Beijing, China, pp. 225–230, 2018.

[6] G. Corani and G. Guariso, "Coupling fuzzy modeling and neural networks for river flood prediction," *IEEE Transactions on Systems, Man and Cybernetics, Part C (Applications and Reviews)*, vol. 35, no. 3, pp. 382–390, 2005.

[7] F. M. Fan, D. Schwanenberg, W. Collischonn, and A. Weerts, "Verification of inflow into hydropower reservoirs using ensemble forecasts of the TIGGE database for large scale basins in Brazil," *Journal of Hydrology: Regional Studies*, vol. 4, pp. 196–227, 2015.

[8] P. R. M. Pontes, F. M. Fan, A. S. Fleischmann et al., "MGB-IPH model for hydrological and hydraulic simulation of large floodplain river systems coupled with open source GIS," *Environmental Modelling & Software*, vol. 94, pp. 1–20, 2017.

[9] P. R. M. Pontes, R. B. L. Cavalcante, P. K. Sahoo et al., "The role of protected and deforested areas in the hydrological processes of Itacaiúnas river Basin, eastern Amazonia," *Journal of Environmental Management*, vol. 235, pp. 489–499, 2019.

[10] H. Wang, C. Wang, Y. Wang, X. Gao, and C. Yu, "Bayesian forecasting and uncertainty quantifying of stream flows using Metropolis-Hastings Markov chain Monte Carlo algorithm," *Journal of Hydrology*, vol. 549, pp. 476–483, 2017.

[11] P.-S. Yu, S.-T. Chen, and I.-F. Chang, "Support vector regression for real-time flood stage forecasting," *Journal of Hydrology*, vol. 328, no. 3-4, pp. 704–716, 2006.

[12] J. Liu, G. Wang, P. Hu, L. Duan, and A. C. Kot, "Global context-aware attention LSTM networks for 3D action recognition," in *Proceedings of 2017 IEEE Conference on Computer Vision and Pattern Recognition*, pp. 3671–3680, Honolulu, HI, USA, July 2017.

[13] J. Juliang, W. Yiming, and Y. Xiaohua, "Genetic algorithm based neural network and application in modeling vulnerability of flood disaster bearing body," *Journal of Natural Disasters*, no. 2, pp. 53–60, 1998.

[14] W. Minghua, D. Peng, and L. Zhijia, "Comparison between applications of artificial neural network model and Xinanjiang model," *Hydrology*, vol. 28, no. 6, pp. 33–35, 2008.

[15] C. T. Cheng, W. J. Niu, Z. K. Feng, J. J. Shen, and K. W. Chau, "Daily reservoir runoff forecasting method using artificial neural network based on quantum-behaved particle swarm optimization," *Water*, vol. 7, no. 8, pp. 4232–4246, 2015.

[16] C. H. R. Lima, U. Lall, T. Troy, and N. Devineni, "A hierarchical Bayesian GEV model for improving local and regional flood quantile estimates," *Journal of Hydrology*, vol. 541, pp. 816–823, 2016.

[17] D. R. H. O'Connell, "Nonparametric Bayesian flood frequency estimation," *Journal of Hydrology*, vol. 313, no. 1–2, pp. 79–96, 2005.

[18] D. Biondi, P. Versace, and B. Sirangelo, "Uncertainty assessment through a precipitation dependent hydrologic uncertainty processor: an application to a small catchment in southern Italy," *Journal of Hydrology*, vol. 386, no. 1-4, pp. 38–54, 2010.

[19] X. Xu, Y. Li, T. Huang et al., "An energy-aware computation offloading method for smart edge computing in wireless metropolitan area networks," *Journal of Network and Computer Applications*, vol. 133, pp. 75–85, 2019.

[20] L. Qi, Y. Chen, Y. Yuan, S. Fu, X. Zhang, and X. Xu, "A QoS-aware virtual machine scheduling method for energy conservation in cloud-based cyber-physical systems," *World Wide Web*, vol. 23, no. 2, pp. 1275–1297, 2020.

[21] X. Xu, X. Zhang, H. Gao, Y. Xue, L. Qi, and W. Dou, "Become: blockchain-enabled computation offloading for IOT in mobile edge computing," *IEEE Transactions on Industrial Informatics*, vol. 16, no. 6, pp. 4187–4195, 2020.

[22] X. Xu, C. He, Z. Xu, L. Qi, S. Wan, and M. Z. A. Bhuiyan, "Joint optimization of offloading utility and privacy for edge computing enabled IoT," *IEEE Internet of Things Journal*, p. 1, 2019.

[23] L. Qi, R. Wang, C. Hu, S. Li, Q. He, and X. Xu, "Time-aware distributed service recommendation with privacy-preservation," *Information Sciences*, vol. 480, pp. 354–364, 2019.

[24] X. Xu, S. Fu, L. Qi et al., "An IoT-oriented data placement method with privacy preservation in cloud environment," *Journal of Network and Computer Applications*, vol. 124, pp. 148–157, 2018.

[25] X. Xu, Q. Liu, Y. Luo et al., "A computation offloading method over big data for IoT-enabled cloud-edge computing," *Future Generation Computer Systems*, vol. 95, pp. 522–533, 2019.

[26] X. Xu, Y. Chen, X. Zhang, Q. Liu, X. Liu, and L. Qi, "A blockchain-based computation offloading method for edge computing in 5G networks," *Software: Practice and Experience*, 2019.

[27] X. Xu, Y. Xue, L. Qi et al., "An edge computing-enabled computation offloading method with privacy preservation for internet of connected vehicles," *Future Generation Computer Systems*, vol. 96, pp. 89–100, 2019.

[28] L. Qi, X. Zhang, W. Dou, C. Hu, C. Yang, and J. Chen, "A two-stage locality-sensitive hashing based approach for privacy-preserving mobile service recommendation in cross-platform edge environment," *Future Generation Computer Systems*, vol. 88, pp. 636–643, 2018.

[29] V. Mnih, N. Heess, A. Graves, and K. Kavukcuoglu, "Recurrent models of visual attention," in *Proceedings of Neural Information Processing Systems*, pp. 2204–2212, Montreal, Canada, December 2014.

[30] T. He, W. Huang, Y. Qiao, and J. Yao, "Text-attentional convolutional neural network for scene text detection," *IEEE Transactions on Image Processing*, vol. 25, no. 6, pp. 2529–2541, 2016.

[31] S. Song, C. Lan, J. Xing, W. Zeng, and J. Liu, "An end-to-end spatio-temporal attention model for human action recognition from skeleton data," in *Proceedings of AAAI Conference on Artificial Intelligence*, pp. 4263–4270, San Francisco, CA, USA, February 2017.

[32] J. Liu, A. Shahroudy, M. L. Perez, G. Wang, L. Y. Duan, and A. K. Chichung, "Ntu RGB+D 120: a large-scale benchmark for 3D human activity understanding," *IEEE Transactions on Pattern Analysis and Machine Intelligence*, p. 1, 2019.

[33] S. Yeung, O. Russakovsky, N. Jin, M. Andriluka, G. Mori, and F. Li, "Every moment counts: dense detailed labeling of actions in complex videos," *International Journal on Computer Vision*, vol. 126, no. 2–4, pp. 375–389, 2018.

[34] K. Chen, L. Yao, D. Zhang, X. Wang, X. Chang, and F. Nie, "A semisupervised recurrent convolutional attention model for human activity recognition," *IEEE Transactions on Neural Networks and Learning Systems*, pp. 1–10, 2019.

[35] P. Anderson, X. He, C. Buehler et al., "Bottom-up and top-down attention for image captioning and visual question answering," in *Proceedings of 2018 IEEE Conference on Computer Vision and Pattern Recognition*, pp. 6077–6086, Salt Lake City, UT, USA, June 2018.

[36] L. Ren, X. Cheng, X. Wang, J. Cui, and L. Zhang, "Multi-scale dense gate recurrent unit networks for bearing remaining useful life prediction," *Future Generation Computer Systems*, vol. 94, pp. 601–609, 2019.

[37] L. Jintao, L. Xiaopeng, C. Xi, and M. Can, "Soil moisture content distribution in intermittent rainfall and its effect on infiltration," *Journal of Soil and Water Conservation*, vol. 23, no. 5, pp. 96–100, 2009.

Hindawi
Complexity
Volume 2019, Article ID 1635793, 8 pages
https://doi.org/10.1155/2019/1635793

Research Article

Dynamic Cross-Correlations between Participants' Attentions to P2P Lending and Offline Loan in the Private Lending Market

Yingxiu Zhao,[1] Wei Zhang,[1,2] and Xiangyu Kong[1]

[1]*College of Management and Economics, Tianjin University, Tianjin, China*
[2]*China Center for Social Computing and Analytics, Tianjin University, Tianjin, China*

Correspondence should be addressed to Xiangyu Kong; hector_kong@tju.edu.cn

Received 19 August 2019; Revised 15 October 2019; Accepted 15 November 2019; Published 12 December 2019

Guest Editor: Shu-Heng Chen

In this paper, we examine the dynamic cross-correlations between participants' attentions to the P2P lending and offline loan (lending) with the method of multifractal detrended cross-correlation analysis (MF-DCCA). The empirical result mainly shows that (1) the power-law cross-correlation exists between participants' attentions to the P2P lending and offline loan and is persistent, (2) the cross-correlation is more stable in the short term, and (3) the relation subjected to a small fluctuation is more cross-correlated than that under larger ones. Furthermore, we carry out the robustness test to verify the result. The Granger causality test indicates that participants' attentions to P2P lending and offline loan Granger cause each other in the short term.

1. Introduction

The formal credit market, the subject of which includes banks, mainly provides loans for enterprises and institutions and seldom provides funds for either small and medium enterprises (SMEs) or individuals [1, 2]. Therefore, it is difficult for SMEs and individuals to raise funds [3, 4]. Luckily, the informal credit market serves SMEs and individuals, mitigating this problem effectively [5–7]. Schreiner [5] describes multiple ways for microfinance to acquire the virtues of informal finance, such as using collateral that is easy to repossess. Barslund and Tarp [6] and Khoi et al. [7] find that informal finance has effectively alleviated the problem of Vietnamese farmers' borrowing. The informal credit market, in which present cash is exchanged for promises of cash in the future through contracts or agreements conducted without reference or recourse to the legal system, primarily comprises private lending, and savings group [8–10]. In China, lending is the dominant part of informal finance [11]. The offline loan (lending) has a smaller business radius and a stronger social network and is more conducive to obtaining "soft" information on borrowers by reducing the geographical distance between borrowers and lenders and strengthening the social network [12, 13]. Before 2007, the offline loan is the main body of the informal credit market. With the development of Internet finance, the P2P (peer-to-peer) lending platform has received more attention [14]. So far, online lending and offline loan constitute the private lending system, forming the major constituent of the informal finance network.

While offline loan has existed for quite a long time, the first online lending platform in China came into being in 2007. From then on, the P2P lending platform has been growing rapidly, with the number of platforms soaring to more than 6000 and the quantity of participants reaching as high as 10 million at the peak (https://shuju.wdzj.com/industry-list.html). However, after the government implemented regulatory measures aiming to standardize market behavior and guard against financial risks, a pyramid of P2P lending platforms that did not meet the requirements of provisions were squeezed out of market (http://wdzjosscdn.oss-cn-hangzhou.aliyuncs.com/pdf/2018年中国网络借贷 行业年报.pdf). At present, there are only about 600 platforms, and the quantity of participants has been reduced to 4 million (https://shuju.wdzj.com/industry-list.html). It is intuitive to come up with the anticipation that offline loan would rise to fill the vacancy of vanishing P2P lending, and consequently investors would be more likely to turn to offline loan to attend

their need, but further consideration and reflection render the speculation to criticism. For platforms, policy orientation is sure to cast enormous influence on their subsistence and operation, but for participants, a common influence factor of more importance is price of money, which is determined by the base interest rate and market support demand. The credit side and the debtor agree on the lending rate and then conclude a transaction. From this point of view, the lending rate partly affects participants in selecting the way of lending. While P2P lending and offline lending organizations share the overall same fluctuation trend in the loan interest rate [13], participants' attentions to offline loan and P2P lending show difference to a more sophisticated and complex extent: when investors are eager to obtain funds from offline loan institutions, they either withdraw their appeal from P2P lending platforms to lower capital cost or do not mind borrowing in two different ways to catch market opportunity, and vice versa. In this paper, we employ Baidu Search Index on P2P lending and offline loan as proxies of participants' attentions to P2P lending and offline loan, respectively. Baidu Search Index can represent participants' attentions. (Baidu Search Index is a data sharing platform based on Baidu's massive behavior data of Internet users. Here, you can study keyword search trends and insight into the interests and needs of netizens and monitor public opinion trends (http://zhishu.baidu.com/Helper/?tpl=duty). There exist other factors that influence the selection between P2P lending and offline loan, such as qualification review, i.e., the level of difficulty to grant a loan, yet they are not the focus of this paper. As discussed above, the nexus between participants' attention to P2P lending and that to offline loan is complex and dynamic. And, it is meaningful to explore the correlation of participants' attentions in the whole private lending market in China. Recent research on the private lending market system mainly includes (1) the related research on the P2P lending market, such as borrowing success rate and default rate [14–18], investor behavior [19–22], and credit evaluation and market mechanism [23–28]; (2) the relationship between the informal credit market and the formal credit market [6, 29–32]; and (3) the research on offline loan [33–35]. Therefore, this paper expands the research scope of the existing literature by investigating the extent of interdependence across time to clarify whether participants' attentions to P2P lending and offline loan are segmented or becoming more integrated.

The Pearson, Spearman, and Kendall correlations are conventional methods extensively used in investigating the relationship between two variables. The Pearson coefficient measures linear correlation, yet its application relies on the precondition that the time series are stationary and obey the normal distribution. Different from the Pearson correlation, Spearman and Kendall correlations are nonparametric tests of rank correlation. Each of them does not depend on any assumptions on the distribution and assesses the significance of the relation by comparing rankings of the variables. While multifractality is ubiquitously observed in socioeconomic systems [36], the aforementioned traditional correlation methodologies are not tested and verified by existing documents to examine multifractality. Therefore, both detrended cross-correlation analysis (DCCA) advanced by Podobnik and Stanley [37] and multifractal detrended cross-correlation analysis (MF-DCCA) proposed by Zhou [38] are selected to study the cross-correlations between participants' attentions to P2P lending and offline loan. After implementing numerical experiments with mathematical models, researchers have confirmed the characteristics of the DCCA coefficient and justified its advantage over the Pearson coefficient [36, 39–44]. Kristoufek [40] confirms that, for the nonstationary series, the DCCA coefficient measures correlation accurately despite various levels of nonstationarity and dominates the Pearson coefficient. Compared with the Pearson correlation coefficients, the DCCA coefficients are scale-dependent and more robust to the amplitude ratio between slow and fast components and contaminated noises [45].

The remainder of this paper is organized as follows: Section 2 describes the data used in this paper and their statistical characteristics. Section 3 describes the procedure of the methodology of MF-DCCA. Section 4 reports the relevant empirical results of MF-DCCA, and Section 5 concludes this paper.

2. Data Description

We obtain daily search volume data of P2P lending and offline loan from Baidu Search Index. Like Google Trends [46], Baidu Search Index has been used as a proxy of attention [47, 48]. In this paper, we choose the keywords "P2P lending" and "offline loan" to achieve searching volumes. The P2P lending search volume reflects participants' attention. The higher the index, the more the attention P2P lending arouses. The offline loan search volume has a similar meaning. P2P lending and offline loan constitute the private lending network system. So the search volumes can represent participants' attention to the approach of borrowing or lending in the private lending network. The whole sample period extends from January 1, 2011, to July 3, 2019.

In order to explore cross-correlations between participants' attention to P2P lending and that to offline loan, we define two variables as follows:

$$\begin{aligned} \mathrm{P2P}_t &= \ln\left(\mathrm{P2P}_t\right), \\ \mathrm{loan}_t &= \ln\left(\mathrm{loan}_t\right), \end{aligned} \tag{1}$$

where $\mathrm{P2P}_t$ is the Baidu index of P2P lending and loan_t is the Baidu index of offline loan in time t, respectively.

Table 1 shows the statistical properties of P2P lending and offline loan searching indices, including mean, median, stand deviation, kurtosis, max value, min value, skewness, and Jarque–Bera test values. As we can see in Table 1, the mean, median, min, and max values of the P2P lending searching index are larger than those of the offline loan searching index, indicating keen interest for P2P lending. It is reasonable to speculate that P2P lending raises far more attention than does offline loan because of its Internet foundation. Both the KPSS test and augmented Dickey–Fuller test reject the null hypothesis that a unit root exists at

Table 1: Statistics of searching indices.

Var.	Obs.	Mean	Median	Std.	Max	Min	Ske.	Kur.	Jar.
P2P	3106	9436.146	7496.5	5102.071	63190	1868	1.841	9.923	7957.118***
Loan	3106	1404.857	1279	549.201	10784	218	2.939	38.905	171316.870***

***indicates statistical significance at the 1% level. Ske. is skewness; Kur. is Kurtosis; Jar. is Jarque–Bera; Std. is standard deviation.

the 1% significance level and justify the appropriateness of the Jarque–Bera test. The Jarque–Bera test values of two variables are all significant, and the null hypothesis of following a normal distribution is rejected.

3. Empirical Methodology

We employ the method of MF-DCCA introduced by Zhou [38] to analyze the cross-correlation between participants' attention to P2P lending and that to offline loan. Consider two equal time series $\{x_i\}$ and $\{y_i\}$, where $i = 1, 2, \ldots, N$. The detailed steps of the methodology can be described as follows:

Step 1: construct two profiles by the two time series as

$$X_i = \sum_{k=1}^{i} (x_k - \overline{x}), \quad Y_i = \sum_{k=1}^{i} (y_k - \overline{y}), \quad i = 1, 2, \ldots, N, \tag{2}$$

where $\overline{x} = 1/N\sum_{k=1}^{N} x_k$ and $\overline{y} = 1/N\sum_{k=1}^{N} y_k$.

Step 2: the two profiles are divided into $N_s = [N/s]$ nonoverlapping segments of equal length s. If the length N cannot be divisible by scale s, a short part segment at the end of each profile will be left. In order to extract all the information involved in the profiles, the same division procedure is repeated from the other end of the profile and we obtain $2N_s$ segments of each profile consequently. According to the research of Zhang et al. [43], which employs Internet-based data as is the case in this paper, we set the scale s as $10 < s < N/4$, and the step is 1 in this paper.

Step 3: the detrended covariance is calculated by

$$F^2(s, v) = \frac{1}{s}\sum_{j=1}^{s}\left[X_{(v-1)s+j} - \widetilde{X}_{(v-1)s+j}\right]\left[Y_{(v-1)s+j} - \widetilde{Y}_{(v-1)s+j}\right], \quad \text{for } v = 1, 2, \ldots, N_s, \tag{3}$$

$$F^2(s, v) = \frac{1}{s}\sum_{j=1}^{s}\left[X_{N-(v-N_s)s+j} - \widetilde{X}_{N-(v-N_s)s+j}\right]\left[Y_{N-(v-N_s)s+j} - \widetilde{Y}_{N-(v-N_s)s+j}\right], \tag{4}$$

for $v = N_s + 1, N_s + 2, \ldots, 2N_s$, where $\widetilde{X}$ and $\widetilde{Y}$ are local trends estimated in each segment through the OLS method.

Step 4: average all detrended segments to get the q th-order fluctuation function as

$$F_q(s) = \left\{\frac{1}{2N_s}\sum_{v=1}^{2N_s} F^2(s, v)^{q/2}\right\}^{1/q}. \tag{5}$$

When $q = 0$, the equation is defined as

$$F_0(s) = \exp\left\{\frac{1}{4N_s}\sum_{v=1}^{2N_s} \ln\left[F^2(s, v)\right]\right\}. \tag{6}$$

Step 5: observe the log-log plots of $F_q(s)$ versus s and analyze the scaling behavior of the fluctuation function. If the two series are long-range cross-correlated, there exists a following power-law relation between them:

$$F_q(s) \propto s^{H_{xy}(q)}. \tag{7}$$

The slope of the log-log plots of $F_q(s)$ versus s can be estimated with the method of OLS and denoted as $H_{xy}(q)$, which is an indicator of the cross-correlation of the two time series. If $H_{xy}(q) < 0.5$, the cross-correlation between them is antipersistent (negative); if $H_{xy}(q) > 0.5$, the cross-correlation between them is persistent (positive); when $H_{xy}(q) = 0.5$, no cross-correlation exists between the two time series. In particular, when $q = 2$, the scaling exponent $H_{xy}(q)$ turns into the generalized Hurst exponents.

4. Empirical Results

4.1. Cross-Correlation Test. In order to have a macroscopic and qualitative view of the correlation participants' attention in the private lending market to P2P lending and that to offline loan, we first carry out a cross-correlation test advanced by Podobnik and Stanley [37], which is defined as

$$Q_{cc}(m) = N^2 \sum_{i=1}^{m} \frac{X_i^2}{N - i}, \tag{8}$$

where X_i^2 is the cross-correlation function defined as

$$X_i^2 = \frac{\sum_{k=i+1}^{N} x_k y_{k-i}}{\sqrt{\sum_{k=1}^{N} x_k^2 \sum_{k=1}^{N} y_k^2}}, \tag{9}$$

where $\{x_i\}$ and $\{y_i\}$ are the two time series that have the same length N.

The test statistic $Q_{cc}(m)$ is approximately chi square distributed with m degrees of freedom. The null hypothesis of this cross-correlation test is that none of the first m cross-correlation coefficient is different from zero. Thereby, if the value of the test statistic $Q_{cc}(m)$ exceeds the critical value of $\chi^2(m)$, a significant cross-correlation between the two time series exists.

Figure 1 shows the results of the test statistic $Q_{cc}(m)$ between P2P lending and offline loan. The degrees of freedom vary from 1 to 1000, and the black line denotes the critical value of $\chi^2(m)$ at the 5% significant level. The $Q_{cc}(m)$ statistics are always larger than the critical value, and thus, the null hypothesis of no cross-correlations can be rejected. There are long-range cross-correlations in series of participants' attentions to P2P lending and offline loan.

4.2. Multifractal Detrended Cross-Correlation Analysis. Now that the test statistic $Q_{cc}(m)$ provides qualitative evidence that the long-range cross-correlation between attention to P2P lending and that to offline loan is existent, we then conduct the quantitative method, MF-DCCA, to analyze the cross-correlations of attentions. In this paper, the order q is set from -10 to 10, and the step is 1. If $q < 0$, the paired time series means a small fluctuation; if not, it symbolizes a large fluctuation. Figure 2 depicts the log-log plots of $F_{xyq}(s)$ versus s for P2P lending and offline loan, and the order q of lines increases from the bottom to the top. As we can see, all lines fit the log-log line of $F_{xyq}(s)$ versus s, proving that the power-law cross-correlation between the pair exists.

Figure 3 shows the scaling exponents of cross-correlation for P2P lending-offline loan with the varying order of q. The values of $H_{xy}(q)$ for P2P-loan are both above 0.5, indicating that the cross-correlation between attention to P2P lending and that to offline loan is persistent. As q increases, $H_{xy}(q)$ for P2P-loan has a mainly downward trend, demonstrating that the relation during a small fluctuation is more cross-correlated than that during the large one.

Podobnik et al. [49] suggest that a turning point S^* referred to as the "crossover" can indicate the fundamental change in the linear trend of the curves. In this paper, we can find $S^* = 2.37$ (about 234 days) in Figure 2. As is vividly pictured in Figure 4, the scaling exponents for P2P-loan in the long term $(S > S^*)$ are larger than those in the short term $(S < S^*)$, implying that the cross-correlations in the short term are less persistent. As q increases, P2P-loan scale exponents in both long and short terms incline to reduce in general, and we can infer that relations subjected to small fluctuations are more cross-correlated than those under larger ones. ΔH_q is introduced to explore the degree of multifractality by Yuan et al. [50], and the larger the ΔH_q, the higher the degree of multifractality.

$$\Delta H_q = \max\left(H_q\right) - \min\left(H_q\right). \tag{10}$$

ΔH_q of P2P-loan in the short term reported in Table 2 is smaller than that in the long term. From ΔH_q, we can conclude that the cross-correlation of attention to P2P lending and that to offline loan is more stable in the short term.

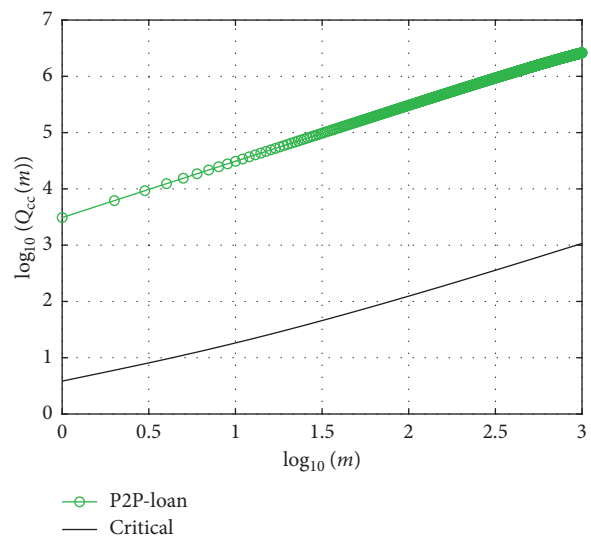

Figure 1: Cross-correlation test $(Q_{cc}(m))$.

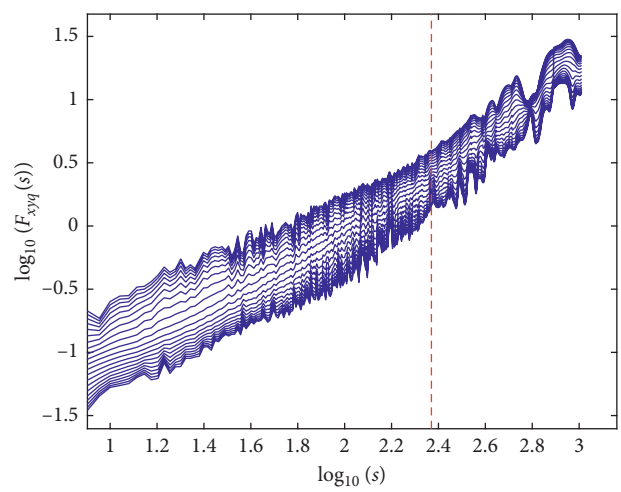

Figure 2: Log-log plots of $F_{xyq}(s)$ versus s for P2P-loan.

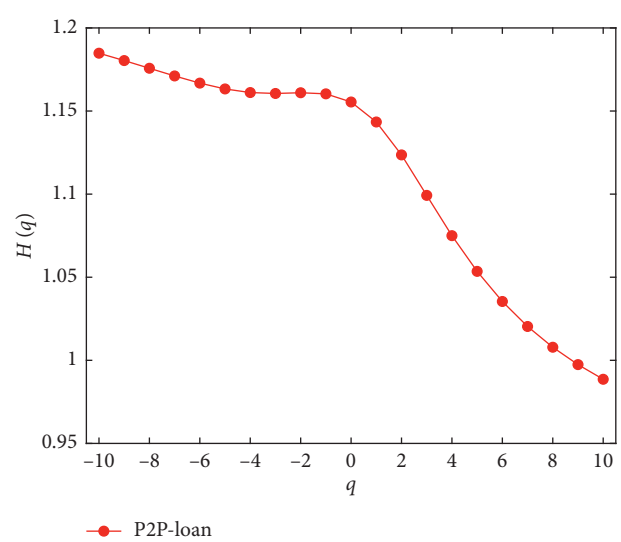

Figure 3: MF-DCCA scaling exponents for P2P-loan.

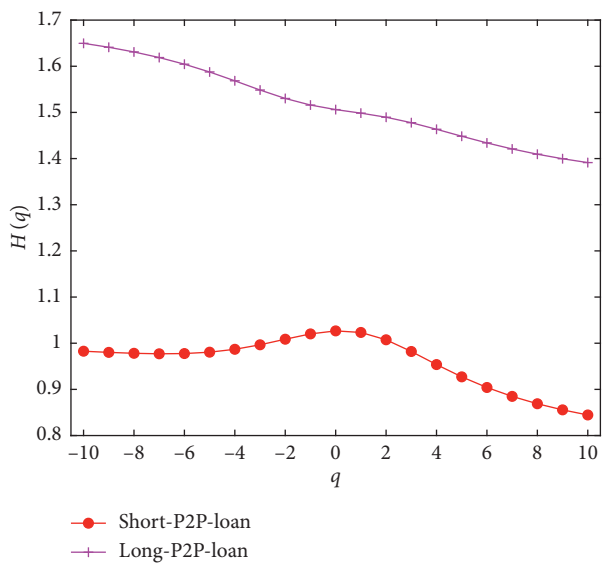

Figure 4: Short and long scaling exponents for P2P lending-offline loan.

Table 2: Cross-correlation scaling exponents $H_{xy}(q)$ for P2P-loan with q varying from −10 to 10.

q	P2P-loan $S^* = 234$	
	$S < S^*$	$S > S^*$
−10	0.9827	1.6497
−9	0.9802	1.6411
−8	0.9782	1.6310
−7	0.9771	1.6189
−6	0.9776	1.6045
−5	0.9806	1.5875
−4	0.9868	1.5684
−3	0.9966	1.5485
−2	1.0087	1.5302
−1	1.0202	1.5159
0	1.0267	1.5061
1	1.0233	1.4984
2	1.0074	1.4895
3	0.9821	1.4777
4	0.9537	1.4634
5	0.9271	1.4484
6	0.9041	1.4339
7	0.8848	1.4208
8	0.8689	1.4094
9	0.8556	1.3996
10	0.8445	1.3913
ΔH_q	0.1821	0.2584

S^* is a turning point at which the linear tendency of the curve changes fundamentally. When $S < S^*$, the scale exponent denotes short-term-related behavior. And when $S > S^*$, the scale exponent reflects long-term-related behavior. q indicates the order of fluctuation function described in equation (5). ΔH_q denotes the degree of multifractality.

4.3. Quantile Regression. The above nonlinear pattern motivates a further examination of the relationship between search volumes of P2P lending and offline loan. We apply a quantile regression to examine whether such a relationship exhibits a systematic change. Quantile regression is first proposed by Koenker and Bassett [51] and, more recently, is employed to study stock return autocorrelations [52], research the effect of investor sentiment on stock returns [53], and examine the relationship between the magnitude of the herding effect and the number of investors [54]. In this paper, the quantiles including 5%, 10%, 25%, 50%, 75%, and 90% are chosen to conduct the quantile regression analysis. The regression model is

$$\text{loan}_{(\tau)t} = \alpha_{(\tau)} + \beta_{(\tau)}\text{P2P}_{(\tau)t}, \tag{11}$$

in which τ represents the quantile and $\alpha_{(\tau)}$ and $\beta_{(\tau)}$ denote the coefficient of regression terms. From Table 3, we see that the estimated coefficients for cross-correlation remain statistically significant across different quantiles, indicating the robustness of cross-correlations between attentions to P2P lending and offline loan.

4.4. Granger Causality Test. Before performing the Granger causality test, we tested the stationary property of the time series in the regression model by carrying out the augmented Dickey–Fuller test and KPSS test. And the null hypothesis that a unit root exists is rejected. The pairwise Granger causality test employed in this paper follows the following equation:

$$\begin{aligned} \text{P2P}_t &= \sum_{i=1}^{m} \alpha_i \text{loan}_{t-i} + \sum_{j=1}^{m} \beta_j \text{P2P}_{t-j} + \mu_{1t}, \\ \text{loan}_t &= \sum_{i=1}^{n} \lambda_i \text{loan}_{t-i} + \sum_{j=1}^{n} \delta_j \text{P2P}_{t-j} + \mu_{2t}, \end{aligned} \tag{12}$$

in which m and n signify "model order," i.e., the quantity of lagged observations contained in the multivariate regression model. And the result of the pairwise Granger causality test is depicted in Figure 5. A low p value (<0.1) rejects the hypothesis of no causality and indicates a significant causal relation. When lag < 32, the attention to P2P lending always Granger causes that to offline loan at the 10% significance level; when lag = [2, 3, 4, 6, 7, 8, 9, 10], the attentions to P2P lending and offline loan Granger cause each other at the 10% significance level.

However, there might exist a large number of neutral participants in the credit market that have no preference for either of the two types of lending and search both P2P lending and offline loan on Baidu to get informed before making decisions. In this case, the empirical result that participants' attentions to P2P lending and offline loan Granger cause each other in the short run can even be reduced to unreliable. To ruling out this possibility, we construct two new series, i.e., loan_P2P_t and P2P_loan_t, both of which are derived from the following equation:

$$\begin{aligned} \text{loan\_P2P}_t &= \max\left(\text{loan}'_t - \text{P2P}'_t, 0\right), \\ \text{P2P\_loan}_t &= \max\left(\text{P2P}'_t - \text{loan}'_t, 0\right), \end{aligned} \tag{13}$$

in which loan'_t and $\text{P2P}'_t$ are obtained from normalizing loan_t and P2P_t to the scale of 0 to 100, respectively.

Table 3: Estimation results of quantile regression.

Quantile	$\alpha_{(\tau)}$	$\beta_{(\tau)}$
0.05	426.9315 (0.0000)***	0.0369 (0.0000)***
0.10	488.3254 (0.0000)***	0.0426 (0.0000)***
0.25	739.9957 (0.0000)***	0.0386 (0.0000)***
0.50	933.3032 (0.0000)***	0.0402 (0.0000)***
0.75	1055.0440 (0.0000)***	0.0654 (0.0000)***
0.90	1550.3950 (0.0000)***	0.0550 (0.0000)***

The regression model is $\text{loan}_{(\tau)t} = \alpha_{(\tau)} + \beta_{(\tau)}\text{P2P}_{(\tau)t}$, in which $\text{P2P}_{(\tau)t}$ is the Baidu index of P2P lending, $\text{loan}_{(\tau)t}$ is the Baidu index of offline loan in time t, τ represents the quantile, and $\alpha_{(\tau)}$ and $\beta_{(\tau)}$ denote the coefficient of regression terms. p values and t statistics are in parentheses $^{*}p < 0.10$, $^{**}p < 0.05$, $^{***}p < 0.01$.

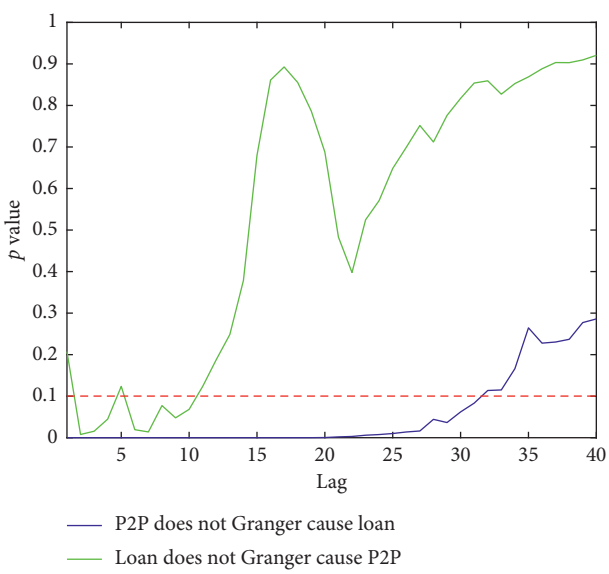

Figure 5: Granger causality test. The dashed line represents the significance level of 10%.

loan_P2P_t (P2P_loan_t) is supposed to capture the participants' attention to offline loan (P2P-lending) with neutral participants' searching behavior for P2P lending (offline loan) excluded. Then, we employ the Granger causality test with the two new series. As Figure 6 depicts, the consequent robustness result is consistent with the empirical result in the short term: when lag < 6, the attentions to P2P lending and offline loan Granger cause each other at the 10% significance level.

5. Conclusions

In this paper, we focus on the private lending network system which consists of P2P lending and offline loan and investigate the cross-correlations of participants' attention between two types of lending. In particular, we conduct the cross-correlation test with multifractal detrended cross-correlation analysis (MF-DCCA). Based on the search volumes of P2P lending and offline loan from Baidu Search Index, the empirical results show that (1) there are long-range cross-correlations in series of attentions to P2P lending and offline loan, (2) the cross-correlation exponents $H_{xy}(q)$ of attentions to P2P lending and offline loan are both above 0.5, denoting persistent correlation between attentions to P2P lending and offline loan in the private lending, and (3) as order q increases, $H_{xy}(q)$ for P2P lending and offline loan has a mainly downward trend, and the small fluctuation is more cross-correlated than the large one. Furthermore, quantile regression and Granger causality test consolidate the conclusion. The Granger causality test further indicates that participants' attentions to P2P lending and offline loan Granger cause each other during a period less than two weeks, while in a relatively longer time span, i.e., a month, the attention to P2P lending always Granger causes that to offline loan.

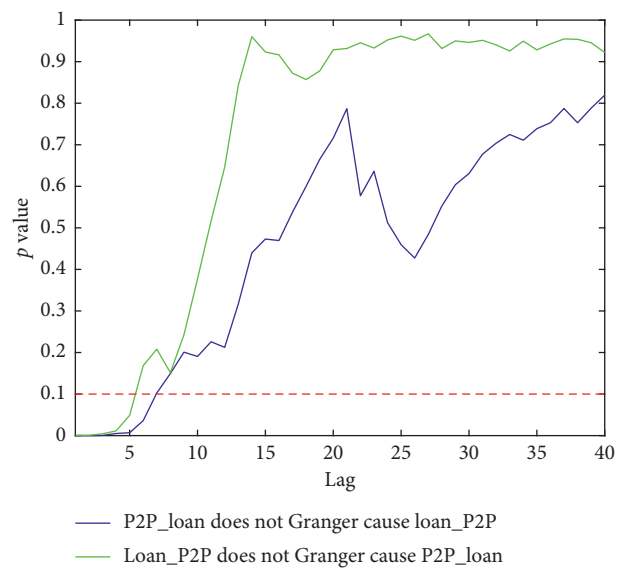

Figure 6: Granger causality test with the new series. The dashed line represents the significance level of 10%.

Admittedly, the above results cannot completely reveal the relationship between attentions to the two types of lending. To further explore the attentions to P2P lending and offline loan in the credit market, factors such as the interest rate, qualification examination, and mutual transformation between offline loan and P2P lending remain to be investigated in the future.

Data Availability

The data of participants' preferences for P2P lending and offline loan used to support the findings of this study are currently under embargo, while the research findings are commercialized. Requests for data, 12 months after publication of this article, will be considered by the corresponding author. Our data are derived from Baidu Search Index, and we have complied with terms of use stated on the website http://index.baidu.com.

Conflicts of Interest

The authors declare that they have no conflicts of interest.

Acknowledgments

This research was supported by the National Natural Science Foundation of China (71532009 and 71661137001).

References

[1] M. J. Fry, *Money, Interest, and Banking in Economic Development*, John Hopkins University Press, Baltimore, MD, USA, 1995.

[2] R. I. McKinnon, *Money and Capital in Economic Development*, The Brookings Institution, Washington, DC, USA, 1973.

[3] C. G. Turvey, R. Kong, and X. Huo, "Borrowing amongst friends: the economics of informal credit in rural China," *China Agricultural Economic Review*, vol. 2, no. 2, pp. 133–147, 2010.

[4] A. N. Berger, W. Goulding, and T. Rice, "Do small businesses still prefer community banks?," *Journal of Banking & Finance*, vol. 44, pp. 264–278, 2014.

[5] M. Schreiner, "Informal finance and the design of microfinance," *JSTOR*, vol. 11, no. 5, 2001.

[6] M. Barslund and F. Tarp, "Formal and informal rural credit in four provinces of Vietnam," *The Journal of Development Studies*, vol. 44, no. 4, pp. 485–503, 2008.

[7] P. D. Khoi, C. Gan, G. V. Nartea, and D. A. Cohen, "Formal and informal rural credit in the Mekong River Delta of Vietnam: interaction and accessibility," *Journal of Asian Economics*, vol. 26, pp. 1–13, 2013.

[8] S.-Y. Tang, "Informal credit markets and economic development in Taiwan," *World Development*, vol. 23, no. 5, pp. 845–855, 1995.

[9] M. S. Floro and D. Ray, "Vertical links between formal and informal financial institutions," *Review of Development Economics*, vol. 1, no. 1, pp. 34–56, 1997.

[10] K. Hoff and J. E. Stiglitz, "Introduction: imperfect information and rural credit markets-puzzles and policy perspectives," *The World Bank Economic Review*, vol. 4, no. 3, pp. 235–250, 1990.

[11] H. Li, "On the Regulatory Model and Improvement of Private Lending," Research on Rule of Law, 2011.

[12] C. Zhang, Z. Xu, and D. Qing, "Private lending rate and the way out for private capital: case study," *Financial Research*, vol. 3, 2013.

[13] B. Wang, H. Liang, and X. Zhang, "Interest rate marketization, monetary policy shocks and on-line and off-line private lending," *China Industrial Economics*, vol. 6, pp. 60–78, 2019.

[14] G. Dorfleitner, C. Priberny, S. Schuster et al., "Description-text related soft information in peer-to-peer lending evidence from two leading European platforms," *Journal of Banking and Finance*, vol. 64, pp. 169–187, 2016.

[15] J. Duarte, S. Siegel, and L. Young, "Trust and credit: the role of appearance in peer-to-peer lending," *Review of Financial Studies*, vol. 25, no. 8, pp. 2455–2484, 2012.

[16] R. Emekter, Y. Tu, B. Jirasakuldech, and M. Lu, "Evaluating credit risk and loan performance in online peer-to-peer (P2P) lending," *Applied Economics*, vol. 47, no. 1, pp. 54–70, 2015.

[17] R. Iyer, A. I. Khwaja, E. F. P. Luttmer, and K. Shue, "Screening peers softly: inferring the quality of small borrowers," *Management Science*, vol. 62, no. 6, pp. 1554–1577, 2016.

[18] M. Lin, N. R. Prabhala, and S. Viswanathan, "Judging borrowers by the company they keep: friendship networks and information asymmetry in online peer-to-peer lending," *Management Science*, vol. 59, no. 1, pp. 17–35, 2013.

[19] M. Herzenstein, U. M. Dholakia, and R. L. Andrews, "Strategic herding behavior in peer-to-peer loan auctions," *Journal of Interactive Marketing*, vol. 25, no. 1, pp. 27–36, 2011.

[20] D. Paravisini, V. Rappoport, and E. Ravina, "Risk aversion and wealth: evidence from person-to-person lending portfolios," *Management Science*, vol. 63, no. 2, pp. 279–297, 2017.

[21] D. J. Brass, "Friendships in online peer-to-peer lending: popes, prisms, and relational herding," *MIS Quarterly*, vol. 39, no. 3, pp. 729–742, 2015.

[22] J. Zhang and P. Liu, "Rational herding in microloan markets," *Management Science*, vol. 58, no. 5, pp. 892–912, 2012.

[23] Y. H. Guo, W. J. Zhou, C. Y. Luo, and H. Xiong, "Instance-based credit risk assessment for investment decisions in P2P lending," *European Journal Operational Research*, vol. 249, no. 2, pp. 417–426, 2015.

[24] Y. Gao, J. Sun, and Q. Zhou, "Forward looking versus backward looking: an empirical study on the effectiveness of credit evaluation system in China's online P2P lending market," *China Finance Review International*, vol. 7, no. 2, pp. 228–248, 2017.

[25] O. Rigbi, "The effects of usury laws: evidence from the online loan market," *Review of Economics and Statistics*, vol. 95, no. 4, pp. 1238–1248, 2013.

[26] Z. Y. Wei and M. Lin, "Market mechanisms in online peer-to-peer lending," *Management Science*, vol. 63, no. 12, pp. 4236–4257, 2013.

[27] H. Liu, H. Qiao, S. Wang, and Y. Li, "Platform competition in peer-to-peer lending considering risk control ability," *European Journal of Operational Research*, vol. 274, no. 1, pp. 280–290, 2019.

[28] H. Tang, "Peer-to-peer lenders versus banks: substitutes or complements?," *The Review of Financial Studies*, vol. 32, no. 5, pp. 1900–1938, 2019.

[29] X. Giné, "Access to capital in rural Thailand: an estimated model of formal vs. informal credit," *Journal of Development Economics*, vol. 96, no. 1, pp. 16–29, 2011.

[30] T. B. Andersen and N. Malchow-Møller, "Strategic interaction in undeveloped credit markets," *Journal of Development Economics*, vol. 80, no. 2, pp. 275–298, 2006.

[31] M. W. Peng and J. Q. Zhou, "How network strategies and institutional transitions evolve in Asia," *Asia Pacific Journal of Management*, vol. 22, no. 4, pp. 321–336, 2005.

[32] M. R. Gupta and S. Chaudhuri, "Formal credit, corruption and the informal credit market in agriculture: a theoretical analysis," *Economica*, vol. 64, no. 254, pp. 331–343, 1997.

[33] H. Ngalawa and N. Viegi, "Interaction of formal and informal financial markets in quasi-emerging market economies," *Economic Modelling*, vol. 31, pp. 614–624, 2013.

[34] A. Madestam, "Informal finance: a theory of moneylenders," *Journal of Development Economics*, vol. 107, pp. 157–174, 2014.

[35] D. Qin, Z. Xu, and X. Zhang, "How much informal credit lending responded to monetary policy in China? The case of Wenzhou," *Journal of Asian Economics*, vol. 31-32, pp. 22–31, 2014.

[36] Z. Q. Jiang, W. J. Xie, W. X. Zhou, and D. Sornette, "Multifractal analysis of financial markets," 2018, https://arxiv.org/abs/1805.04750.

[37] B. Podobnik and H. E. Stanley, "Detrended cross-correlation analysis: a new method for analyzing two nonstationary time series," *Physical Review Letters*, vol. 100, no. 8, pp. 1–4, 2008.
[38] W.-X. Zhou, "Multifractal detrended cross-correlation analysis for two nonstationary signals," *Physical Review E*, vol. 77, no. 6, Article ID 066211, 2008.
[39] B. Podobnik, Z.-Q. Jiang, W.-X. Zhou, and H. E. Stanley, "Statistical tests for power-law cross-correlated processes," *Physical Review E*, vol. 84, no. 6, pp. 1–8, 2011.
[40] L. Kristoufek, "Measuring correlations between non-stationary series with DCCA coefficient," *Physica A: Statistical Mechanics and Its Applications*, vol. 402, pp. 291–298, 2014.
[41] L. Kristoufek, "Fractal approach towards power-law coherency to measure cross-correlations between time series," *Communications in Nonlinear Science and Numerical Simulation*, vol. 50, pp. 193–200, 2017.
[42] L. Kristoufek, "Detrending moving-average cross-correlation coefficient: measuring cross-correlations between non-stationary series," *Physica A: Statistical Mechanics and Its Applications*, vol. 406, pp. 169–175, 2014.
[43] Z. Zhang, Y. Zhang, D. Shen, and W. Zhang, "The cross-correlations between online sentiment proxies: evidence from Google Trends and Twitter," *Physica A: Statistical Mechanics and Its Applications*, vol. 508, pp. 67–75, 2018.
[44] W. Zhang, P. Wang, X. Li, and D. Shen, "Multifractal detrended cross-correlation analysis of the return-volume relationship of bitcoin market," *Complexity*, vol. 2018, Article ID 8691420, 20 pages, 2018.
[45] L. Piao and Z. Fu, "Quantifying distinct associations on different temporal scales: comparison of DCCA and Pearson methods," *Scientific Reports*, vol. 6, no. 1, pp. 36–59, 2016.
[46] Z. Da, J. Engelberg, and P. Gao, "In search of attention," *The Journal of Finance*, vol. 66, no. 5, pp. 1461–1499, 2011.
[47] W. Zhang, D. Shen, Y. Zhang, and X. Xiong, "Open source information, investor attention, and asset pricing," *Economic Modelling*, vol. 33, pp. 613–619, 2013.
[48] D. Shen, Y. Zhang, X. Xiong, and W. Zhang, "Baidu index and predictability of Chinese stock returns," *Financial Innovation*, vol. 3, no. 1, pp. 1–8, 2017.
[49] B. Podobnik, I. Grosse, D. Horvatić, S. Ilic, P. C. Ivanov, and H. E. Stanley, "Quantifying cross-correlations using local and global detrending approaches," *The European Physical Journal B*, vol. 71, no. 2, pp. 243–250, 2009.
[50] Y. Yuan, X.-T. Zhuang, and X. Jin, "Measuring multifractality of stock price fluctuation using multifractal detrended fluctuation analysis," *Physica A: Statistical Mechanics and Its Applications*, vol. 388, no. 11, pp. 2189–2197, 2009.
[51] R. Koenker and G. Bassett, "Regression quantiles," *Econometrica*, vol. 46, no. 1, pp. 33–50, 1978.
[52] D. G. Baur, T. Dimpfl, and R. C. Jung, "Stock return autocorrelations revisited: a quantile regression approach," *Journal of Empirical Finance*, vol. 19, no. 2, pp. 254–265, 2012.
[53] Z.-X. Ni, D.-Z. Wang, and W.-J. Xue, "Investor sentiment and its nonlinear effect on stock returns—new evidence from the Chinese stock market based on panel quantile regression model," *Economic Modelling*, vol. 50, pp. 266–274, 2015.
[54] Y. Jiang, Y.-C. Ho, X. Yan, and Y. Tan, "Investor platform choice: herding, platform attributes, and regulations," *Journal of Management Information Systems*, vol. 35, no. 1, pp. 86–116, 2018.